VOL. 126, PART 1
31 MAY, 2002

Transactions of the Royal Society of South Australia Incorporated

Contents

PUBLISHED AND SOLD AT THE SOCIETY'S ROOMS
SOUTH AUSTRALIAN MUSEUM, NORTH TERRACE, ADELAIDE, S.A. 5000

TRANSACTIONS OF THE

ROYAL SOCIETY OF SOUTH AUSTRALIA

INCORPORATED

VOL. 126, PART 1

TRANSACTIONS OF THE

ROYAL SOCIETY OF SOUTH AUSTRALIA INC.

CONTENTS, VOL. 126, 2002

PART 1, 31 MAY, 2002

PART 2, 29 NOVEMBER, 2002

A REVIEW OF THE INVERTEBRATE PHYLUM KAMPTOZOA (ENTOPROCTA) AND SYNOPSIS OF KAMPTOZOAN DIVERSITY IN AUSTRALIA AND NEW ZEALAND

By Kerstin Wasson

Summary

Wasson, K. (2002) A review of the invertebrate phylum Kamptozoa (Entoprocta) and synopsis of kamptozoan diversity in Australia and New Zealand. Trans. R. Soc. S. Aust. 126(1), 1-20, 31 May, 2002.

Kamptozoans are tiny suspension-feeders superficially resembling bryozoans or hydroids, but phylogenetically affiliated with spiralians such as polychaetes. All 150 of the described species undergo budding, either to form clonal aggregations or interconnected colonies. This review provides a synthesis of current knowledge about Kamptozoa, updating the last general English-language description of the phylum provided by Hyman in 1951. Kamptozoan morphology, reproduction, and phylogenetic relationships are characterized. Finally, each of the three major kamptozoan families is described with examples drawn from Australia and New Zealand. Currently 37 species are known from this region, but many more remain to be discovered. The Australian fauna is unusually rich and varied and includes the world's largest kamptozoan species.

Transactions of the Royal Society of S. Aust. (2002), **126**(1), 1–20.

A REVIEW OF THE INVERTEBRATE PHYLUM KAMPTOZOA (ENTOPROCTA) AND SYNOPSIS OF KAMPTOZOAN DIVERSITY IN AUSTRALIA AND NEW ZEALAND

by KERSTIN WASSON*

Summary

WASSON, K. (2002) A review of the invertebrate phylum Kamptozoa (Entoprocta) and synopsis of kamptozoan diversity in Australia and New Zealand. *Trans. R. Soc. S. Aust.* **126**(1), 1–20, 31 May 2002.

Kamptozoans are tiny suspension-feeders superficially resembling bryozoans or hydroids, but phylogenetically affiliated with spiralians such as polychaetes. All 150 of the described species undergo budding, either to form clonal aggregations or interconnected colonies. This review provides a synthesis of current knowledge about Kamptozoa, updating the last general English-language description of the phylum provided by Hyman in 1951. Kamptozoan morphology, reproduction, and phylogenetic relationships are characterized. Finally, each of the three major kamptozoan families is described with examples drawn from Australia and New Zealand. Currently 37 species are known from this region, but many more remain to be discovered. The Australian fauna is unusually rich and varied and includes the world's largest kamptozoan species.

Introduction

Kamptozoans are tiny, tentaculate suspension feeders that live in all oceans of the world. Clonal aggregations of independent zooids (Fig. 1a) are found on invertebrate hosts, while colonies of interconnected zooids (Fig. 1b, c) grow on various substrata. Each zooid has the shape of a wine glass: a bowl-shaped calyx is supported by a slender, flexible stalk that attaches basally to the substratum. The calyx is ringed by a horseshoe of ciliated feeding tentacles and contains a U-shaped gut, a small ganglion, a pair of protonephridia and one or two pairs of gonads. The space enclosed by the tentacles forms an atrium, the deepest part of which serves as a brood chamber for developing embryos.

Kamptozoan zooids actively bend and twist. Their characteristic motion is reflected in the phylum's scientific name (Greek: *kamptestai* = to bend) and its common name, "nodding heads". Another name for the phylum, Entoprocta, is less appropriate because it suggests an affiliation with the Ectoprocta (Bryozoa) and it implies erroneously that the anus is completely enclosed by the tentacular ciliation. Kamptozoans bear only a superficial resemblance to bryozoans, with which they were once grouped. Developmentally, kamptozoans are spiralians but their phylogenetic relationships to other metazoans remain enigmatic.

About 150 species have been described worldwide but kamptozoan diversity probably exceeds 500 species (Nielsen 1989). While they are widespread and are quite abundant in some microhabitats, most of the world's kamptozoans are poorly characterized or not known at all, because most species are tiny and easily overlooked. Kamptozoans occur in all oceans, from the intertidal zone to several hundred metres depth. A few colonial species live in brackish water, and one in freshwater. Representatives of all three major families (Loxosomatidae, Pedicellinidae, Barentsiidae) have been found in every marine region that has been thoroughly surveyed. The fourth family (Loxokalypodidae) has been found only once, in the northeastern Pacific.

The main purpose of this review is to synthesize current knowledge about the Kamptozoa. The last general English-language description of this phylum was provided by Hyman (1951), and there have been many advances in our understanding since that time. In summarizing what is known about kamptozoans, I draw heavily on work by two recent pioneers in kamptozoology, P. Emschermann (e.g. Emschermann 1972, 1982) and C. Nielsen (e.g. Nielsen 1971, 1996; Nielsen and Jespersen 1997). A second objective of this review is to highlight the rich and unusual kamptozoan fauna of Australia and New Zealand.

History of study

Kamptozoans were first illustrated by Ellis (1756). Pallas (1774a, b) described the first species as *Brachionus cereus*, placing it in a genus of rotifers. The same species was placed in the new genus *Pedicellina* by Sars (1835), who considered it a naked bryozoan. Van Beneden (1845) contributed the first thorough monograph of kamptozoan morphology and reproduction. The genus *Urnatella* was described by Leidy (1851) and *Loxosoma* by Keferstein (1862). Allman (1856) pointed out the uniqueness of kamptozoan calyx and tentacle structure. Nitsche (1870) conceived of *Pedicellina*,

* Elkhorn Slough National Estuarine Research Reserve, Royal Oaks, CA 95076, U.S.A. E-mail: research@elkhornslough.org

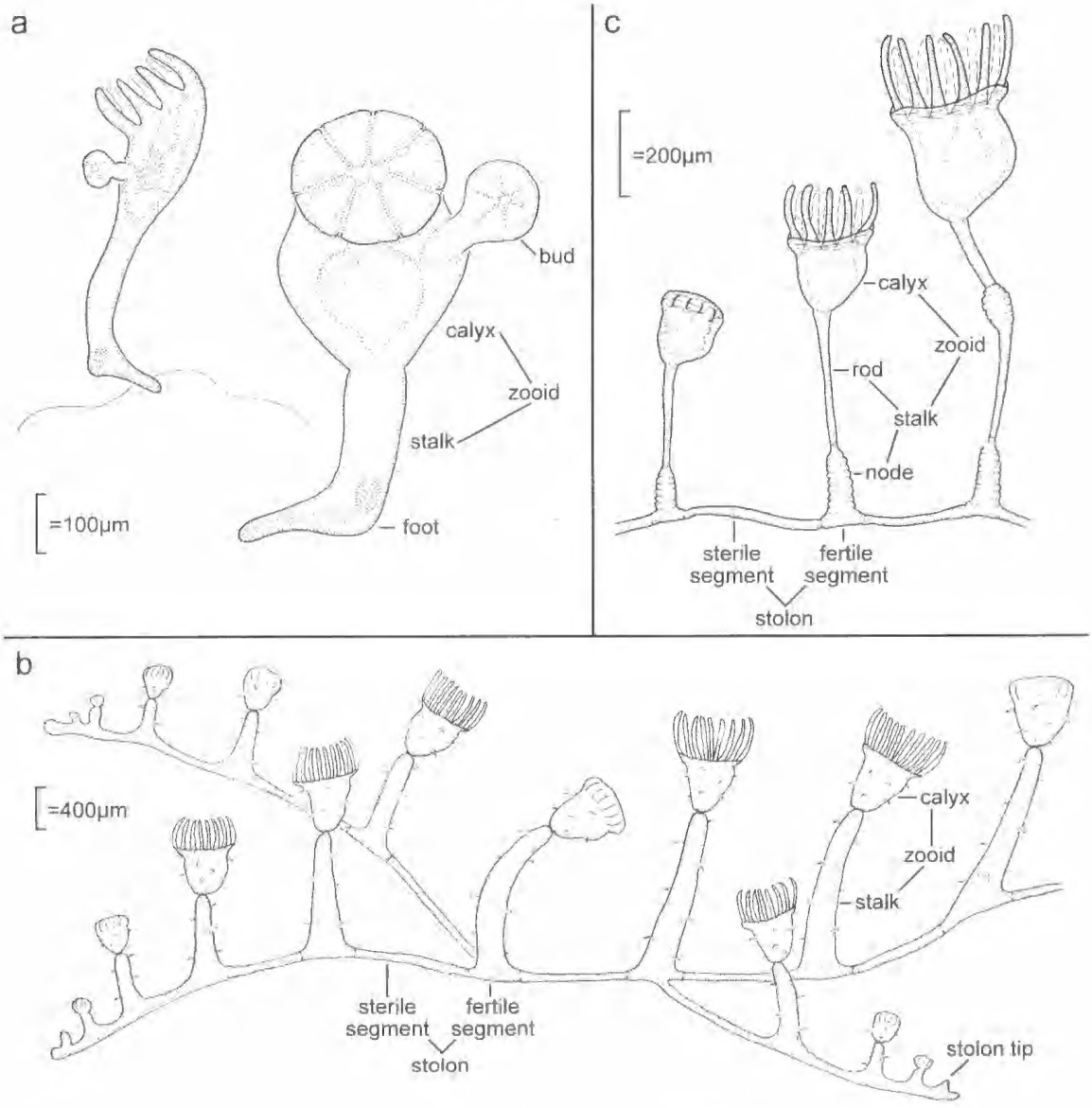

Fig. 1. Structure of kamptozoan zooids. (a). *Loxosomella* sp. 3 on sponge. (b). *Pedicellina whiteleggii*. (c). *Barentsia* sp. 1.

Urnatella and *Loxosoma* as a natural grouping, the Entoprocta, and separated them from all other bryozoans, the Ectoprocta. Hatschek (1888) first raised the entoprocts to the level of phylum. Clark (1921) proposed the name Calyssozoa to distinguish this phylum further from the bryozoans; Cori (1929) agreed with this intent, but changed the name to Kamptozoa, since the name Calyssozoa had already been applied to another taxon (the cnidarian Stauromedusae). Late in the 19th century, a number of prominent scientists investigated kamptozoans, emphasizing embryological and phylogenetic questions (e.g. Barrois 1877; Harmer 1885; Seeliger 1890). Since then, only a few researchers at any one time have focused on kamptozoans.

Morphology and physiology

External characteristics

Kamptozoan zooids are generally constructed of a stalk, basal attachment and calyx (Fig. 1). The height of individual zooids ranges among species from 0.3-30 mm. The stalk develops as an outgrowth of the calyx to form a flexible, roughly cylindrical support. Clonal forms (Family Loxosomatidae) have a specialized basal organ (either a muscular suction

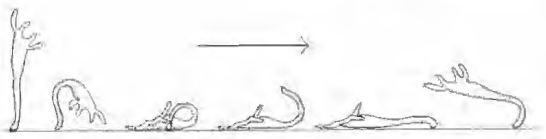

Fig. 2. Locomotion of *Loxosoma agile*. Modified from Nielsen (1966).

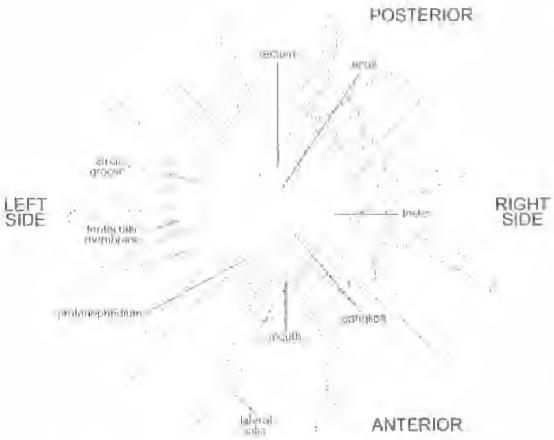

Fig. 3. Diagrammatic top view of a pedicellinid calyx.

disc or a differentiated "foot" with an associated gland (Fig. 1a)) with which they attach to invertebrate hosts. Beneath the stalks of most colonial forms (Families Pedicellinidae and Barentsiidae), stolons (Fig. 1b, c) adhere to various living and non-living substrata with cuticular adhesions. The cup-like calyces range in height from 0.2-1.2 mm and are ringed by a horseshoe of tentacles. The mouth and anus are at opposite sides of the calyx, regarded as anterior and posterior respectively (Figs 3, 4b). The calyx is bilaterally symmetrical; a vertical plane through mouth and anus divides the calyx into right and left mirror images (Fig. 3). The region above the stomach is ventral (this region was below the stomach in the larva); the bottom of the calyx and stalk are dorsal (Fig. 4b).

Body wall, musculature and support

The body wall is a single-layered epithelium, covered by a glycoprotein cuticle containing a trace (0.06-0.45%) of chitin (Jeuniaux 1982) but no collagen (Emschermann 1982). The cuticle is generally thickest on the stalk, which may be darkly pigmented, moderately thin and transparent on the calyx, where the internal anatomy can be readily

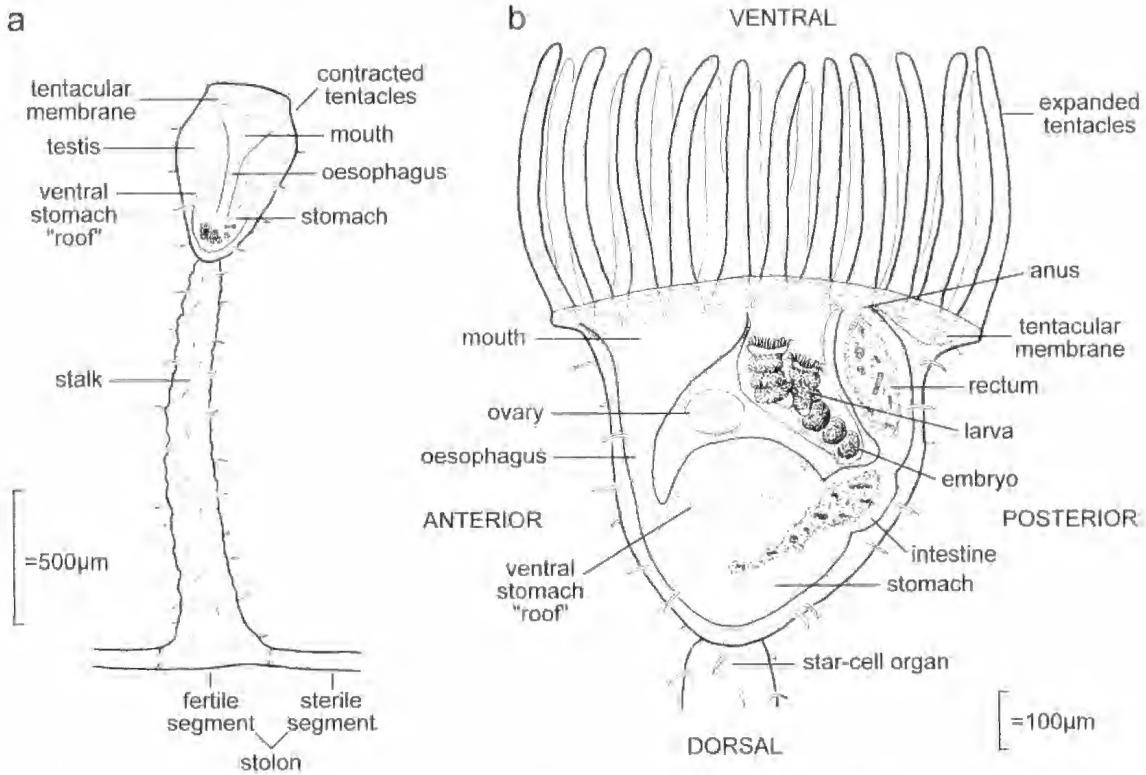

Fig. 4. Structure of a kamptozoan calyx. (a). Anterior view of contracted male *Pedicellina whiteleggii* zooid. (b). Side view of expanded female *P. whiteleggii* calyx.

observed through the body wall, and thinnest on the inner (frontal) side of the tentacles (Nielsen & Jespersen 1997).

Strong longitudinal muscle fibres beneath the stalk epithelium produce the characteristic bending motions of kamptozoan zooids. Circular muscles are limited to the tentacular membrane and sphincters between parts of the gut. The structure of muscle fibres has been described by Emschermann (1969b, 1982), Reger (1969) and Nielsen and Jespersen (1997). Kamptozoans lack a coelom. The cavity surrounding the calycal organs and extending into the tentacles and stalk is filled by a loose fluid matrix of mesenchyme cells which acts as a hydrostatic skeleton and, together with the cuticle, lends the stalk rigidity (Brien 1959).

Locomotion and movement

All kamptozoans have larvae that swim or creep by ciliary action. While larvae represent the main dispersal mode for most colonial, and perhaps many solitary species, some species are mobile at other stages in the life-cycle. In some loxosomatid species, newly released, asexually produced buds can swim with their stalk forward, propelled by their tentacular cilia; in a few loxosomatids, adults may also be capable of such swimming (Atkins 1932; Ryland & Austin 1966; Nielsen 1966). In loxosomatid species whose adults can attach repeatedly to the substratum, passive drifting of detached zooids may also serve for dispersal. Most colonial forms are sessile as adults, but in the freshwater species *Urnatella gracilis* Leidy 1851, short propagation stolons of two or three zooids often break from a larger colony, leading to rapid colonization of a favourable area by fragments of the same original colony which have spread by drifting (Emschermann 1987).

In some species in the genus *Loxosoma*, zooids employ their basal suction discs to somersault across the substratum (Assheton 1912; Nielsen 1964), "moving...in a manner fascinating and unique by a series of gymnastic efforts, which combine the agility of the kangaroo and the deliberation of a geometer caterpillar" (Assheton 1912). The zooid bends down until the calyx attaches by four long oral tentacles to the substratum; the suction disc then detaches from the substratum and flips over the calyx to reattach some distance from its original site; the zooid then returns to an upright orientation (Fig. 2).

While adult locomotion occurs in only some species, the non-locomotory bending motions of attached zooids are characteristic of all members of the phylum. Although the rapid and vigorous nodding of kamptozoans immediately catches the observer's eye, the mechanisms and stimuli involved have not been thoroughly examined. Bending of the stalk results from shortening of longitudinal muscles on one side (Brien 1959). A stronger bending response is obtained by stimulation of calyces than of stalks (Cori 1936). The nodding and writhing may help zooids escape predators, may diminish overgrowth by fouling organisms, or may prevent the calyces from repeatedly filtering the same water.

Finally, individual calyces have a characteristic response to disturbance. When irritated, the tentacles curl inwards and are enclosed by a delicate layer of tissue, the tentacular membrane (Figs 3, 4), which tightens like a draw-string purse by means of circular musculature. This infolding of the tentacles resembles the contraction of a sea anemone more than the retraction a bryozoan lophophore.

Feeding and digestive system

Kamptozoans are suspension feeders on phytoplankton and other particulate food. Each tentacle has five longitudinal rows of ciliated cells (Atkins 1932; Mariscal 1965; Nielsen & Rostgaard 1976). On the sides of each tentacle (Fig. 3), large lateral cells bear compound cilia that beat towards the tentacle's frontal midline (Nielsen & Rostgaard 1976); these cilia generate the feeding currents. Water is drawn between the tentacles from below the tentacular crown, then sent upward away from the calyx (Atkins 1932). The lateral cilia also capture particulate food from the water currents they create; kamptozoans employ a downstream collecting mechanism (Nielsen & Rostgaard 1976). Inside the rows of lateral cells, rows of narrow laterofrontal cells bear short cilia that presumably transfer food from lateral to frontal cilia (Mariscal 1965). The frontal midline of each tentacle has a single row of large frontal cells bearing short cilia and small mucus vesicles; these cilia beat with the effective stroke towards the base of the tentacle, and transport captured particles in a band of mucus to the base of the tentacles (Nielsen & Rostgaard 1976). Food particles then travel in ciliated gutters, the right and left atrial grooves (Fig. 3) to the mouth (Atkins 1932).

Some kamptozoans apparently trap ciliates and other organisms by rapidly contracting the tentacular crown (Atkins 1932). One Antarctic kamptozoan has special multicellular extrusive organs ("lime-twig glands") that discharge hollow, sticky threads, presumably to capture larger prey items that supplement its diet of suspended particles (Emschermann 1993b).

Kamptozoans have a U-shaped gut, with both the mouth and anus opening ventrally (Figs 3, 4b). The digestive tracts of larvae and adults are simple tubes of ciliated epithelium divided into four regions, and have been characterized by Beck (1938) and Nielsen and Jespersen (1997). The crescent-shaped mouth (Fig. 3) leads to a funnel-like buccal cavity, then to a

narrow oesophagus that opens into a voluminous stomach filling much of the calyx (Fig. 4b). Ingested particles are embedded in strands of mucus that are kept in constant rotation by cilia in the stomach; the gut lacks musculature except at sphincters between regions and food is transported entirely by ciliary action (Beeker 1938). The strands gradually consolidate into clumps as they pass towards the intestine. Digestive enzymes are secreted by glandular cells in the ventral "roof" of the stomach; absorption occurs both in this region of the stomach and in the intestine (Beeker 1938). The stomach leads to a short intestine, and then to the rectum, which projects above the floor of the atrium (Figs 3, 4b), such that faeces released into the tentacular water current are swept away from the calyx. When the tentacles are contracted, the rectum folds lid-like over the atrium.

Circulatory and respiratory systems

Since kamptozoan calyces are tiny, diffusion is a sufficient transport mechanism; no special organs facilitate circulation within the calyx. Loose mesenchyme surrounding the organs allows for the free circulation of dissolved gases and nutrients. Contrary to earlier indications (e.g. Hyman 1951), there are no free amoebocytes enhancing nutrient transport within the mesenchyme matrix (Emschermann 1969a). In loxosomatids, fluids also pass freely between the calyx and the stalk, helped on their way by muscular movements. In many colonial kamptozoans, diffusion may not suffice for circulation throughout the zooid because the stalk is often much longer than in loxosomatids and is partly separated from the calyx by a cuticular septum. Pedicellinids and barentsiids have a circulatory structure, the star-cell organ (Emschermann 1969a). A stack of flattened, stellate cells spans the narrow zone between the stalk and calyx (Fig. 4b). The topmost cell contracts and expands like a pipette-bulb; rhythmic pulsations of the stacked cells pump fluids between calyx and stalk (Emschermann 1969a).

Excretion

A pair of flame-bulb protonephridia, located just posterior of the oesophagus (Fig. 3), apparently functions mainly in ion regulation and osmoregulation (Emschermann 1982). Each protonephridium is composed of four multiciliated cells. Two of the cells form a terminal organ, with a filtration area where they interdigitate; the third and fourth cells encircle the nephridial lumen, and the fourth cell forms the nephridiopore (Franke 1993). In loxosomatid calyces, the two protonephridia open separately into the atrium, while in stolonates they open through a common nephridiopore (Franke 1993). The freshwater kamptozoan *Urnatella gracilis* has a more highly developed excretory system, with 30-40 protonephridia in the calyx, and many others in the stalk (Emschermann 1965).

Excretion of metabolites takes place in the ventral stomach "roof" (Fig. 4), a region that is often eye-catching because it is conspicuously coloured by the pigments of consumed phytoplankton. The large vacuoles of cells in this region contain precipitated uric acid and guanine as well as algal pigments (Beeker 1938; Emschermann 1965). These intracellular inclusions are eventually expelled into the stomach and voided.

Nervous system and sense organs

A large, dumbbell-shaped ganglion lies ventral to the stomach, just posterior to the protonephridia (Fig. 3). Nerves radiate from this subenteric ganglion to the tentacles, to other parts of the calyx, and to the stalk. Many kamptozoans have unicellular tactile receptors on the tentacles and on the surface of the calyx (Nielsen & Rostgaard 1976). In addition, loxosomatids often have a pair of lateral sense organs consisting of ciliated papillae on the right and left sides of the calyx. There are no nervous connections between zooids in a colony; earlier suggestions (Hilton 1923) of an interzooidal nervous system have been rejected (Emschermann 1982).

The larvae of many loxosomatids have a pair of eyes, each consisting of a cup-shaped pigment cell, a lens cell and a sensory cell. The structure of the eye is unusual in that light enters perpendicular to, rather than parallel to the long axes of the sensory cilia (Woollacott & Eakin 1973). No adult kamptozoans are known to have eyes but zooids of some species contract in response to sudden exposure to bright light (Emschermann 1982).

Reproduction and development

Asexual reproduction

All kamptozoans grow by budding. In loxosomatids, which live on other invertebrates, buds form in two anterior or anterolateral regions of the calyx, often roughly level with the top of the stomach (Figs 1a, 5a, b, 8a, b). Buds may be produced alternately or simultaneously at the two budding sites. The basal part of the bud's stalk develops an attachment organ. The bud may remain attached to its "parent" for some time, feeding and even becoming sexually mature, but it eventually breaks away, often attaching to a nearby spot on the invertebrate host.

Colonial kamptozoans also bud at the anterior face of zooids, but budding occurs earlier in the life of zooids than in loxosomatids (Brien 1959). The zooids producing buds are often themselves still tiny

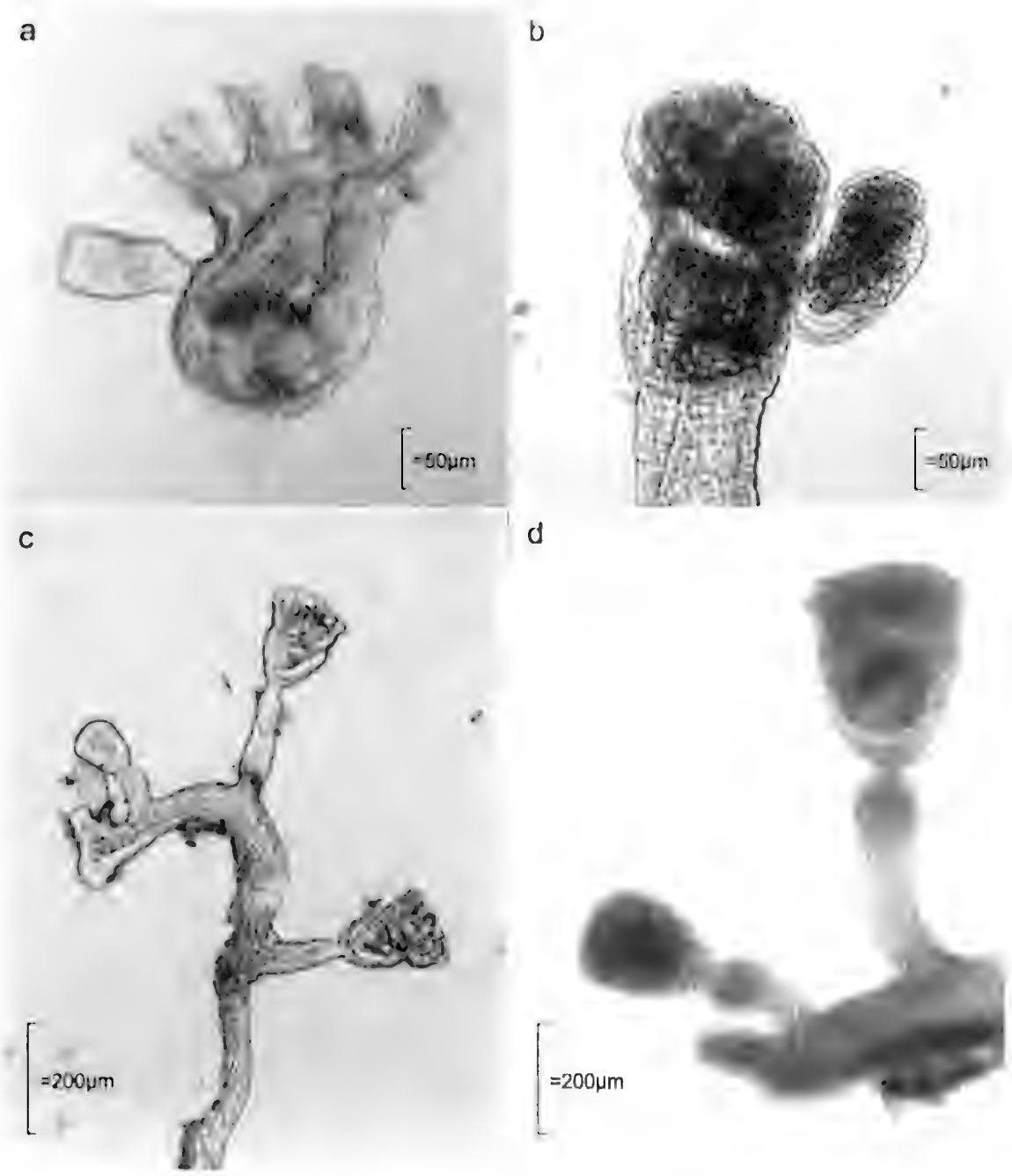

Fig. 5. Asexual reproduction. (a). Calycal budding in *Loxosomella* sp. 5. (b). Calycal budding in *Loxosoma* sp. 1. (c). Budding at the stolon tip in *Barentsia matsushimana*. (d). Budding at the stolon tip in *Pedicellina pyriformis*.

buds; each stolon tip is a bud primordium forming anterior to the next youngest bud (Figs 1b, 5c, d). As the buds grow and differentiate into fully formed zooids, they are separated by intercalating growth of the stolon. Eventually this growth ceases and a septum with a central opening forms on each side of the zooid, partitioning the stolon into fertile (zooid bearing) and sterile (without zooids) segments (Figs 1b, c, 4a). Because of this pattern of formation, the anterior side of every zooid along a stolon faces the growing stolon tip. Colony form can be more complex in some barentsiids, which bud from specialized stalk regions. In some species, resting buds (hibernacula) are formed at stolon tips. These

undifferentiated buds are enclosed in single or multiple chambers and are covered by a thick cuticle. They germinate only after the stolonic connection to the rest of the colony is severed, and following exposure to low temperatures (Toriumi 1951; Emschermann 1961, 1982).

Pedicellinids and barentsiids, unlike most loxosomatids, can regenerate calyces. Old calyces degenerate and are shed and are replaced by a budding process at the apical stalk tip comparable to that at stolon tips. Injured barentsiid zooids can regenerate new calyces and stalks even from basal stalk and stolon remnants (Hyman 1951; Brien 1959; Mukai & Makioka 1978).

Patterns of bud formation at the histological level are very similar in all kamptozoans (Seeliger 1889, 1890; Brien 1959). An epidermal proliferation of the anterior body wall of a zooid results in an evagination that forms the bud primordium. Budding is essentially an ectodermal process; while some mesenchyme cells migrate from the "parent" into the bud, no endoderm is contributed. At the apex of the bud primordium, an invagination forms, then constricts into an upper and lower vesicle, which become the atrium and the digestive tract, respectively. A narrow passage connecting the vesicles becomes the mouth, while the anus breaks through at a later stage. A constriction soon separates calyx and stalk and the latter elongates. Eventually the atrial cavity breaks through, freeing the tentacles, and the bud begins to feed.

Sexual reproduction

Most loxosomatid calyces are protandric, with a discrete male phase followed by a female phase (Nielsen 1971; Emschermann 1993a); calyx gonochorism has also been reported (Harmer 1915; Prenant & Bobin 1956). Barentsiid calyces are typically gonochoric (Wasson 1997). Some barentsiid colonies are gonochoric, too, containing calyces of only one sex; other barentsiid colonies are simultaneously hermaphroditic, with both male and female calyces formed along the same stolon (Mukai & Makioka 1980; Emschermann 1985; Wasson 1997). A very few barentsiid species have simultaneously hermaphroditic calyces (Johnston & Angel 1940; Wasson 1997). Some pedicellinids have gonochoric calyces in gonochoric colonies (Marcus 1939); others have gonochoric calyces in simultaneously hermaphroditic colonies (Dublin 1905); still others have simultaneously hermaphroditic calyces (Brien 1959; Emschermann 1985).

The reproductive system is rather simple in both sexes. Gonad rudiments derived from mesenchymal cells first appear above the stomach as a pair of tiny oval translucent vesicles (Mukai & Makioka 1980). These grow into large ovoid sacs, consisting of a one-layered epithelium which is the germinal layer from which the gametes arise (Brien 1959). In simultaneously hermaphroditic calyces, a pair of testes lies posterior to the pair of ovaries. Each gonad feeds into a gonoduct, and the right and left gonoducts merge at the ventral midline to open through a common gonopore posterior to the ganglion (Brien 1959).

The testes grow rapidly and may fill much of the calyx (Figs 3, 4a). The spermatozoa have elongate heads (Emschermann 1982; Franzen 1983b). Spawning has rarely been observed; apparently a cloud of sperm is released following a sudden contraction of the calyx (Dublin 1905).

All kamptozoans brood their embryos and release fully formed larvae. The ovaries remain much smaller than the testes (Fig. 4b), with only a few germinal cells at any one time differentiating into oocytes. The small (40–80 μm) but yolky eggs (Franzen 1983a) are fertilized in the ovary, then discharged into the deepest part of the atrium, the brood chamber (Cori 1936; Marcus 1939; Mukai & Makioka 1980). A glandular region of the oviduct secretes a pliant envelope, which encloses the embryo and extends into a cord which tethers it to the floor of the brood chamber (Marcus 1939; Brien 1959). The ovaries release one or a few eggs per day in alternation, the youngest embryos pushing the older ones farther from the gonopore (Brien 1959). The tethered embyros, like a varied bouquet of balloons, can occupy a substantial portion of their mother's calyx (Fig. 4b). The brood chamber contains many embryos in a regular succession of stages from cleaving eggs to contractile larvae. When larvae hatch out of their envelopes, they remain attached to the atrial wall by the cord, with their mouth and ciliary band upward, allowing them to feed on particles in their mother's current (Brien 1959; Mariscal 1965). Swimming larvae are released about a week after fertilization (Mukai & Makioka 1980).

Embryology and development

Kamptozoans show typical spiralian, determinate development (Barrois 1877; Hatschek 1877; Harmer 1885; Lebendinsky 1905; Marcus 1939; Malakhov 1990). Cleavage is spiral and the 4d cell is a mesentoblast cell that proliferates loose mesenchyme in the interior of the embryo, eventually giving rise to the muscles (Marcus 1939). The arrangement of cells at the animal pole resembles an annelidan rather than a molluscan cross (Marcus 1939). The larval mouth forms very near to the anterior margin of the blastopore, which eventually closes; the anus forms secondarily as well. There is never any hint of coelom formation (Marcus 1939).

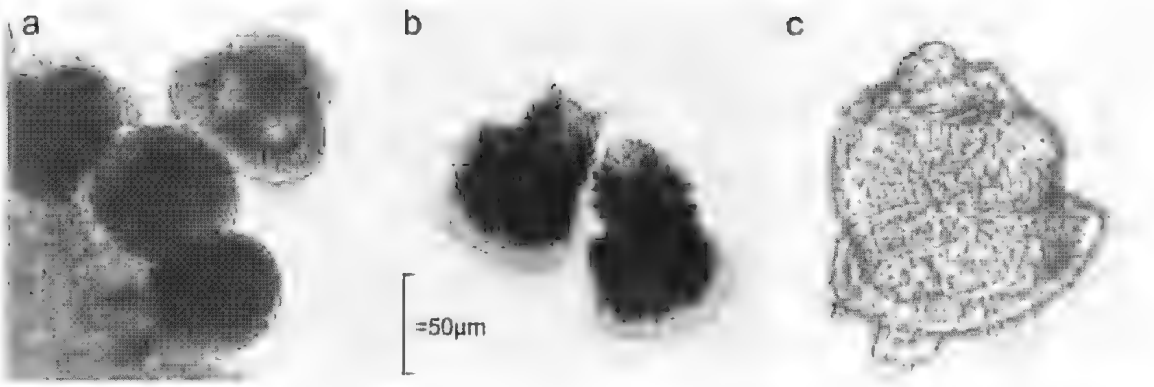

Fig. 6. Tholophores. (a). Embryos and larvae of *Loxosomella* sp. 1. (b). Larvae of *Pedicellina whiteleggii*. (c). Larva of *P. gracilis* var. *simplex*. All figures to same scale.

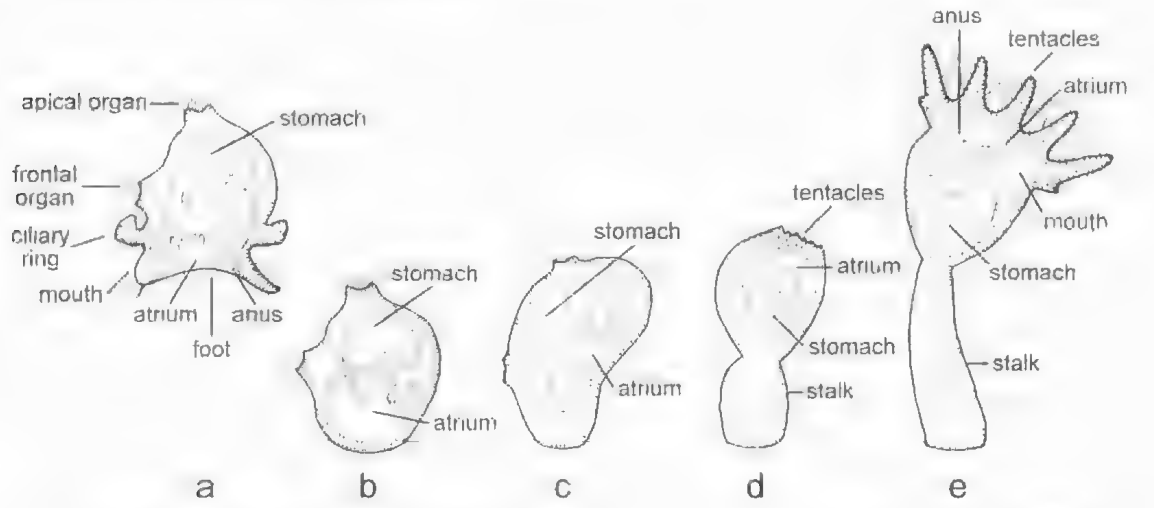

Fig. 7. Schematic representation of metamorphosis in *Pedicellina cernua*. (a). Swimming larva. (b). Newly settled larva. (c). Period of vigorous anterior growth. (d). Zooid with separation between stalk and calyx; tentacles forming. (e). Feeding zooid. Modified from Cori (1929).

Kamptozoan larvae are generally hat-shaped (Figs 6, 7a). Salvini-Plawen (1980) suggested the name tholophora (Greek: *tholos* - dome; *tholia* - straw hat) for them. There are a number of detailed descriptions of larvae (e.g. Barrois 1877; Cori 1929; Marcus 1939; Mariscal 1965; Nielsen 1971) from various regions of the world. The hyposphere of the larva is deeply indented into the prominent, hat-like episphere when the larva is swimming. The curve of the U-shaped gut is in the upper part of the hat; mouth and anus open on the ventral surface (Fig. 7a). There is an apical organ at the top of the hat, a frontal organ at the front of the hat, and a ring of long compound cilia around the brim, just above the mouth (Figs 6, 7a). Below (ventral to) the mouth, there is a second band of shorter compound cilia in the shape of a horseshoe, with the opening of the horseshoe at the anus; the band is also broken behind the mouth. These two ciliary bands beat in opposition and capture particles that are then transported to the mouth by short cilia in the atrial grooves, which run between the two bands of longer cilia from anus to mouth on both sides, as in the adults (Fig. 3). Often there is a ciliated creeping foot in the ventral area between mouth and anus (Fig. 7a). Some tholophores show unusual features (stalked vesicles, a spiderweb pattern of ornamentation, an adhering layer of detritus, etc.) that are not yet understood (Nielsen 1971).

Tholophores resemble the trochophores of some spiralians (Balfour 1885; Cori 1936; Nielsen 1971, 1995; Emschermann 1982). The downstream-collecting ciliary bands of tholophores are similar to those of trochophores in cell-lineage, structure, and function (Nielsen 1995). The apical organs of tholophores also resemble those of trochophores. But

unlike trochophores, most tholophores have a frontal organ and a ciliated foot, and their hyposphere is deeply indented into the episphere when the larva is swimming. A few loxosomatid larvae lack the frontal organ and foot and have a more pronounced hyposphere, thus more strongly resembling trochophores, but these forms are considered derived, not ancestral within the phylum (Nielsen 1971). The strongest resemblance of tholophores is to adult kamptozoan calyces; larva and adult share the same shape, structure of the digestive system, atrium with atrial grooves, and a very similar ciliary feeding mechanism.

Larvae from only a few Australian species are known. One *Loxosomella* larva (Fig. 6a) is elongate in the anterior-posterior axis, with adhering particles and a well-developed foot. The *Pedicellina whiteleggii* Johnston & Walker 1917 larva (Fig. 6b) is tall in the ventral-dorsal axis, covered with a remarkably dense layer of detritus, and lacks a foot (Wasson 1995). The *Barentsia gracilis* larva (Fig. 6c) is relatively big, occupying a large portion of the parental calyx. It is about as high as wide and is free of adherent particles.

Most tholophores appear capable of both swimming and creeping; it is not known to what extent the larval period of most species is pelagic or benthic. Most tholophores are feeding larvae with a functional gut. However, the larval period of many kamptozoans appears to be extremely short - hours to days (Nielsen 1971; Emschermann 1982, Wasson 1998) - so the larva's feeding while still in the brood chamber may be more important than feeding after release. On the other hand, some *Loxosoma* larvae are often caught in the plankton and are presumed to have a long pelagic phase (Jägersten 1964; Nielsen 1966).

Metamorphosis has been carefully described in a few kamptozoan species (Barrois 1877; Harmer 1887; Cori 1936; Marcus 1939; Nielsen 1971; Emschermann 1982). The larva creeps on the substratum, testing it with the frontal organ, before attaching by the region around the frontal organ, settling on the anterior side (loxosomatids) or by attaching by the foot region, settling on the circumference of the retracted ventral ciliary girdle (pedicellinids and barentsiids). The atrium becomes enclosed by a constriction of the episphere dorsal to the ciliary girdle (Fig. 7b). The atrium and digestive tract are rotated upwards as a result of rapid growth of the anterior region of the episphere (Fig. 7c). Next, a separation forms between calyx and stalk and the latter elongates (Fig. 7d). Ciliated tentacles form as ectodermal protuberances at the periphery of the atrium (Fig. 7d), roughly in the location of the degenerating larval ciliary bands. Finally, the atrium breaks open, releasing the tentacles, and feeding begins (Fig. 7e).

While in all colonial and many clonal species the larva does metamorphose directly into the adult, some loxosomatids have precocious budding in which the larva does not metamorphose, but instead dies as the buds it bears grow and are released (Harmer 1885; Jägersten 1964; Nielsen 1971). In effect, the larval bud, rather than the larva itself, is the route to adulthood in these species. In the most extreme cases, the larva is completely consumed by an internal bud that forms while the larva is still within its parent, and the larval gut is absent (Nielsen 1971). Some remarkable species display further heterochrony: the buds themselves already have buds in turn or even are sexually mature while still contained in the larva (Jägersten 1964).

Phylogeny

Fossil record

Kamptozoans fossilized by bioimmuration occur in upper Jurassic rocks in Great Britain (Todd & Taylor 1993) and northern France (J. Todd, pers. comm. 1995). The structure of zooids unambiguously identifies them as members of the extant genus *Barentsia*. These Mesozoic fossils set a minimum time for the divergence of what is probably the most derived family, suggesting that ancestral members of the phylum may date back much further.

Relationships with other invertebrate taxa

Historically, there have been several proponents of a close relationship between kamptozoans and bryozoans (e.g. Harmer 1885; Marcus 1939; Prenant & Bobin 1956; Nielsen 1971, 1995). Zooids of both taxa have a U-shaped gut and are ringed by ciliated tentacles. Budding and hibernacula occur in both taxa and neither has an endodermal contribution from "parent" to bud. In both groups, larval eyespots have sensory cilia oriented at right angles to the incoming light (Woollacott & Eakin 1973). However, many other workers reject a close evolutionary affiliation of kamptozoans with bryozoans (e.g. Allman 1856; Hatschek 1888; Cori 1936; Hyman 1951; Brien 1959; Jägersten 1972; Emschermann 1982). They attribute the similar body plans of adults to common suspension feeding habits and tiny body sizes. Budding and hibernacula are found in many sessile taxa and lack of endodermal contribution to buds is found in pterobranchs and some ascidians, as well as kamptozoans and bryozoans. The similarity of the larval eyes is striking but, since the eyes are constructed somewhat differently (Woollacott & Eakin 1973), they are not necessarily homologous.

Beyond ascribing similarities to convergence, opponents of a close relationship between

kamptozoans and bryozoans emphasize the differences between the two taxa. Kamptozoans have no coelom; bryozoans do, although it is rather unusual. Kamptozoans have protonephridia and gonads; bryozoans do not (Emschermann 1982). Kamptozoans retract their tentacles by curling them inwards and pulling the tentacular membrane around them; bryozoans retract the whole polypide and the lophophore shuts like an inverted umbrella (Brien 1960). Kamptozoans have downstream-collecting ciliary bands, while bryozoans have upstream-collecting ciliary bands (Nielsen & Rostgaard 1976; Nielsen 1995). A key component of the bryozoan body plan is the box-like cystid, absent in kamptozoans. There is little evidence of communication or nutrient flow between kamptozoan zooids, or of polymorphism among zooids; these features are characteristic of bryozoans (Brien 1960). Kamptozoan nervous systems are limited to single zooids, while bryozoans have colonial nervous systems linking zooids (Emschermann 1982). Kamptozoan metamorphosis usually involves retention of the larval gut and other larval structures; bryozoan metamorphosis is a "catastrophic" reorganization without retention of larval features (Brien 1959). A recent molecular analysis of complete 18S rRNA sequences (Mackey *et al.* 1996) provides further evidence against a close relationship between kamptozoans and bryozoans.

If kamptozoans are not closely related to bryozoans, with what group of animals are they allied? Based on embryology (Brien 1959; Nielsen 1971, 1995; Emschermann 1982) and molecular sequence data (Mackey *et al.* 1996), affinities must be sought among other spiralians. Some authors have been impressed by similarities between kamptozoans (especially loxosomatid larvae) and rotifers (Barrois 1877; Harmer 1885; Davenport 1893; Hyman 1951), or turbellarian flatworms (Salvini-Plawen 1980). Haszprunar (1996) proposes a sister group relationship between kamptozoans and molluscs, emphasizing similarities such as a chitinous cuticle, a circulatory system with sinuses, and a ventral, ciliary gliding sole (at some stage in the life-cycle) and a pedal gland. Alternatively, kamptozoans may be more closely allied with annelids (Emschermann 1982). Until further evidence resolves the question, the precise phylogenetic position of kamptozoans remains an enigma.

The similarity between adult kamptozoan calyces and tholophores has led to the proposition that the phylum originated by paedomorphosis. This hypothesis is developed in depth by Jägersten (1972), who envisages the original kamptozoan life-cycle as consisting of a planktotrophic trochophore larva and a benthic creeping adult with a ciliated foot. In this paedomorphic scenario, the original motile adult was eliminated but its ciliated foot was retained by the larva, which became sexually mature. This larva then gave rise to a secondary benthic adult, which retained the same ciliary feeding mechanism as the larva, although the ciliary bands eventually were drawn out on to tentacles. The new adult developed a stalk, an attachment organ, and the ability to bud. Haszprunar *et al.* (1995) recently presented a similar scenario of a paedomorphic origin for the phylum, but beginning with a lecithotrophic larva.

Key to the orders and families

1 (a) clonal: new zooids budded at calyx and then released; musculature continuous between stalk and calyx; star-cell organ absent; larva usually with paired frontal organ .....O. SOLITARIA, F. Loxosomatidae
(b) colonial: new zooids budded at base of older zooids or from stalks and remain connected to each other.....O. COLONIALES; 2

2 (a) zooids connected by non-septate basal plate; musculature continuous between stalk and calyx; star-cell organ absent; larva with paired frontal organ .....Sub.O. ASTOLONATA, F. Loxokalypodidae [known only from North-eastern Pacific]
(b) zooids connected by septate stolon or rarely (*Urnatella*) septate basal plate; musculature not continuous between stalk and calyx; star-cell organ present; larva with unpaired frontal organ .....Sub.O. STOLONATA; 3

3 (a) stalk of zooids with continuous longitudinal musculature, fairly wide throughout whole length, stalk and calyx often with cuticular spines .....F. Pedicellinidae
(b) stalk of zooids alternating between wide muscular nodes and narrow rigid rods; rods often with cuticular pores; stalk and calyx generally without cuticular spines .....F. Barentsiidae

Systematics and Australian diversity

Order Solitaria Emschermann, 1972
Family Loxosomatidae (Hincks, 1880)

The order Solitaria contains only a single family, the Loxosomatidae. Nevertheless, it is the largest natural grouping of kamptozoans, with about 100 of the 150 described species. Three loxosomatid genera are currently recognized (Nielsen 1996): *Loxosomella*, *Loxomespilon*, and *Loxosoma*, and are distinguished primarily by their basal attachment structures. About 20 species of loxosomatids have been reported from Australia and New Zealand but only seven of them are described (Appendix). Many more species certainly remain to be discovered; until

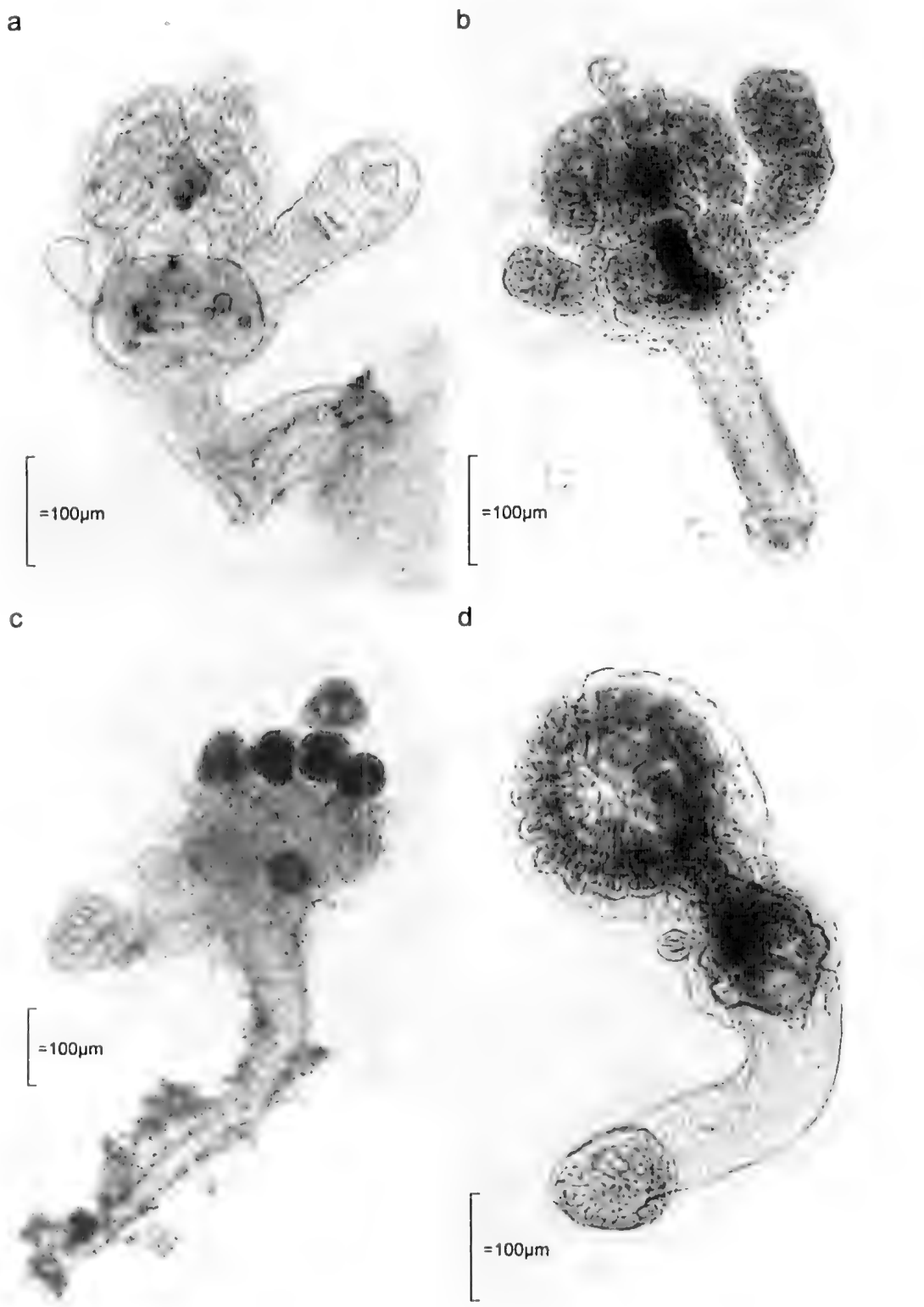

Fig. 8. Loxosomatid diversity. (a). *Loxosomella* sp. 3 showing foot. (b). *Loxosomella velatum*. (c). *Loxosomella* sp. 1 with larvae at top of calyx. (d). *Loxosoma* sp. 2 showing basal muscular disc.

more thorough surveys are undertaken, it is impossible to assess the true diversity Australia's loxosomatids.

Loxosomatids, which form clonal aggregations by calycal budding, are considered the most plesiomorphic group of kamptozoans (Emschermann 1972). The highly contractile zooids are often very small (less than 1 mm high). Calyx and stalk are not sharply separated and longitudinal musculature is continuous between them. The calyx and tentacles are generally oriented obliquely to the stalk (Figs 1a, 8). The calyces are often compressed in the anterior-posterior axis, sometimes so strongly that the zooids resemble paddles.

In *Loxosomella*, the basal part of the stalk of buds is differentiated into a structure resembling a human foot (Figs 1a, 8a). The heel of the foot is anterior and contains a conspicuous gland. A groove lined by accessory gland cells runs from the heel to the posterior toe, where it opens. When a bud is released from its "parent", it attaches to the substratum by its toe. In some species the zooid retains the glandular foot for its entire existence and is able to detach and reattach repeatedly over its lifetime. In other species, the foot of the bud degenerates after attachment and the adult becomes permanently cemented to the substratum (Figs 8b, c). Zooids of the monotypic genus *Loxomespilon* have a very reduced stalk and foot but otherwise resemble *Loxosomella* zooids (Bobin & Prenant 1953; Nielsen 1996). Seven described and eight undescribed species of *Loxosomella* are known from Australia and New Zealand, and most of the species in the Appendix whose basal attachment structures could not be assessed (and so are listed merely as "Loxosomatid sp.") probably belong to *Loxosomella* as well.

In *Loxosoma*, each zooid is attached by a muscular suction disc at the base of the stalk (Fig. 8d); additional suction discs may occur posteriorly and/or at the base of the tentacles (Nielsen 1996). Zooids retain the ability to detach and reattach, sometimes moving actively across the substratum (Fig. 2). All known *Loxosoma* larvae have stalked vesicles on the episphere and undergo budding rather than a normal metamorphosis (Nielsen 1996). Only three (undescribed) *Loxosoma* species are known from Australia and New Zealand.

Most loxosomatids dwell on other invertebrates. In Australia and New Zealand they have been reported from various sponges, a sipunculan, various polychaetes, two hirudineans, a squat lobster, two prawns, and various bryozoans (Appendix). As more potential hosts in this region are examined for the presence of loxosomatid symbionts, this list will certainly grow. Each loxosomatid species appears to have either a single host species or a limited set of potential host species. Larvae, and possibly also buds and motile adults, can colonize new hosts; it is not known whether propagule preference or differential mortality on different host species is responsible for the later distribution of adults. Association with other invertebrates has clear benefits for the loxosomatid. The zooids are often located in the pathway of the host's feeding or respiratory water currents, which they may use for their own ciliary feeding (Nielsen 1964). The host probably offers the fragile zooids protection from predation or other damage. Whether the presence of loxosomatids negatively affects their hosts is not known; Williams (2000) has shown that host epidermis may be modified by loxosomatid symbionts.

Worldwide, many loxosomatid species (about 50%) live on polychaetes; they are found on or between the parapodia, on the gills, on the setae, or under the elytra of members of ten polychaete families (Nielsen 1989). *Loxosomella diopatricola* Williams 2000 and seven undescribed species of loxosomatids are known from polychaetes in Australia and New Zealand (Figs 5a, b, 8d; Appendix).

While loxosomatid species diversity is highest on polychaetes, loxosomatid density is probably highest on sponges. Loxosomatids may form strikingly dense aggregations on sponges — sometimes 100,000 zooids on a fist-sized sponge (Rützler 1968). Some of these sponge-dwelling forms are unusually darkly pigmented, and an aggregation against the background of a brightly coloured sponge can be eye-catching. Two undescribed species of *Loxosomella* are known from sponges in Australia and New Zealand (Figs 1a, 8a).

Six loxosomatid species in Australia (*Loxosomella breve*, *L. circulare*, *L. cirriferum*, *L. pusillum*, *L. velamen* (all Harmer 1915), *L.* sp. 1) grow on bryozoans (Appendix). Most of these species are ornamented by odd cirriform organs or papillae (Fig. 8b, c), and share other similarities that suggest they comprise a clade; both the ecology and the taxonomy of bryozoan-dwelling species merit further attention. Some bryozoan-dwelling loxosomatids, originally described by Harmer (1915) from *Siboga* expedition material, live in very close association with their hosts. One minisente loxosomatid species even lives in the compensation sac of its host: almost every compensation sac in an infested bryozoan colony contains a loxosomatid zooid (Harmer 1915).

Order Coloniales Emschermann, 1972

Sub-Order Stolonata Emschermann, 1972

The sub-order Stolonata is the other large natural grouping of kamptozoans and exhibits the second basic body plan within the phylum. The calyces of stolonates are generally larger than those of loxosomatids, with stronger ciliary currents that

apparently free the zooids from dependence on hosts' ciliary currents (Emschermann 1972). Stolonate calyces are generally laterally compressed (Fig. 4a v. 4b; Fig. 10a v. 10b) and musculature is reduced, often to just a few longitudinal strands, the atrial retractor muscles, which extend from the base of the calyx to the atrium and serve to depress it (Emschermann 1972). Calyx and stalk are separated by a cuticular diaphragm and the calyx-stalk junction is spanned by the circulatory star-cell organ (Emschermann 1969a); the longitudinal musculature of the stalk is not continuous with that of the calyx. The stalk often bears cuticular pores or spines which vary in size and density with environmental conditions. Stolonate zooids, as their name implies, grow on cylindrical stolons that are usually divided into fertile (zooid-bearing) and sterile (no zooids) segments by transverse septa (Figs 1b, c, 4a). The septa may function to space the zooids, thus avoiding interference in feeding, or may prevent damage by sealing off intact sections from harmed ones.

Stolonate kamptozoans are members of the sessile benthic community and often grow together with hydroids and bryozoans. They are preyed upon by nudibranch molluses, some of which appear to specialize on barentsiid species (MacDonald & Nybakken 1978); predation by turbellarian flatworms has also been observed (Canning & Carlton 2000). Although seldom conspicuous, stolonate kamptozoans are often fairly abundant. I have found stolonates intertidally at every site surveyed in Australia and New Zealand by collecting various substrata (mostly sponges, ascidians, bryozoans, worm tubes and bivalve shells) in the field and examining them in the laboratory. In some localities, an astounding 50%–75% of all substrata searched were infested with stolonate kamptozoans, although the level was usually about 5–10% at other sites.

Family Pedicellinidae (Johnston, 1847)

The family Pedicellinidae is considered more plesiomorphic than the Barentsiidae (Emschermann 1972): pedicellinid zooids retain a fairly simple zooidal structure, with undifferentiated stalks that have continuous musculature. Five genera are recognized but four of these (*Chitaspis*, *Loxosomatoides*, *Myosoma*, *Sangavella*) contain only one or two species, and have not been reported from Australia or New Zealand. The larger genus *Pedicellina* comprises about twelve species worldwide, six of which are known from Australia and New Zealand (Appendix).

In colder waters of this region, *P. whiteleggii* Johnston & Walker 1917 (Figs 1b, 4a, b, 9c) is ubiquitous and can be collected readily from coastal habitats (Wasson 1995). This species is recognized by its spination, by the distinctive, glistening, double rows of large cells on the tentacles, and by its tall, particle-covered larva (Fig. 6b). In warmer waters, *P. whiteleggii* is replaced by another abundant species, *P. compacta* Harmer 1915 (Fig. 9a), which is characterized by short, squat zooids ornamented with filiform spines (Wasson 1995).

A rarer pedicellinid from Otago, New Zealand, and Tasmania is *Pedicellina pyriformis* Ryland 1965 (Fig. 9b). The stalks grow up to 6 mm high, and calyces can be almost 1 mm high; this species is a giant among the world's pedicellinids. Zooids are also more densely clustered in this species than in other pedicellinids. The wide stolons lack septa; the absence of intervening sterile segments allows zooids to grow very close together along the stolon.

Family Barentsiidae Emschermann, 1972

This family is characterized by the division of the stalk into wide, flexible, muscular nodes and narrow, rigid, non-muscular rods that are often perforated by pores (Figs 1c, 10c, 11c). An incomplete cuticular septum separates each node from the rod above it. There is a minimum of one basal node and one rod apical to it, but many species have multiple alternating nodes and rods, lending a segmented appearance to the stalk.

Five genera of barentsiids are recognized. *Corella*, *Pseudopedicellina*, *Pedicellinopsis* and *Urnatella* (the sole freshwater form) each contain a single species; most of the roughly thirty known barentsiid species belong to the genus *Barentsia*. Seven barentsiid species are known from Australia and New Zealand (Appendix), six in the genus *Barentsia* and one in the genus *Pedicellinopsis*. The common species of colder waters, *Barentsia* sp. 1 (Figs 1c, 10a, b), is characterized by small, delicate zooids only about 1 mm high, usually with 1–3 series of stalk nodes and rods. In warmer waters, *B.* sp. 1 is supplemented by *B. geniculata* Harmer 1915 (Fig. 10c) which has many (average 4–5) series of stalk nodes and rods. In its segmented stalk structure, *B. geniculata* resembles the cosmopolitan species *B. benedeni* (Foettinger 1887) (found in Australian harbours), from which it can be distinguished by its wider, shorter nodes and by the less pronounced anterior orientation of the calyx.

Pedicellinopsis frutescens Hincks 1884 (Fig. 11) is a remarkable barentsiid apparently endemic to southern Australian waters (Appendix). Zooids spiral around a hard central stem (Fig. 11a), from which each zooid is separated by a septum. Each stem resembles a tree-fern, with the newest zooids at the apical growing tip; older regions of the stem where zooids have degenerated have spiral patterns of zooid scars as do lower regions of tree-fern trunks. The thick, rigid stems branch, forming bushy

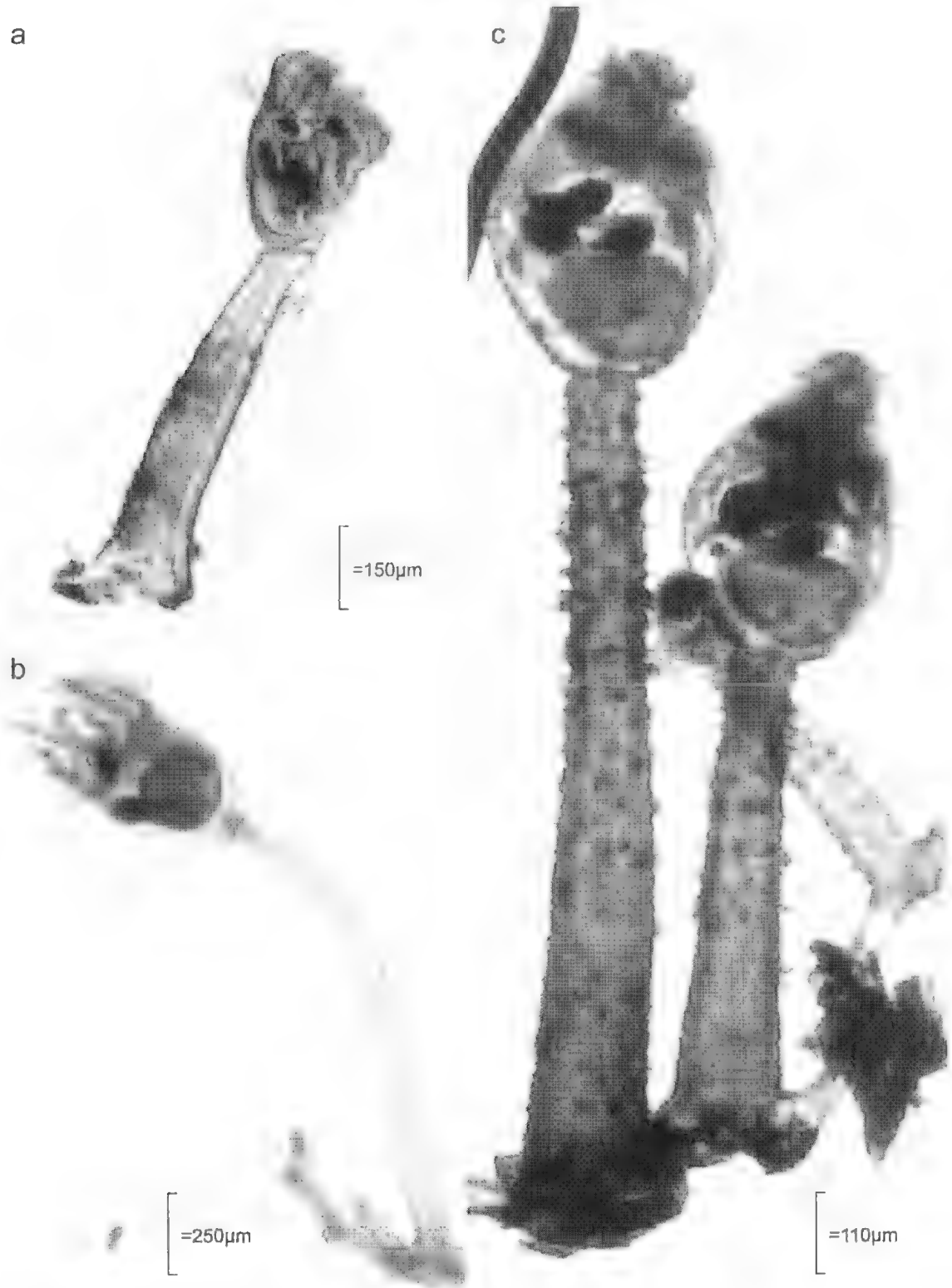

Fig. 9. Pedicellinid diversity. (a). *Pedicellina compacta*. (b). *P. pyriformis*. (c). *P. whiteleggii*.

Fig. 10. Barentsiid diversity. (a), and (b). *Barentsia* sp. 1 in side and anterior view, respectively. (c). *B. geniculata*.

colonies that may reach 30 cm across, far and away the record for a kamptozoan. They are anchored to the substratum by a lush basal growth of free stolons, which extend downwards to serve as rhizoids and secondarily back up the stem, becoming intertwined with it. Individual zooids, although unsegmented, grow to a length of 6 mm. The nodes are large and annulate (Fig. 11c). The rods are a deep golden brown due to a very thick cuticle and make a striking contrast to the pale calyces and nodes. The rods are decorated with alternating rows of bubble-like pores and pairs of lateral cuticular ridges (Fig. 11b, c), a pattern of stalk ornamentation not known from any other barentsiid. A large cuticular spine extends up past the stalk-calyx junction on the aboral side of the zooid (Fig. 11b). With its long list of unique features, *Pedicellinopsis fruticosa* may be the most highly derived member of the phylum Kamptozoa. It has yet to be observed alive.

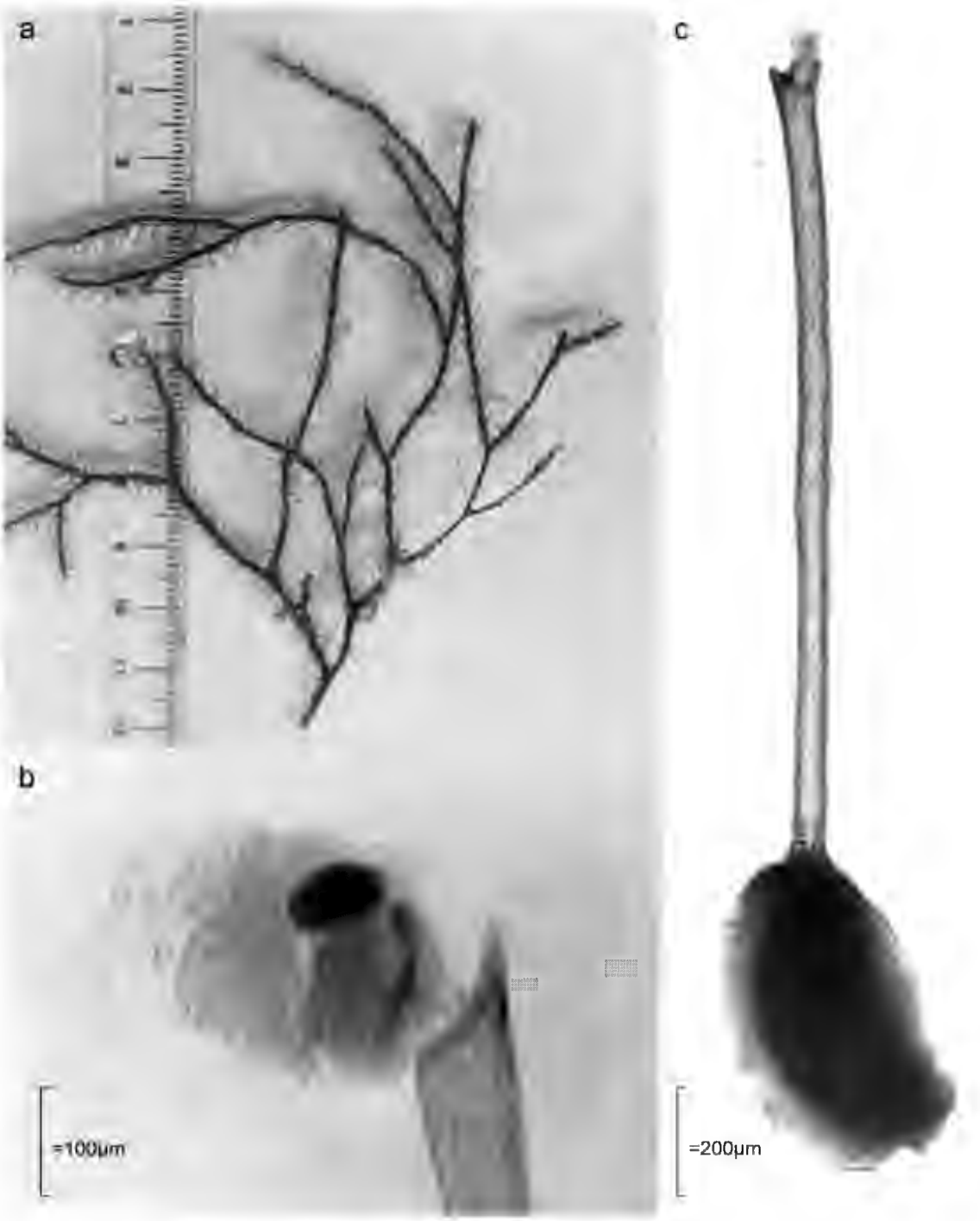

Fig. 11. The barentsiid *Pedicellinopsis fruticosa*. (a). Colony, showing zooids spiraling off of thick main stem. (b). Calyx and posterior spine. (c) Stalk, showing large annulate node and regularly ornamented rod.

Perspectives on the Australian fauna

Reports of kamptozoans from Australian waters are scarce, and currently only about 37 species of kamptozoans are known from Australia and New Zealand (Appendix). However, the Australian kamptozoan fauna is unusually varied, encompassing extremes of the body plan. The world's largest kamptozoan, *Pedicellinopsis*

frutticosa, dwells in these waters, as do some of the world's smallest kamptozoans, tiny *Loxosomella* species on bryozoan hosts. Australian species may also hold the record for the greatest density of zooids in colonies: *Pedicellina pyriformis* packs in one giant zooid after another along its peculiar non-septate stolon, while in *Pedicellinopsis fruticosa*, zooids spiral around a rigid central stem resulting in a density of zooids and a growth pattern unknown in other kamptozoans.

Kamptozoans in Australia are neither rare nor hard to find. The fauna of Australia is so poorly characterized that new and unreported species (as well as those listed in the Appendix) probably can be collected in only a few hours anywhere along the coast. Beyond taxonomic identity, we know virtually nothing about the biology of Australian species. The little we do know leads us to suspect that further investigations hold much promise for new insights into kamptozoan ecology, symbiotic relationships, larval biology, biogeography and phylogeny. Certainly, given the geographical dimensions and ecological diversity of this country, many new morphological adaptations and life history variations are likely to be revealed when the Australian kamptozoan fauna is more thoroughly examined.

Acknowledgments

I am deeply grateful to P. Arnold, E. & M. Barker, P. Berents, D. Gordon, K. L. Gowlett-Holmes, S. O'Shea, S. Shepherd, and W. Zeidler for their hospitality and for their assistance in accessing museum collections and carrying out fieldwork in Australia and New Zealand. Environment Australia generously funded my fieldwork and, through the Australian Biological Resources Study (ABRS), commissioned this review as a part of the *Fauna of Australia*, which series was closed prior to publication of this chapter. I am indebted to A. T. Newberry, C. Nielsen, J. Pearse, and D. Potts for their thoughtful comments that greatly improved the content, and to A. T. Newberry in particular for invaluable guidance with the writing. Finally, many thanks to a team of delightfully supportive editors: from ABRS, C. Glasby for initiating this project, and G. Ross and A. Wells for tending to its development; and, from the Royal Society of South Australia, J. Bird for bringing it to fruition. The figures are published with the kind permission of ABRS.

References

ALLMAN, G. J. (1856) "Monograph of the Freshwater Polyzoa" (Ray Society, London)

ASSHETON, R. (1912) *Loxosoma loxalina* and *Loxosoma valians* – two new species. *Quart. J. Microsc. Sci.* **58**, 117-143

ATKINS, D. (1932) The ciliary feeding mechanism of the entoproct Polyzoa, and a comparison with that of the ectoproct Polyzoa. *Ibid.* **75**, 393-423

BALFOUR, F. M. (1885) "Comparative Embryology", Vol. 1 (Macmillan, London)

BARROIS, J. (1877) Mémoire sur l'embryologie des Bryozoaires. *Theses presentées à la Faculté des Sciences de Paris* **396**, 1-298.

BECKER, G. (1958) Untersuchungen über den Darm und die Verdauung von Kamptozoen, Bryozoen und Phoroniden. *Z. Morph. Ökol. Tiere* **33**, 72-127.

BOBIN, G. & PRENANT, M. (1953) Deux Loxosomes nouveaux de Roscoff. *Arch. Zool. Exp. Gen.* **91**, 25-33

BRIEN, P. (1959) Classe des Endoproctes ou Kamptozoaires pp. 927-1080 *In* Grassé, P. (Ed.) "Traité de Zoologie" Vol. 5 (Masson, Paris).

_____ (1960) Le bourgeonnement et la phylogenèse des Endoproctes et des Ectoproctes. Reflexions sur les processus de l'évolution animale. *Bull. Cl. Sci. Acad. Roy. Belg.* (5th Ser.) **46**, 748-766.

BUSK, G. (1886) Report on the Polyzoa collected by H.M.S. Challenger during the years 1873-1876. Part II. The Cyclostomata, Ctenostomata, and Pedicellinea. *Rep. Sci. Res. Voy. H.M.S. Challenger (Zool.)* **17**, 1-47

CARMINO, M. H. & CARLOS, J. L. (2000) Predation on kamptozoans (Entoprocta). *Invert. Biol.* **119**, 386-387

CLAPAREDE, E. (1867) Miscellanées zoologiques. V. Sur le *Loxosoma kefersteinii* n. sp., Bryozoaire mou du golfe de Naples. *Ann. Sci. Nat.* 5th Ser. (Zool.) **8**, 28-30.

CLARK, A. H. (1921) A new classification of animals. *Bull. Inst. Oceanogr.* (Monaco) **400**, 1-24.

CORI, C. J. (1929) Kamptozoa pp. 1-64 *In* Kükenthal, W. & Krumbach, T. (Eds) "Handbuch der Zoologie" Vol. 2 (W. de Gruyter, Berlin).

_____ (1936) Kamptozoa pp. 1-119 *In* Bronn, H.G. (Ed.) "Klassen und Ordnungen des Tierreichs" Vol. 4, Pt. 2, Book 4 (Akademische Verlagsgesellschaft, Leipzig)

DAVENPORT, C. B. (1893) On *Urnatella gracilis*. *Bull. Mus. Comp. zool.* (Harvard Univ.) **24**, 1-44

DOBLIN, L. J. (1905) The history of the germ cells in *Pedicellina americana*. *Ann. N. Y. Acad. Sci.* **16**, 1-64.

ELLIS, J. (1756) "Essay towards a natural history of the corallines" (Millar, London)

EMSCHERMANN, P. (1961) Über Brutkörper bei dem Kamptozoon *Barentsia gracilis* Sars. *Zool. Jahrb.* (Physiol.) **69**, 333-338.

_____ (1965) Das Protonephridiensystem von *Urnatella gracilis* Leidy (Kamptozoa). *Zeit. Morphol. Ökol. Tiere* **55**, 859-914

_____ (1969a) Ein Kreislauforgan bei Kamptozoen. *Zeit. Zellforsch.* **97**, 576-607

_____ (1969b) Spiralig angeordnete Untereinheiten in den A-Filamenten der Kamptozoenmuskulatur. *Experientia* **25**, 975-976.

_____ (1972) *Loxokalypus socialis* gen. et sp. nov. (Kamptozoa, Loxokalypodidae fam. nov.), ein neuer Kamptozoentyp aus dem nördlichen Pazifischen Ozean. Ein Vorschlag zur Neufassung der Kamptozoen systematik. *Mar. Biol.* **12**, 237-254.

_____ (1982) Les kamptozoaires. Etat actuel de nos connaissances sur leur anatomie, leur developpement, leur biologie et leur position phylogenetique. *Bull. Soc. Zool. Fr.* **107**, 317-344.

_____ (1985) Factors inducing sexual maturation and influencing the sex determination of *Barentsia discreta* Bush (Entoprocta, Barentsiidae) pp. 101-108 *In* Nielsen, C. and Tarwood, G.P. (Eds) "Bryozoa: Ordovician to Recent" (Olsen & Olsen, Fredensborg, Denmark).

_____ (1987) Creeping propagation stolons - an effective propagation system of the freshwater entoproct *Urnatella gracilis* Leidy (Barentsiidae) *Arch. Hydrobiol.* **108**, 439-448.

_____ (1993a) On Antarctic Entoprocta: nematocyst-like organs in a loxosomatid, adaptive developmental strategies, host specificity, and bipolar occurrence of species. *Biol. Bull.* **184**, 153-185.

_____ & _____ (1993b) Lime-twig glands: a unique invention of an Antarctic entoproct. *Ibid.* **185**, 97-108.

Ermak, M. (1993) Ultrastructure of the protonephridia in *Loxosomella fauveli*, *Barentsia matsushimana* and *Pedicellina cernua*. Implications for the protonephridia in the ground pattern of the Entoprocta (Kamptozoa). *Microf. Mar.* **8**, 7-38.

Franzen, Å. (1983a) Bryozoa Entoprocta pp. 561-569 *In* Adiyodi K.G. & Adiyodi R.G. (Eds) "Reproductive Biology of Invertebrates" Vol. 1 (Wiley & Sons, New York).

_____ (1983b) Bryozoa Entoprocta pp. 505-517 *In* Adiyodi K.G. & Adiyodi R.G. (Eds) "Reproductive Biology of Invertebrates" Vol. 2 (Wiley & Sons, New York).

Goddard, E. T. (1909) Contribution to our knowledge of Australian Hirudinea. Pt 4, *Proc. Linn. Soc. N. S. W.* **34**, 721-732.

Gordon, D. P. (1972) Biological relationships in an intertidal bryozoan population. *J. Nat. Hist.* **6**, 503-514.

_____ & Ballantine, W. J. (1977) Cape Rodney to Okakari Point Marine Reserve: review of knowledge and bibliography to 1976. *Tane (J. Auckland Univ. Field Club)* **22** (suppl.), 1-146.

Harmer, S. F. (1885) On the structure and development of *Loxosoma*. *Quart. J. Microsc. Sci.* **25**, 261-337.

_____ (1887) On the life-history of *Pedicellina*. *Ibid.* **27**, 239-263.

_____ (1915) The Polyzoa of the Siboga Expedition. Pt 1. Entoprocta, Ctenostomata and Cyclostomata. *Siboga. Exp. Rep.* **28 A**, 1-180.

Hastings, A. (1932) The Polyzoa. *Gt. Barr. Reef Exp. 1928-1929 Sci. Rep.* **4**, 399-455.

Haswell, W. A. (1891) Observations on the Chloraemidae, with special reference to certain Australian forms. *Proc. Linn. Soc. N. S. W.* **22**, 329-356.

Haszprunar, G. (1996) The Mollusca: coelomate turbellarians or mesenchymate annelids? pp. 1-28 *In* Taylor, J.D. (Ed.) "Origin and Evolutionary Radiation of the Mollusca" (Oxford University Press, London).

_____, Salvini-Plawen, L. v. & Rieger, R. M. (1995) Larval planktotrophy - a primitive trait in the bilateria? *Acta Zool.* **76**, 141-154.

Haszprunar, H. (1877) Embryonalentwicklung und Knospung der *Pedicellina echinata*. *Zeit. Wiss. Zool.* **29**, 502-549.

_____ (1888) "Lehrbuch der Zoologie" (G. Fischer, Jena).

Hedley, C. (1915) An ecological sketch of the Sydney Beaches (Presidential address). *J. Proc. Roy. Soc. N. S. W.* **49**, 15-77.

Hutton, F. W. (1898) On the occurrence of *Pedicellina* in New Zealand. *Trans. Proc. N. Z. Inst. (N. S.)* **31**, 30, 218.

Hyman, W. A. (1925) A study of the movements of entoproctan bryozoans. *Trans. Amer. Microsc. Soc.* **42**, 135-141.

Hyman, L. (1880) "A history of the British marine Polyzoa" (Van Voorst, London).

_____ (1884) Contributions towards a general history of the marine Polyzoa. *Ann. Mag. Nat. Hist.* (Ser. 5) **13**, 356-369.

Hyman, L. H. (1951) "The Invertebrates" Vol. 3 (McGraw-Hill, New York).

Jägersten, G. (1964) On the morphology and reproduction of entoproct larvae. *Zool. Bid. Upp.* **36**, 295-314.

_____ (1972) "Evolution of the Metazoan Life Cycle" (Academic Press, New York).

Jeuniaux, C. (1982) Composition chimique comparée des formations squelettiques chez les lophophoriens et les endoproctes. *Bull. Soc. Zool. Fr.* **107**, 233-249.

Johnston, G. (1847) "A history of British zoophytes" 2nd ed. (Van Voorst, London).

Johnston, T. H. & Walker, M. J. (1917) A new species of *Pedicellina* from Sydney Harbour. *Proc. R. Soc. Qld* **29**, 61-65.

_____ & Angel, L. M. (1940) Endoprocta. *B.A.N.Z. Antarc. Res. Exp. 1929-1931 Rep. (Ser. B; Zool. & Bot.)* **4**, 219-231.

Kefferstein, W. (1862) Über *Loxosoma simulans* gen. et sp. n., den Schmarotzer einer Annelide. Untersuchungen über niedere Seethiere. *Zeit. Wiss. Zool.* **12**, 131-132.

Kirkpatrick, R. (1890a) Reports on the zoological collections made in Torres Straits by Professor A.C. Haddon, 1888-1889, Hydroida and Polyzoa. *Sci. Proc. Roy. Dubl. Soc.* **6**, 603-626.

_____ (1890b) Polyzoa from Port Phillip. *Ann. Mag. Nat. Hist.* **6**, 12-21.

Lidbansky, I. (1905) Die Embryonalentwicklung der *Pedicellina echinata* Sars. *Biol. Zent.* **25**, 536-548.

Leidy, J. (1851) On some American Polyzoa. *Proc. Acad. Nat. Sci. Phil.* **5**, 320-322.

McDonald, G. R. & Nybakken, J. W. (1978) Additional notes on the food of some California nudibranchs with a summary of known food habits of California species. *Veliger* **21**, 110-118.

MacGillivray, P. H. (1887) A catalogue of the marine Polyzoa of Victoria. *Proc. Roy. Soc. Vict.* **23**, 187-224.

Mackey, L. Y., Winnepenninckx, B., De Wachter, R., Backeljau, T., Emschermann, P. & Garey, J. R. (1996) 18S rRNA suggests that Entoprocta are protostomes, unrelated to Ectoprocta. *J. Molec. Evol.* **42**, 552-559.

Malakhov, V. V. (1990) Description of the development of *Arcopedicula discreta* (Coloniales, Barentsiidae) and discussion of the Kamptozoa status in the animal kingdom. (In Russian, English summary.) *Zool. Zhur.* **69**, 20-30.

Marcus, E. N. (1965) The adult and larval morphology and life history of the entoproct *Barentsia gracilis* (M. Sars, 1835). *J. Morphol.* **116**, 311-338.

_____ (1975) Entoprocta pp. 1-41 *In* Giese, A.C., & Pearse, J.S. (Eds) "Reproduction of Marine Invertebrates" Vol. 2 (Academic Press, New York).

Marcus, E. (1939) Briozoários marinhos brasileiros. III. *Bol. Fac. Fil. Ciê. Let.* (Univ. São Paulo) *Zool.* **3**, 111-295.

Mokai, H. & Makioka, T. (1978) Studies on the regeneration of an entoproct, *Barentsia discreta*. *J. Exp. Zool.* **205**, 261-276.

_____ _____ (1980) Some observations on the sex differentiation of an entoproct, *Barentsia discreta* (Bush). *Ibid.* **213**, 45-59.

Nielsen, C. (1964) Studies on Danish Entoprocta. *Ophelia* **1**, 1-76.

_____ (1966) On the life-cycle of some Loxosomatidae (Entoprocta). *Ibid.* **3**, 221-247.

_____ (1971) Entoproct life-cycles and the entoproct/ectoproct relationship. *Ibid.* **9**, 209-341.

_____ (1989) "Entoprocts". Synopses of the British Fauna, New Series, Vol. 41. (E.J. Brill, Leiden).

_____ (1995) "Animal Evolution" (Oxford University Press, Oxford).
_____ (1996) Three new species of *Loxosoma* (Entoprocta) from Phuket, Thailand with a review of the genus. *Zool. Scr.* **25**, 61-75.
_____ & JESPERSEN, A. 1997. Entoprocta pp. 13-43 *In* Harrison, F.W. (Ed.) "Microscopic Anatomy of Invertebrates" Vol. 13 (Wiley-Liss, Inc., New York).
_____ & ROSTGAARD, J. (1976) Structure and function of an entoproct tentacle with a discussion of ciliary feeding types. *Ophelia* **15**, 115-40.
NITSCHE, H. (1870) Beiträge zur Kenntniss der Bryozoen. *Zeit. Wiss. Zool.* **20**, 1-36.
PALLAS, P. S. (1774a) "Spicilegia Zoologica, quibus novae et imprimis obscurae animalium species iconibus, descriptionibus atque commentariis illustrantur" Vol. 1 (G.A. Lange, Berlin).
_____ (1774b) "Naturgeschichte merkwürdiger Thiere. Zoophyta" (G. A. Lange, Berlin).
PRENANT, M. & BOBIN, G. (1956) Bryozoaires. Pt 1. Entoproctes, Phylactolèmes, Cténostomes. *Faune Fr.* **60**, 1-398.
RIGER, J. F. (1969) Studies on the fine structure of muscle fibers and contained crystalloids in basal socket muscle of the Entoproct, *Barentsia gracilis*. *J. Cell Sci.* **4**, 305-325.
RÜTZLER, K. (1968) *Loxosomella* from *Tedania ignis*, the Caribbean fire sponge. *Proc. U. S. Nat. Mus.* **124**, 1-11.
RYLAND, J. S. (1965) Some New Zealand Pedicellinidae (Entoprocta), and a species new to Europe. *Trans. Roy. Soc. N. Z.* **6**, 189-205.
_____ & AUSTIN, A. P. (1960) Three species of Kamptozoa new to Britain. *Proc. Zool. Soc. London* **133**, 423-433.
SALVINI-PLAWEN, L. v. (1980) Was ist eine Trochophora? Eine Analyse der Larventypen mariner Protostomier. *Zool. Jahrb. (Anat.)* **103**, 389-423.
SARS, M. (1835) "Beskrivelser og Iagttagelser over nogle maerkelige eller nye i Havet ved den Bergenske Kyst levende Dyr af Polypernes, Acalephernes, Radiaternes, Annelidernes og Molluskernes Classer" (T. Hallager, Bergen).
SELIGER, O. (1889) Die ungeschlechtliche Vermehrung der endoprokten Bryozoen. *Zeit. Wiss. Zool.* **49**, 168-208.
_____ (1890) Bemerkungen zur Knospenentwicklung der Bryozoen. *Ibid.* **50**, 560-599.
TODD, J. A. & TAYLOR, P. D. (1992) The first fossil entoproct. *Naturwiss.* **79**, 311-314.
TORIUMI, M. (1951) Some entoprocts found Matsushima Bay. *Sci. Rep. Tôhoku Univ., 4th Ser. (Biol.)* **19**, 17-22.
VAN BENEDEN, P. J. (1845) Recherches sur l'anatomie, la physiologie et le développement des Bryozoaires qui habitent la Côte d'Ostende. Histoire naturelle du genre *Pedicellina*. *Nouv. Mem. Acad. Roy. Sci. Bel. Let. Brux.* **19**, 1-31.
WASSON, K. (1995) The kamptozoan *Pedicellina whiteleggii* Johnston and Walker, 1917 and other pedicellinids in Australia and New Zealand. *Rec. S. Aust. Mus.* **28**, 131-141.
_____ (1997) Sexual modes in the colonial kamptozoan genus *Barentsia*. *Biol. Bull.* **193**, 163-170.
_____ (1998) Sexual reproduction in the colonial kamptozoan *Barentsia hildegardae*. *Invert. Biol.* **117**, 123-128.
_____ & SHEPHERD, S. A. (1997) Nodding heads (Phylum Kamptozoa or Entoprocta) pp. 975-992 *In* Shepherd, S. A. & Davies, M. (Eds) "Marine Invertebrates of Southern Australia" Pt 3. (South Australia Fauna and Flora Handbooks Committee, Adelaide).
WATERS, A. W. (1904) Bryozoa pp. 1-113 *In* "Résultats du Voyage du S.Y. Belgica" (J. E. Buschmann, Anvers).
WHITELEGGE, T. (1889) List of the marine and fresh-water invertebrate fauna of Port Jackson and the neighbourhood. *J. Proc. Roy. Soc. N. S. W.* **23**, 163-323.
WILLIAMS, J. B. (2000) Descriptions of two loxosomatids (Entoprocta), with emphasis on a relationship between symbiont attachment structures and host cuticle. *Canad. J. Zool.* **78**, 110-120
WOOLLACOTT, R. M. & EAKIN, R. M. (1973) Ultrastructure of a potential photoreceptoral organ in the larva of an entoproct. *J. Ultrastruct. Res.* **43**, 412-425.

Appendix

Known kamptozoan diversity in waters around Australia and New Zealand.

This appendix lists the 19 described and 18 undescribed species of kamptozoans known from Australia and New Zealand. The first column gives the species name. Undescribed species have been assigned a number. Those loxosomatids whose basal attachment (generic character) could not be determined are listed simply as "loxosomatid". The second column gives the author of the original species description for described species, or a brief descriptive phrase (for loxosomatids, host is given) for undescribed species. The third column gives the citation for occurrence of this species in Australia or New Zealand. For new records (Wasson, this paper), the name of the collector is given in parentheses. The fourth column lists (abbreviated) the Australian State or the Island of New Zealand where the species was found.

FAMILY LOXOSOMATIDAE (7 described + 17 undescribed species)

Loxosomella breve	(Harmer, 1915)	Hastings 1932	QLD
Loxosomella circulare	(Harmer, 1915)	Hastings 1932	QLD
Loxosomella cirriferum	(Harmer, 1915)	Hastings 1932; Wasson, this paper (R. A. Birtles & P. Arnold)	QLD
Loxosomella diopatricola	Williams, 2000	Williams 2000	VIC
Loxosomella kefersteinii	(Claparède, 1867)	Wasson & Shepherd 1997	SA
Loxosomella pusillum	(Harmer, 1915)	Hastings 1932	QLD
Loxosomella velatum	(Harmer, 1915)	Wasson, this paper (R. A. Birtles & P. Arnold)	QLD
Loxosomella sp. 1	on bryozoan	Wasson & Shepherd 1997	SA
Loxosomella sp. 2	dark zooids on sponge	Wasson & Shepherd 1997	SA
Loxosomella sp. 3	light zooids on sponge	Wasson, this paper (M. Barker & K. Wasson)	SNZ

Loxosomella sp. 4	on polychaete *Sthenelais*	Hastings 1932	QLD
Loxosomella sp. 5	on polynoid polychaete	Wasson, this paper (M. Barker & K. Wasson)	SNZ
Loxosomella sp. 6	on prawns	Wasson, this paper (R. Lester)	NT
Loxosomella sp. 7	on polychaete	Wasson, this paper (D. Gordon)	NNZ
Loxosomella sp. 8	on polychaete *Eunice*	Williams 2000	VIC
Loxosoma sp. 1	on polychaete *Copperingeria*	Haswell 1891; Hastings 1932; Wasson, this paper (R. A. Birtles & P. Arnold)	QLD QLD
Loxosoma sp. 2	on polychaete *Pectinaria*	Wasson, this paper (J. Collins)	QLD
Loxosoma sp. 3	on polychaete *Aviothella*	Wasson, this paper (D. Gordon)	NNZ
Loxosomatid sp. 1	on sipunculan *Phascolosoma*	Whitelegge 1889	NSW
Loxosomatid sp. 2	on hirudinean *Branchellion*	Goddard 1909	WA
Loxosomatid sp. 3	on hirudinean *Pontobdella*	Goddard 1909	WA, NSW
Loxosomatid sp. 4	on bryozoan *Amathia*	Harmer 1915	VIC
Loxosomatid sp. 5	on squat lobster *Thenus*	Wasson, this paper (R. Lester)	QLD
Loxosomatid sp. 6	on aquarium walls	Gordon & Ballantine 1977	NNZ

FAMILY PEDICELLINIDAE (6 described species)

Pedicellina cernua	(Pallas, 1774)	Kirkpatrick 1890b; Chittleborough[1]; Wasson 1995	VIC, SA
Pedicellina compacta	Harmer, 1915	Hastings 1932; Wasson 1995	QLD
Pedicellina grandis	Ryland, 1965	Ryland 1965	SNZ
Pedicellina pernae	Ryland, 1965	Ryland 1965	SNZ
Pedicellina pyriformis	Ryland, 1965	Ryland 1965, Wasson 1995	SNZ, TAS
Pedicellina whiteleggii	Johnston & Walker, 1917	Wasson 1995 (and others cited therein)	NSW, VIC, SA, NNZ, SNZ

FAMILY BARENTSIIDAE (6 described + 1 undescribed species)

Barentsia benedeni	(Foettinger, 1887) [misidentified as *B. gracilis*]	Wasson & Shepherd 1997; Chittleborough[1]	NSW, SA SA
Barentsia discreta	(Busk, 1886)	Wasson & Shepherd 1997 Wasson, this paper (D. Gordon & S. O'Shea)	VIC NNZ
Barentsia geniculata	Harmer, 1915	Wasson, this paper (R. A. Birtles & P. Arnold)	QLD
Barentsia laxa	Kirkpatrick, 1890a	Kirkpatrick 1890a	NT
Barentsia matsushimana	Toriumi, 1951	Wasson, this paper (M. Barker & K. Wasson)	SNZ
Barentsia sp. 1	minute, delicate zooids [misidentified as *B. gracilis*]	Wasson & Shepherd 1997; Kirkpatrick 1890b; Waters 1904; Hastings 1932; Hilgendorf 1898; Gordon 1972	NSW, SNZ, SA VIC, QLD SNZ, NNZ
Pedicellinopsis fruticosa	Hincks, 1884	Hincks 1884; Busk 1886; MacGillivray 1887; Whitelegge 1889; Hedley 1915; Johnston & Angel 1940; Wasson & Shepherd 1997	VIC, NSW, TAS

[1] Chittleborough, R. G. (1952) Marine Fouling at Port Adelaide. MSc Thesis, The University of Adelaide (unpub.).

AMINO ACID RACEMISATION DATING OF A RAISED GRAVEL BEACH DEPOSIT, SELLICKS BEACH, SOUTH AUSTRALIA

By C. V. Murray-Wallace & R. P. Bourman†*

Summary

Murray-Wallace, C. V. & Bourman, R. P. (2002). Amino acid racemisation dating of a raised gravel beach deposit, Sellicks Beach, South Australia. Trans. R. Soc. S. Aust. 126(1), 21-28, 31 May, 2002.

The extent of racemisation (total acid hydrolysate) of the amino acids aspartic acid, glutamic acid, leucine, phenylalanine and valine indicates a minimum age of last interglacial for fossil molluscs occuring within a raised gravel beach deposit at Sellicks Beach, South Australia. The base of the raised gravel beach occurs up to 5.5 m above Australian Height Datum (AHD) and possibly indicates 3 m of local uplift since the last interglacial maximum (c. 125 ka; Oxygen Isotope Substage 5e). Emergence of the gravel beach is attributed to ongoing neotectonic uplift of Fleurieu Peninsula.

Key Words: amino acid racemisation, last interglacial, neotectonics, sea-levels, South Australia.

Transactions of the Royal Society of S. Aust. (2002), **126**(1), 21-28.

AMINO ACID RACEMISATION DATING OF A RAISED GRAVEL BEACH DEPOSIT, SELLICKS BEACH, SOUTH AUSTRALIA

by C.V. MURRAY-WALLACE* & R.P. BOURMAN†

Summary

MURRAY-WALLACE, C.V. & BOURMAN, R.P. (2002). Amino acid racemisation dating of a raised gravel beach deposit, Sellicks Beach, South Australia. *Trans. R. Soc. S. Aust.* **126** (1), 21-28, 31 May, 2002.

The extent of racemisation (total acid hydrolysate) of the amino acids aspartic acid, glutamic acid, leucine, phenylalanine and valine indicates a minimum age of last interglacial for fossil molluscs occurring within a raised gravel beach deposit at Sellicks Beach, South Australia. The base of the raised gravel beach occurs up to 5.5 m above Australian Height Datum (AHD) and possibly indicates 3 m of local uplift since the last interglacial maximum (c. 125 ka; Oxygen Isotope Substage 5e). Emergence of the gravel beach is attributed to ongoing neotectonic uplift of Fleurieu Peninsula.

KEY WORDS: amino acid racemisation, last interglacial, neotectonics, sea-levels, South Australia.

Introduction

A resurgence of interest in recent years in Quaternary emergent shoreline successions has arisen from the increasing ability to determine the age of these features due to technological advances in geochronology (Rutter & Catto 1995; Noller *et al.* 2000). Similarly, an increasing awareness that coastal successions, particularly those deposited during the last interglaciation (c.125 ka), are sufficiently old to quantify even modest rates of neotectonism, has bolstered this research endeavour. Accordingly, the elevation of last interglacial coastal deposits has been widely used as a benchmark to delineate recent tectonic behaviour at continental scales (Murray-Wallace & Belperio 1991; Ota 1994; Bourman *et al.* 1999; Zazo *et al.* 1999). In this work, the age of a raised beach deposit at southern Sellicks Beach, South Australia, is determined based on the extent of racemisation of several amino acids within molluscs from the fossil assemblage. In addition, the neotectonic significance of this deposit and its relation to other emergent shoreline deposits on Fleurieu Peninsula is examined.

Materials and Methods

Field investigations

The elevation and lateral extent of the gravel beach deposit was surveyed to Australian Height Datum (AHD) using an automatic level. In addition to a general field description of the deposit, shell samples were collected for amino acid racemisation dating and to document the fossil mollusc assemblage. Species identification followed that set out in Ludbrook (1984).

Amino acid racemisation analyses

Samples of fossil molluscs for amino acid racemisation analyses (total acid hydrolysate) were collected from the gravel beach deposit. Shells were removed from the matrix of the deposit and their depth of burial recorded. Analyses were undertaken on specimens of *Patella (Scutellastra) laticostata* Blainville, *Thais orbita* (Gmelin), *Sydaphera undulata* (Sowerby), *Nerita (Melanerita) atramentosa* Reeve and *Ostrea* sp. Linnaeus.

Sediment adhering to the surfaces of shell samples and diagenetically modified aragonite, particularly chalky surfaces, were removed with a dental drill, followed by successive washes in distilled water using an ultrasonic bath. A dilute acid etch (2 mol HCl) was subsequently undertaken to remove the outer surfaces (c. 10-15% by mass) of the shells that had been in contact with the host sediment. Samples were subsequently hydrolysed for 22 hours at 110° C in 8 mol HCl. Following cation exchange isolation of the amino acid residues, samples were freeze dried and derivatized. Chromatography of the N-penta-fluropropionyl D, L-amino acid 2-propyl esters was performed using a Hewlett-Packard 5890A Series II gas chromatograph with a flame ionisation detector and a 25 m coiled, fused silica capillary column coated with the stationary phase Chirasil-L-Val. Full details of the analytical techniques followed in this work are reported elsewhere (Murray-Wallace 1993). Enantiomeric ratios were determined for the amino acids aspartic acid (ASP), glutamic acid (GLU), leucine (LEU), phenylalanine (PHE) and valine (VAL).

* School of Geosciences, University of Wollongong, NSW 2522.
† School of Environment and Recreation Management, University of South Australia, Mawson Lakes, SA 5095.

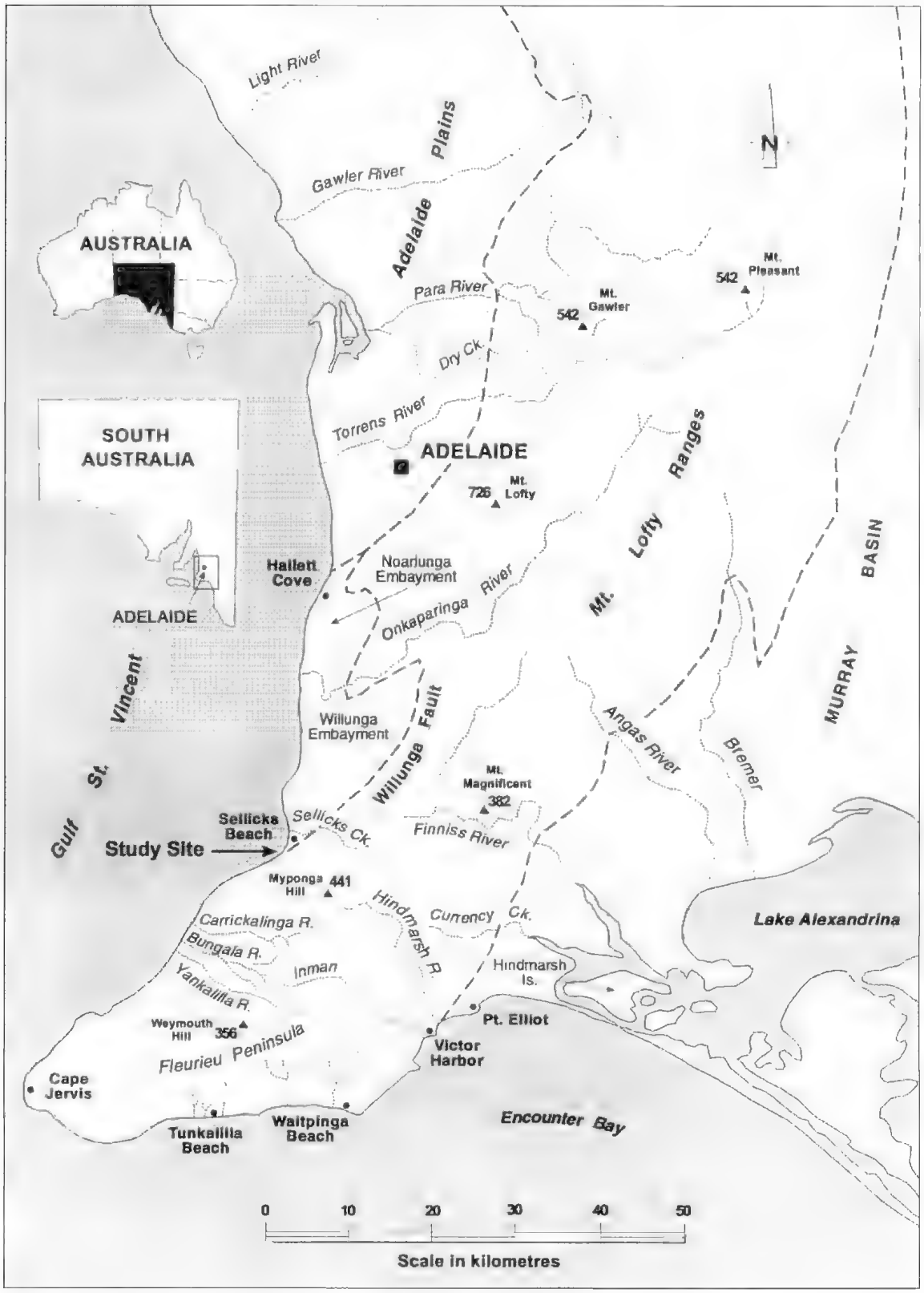

Fig. 1 Location of the raised gravel beach deposit, Sellicks Beach, South Australia.

Fig 2. View looking south along southern Sellicks Beach towards the southern Adelaide Hills and coastal cliffs developed on Pleistocene alluvial fan successions. The location of the raised beach deposit, which occurs in the scarp foot zone is indicated by an arrow.

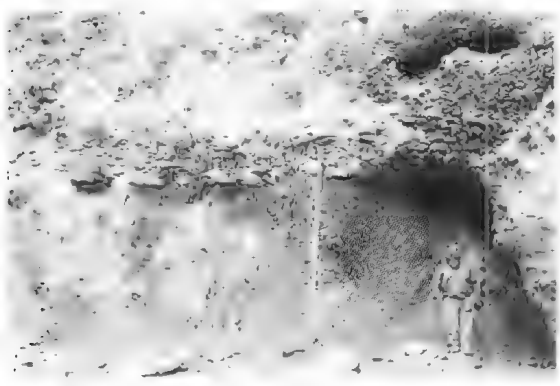

Fig. 4. A shore-normal view of the raised gravel beach deposit at Sellicks Beach. The steeply dipping Ochre Cove Formation is visible near the survey staff. The staff, which is fully extended, is 5 m long.

Geomorphological Setting And Site Description

The raised gravel beach deposit is situated near the Willunga Fault at the southern-most part of Sellicks Beach (35° 21' 09.8" S; 138° 26' 07.5" E), landward of a modern, gently seaward sloping intertidal shore platform (Figs 1, 2). The modern intertidal platform is approximately 20 m wide in a shore-normal transect, is partially covered with boulders and cobbles and represents a modern analogue for the relict platform (Fig. 3). An accumulation of boulders and cobbles occurs at the foot of the modern cliff and represents a further modern analogue of the raised beach deposit. The emergent gravel beach facies rests on a strongly eroded remnant of a shore platform that is developed on the steeply dipping Oligo-Miocene Port Willunga Beds (Daily *et al.*

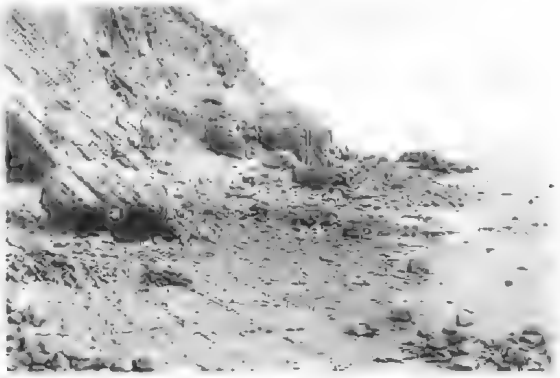

Fig. 3. View looking southwest towards the raised gravel beach deposit at Sellicks Beach. The gravels rest unconformably on the Oligo-Miocene Port Willunga Beds and the Middle Pleistocene Ochre Cove Formation. The gravel deposit dips gently seawards. The unconformity surface represents a relict intertidal shore platform. The modern intertidal platform occurs in the foreground, dips gently seaward and is partially covered by boulders and cobbles. The maximum difference in elevation between the two platforms is 5 m as determined in the most landward exposure, not visible in this photograph. Small, isolated, sea stacks representing erosional remnants of the formerly more extensive Pleistocene shore platform occur within this area (e.g. "a" in the middle distance).

1976), and in part, a steeply dipping portion of the Middle Pleistocene Ochre Cove Formation (Ward 1966; Pillans & Bourman 1996; Figs 3, 4, 5). The gravel deposit occurs within a former scarp foot zone excavated at a time of higher sea level, and abuts fanglomerates of the Ochre Cove Formation (May & Bourman 1984).

The bedrock surface on which the gravel beach facies rests, grades in a seaward direction from 5.55 m to 4.95 m above Australian Height Datum (AHD). The platform extends out seaward from the deposit some 1-1.5 m forming a well-defined bench (Fig. 6). The gravel beach facies crops out over a shore-parallel distance of approximately 50 m, and ranges in thickness between 1 and 1.5 m (Fig. 6).

The gravel deposit is poorly sorted and comprises sub-rounded to subangular clasts of siltstone, quartzite and bryozoal limestone that range from boulder to pebble size, although the modal clast size is boulder-cobble (700-70 mm). The lithoclasts are tightly packed. Numerous entire and fragmental fossil molluscs occur within the granular matrix of the gravel deposit.

A pale grey, clean, free-flowing sand is thinly draped over the gravel deposit and the underlying fanglomerates and extends up to 2.5 m above the upper bounding surface of the deposit. The sand also

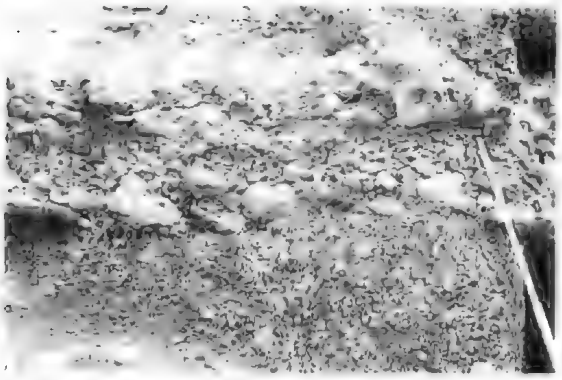

Fig. 5. Detail from figure 4 showing the tightly packed arrangement of lithoclasts.

Fig. 6. View looking eastnortheast showing part of the shore-parallel lateral extent of the raised beach deposit. The letter "a" denotes the general level of the gravel deposit which is approximately 4 m above the gravel covered footslope of the small cliff in the foreground. A planated surface representing remnants of an intertidal shore platform is visible on the seaward side of the deposit. Pleistocene conglomerates are evident in the upper right-hand portion of the photograph "b". The raised beach deposit is overlain by a thin veneer of sand which also partially covers the conglomerate, but is difficult to discern in this photograph.

occurs within the uppermost part of the matrix of the gravel bed near the contact between the gravel and the overlying sand. A thermoluminescence age of 34.0±2.9 ka (W2317) was previously reported for this sandy unit (Bourman *et al.* 1999). In addition, a radiocarbon age (minimum age) of >30 ka (GaK-6095) has previously been reported for molluscs from the gravel beach deposit (May & Bourman 1984).

Results and Discussion

Mollusc assemblage

The gravel unit contains a relatively diverse assemblage of fossil molluscs, principally gastropods, within the sediment matrix. Molluscs include *Patella (Scutellastra) laticostata* Blainville, *Mactra rufescens* (Lamarck), *Ostrea angasi* Sowerby, *Monodonta (Austrocochlea) constricta* Lamarck, *Nerita (Melanerita) atramentosa* Reeve, *Cymatiella lesueuri* Iredale; *Conus* sp., Linnaeus, *Diloma (Chlorodiloma) adelaidea* (Philippi), *Bembicium melanostoma* (Gmelin), *Sydaphera undulata* (Sowerby) and opercula of *Turbo* sp., Linnaeus. Many of the shells also occur as large fragments, highly abraded and of unrecognizable affinity. Collectively, the fossil assemblage indicates deposition in an environment comparable to the modern coast at southern Sellicks Beach, with molluscs found in sand or attached to rocks, in a relatively sheltered setting of the lower littoral zone (Ludbrook 1984).

Dating

A generally high degree of racemisation (expressed as a D/L ratio) is evident for the five different enantiomeric amino acids measured in each of the fossil molluscs from the gravel beach deposit (Table 1). The relative extent of racemisation for the different amino acids, within the single mollusc samples, generally follows the relation VAL<LEU<GLU<PHE≤ASP. Similar trends are reported for fossil molluscs from United States Pacific coastal plain sites (Lajoie *et al.* 1980).

Three specimens of *Patella (Scutellastra) laticostata* (samples UWGA-695, 696 and 763) reveal good concordance in measured enantiomeric ratios (i.e. between-shell D/L ratio variation) with coefficients of variation less than 5.6% for all amino acids for the combined data (actual values include VAL 2.2%, LEU 5.6%, ASP 0.3%, PHE 1.9% and GLU 5%). The consistently lower degree of racemisation for all amino acids in the specimen of *Patella* sp. (sample UWGA-697), compared with the other three *Patella* samples is possibly due to the diffusive loss of the more highly racemised, lower molecular weight peptide fraction from the shell carbonate matrix. Accordingly, the degree of racemisation as determined in the total acid hydrolysate, would be disproportionately weighted towards the less racemised, higher molecular weight peptide residues that remain within the shell aragonite matrix. This explanation is consistent with the poorly preserved nature of some of the molluscs within the gravel deposit (e.g. chalky appearance).

The high extent of racemisation measured in all the fossil molluscs from the raised beach deposit far exceeds values typically determined in Holocene fossils (Murray-Wallace & Bourman 1990; Murray-Wallace & Goede 1995; Murray-Wallace 2000; Table 1). The extent of racemisation in the molluscs

TABLE 1. *Extent of amino acid racemisation (total acid hydrolysate) in fossil molluscs from a raised gravel beach deposit, Sellicks Beach and other localities for comparison*

Species & Location	Lab. Code or reference	Amino acid D/L ratio[†] VAL	LEU	ASP	PHE	GLU
Sellicks Beach, raised beach deposit						
Thais orbita (columella)	UWGA-733	0.284±0.021	0.369	0.556±0.015	-	-
Sylaphera undulata	UWGA-736	-	0.333	0.322±0.036	-	-
Patella (Scutellastra) laticostata	UWGA-697	0.309±0.008	0.370±0.018	0.613±0.033	0.541±0.006	0.549±0.051
Patella (Scutellastra) laticostata	UWGA-696	0.412	0.582±0.021	0.800±0.004	0.798±0.029	0.606±0.008
Patella (Scutellastra) laticostata	UWGA-695	0.405±0.003	0.551±0.007	0.799±0.007	0.777±0.017	0.557±0.002
Patella (Scutellastra) laticostata	UWGA-763	0.423±0.008	0.520±0.003	0.804±0.001	0.770±0.009	0.611±0.009
Nerita (Melanerita) atramentosa	UWGA-766	0.386±0.008	0.411±0.006	0.702±0.029	0.599±0.005	0.671±0.006
Ostrea sp.	UWGA-768	0.365±0.010	0.403±0.013	0.835±0.023	0.727±0.008	0.789±0.026
Late Pleistocene, Glanville Formation, Normanville, SA						
Mactra australis	Bourman *et al.* (1999)	0.283±0.011	0.273±0.012	0.590±0.010	-	0.333±0.006
Hindmarsh Island, SA						
Mactra australis		0.26±0.003	0.37±0.002	0.56±0.001	-	0.36±0.002
Port Wakefield, SA						
Anadara trapezia	Murray-Wallace *et al*	0.32±0.06	0.51±0.02	0.54±0.03	-	0.43±0.01
Katelysia rhytiphora	(1988)	0.32±0.04	0.51±0.07	0.46±0.02	-	0.38±0.04
Holocene Three Rivers Creek, King Island, TAS						
Patella laticostata (790±60 yr BP; SUA-2927)	Murray-Wallace & Goede (1995)	0.01	0.05±0.02	-	0.04±0.001	0.05±0.001
Sir Richard Peninsula, SA						
Donax deltoides (2260±140 yr BP; SUA-2881)	Murray-Wallace & Bourman (1990)	0.07±0.01	-	0.27±0.01	0.19±0.01	0.12±0.005

[†] amino acids: VAL - valine; LEU - leucine; ASP - aspartic acid, PHE - phenylalanine and GLU - glutamic acid.

from the Sellicks Beach deposit also exceeds that apparent for representative examples from the Late Pleistocene Glanville Formation at Normanville and Hindmarsh Island, two localities with comparable current mean annual air temperatures and, as a corollary, two deposits likely to have experienced similar diagenetic temperature histories to the Sellicks Beach deposit, given the caveat that the shells from each deposit remained buried at depths ≥1 m for much of their diagenetic histories (Murray-Wallace *et al.* 1988; Bourman *et al.* 1999; Table 1). The Glanville Formation, as originally defined in the Adelaide region (Ludbrook 1976; Cann 1978) has been correlated with the last interglacial maximum (125 ka; Oxygen Isotope Substage 5e) based on thermoluminescence, amino acid racemisation and uranium-series dating of correlative deposits from other parts of the South Australian coastline (Belperio *et al.* 1984; Schwebel 1984; Huntley *et al.* 1993, 1994; Murray-Wallace 2000).

Although the fossil molluscs from the raised beach deposit at Sellicks Beach were obtained from near-surface contexts (<50 cm), the geomorphological and stratigraphical evidence suggest that for part of

their diagenetic history, the fossils were more deeply buried (i.e. at least 1 m). However, these molluscs will have experienced a higher integrated diagenetic temperature than for fossils that have remained in more deeply buried contexts (Table 1). Current mean annual air temperatures (CMAT) at Sellicks Beach, Normanville and Hindmarsh Island are all approximately 16° C, and 17° C for Port Wakefield.

The extent of racemisation for the majority of amino acids is significantly higher in the molluscs from Sellicks Beach compared with those from Normanville and Hindmarsh Island (Table 1). The difference in extent of racemisation is less pronounced when compared with the molluscs from Port Wakefield which have experienced a higher diagenetic temperature (Table 1). As current mean annual temperature at the Port Wakefield site is approximately 1° C warmer than at Sellicks Beach, and given that rates of racemisation are known to increase by up to 20 per cent for such a temperature difference (McCoy 1987), the implication is that the shallow burial depth of the shells at Sellicks Beach has contributed to the high degree of racemisation of amino acids within these fossils.

Amino acid D/L ratios for the molluscs from the Sellicks Beach deposit range from the envelope of values representative of last interglacial age to potentially the penultimate interglacial (c. 220 ka; Oxygen Isotope Stage 7), as revealed in a plot of the extent of racemisation against current mean annual temperature (and as a corollary, latitude) (Fig. 7). The lack of clustering and chronological consistency of the data suggests a diagenetic basis for the observed variation in enantiomeric ratios rather than a genuine age variation between shells. The range in D/L ratios for the shells from Sellicks Beach exceeds that typically found for a single isotopic stage (Murray-Wallace 2000).

Although racemisation rates are known to be genus-specific (Miller & Brigham-Grette 1989) this is unlikely to account solely for the higher degree of racemisation in the fossil *Patella (Scutellastra) laticostata* from the Sellicks Beach deposit, compared with other genera from the Glanville Formation. It is therefore concluded that the higher degree of racemisation in the molluscs from Sellicks Beach is due to faster rates of racemisation, due to their shallow burial depth during late diagenesis resulting from the progressive exhumation of the deposit, and a genus-effect on racemisation.

As the shells have been subjected to variable burial depths during late diagenesis, the integrated rate expression for racemisation was rearranged with temperature as the subject to assess whether it is possible to induce the high extent of racemisation at ambient diagenetic temperatures over the course of the Holocene. As the amino acid analyses reported

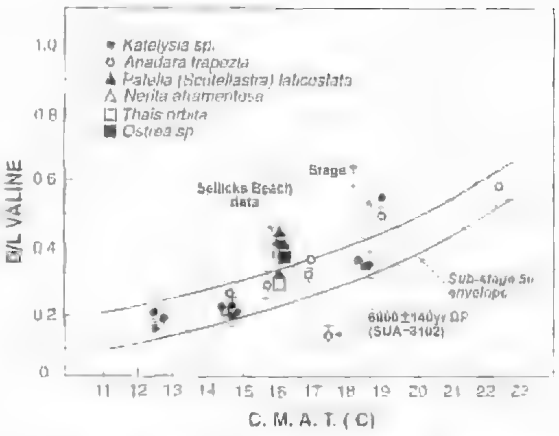

Fig. 7. The extent of valine racemisation (total acid hydrolysate) in fossil molluscs of last interglacial age (Oxygen Isotope Substage 5e) from southern Australia plotted against current mean annual air temperature (°C) to illustrate the Sellicks Beach data within a broader regional context. Details of samples from elsewhere in southern Australia are reported by Murray-Wallace & Belperio (1991) and Murray-Wallace *et al.* (1999). The amino acid data for the last interglacial molluscs are in accord with the exponential trend of increasing extent of racemisation with higher diagenetic temperatures, and as a corollary, higher current mean annual temperatures. The fossil molluscs from the raised beach deposit at Sellicks Beach reveal a broad range in extent of racemisation from the envelope of the last interglacial to values consistent with a penultimate interglacial age (Oxygen Isotope Stage 7 c. 220 ka). Amino acid results for Holocene and Stage 7 molluscs are presented as a framework for comparison.

here were undertaken on different fossils from those used for the radiocarbon assay (~30 ka age; May & Bourman 1984), the integrated diagenetic temperature was calculated to examine the possibility that the radiocarbon age was the result of chance sampling of reworked Pleistocene shells within a Holocene deposit. A minimum age of 7000 years was selected for the calculation, representing the timing of the culmination of the post-glacial marine transgression in southern Australia (Belperio *et al.* 2002), and, therefore, the oldest age likely for an undisturbed Holocene coastal deposit. The rationale for this is that the early Holocene is the only time in the Late Quaternary, apart from the last interglacial maximum, that sea level was sufficiently high potentially to form the raised beach. Present sea level is not sufficiently high to form the deposit. Furthermore, interstadial sea levels of the Late Pleistocene (Chappell *et al.* 1996) were significantly below present sea level and would imply rates of tectonic uplift of a magnitude inconsistent with the

well-established tectonic framework for the region (Bourman *et al.* 1999; Belperio *et al.* 2002).

An average diagenetic temperature required to induce the degree of racemisation measured in the fossils assuming an age of 7 ka was determined thus:

$$T = \frac{5939}{15.77 - \log_e \ln\left[\frac{(1+D/L_f)}{(1-D/L_f)}\right] - \ln\left[\frac{(1+D/L_\infty)}{(1-D/L_\infty)}\right] / 2t}$$

where T is the absolute temperature (°K), D/L_f and D/L_∞ are the enantiomeric ratios of the fossils and their modern equivalents respectively, t is an assumed age (i.e. 7000 years) and 15.77 and 5939 are constants derived from the empirical rate constant expression (Wehmiller 1982, 1993). Accordingly, an average diagenetic temperature of 24° C would be necessary to induce the extent of racemisation measured in the three specimens of *Patella (Scutellastra) laticostata* (UWGA-695, -696 and -763) from the raised beach deposit if they were only 7 ka. A diagenetic temperature of this value is unlikely, however, given that the current mean annual air temperature at Sellicks Beach is approximately 16° C. A prolonged, higher mean annual temperature by as much as 8° C is unlikely over the course of the Holocene for this region (Chappell 1991). Thus, the extent of racemisation measured in the fossil molluscs from the raised beach deposit could not have been attained during the Holocene. A penultimate interglacial age is also not favoured, as the gravel beach deposit is unlikely to have survived erosional processes of the last two glacial cycles. On this basis a last interglacial age is favoured for the raised gravel beach deposit at Sellicks Beach.

Neotectonics

The raised gravel beach deposit at Sellicks Beach provides a further opportunity to examine the neotectonic behaviour of Fleurieu Peninsula. Previous investigations have revealed that the region has experienced geologically recent uplift as indicated by the elevation of last interglacial coastal deposits (Bourman *et al.* 1999).

Although many gravel beach deposits represent relational sea-level indicators (i.e. always form above tidal datum) and are therefore of only modest reliability (Chappell 1987), several attributes of the deposit at Sellicks Beach render it more reliable for quantifying rates of neotectonism. The adjacent modern intertidal platform has clearly formed within a narrow range of tidal datum and represents an analogous feature to the Pleistocene equivalent. The upper reaches of the modern shore platform are covered by boulders and cobbles presumably accumulated during storm events. However, the steep backing slope of the cliff prevents boulders or finer clasts from being deposited at any significantly higher elevation above tidal datum.

Estimates of a glacio-eustatic sea level for the last interglacial (Oxygen Isotope Substage 5e) from Eyre Peninsula suggest a value of 2 m AHD, and represents a particularly reliable datum given the relative tectonic stability of the Gawler Craton upon which much of the Eyre Peninsula coastline has developed (Murray-Wallace & Belperio 1991). Thus, uplift of the Sellicks Beach deposit by as much as 3 m is indicated based on the elevation of the contact between the gravel deposit and the underlying erosional surface of the relict shore platform.

The amount of uplift since the last interglacial maximum, inferred from the deposit at Sellicks Beach (c. 3 m) is less than that observed at Normanville (c. 10 m) to the south of the Willunga Fault (Bourman *et al.* 1999). The uplift is attributed to the combined effects of ongoing tectonic uplift of the Adelaide Hills and erosional unloading and associated crustal isostatic compensation. Further research is required to model these processes geophysically.

Conclusions

The extent of racemisation for several amino acids in fossil molluscs from a raised gravel beach deposit at Sellicks Beach, South Australia, indicates that the deposit is of Late Pleistocene age, and most likely formed during the last interglacial maximum (c. 125 ka; Oxygen Isotope Substage 5e). The deposit indicates up to 3 m of uplift has occurred in this region since the last interglacial and suggests that the region is still undergoing neotectonic uplift.

Acknowledgments

This research was supported by the Research Centre for Landscape Change at the University of Wollongong. C. Sloss and N. Riggs are thanked for laboratory assistance. The figures were prepared by R. Miller and C. Crothers. This paper is a contribution to IGCP Project 437, 'Coastal Environmental Change During Sea-Level Highstands: A Global Synthesis with Implications for Management of Future Coastal Change'.

References

BELPERIO, A. P., HARVEY, N. & BOURMAN, R. P. (2002) Spatial and temporal variability in the Holocene palaeo sea-level record around the South Australian coastline. *Sed. Geol.* (in press).

_______, SMITH, B. W., POLACH, H. A., NITTROUER, C. A., DEMASTER, D. J., PRESCOTT, J. R., HAILS, J. R. & GOSTIN, V. A. (1984) Chronological studies of the Quaternary marine sediments of northern Spencer Gulf, South Australia. *Mar. Geol.* **61**, 265-296.

BOURMAN, R. P., BELPERIO, A. P., MURRAY-WALLACE, C. V. & CANN, J. H. (1999) A last interglacial embayment fill at Normanville, South Australia, and its neotectonic implications. *Trans. R. Soc. S. Aust.* **123**, 1-15.

CANN, J. H. (1978) An exposed reference section for the Glanville Formation. *Quarterly Geological Notes, Geological Survey of South Australia* **65**, 2-4.

CHAPPELL, J. (1987) Late Quaternary sea-level changes in the Australian region pp. 296-331 *In* Tooley, M. J. & Shennan, I. (Eds) "Sea-Level Changes" (Oxford, Basil Blackwell).

_______ (1991) Late Quaternary environmental changes in eastern and central Australia, and their climatic interpretation. *Quat. Sci. Rev.* **10**, 377-390.

_______, OMURA, A., ESAT, T., MCCULLOCH, M., PANDOLFI, J., OTA, Y. & PILLANS, B. (1996) Reconciliation of late Quaternary sea levels derived from coral terraces at Huon Peninsula with deep sea oxygen isotope records. *Earth Planet. Sci. Lett.* **141**, 227-236.

DAILY, B., FIRMAN, J. B., FORBES, B. G. & LINDSAY, J. M. (1976) Geology pp. 5-42 *In* Twidale, C. R., Tyler, M. J. & Webb, B. P. (Eds.) "Natural History of the Adelaide Region" (Royal Society of South Australia, Adelaide).

HUNTLEY, D. J., HUTTON, J. T. & PRESCOTT, J. R. (1993) The stranded beach-dune sequence of south-east South Australia: a test of thermoluminescence dating, 0-800 ka. *Quat. Sci. Rev.* **12**, 1-20.

_______, _______ & _______ (1994) Further thermoluminescence dates from the dune sequence in the southeast of South Australia. *Ibid.* **13**, 201-207.

LAJOIE, K. R., WEHMILLER, J. F. & KENNEDY, G. L. (1980) Inter- and intra-generic trends in apparent racemization kinetics of amino acids in Quaternary mollusks pp. 305-340 *In* Hare, P. E., Hoering, T. C. & King, K. (Eds) "Biogeochemistry of amino acids" (Wiley, New York).

LUDBROOK, N. H. (1976) The Glanville Formation of Port Adelaide. *Quarterly Geological Notes, Geological Survey of South Australia* **57**, 4-7.

_______ (1984) Quaternary molluscs of South Australia. Department of Mines and Energy, South Australia, Handbook No. **9**.

MAY, R. M. & BOURMAN, R. P. (1984) Coastal landslumping in Pleistocene sediments at Sellicks Beach, South Australia. *Trans. R. Soc. S. Aust.* **108**, 85-94.

MCCOY, W. D. (1987) The precision of amino acid geochronology and paleothermometry. *Quat. Sci. Rev.* **6**, 43-54.

MILLER, G. H. & BRIGHAM-GRETTE, J. (1989) Amino acid geochronology: resolution and precision in carbonate fossils. *Quat. Internat.* **1**, 111-128.

MURRAY-WALLACE, C. V. (1993) A review of the application of the amino acid racemisation reaction to archaeological dating. *The Artefact* **16**, 19-26.

_______ (2000) Quaternary coastal aminostratigraphy: Australian data in a global context pp. 279-300 *In* Goodfriend, G. A., Collins, M. J., Fogel, M. L., Macko, S. A. & Wehmiller, J. F. (Eds) "Perspectives in amino acid and protein geochemistry" (Oxford University Press, New York).

_______ & BELPERIO, A. P. (1991) The last interglacial shoreline in Australia - A review. *Quat. Sci. Rev.* **10**, 441-461.

_______ & BOURMAN, R. P. (1990) Direct radiocarbon calibration for amino acid racemization dating. *Aust. J. Earth Sci.* **37**, 365-367.

_______, BELPERIO, A. P., BOURMAN, R. P., CANN, J. H. & PRICE, D. M. (1999) Facies architecture of a last interglacial barrier: a model for Quaternary barrier development from the Coorong to Mount Gambier Coastal Plain, southeastern Australia. *Mar. Geol.* **158**, 177-195.

_______ & GOEDE, A. (1995) Aminostratigraphy and electron spin resonance dating of Quaternary coastal neotectonism in Tasmania and the Bass Strait islands. *Aust. J. Earth Sci.* **42**, 51-67.

_______, KIMBER, R. W. L., BELPERIO, A. P. & GOSTIN, V. A. (1988) Aminostratigraphy of the last interglacial in southern Australia. *Search* **19**, 33-36.

NOLLER, J. S., SOWERS, J. M. & LETTIS, W. R. (2000) (Eds) "Quaternary Geochronology: methods and applications" (American Geophysical Union, Reference Shelf 4, Washington, DC.)

OTA, Y. (1994) Last Interglacial Shorelines in the Western Pacific Rim. *J. Geog.* **103**, 809-827.

PILLANS, B. J. & BOURMAN, R. P. (1996). The Brunhes/Matuyama polarity transition as a chronostratigraphic marker in Australian regolith studies. *AGSO J. Aust. Geol. & Geophys.* **16**, 289-294.

RUTTER, N. W. & CATTO, N. R. (1995) (Eds) "Dating methods for Quaternary deposits" (Geological Association of Canada, GEOText 2).

SCHWEBEL, D. A. (1984) Quaternary stratigraphy and sea-level variations in the southeast of South Australia pp. 291-311 *In* Thom, B. G. (Ed.) "Coastal geomorphology in Australia" (Academic Press, Sydney).

WARD, W. T. (1966) Geology, geomorphology and soils of the south-western part of County Adelaide, South Australia. *CSIRO Soils Publication No. 23*.

WEHMILLER, J. F. (1982) A review of amino acid racemization studies in Quaternary mollusks: stratigraphic and chronologic applications in coastal and interglacial sites, Pacific and Atlantic Coasts, United States, United Kingdom, Baffin Island and tropical islands. *Quat. Sci. Rev.* **1**, 83-120.

_______ (1993) Applications of organic geochemistry for Quaternary research: aminostratigraphy and aminochronology pp. 755-783 *In* Engel, M. & Macko, S. (Eds) "Organic geochemistry" (Plenum, New York).

ZAZO, C., SILVA, P. G., GOY, J. L., HILLAIRE-MARCEL, C., GHALEB, B., LARIO, J., BARDAJI, T. & GONZALEZ, A. (1999) Coastal uplift in continental collision plate boundaries: data from the Last Interglacial marine terraces of the Gibraltar Strait area (south Spain). *Tectonophys.* **301**, 95-109.

EUROPEAN-INDUCED ENVIRONMENTAL CHANGE IN THE ADELAIDE AREA, SOUTH AUSTRALIA: EVIDENCE FROM DRY CREEK AT MAWSON LAKES

By Robert P. Bourman, Neville F. Alley† & Kristine F. James**

Summary

Bourman, R. P., Alley, N. F. & James, K. F. (2002) European-induced environmental change in the Adelaide area, South Australia: Evidence from Dry Creek at Mawson Lakes. Trans. R. Soc. S. Aust. 126(1), 29-38, 31 May, 2002.

Post-European Settlement Aggradation (PESA) sediments flanking the course of Dry Creek at Mawson Lakes reflect land clearance and agricultural activities in the twenty years or so following the establishment of European settlement in 1836. Sedimentation in this lower section of Dry Creek occurred in response to accelerated erosion on upland slopes related to land clearance and burning activities. A tree trunk, dated at ~400 years BP occurs at the unconformable contact between the PESA and the underlying Pooraka Formation of last interglacial age. Although this might be attributed to Aboriginal firestick farming activities, the discovery of a European artefact from the 1850s favours the view that Aboriginal practices were not responsible for the accelerated erosion and sedimentation in the Dry Creek drainage system.

Key Words: Accelerated erosion, sedimentation, channel incision, European settlement, urban drainage.

Transactions of the Royal Society of S. Aust. (2002), **126**(1): 29-38

EUROPEAN-INDUCED ENVIRONMENTAL CHANGE IN THE ADELAIDE AREA, SOUTH AUSTRALIA: EVIDENCE FROM DRY CREEK AT MAWSON LAKES

by ROBERT P. BOURMAN[1], NEVILLE F. ALLEY[2] & KRISTINE E. JAMES[3]

Summary

BOURMAN, R. P., ALLEY, N. F. & JAMES, K. E. (2002) European-induced environmental change in the Adelaide area, South Australia: Evidence from Dry Creek at Mawson Lakes. *Trans. R. Soc. S. Aust.* **126**(1), 29-38, 31 May, 2002.

Post-European Settlement Aggradation (PESA) sediments flanking the course of Dry Creek at Mawson Lakes reflect land clearance and agricultural activities in the twenty years or so following the establishment of European settlement in 1836. Sedimentation in this lower section of Dry Creek occurred in response to accelerated erosion on upland slopes related to land clearance and burning activities. A tree trunk, dated at ~400 years BP occurs at the unconformable contact between the PESA and the underlying Poonika Formation of last interglacial age. Although this might be attributed to Aboriginal firestick farming activities, the discovery of a European artefact from the 1850s favours the view that Aboriginal practices were not responsible for the accelerated erosion and sedimentation in the Dry Creek drainage system.

KEY WORDS. Accelerated erosion, sedimentation, channel incision, European settlement, urban drainage

Introduction

European-induced accelerated erosion, immediately downstream of the Main North Road crossing of Dry Creek had exposed 6 m deep vertical sections in Quaternary alluvial deposits over a distance of approximately 1 kilometre. Given that channel stabilisation of this section of the creek was to be undertaken in association with the development of the Mawson Lakes housing estate, we decided to examine and describe the exposed sections prior to their destruction, a process which is now complete. The aim of the remediation was to reduce erosion and downstream sedimentation, and to remove deep vertical banks that might present a hazard to people in an urbanised area.

Dry Creek drainage basin

The study area lies on Dry Creek (Fig. 1), which drains an area of approximately 109 km² in the northern and north-eastern suburbs of Adelaide, South Australia, and is bordered by the catchments of the River Torrens to the south and the Little Para River to the north. The drainage divide between Dry Creek and the Little Para River is extremely subdued and difficult to delineate with precision. A series of non-integrated streams such as Cobbler Creek drains from the western side of the Para Escarpment (Fig. 2) and disappears into drains or the alluvium of the plains. Dry Creek rises at the northeastern extremity of the basin, some 400 m asl on the Eden Escarpment from which many first order streams flow, initially in a westerly direction. These streams unite and flow to the southwest along the fault angle depression between the Para and Eden fault blocks, eventually cutting a bedrock gorge at the western edge of the Para block to debouch on to the alluvial North Adelaide Plains. Originally the stream, like so many others of the Adelaide Plains, probably dissipated into the alluvial deposits and rarely reached the sea. Today artificial drains carry discharge from the creek through mangroves and samphire flats into the estuarine/tidal environment of Barker Inlet.

Where it crosses the Main North Road, Dry Creek appears to be relatively insignificant and it is surprising to note that it drains some 40% of the Adelaide suburban area. Because it is so intensively urbanised, there have been many impacts on the drainage basin that have required remedial works to inhibit erosion. The catchment occurs predominantly within the Local Government Authorities of the Cities of Salisbury (50 km²) and Tea Tree Gully (51 km²). A small area also occurs within the City of Port Adelaide/Enfield (4 km²) (PPK E & I & Willing & Partners 1997[4]; BC Tonkin & Associates 1980[5]). The development of an integrated catchment water management plan in

[1] School of Environmental and Recreation Management, University of South Australia, Mawson Lakes Campus, Mawson Boulevard, Mawson Lakes SA 5095.

[2] Offices of Minerals and Energy, PIRSA, GPO Box 1671, Adelaide SA 5001.

[4] PPK ENVIRONMENT & INFRASTRUCTURE IN ASSOCIATION WITH WILLING & PARTNERS (NSW) PTY LTD (1997) "Dry Creek and Little Para Catchments Integrated Catchment Water Management Plan Background and Opportunities" (PPK Environment & Infrastructure, Adelaide), Volume 2.

[5] BC TONKIN & ASSOCIATES (1980) "Hydrology, Dry Creek Drainage Basin" Prepared for the Corporations of the Cities of Salisbury, Tea Tree Gully and Enfield. (BC Tonkin & Associates, Adelaide).

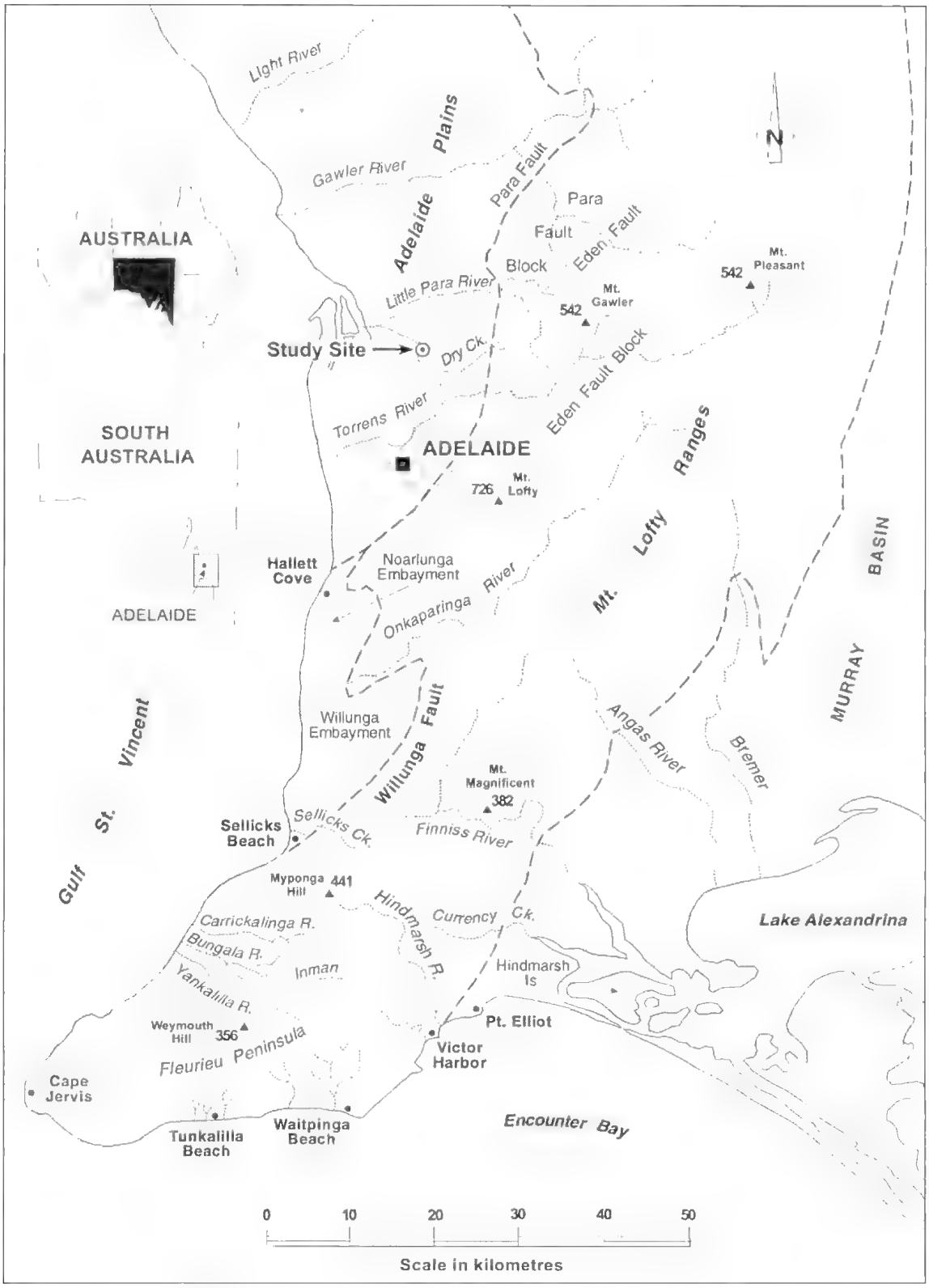

Fig. 1. General location map of the study area.

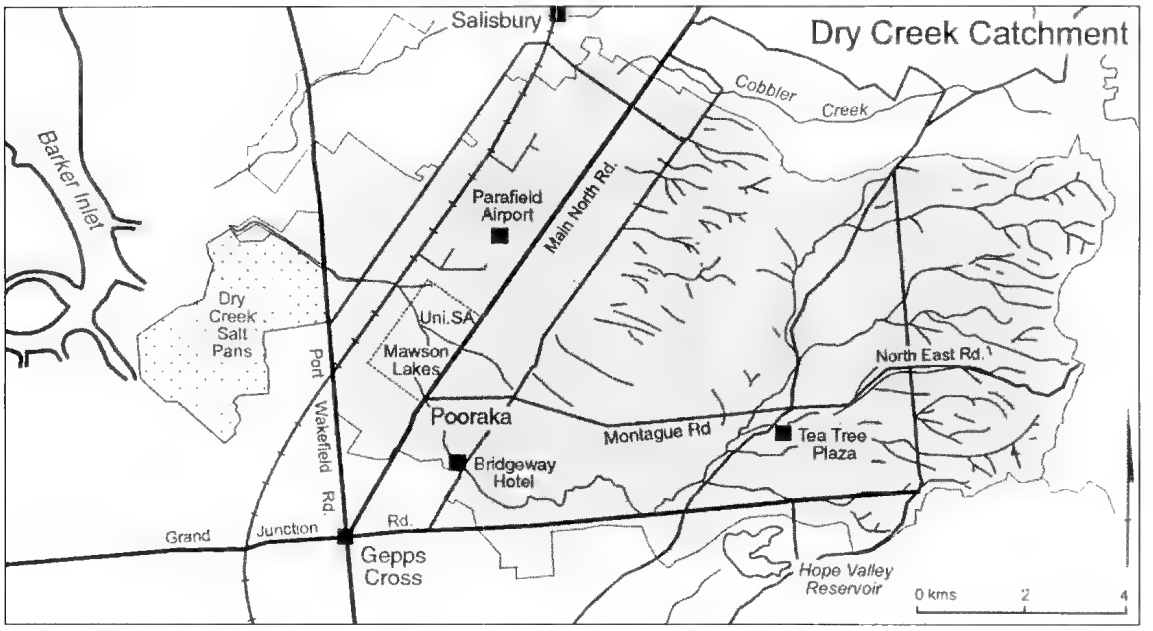

Fig. 2. Map of the drainage basin of Dry Creek.

1997 involving community and technical stakeholders and local drainage authorities should benefit this urbanised creek and its ecology.

Drainage network

The main channel of Dry Creek is 28 km long, with major creeks (81 km) and major drains (54 km) comprising the remainder of the drainage network of 163 km (BC Tonkin & Associates 1980[2]). It is in the lower parts of the catchment that artificial drainage systems have been installed in response to urbanisation, but in the upper parts of the catchment, upstream of the Para escarpment, drainage occurs mostly in natural creeks that are generally protected by flanking reserves. Nevertheless, there has been some development on flood plains, and interruption of watercourses by roads, buildings and other constructions, with the risk of flooding increased by culvert crossings and creek enclosure (BC Tonkin & Associates 1980[2]).

Climate

The Dry Creek catchment occurs in a region of Mediterranean climate with pronounced warm, dry summers and cool, wet winters. The rainfall pattern is strongly seasonal and evaporation rates are high. The annual average rainfall derived from gauging stations located in or around the Little Para and Dry Creek catchments is 531.8 mm (PPK E & I & Willing & Partners 1997[1]), with a tendency for higher rainfall in the eastern part of the catchment.

Land use

Information derived from a digital cadastral database indicates the following land uses in the Dry Creek catchment: mining and quarrying (2%), industrial (3%), open code (3%), commercial (4%), recreation (4%), public utilities (5%), primary production (5%), public institutions (6%), vacant land (23%) and residential (45%), which comprises the largest land use of the catchment (PPK E & I & Willing & Partners 1997[1]. Some 20 years ago, BC Tonkin & Associates (1980[2]) reported that more than "...90% of the catchment comprises either existing or proposed urban development".

In light of the large drainage area, its considerable modification especially by urbanisation, and the strongly seasonal character of rainfall, there is little surprise that accelerated channel changes have occurred in the lower reaches of the Dry Creek drainage basin.

Modification of urban channels

As with many other watercourses in South Australia, Dry Creek has been significantly modified along its length. Some modifications have been directly imposed. Other changes relate to indirect impacts in response to human occupation. In particular, increased urbanisation has resulted in elevated discharges, reduced stream loads and accelerated erosion where there are no protective works, and this has been particularly exacerbated downstream of artificial knickpoints. This has resulted in accelerated sedimentation even further downstream.

The battering of steep bluffs and their landscaping are common features of urban channels. A relatively recent example of this occurred on Dry Creek approximately 2 km upstream from the present study site and immediately downstream of the Bridgeway Hotel at Pooraka. At this locality, from a naturally eroding steep river bluff some 6 m high, Williams (1969) collected samples of detrital carbonised wood and carbonate for radiocarbon dating in order to establish the age of the Pooraka Formation. The Pooraka Formation is a very widespread alluvial unit, which underlies much of the Adelaide Plains (Sheard & Bowman 1996), including the present study site. Bourman *et al.* (1997) were not able to sample from exactly the same site as Williams (1969) in order to date the alluvium, using the different technique of luminescence dating, as the steep river bluff by then had been battered, contoured, rock protected and landscaped. A drilling rig was required to collect samples from approximately the same horizon as the samples of Williams (1969). As well as impacting on research activities, the engineering works have also destroyed the usefulness of the locality as a teaching site.

Materials and Methods

In carrying out this investigation standard sedimentological and stratigraphic techniques were employed. In examining vertical sections, sediment samples were collected every 10 cm. Detailed descriptions of the sections are provided in Table 1. Wood incorporated within the upper suite of sediments was dated by radiocarbon techniques at the Radiocarbon Dating Laboratory, University of Waikato, New Zealand. All exposed sediments were carefully examined and collections were made of foreign materials incorporated within the sediments.

Results

Site description and field observations

The study site occupied a one kilometre section of Dry Creek, downstream of its crossing with the Main North Road (Fig. 3). At this locality channel incision and widening had exposed a 6 m deep section of Late Pleistocene and younger sediments. These recent channel changes have been related to human interference, with the construction of concrete drains under the roadway mentioned above and the construction of an erosion drop structure immediately upstream of the actively eroding zone, causing accelerated erosion. Prior to remedial works being undertaken, both channel deepening and widening were continually exposing fresh faces. The extensive urbanisation of the Dry Creek catchment, reduced sediment loads and increased water yields

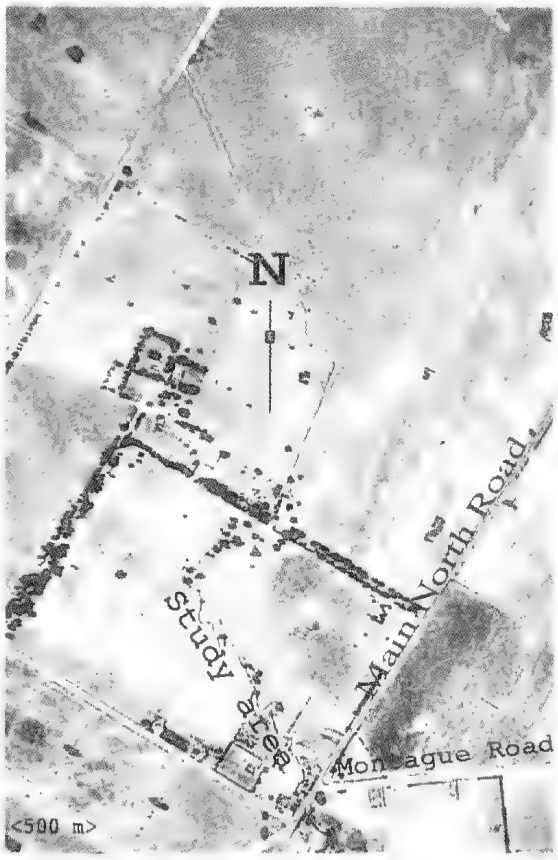

Fig. 3. Aerial photograph of Dry Creek taken in 1935, illustrating that the present course of the creek, downstream from the Main North Road had been incised and established by then. The straight artificial channels downstream of the study site are clearly visible. The length of the section of channel from the Main North Road to where it crosses the next fence line downstream is ~ 1 km. (Source: Commonwealth Government).

have also contributed to the accelerated erosion. Unfortunately, the development of the Mawson Lakes housing project, occurring in the lower part of the catchment west of the Main North Road, has resulted in these informative sections being destroyed or obscured. Consequently, this paper provides the only written account of these formerly exposed sediments. Exposures of the Pooraka Formation are critical to future research on the antiquity of humans on the Australian continent, investigations of the past magnetism of the earth and climatic change. Thus it is disappointing that the trend is to destroy natural exposures of rocks and sediments in urban areas vital for earth science research and teaching activities.

The general elevation of the land surrounding the study site varies between 15 and 11 m. Natural

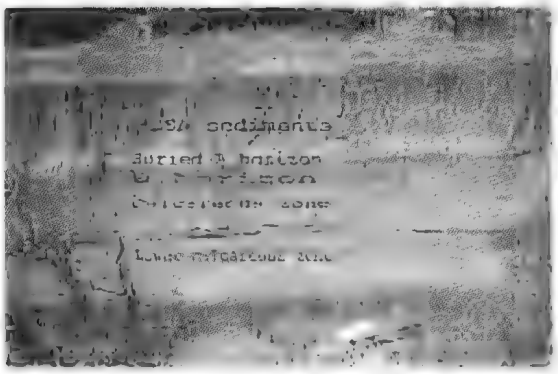

Fig.4. Section in right bank of Dry Creek in the study area. Depth of exposure is approximately 6 m. The upper part of the section (~ 2 m) comprises PESA deposits. A pronounced leached A horizon, which occurs two thirds of the way up the section marks the top of the Pooraka Formation. It overlies a red/brown clay B-horizon containing flecks of calcium carbonate. This forms a wavy boundary above a richer calcareous zone. A second calcareous zone occurs in the base of the section.

Fig. 5. Post European Settlement Aggradation (PESA) sediments overlying Pooraka Formation alluvium on the left bank of Dry Creek. The contact is approximately at the position of the feet of the person on the ladder.

TABLE 1. *Section in left bank of Dry Creek*

0 - 235 cm	**Younger grey brown alluvium**
0 - 40 cm	Grey silty clay. Sour sob. *Oxalis pes-caprae* (L.) bulbs occur down to depths of 40 cm. Sedimentation has occurred over the bulbs. Sediment has vesicular character
40 - 80 cm	Light grey clay silt, slightly calcified, with calcium carbonate diffusing along root channels
80 - 130 cm	Silty clay, buff coloured and mottled with calcium carbonate enrichment. Sediment contains vesicles, with ant nests and footholes to depths of 60 cm.
130 - 170 cm	Grey/brown clay silt with peds and pockets of charcoal. Sediment is a little more clay rich and more lithified than above. Calcium carbonate also more pervasive than above.
170 - 220 cm	Dominantly grey/brown clay displaying some sub horizontal stratification with minor cross-bedding. Only minor quantities of calcium carbonate are present.
220 - 235 cm	Grey/brown coarse gravelly sand, which extends along a disconformity with the underlying Pooraka Formation.
	Disconformity
235 -596 cm Pooraka Formation	
235 - 260 cm	Light grey to whitish grey, silty sand.
260 - 280 cm	Buff coloured, greyish mottled sandy silt with some clay, producing blocky peds as the material dries out.
280 - 292 cm	Red brown clay, slightly mottled.
292 - 352 cm	Lighter coloured calcareous clays, with calcium carbonate penetrating into fissures and root lines.
352 - 522 cm	Grey to buff coloured clay, with the upper 30 cm containing nodules and rhizoliths of calcium carbonate. Some vertical bleaching of sediments along root channels.
522 - 596 cm	Grey to buff coloured clay, with the upper 30 cm containing nodules and rhizoliths of calcium carbonate. Some vertical bleaching of sediments along root channels

levees flanking the stream extend 2 to 3 m above the level of the surrounding alluvial fan deposits. The lower part of the exposed section, from the channel floor up to a level about 4 m above the channel floor is marked by deposits of the Pooraka Formation (Fig. 4), recently dated as of last interglacial age, which is approximately 125,000 years BP (Bourman *et al.* 1997). This alluvium was deposited during a time when global sea level was approximately 2 m higher than at present (Murray-Wallace & Belperio 1995) and the climate was warmer and wetter than now. These climatic conditions would have favoured the aggradation of sediments washed from out of the Mount Lofty Ranges. During this time giant, fossil marsupials, approximately the size of a rhinoceros, the *Diprotodon* spp. roamed the swampy, aggrading Adelaide Plains. Numerous discoveries of *Diprotodon* spp. remains have been made in the Pooraka Formation (Tate 1879; Twidale 1968; N. Pledge pers. comm. 1996) of the Adelaide area.

Pedogenic or soil-forming features are preserved within the Pooraka Formation (Figs 4 & 7). For example, at the top of the Pooraka Formation is a leached, bleached silty sand A horizon, which is underlain by a dark red brown clay B horizon. This, in turn, is underlain by a Bca horizon comprising nodules and cylindroids of calcium carbonate. The above soil is typical of red brown earths. A second, lower Bca horizon illustrates a halt in sedimentation of the Pooraka Formation during its deposition.

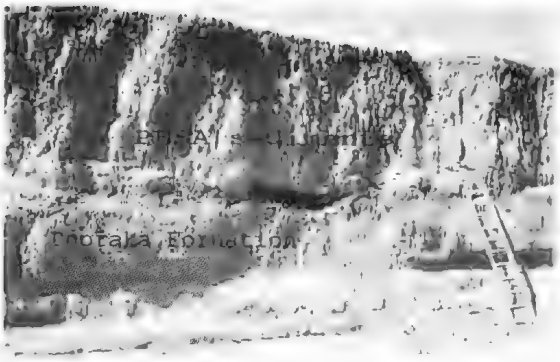

Fig. 6. Post European Settlement Aggradation (PESA) sediments occupying a shallow channel cut into the underlying Pooraka Formation. The contact is near the top of the ladder. The height of the section is 6 m.

Multiple buried soils within the Pooraka Formation are common, such as in Cobbler Creek to the north of Dry Creek.

The distinctively coloured, red-brown Pooraka Formation with its leached, bleached whitish A horizon is overlain by up to 3 m of younger, grey to brown coloured alluvial materials (Fig. 5; Table 1), deposited as levees along the present channel. In places the Pooraka Formation has been eroded cutting through the soil developed on the Pooraka Formation and the channels are infilled with younger sediments (Fig. 6). The young alluvium on the left bank has been largely, although not exclusively, deposited as overbank deposits, whereas those on the right bank have been largely deposited as channel deposits (Fig. 7). The young alluvium contains masses of charcoal, land snails and, possibly, a

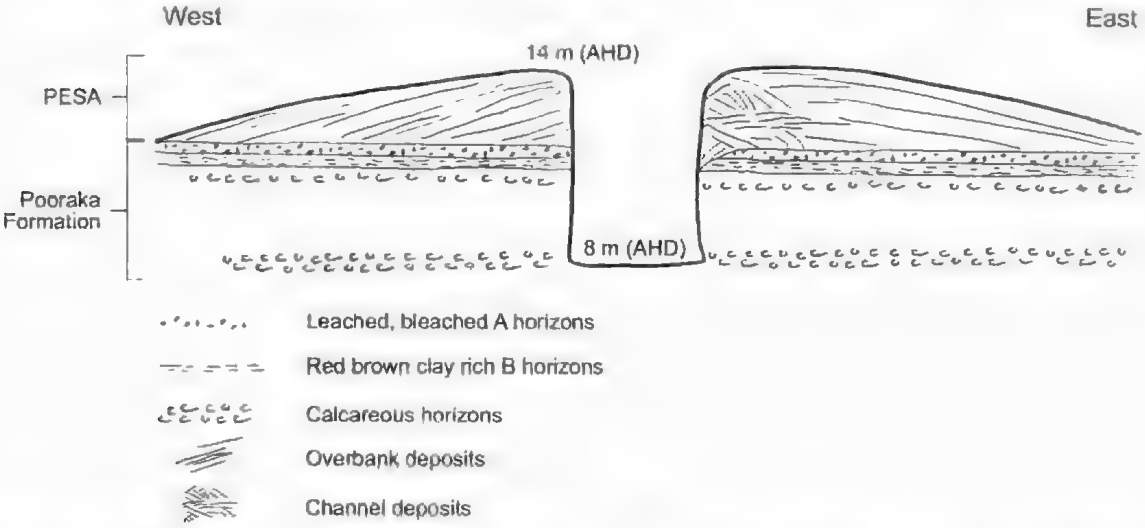

Fig. 7. Diagrammatic sketch of section across Dry Creek at Mawson Lakes. The width of the section is ~ 600 m

Fig. 8. Tree trunk, possibly *E. largiflorens*, sandwiched between the underlying last interglacial Pooraka Formation and Post European Settlement Aggradation (PESA) sediments. The outer part of the trunk was radiocarbon dated at ~ 400 years BP.

Fig. 9. Photograph of the base of a bottle with a shallow punt and with the inscription "CW & Co" located at the contact between the Pooraka Formation and the PESA sediments. The bottle is thought to have been manufactured in the United Kingdom during the 1850s-1860s. The pen is 14 cm long.

microlith artefact. In places there are ripple structures at the unconformity and the ripple structures are preserved both on the base of the sediments and the top of the unconformity.

A tree trunk (Fig. 8), lying horizontally, was located at the contact between the underlying Pooraka Formation and the overlying younger alluvium on the right bank immediately downstream from the drop structure across the channel. A sample of the outer part of the tree trunk, which appeared to be *Eucalyptus largiflorens* (F. Muell), was collected for radiocarbon dating. The outer part of the trunk was sampled to date the youngest part of the trunk.

The study site was revisited after winter rains, which had facilitated further undercutting. Retreat of the channel walls had exposed more of the unconformable contact, revealing the presence of numerous European artefacts that included parts of bottles (both glass and ceramic), cattle bones, fencing wire and other metal objects. Some of these objects were exactly at the base of the unconformity. In particular, the bottom of a black glass bottle with the inscription 'C.W. & Co' was recovered from the base of the unconformity (Fig. 9). The bottle base has an indentation known as a 'punt', 'kickup' or 'kick' (Lachemann 2001[1]).

In the case of Dry Creek there is little evidence of accelerated erosion prior to the deposition of the PESA sediments. A very well developed soil profile on the Pooraka Formation suggests that landscape stability favoured the operation of pedogenic processes. Only in a few minor instances was there evidence of the soil profile developed on the Pooraka Formation being eroded prior to the deposition of the PESA sediments, which have a maximum thickness of ~3 m.

Discussion

Causes of channel erosion

The initiation of gullies and channel erosion is related to many factors. According to Begin & Schumm (1984), gully erosion occurs whenever the power of flows exceeds a threshold value equivalent to the resistance of the valley floor. This may be affected by basin wide external factors such as climate and catchment wide landuse. These factors will initiate erosion on relatively steep and narrow sections of the valley-floor as these sites are closest to the threshold condition and will respond first to altered conditions. Gully development can be, but is not necessarily, related to anthropogenic influences. Gullying has occurred prior to human interferences and may be attributed to the effects of climatic change influencing vegetation and runoff, tectonic uplift including tilting of the land or eustatically-controlled sea level movements. Schumm (1979) has also emphasised that changes can occur as a result of factors inherent within the geomorphic system. For example, an aggrading alluvial fan surface may progressively steepen to such an extent that a critical threshold slope is achieved when the stream may begin to incise its own deposits without external conditions changing. Site specific factors such as ploughing, bridge and culvert construction and drainage schemes can also initiate erosion especially where the changes are most severe (Bourman & James 1995). The potential roles of non-human factors and human influences on stream sedimentation and erosion at the study site will be assessed.

Timing of sedimentation and channel erosion at the study site

The tree trunk at the unconformity between the Pooraka Formation and younger overlying alluvium returned a radiocarbon age of 420 ± 50 years BP (Wk 5825). This radiocarbon date might suggest that there was accelerated erosion in the Mount Lofty Ranges about 400 years ago, possibly related to Aboriginal occupation and burning for firestick farming. This interpretation is supported by the observation of charcoal in the younger alluvium and its occurrence close to the unconformity. A similar situation occurs in the Gawler River, approximately 30 km north of the study site. Radiocarbon dating of wood and charcoal incorporated into alluvium, was undertaken by C. R. Twidale of the University of Adelaide. The samples of carbon and wood collected from within the alluvial deposits near the present day channel were dated at 375 ± 70 Years B.P. (ANU Sample No 204) and 235 ± 70 Years B.P. (ANU Sample No 205) respectively (Bourman 1969[2]). These data, too, are highly suggestive of accelerated sedimentation and erosion related to vegetation disturbance by Aboriginal burning activities.

Bushfires prior to European settlement may have been quite dramatic as illustrated below. Our attention was drawn to the following by B. Taylor, a descendant of one of the early settlers, J. W. Adams, who arrived on the "HMS Buffalo" in 1836 and who penned an account of his early days in the settlement. This included a graphic account of a major summer bushfire in the Mount Lofty Ranges. The "Buffalo" met the "Signet" at Port Lincoln on 24th December, 1836 and they sailed together to Holdfast Bay where they dropped anchor on the 27th December, 1836 (Adams 1902). "When the anchor was dropped the usual bustle commenced for landing. Before we left

[1] LACHEMANN, M. (2001) *The Punt*, [online], accessed 5 Oct. 2001] URL: http://www.virtual-ink.com/articles.php?001.htm

[2] BOURMAN, R. P. (1969) Landform Studies near Victor Harbour, SA (Hons) thesis, The University of Adelaide (unpub.)

the ship we witnessed a grand sight. All the hills and gullies as far as we could see were on fire, and the reflection was so strong that we could see every rope and the men walking the deck of the "Signet". She was about half a mile in shore from us, and we were about five miles out. I have seen many fires since, but nothing to compare with that for grandeur" (Adams 1902).

In combination, the ~ 400 year radiocarbon date on the tree trunk incorporated within the recent alluvial sediments of the plain, plus the first hand account of intensive burning in the adjoining Mount Lofty Ranges (Adams 1902), could suggest that the accelerated erosion and sedimentation may have occurred prior to the arrival of Europeans and had resulted from fires started by Aboriginal people. There is no direct evidence that the fires of late December, 1836 were started by Aboriginal people and may have had natural causes. However, the intense and widespread bushfires of more recent times have occurred later in the fire season, usually in February. This might support the view of Aboriginal influences in starting the fires of 1836.

Regardless of the cause of the 1836 fires and the possible association of Aboriginal burning activities with accelerated erosion and sedimentation, the discovery of European artefacts in the younger alluvium, particularly the base of the glass bottle at the unconformity, indicates that the accelerated landscape change did not occur until some time after European settlement. The occurrence of a ~400 year old tree trunk at the base of the younger sediments does not mean that the sediments were deposited 400 years ago, but only that the tree died 400 years ago. Attempts made to identify the bottle base with the inscription 'CW & Co' unequivocally have not been successful. There is no doubt that it was not manufactured locally as no bottle manufacturing firm with this trademark has existed in South Australia (Shuttard & Tuckwell 1993). Furthermore Hallett Shuttard, an authority on antique bottles, informed the writers (pers. comm. 25/10/01) that the bottle was almost certainly a half pint bottle manufactured in the United Kingdom during the 1850s-1860s, and that the bottle predates the earliest bottle manufacturing in South Australia.

The occurrence of buried soursob bulbs (*Oxalis pes-caprae* L.) to depths of 40 cm also provide data on the timing of sedimentation, which post dated the introduction and dispersal of *Oxalis* from South Africa to South Australia.

The above observations indicate that the younger grey-brown alluvium is actually Post-European Settlement Aggradation (PESA) and probably reflects sedimentation due to accelerated erosion related to land clearance and burning in the upper catchment zones. It also suggests that prior to European occupation there was no alluvium overlying the Pooraka Formation at this site, and that an extremely rapid rate of deposition formed the levees that are up to 3 m in thickness. The sediments were not deposited at least until the 1850s, given the postulated manufacturing date of the "CW & Co" bottle. Furthermore, we know that the present day incised channel was established before 1936 as indicated by an aerial photograph (Fig. 3) so that a minimum rate of sedimentation building the levees is ~ 2.5 cm yr^{-1}.

Causes of sedimentation and channel incision at study site

At the study site there is no evidence for naturally occurring episodes of sedimentation and erosion since the Last Interglacial (125 ka BP) when the Pooraka Formation was deposited. Only minor erosion of the Pooraka Formation has occurred. Preservation of a complete soil profile on the Pooraka Formation is common (Figs 4 & 5), reflecting subaerial exposure and landscape stability. In the wider Adelaide region the youngest alluvial unit that has been recognised as naturally occurring is that of the Middle Holocene Waldeila Formation (~ 5-6 ka BP) (Bourman *et al.* 1997), which has been related to climate change and a slightly elevated sea level. Consequently, within the local area, recent accelerated sedimentation and erosion is most likely due to human factors, especially as sediment containing European artefacts (PESA) is so widespread within and flanking the Mount Lofty Ranges.

It has been suggested that valley side vegetation clearance alone is insufficient to initiate channel erosion, which requires some form of channel disturbance such as by stock grazing and drainage works (Prosser & Slade 1994). However, accelerated deposition of PESA derived from the valley sides following clearance, indirectly leads to erosion by

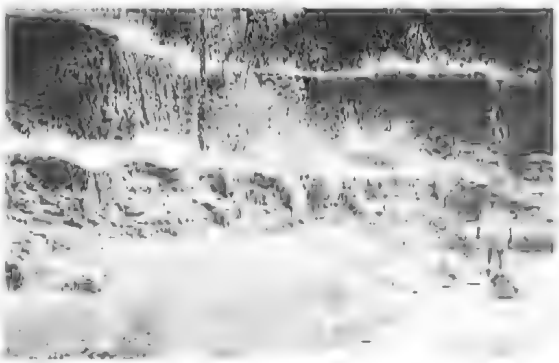

Fig. 10. More recent PESA deposits extending up to 2.2 m above the gully floor. These sediments contained recent European artefacts such as plastics. Total height of section ~ 5 m.

burying vegetation, killing it and steepening slopes. This sets the stage for channel erosion and incision through the PESA sediments and into the underlying units no longer protected by vegetation.

Following deposition of the Post-European Settlement Aggradation (PESA) alluvium the stream cut down through the PESA materials into the Pooraka Formation, developing a deep trench-like channel, stranding the PESA materials high up on the banks. There is evidence of several phases of Post European Settlement Aggradation, based on included artefacts and the level of the PESA filling. At least two infills of younger PESA sediments (Fig. 10) occur within the channel, with the youngest containing plastic materials including bubble plastic. This material had previously in-filled parts of the channel to a depth of 1.5 m before renewed erosion. It is difficult to determine whether these changes were caused by settlement activities, or natural changes in flood periodicity and intensity.

Initial incision of the channel followed accelerated sedimentation associated with land clearance several decades after European settlement. Subsequently many other factors have influenced the sporadic erosion and sedimentation of the channel. Reduced bedloads and increased water yields following urbanisation have impacted on the study site channel as have engineering works such as channelisation and the construction of artificial knickpoints.

Although some of the charcoal in the PESA sediments may have derived from Aboriginal fires, such as that described by Adams (1902), there is no evidence to suggest that the accelerated erosion and aggradation were related to Aboriginal activities. Furthermore, the unburnt, 400 year old tree trunk may have lain around in the landscape for a very long time before being incorporated into the PESA sediments. This interpretation supports the views of Prosser (1990, 1991) who noted no increase in widespread aggradation associated with Aboriginal burning at Wangrah Creek in the Southern Tablelands of NSW. Prosser (1990) also noted no evidence for increased frequency of alluviation at the time of intensified land use.

A tantalisingly similar study was produced by Nelson (1965) from the Chemung River Valley of New York and Pennsylvania. He concluded that overbank deposition on the floodplain accelerated in recent geological time, mainly as a consequence of human interference. Clearing and cultivation increased runoff, erosion and flood heights resulting in higher stream sediment loads and more rapid overbank deposition on the floodplain. A piece of wood recovered 1.68 m from the surface and dated at 410±150 years BP indicated a sedimentation rate of 0.42 cm yr^{-1}. With the appearance of European debris there was a markedly increased rate of sedimentation to 1.7 cm yr^{-1}. Nelson (1965) largely attributed the impacts to European settlement but emphasised the agricultural role of the indigenous Indian inhabitants, who probably initiated the sequence of changes centuries ago.

The shallow channels eroded into the Pooraka Formation and the thick PESA sediments stranded high above the channel floor favour the view that the initiation of channel incision may be related to PESA deposition. This would have buried former shallow and vegetated channels, killed the stabilising vegetation and steepened gradients by deposition. Once initiated, various other factors would have contributed to channel erosion. It is possible that the later construction of a drain in the lower part of Dry Creek, downstream of the study site assisted further channel incision. An aerial photograph taken on 18/11/1935 (Fig. 3) shows the location of the artificial channel and reveals that the channel in the study site was incised prior to extensive urbanisation of the catchment. Consequently, increased runoff related to urbanisation can be dismissed as an initial cause of the channel incision, although it has subsequently been important in causing channel deepening and widening, as have the placement of the channel in concrete conduits and the construction of artificial knickpoints.

The sequence of events described here is similar to those discussed by Schumm (1977) who noted that there may be a sequence or cascade of consequences following initial clearing of catchments for pasture purposes. Such clearance results in accelerated soil erosion on hillslopes, resulting in aggradation along drainage lines that can not accommodate the available sediment load. Eventually, as the supply of erodible materials is exhausted, increased runoff from the valley side slopes continues and inevitably leads to downstream channel incision. Once the initial disturbance of hillslope clearance has occurred the switch from aggradation to incision could occur without further external influences.

Conclusions

Post-European Settlement Aggradation (PESA) sediments flanking the course of Dry Creek at Mawson Lakes are interpreted as the result of European agricultural practices during the period 1836-1860. Accelerated erosion on upland slopes was associated with sedimentation in the lower section of Dry Creek. Subsequently, in response to the sedimentation killing stabilising channel vegetation, channel incision was probably initiated as sediment yield reduced and runoff increased.

A tree trunk occurring at the unconformity between the Pooraka Formation and the PESA deposits dated at ~400 years BP, could be suggestive of Aboriginal

firestick farming activities. However, the discovery of European artefacts of the 1850s favours the view that Aboriginal practices were not responsible for the accelerated erosion and sedimentation in the Dry Creek drainage system. It is possible, however, that some of the charcoal from pre-European fires such as that described by Adams (1902) may have been incorporated into the PESA sediments.

Finally, a disturbing feature of urbanisation has been the loss of many significant geological sites, which have been destroyed or covered in the interests of aesthetics and/or public safety. Two such sites have been described in this paper. There is clearly a need for local government authorities and developers to consult with geologists prior to undertaking major 'restorative' works.

Acknowledgements

The paper was improved by the contributions of the referees Professor Martin Williams and Dr David Dunkerly. Funding for the radiocarbon date was provided by the University of South Australia. Chris Crothers drafted the diagrams.

References

ADAMS, J. W. (1902) "My Early Days in the Colony" (Published by his daughter, Sarah Tilley).

BEGIN, Z. B. & SCHUMM, S. A. (1984) Gradational thresholds and landform singularity: Significance for Quaternary Studies. *Quat. Res.* **21,** 267-274.

BOURMAN, R. P., MARTINAITIS, P., PRESCOTT, J. R., & BELPERIO, A. P. (1997) The age of the Pooraka Formation and its implications, with some preliminary results from luminescence dating. *Trans. R. Soc. S. Aust.* **121,** 83-94.

_____ & JAMES, K. (1995) Gully evolution and management: a case study of the Sellicks Creek drainage basin. *S. Aust. Geog. J.* **94,** 81-105.

MURRAY-WALLACE, C. V. & BELPERIO, A. P. (1995) Aminostratigraphy of Quaternary coastal sequences in Southern Australia - an overview. *Quat. Internat.* **26**, 69-86.

NELSON, J. G. (1965) Man and geomorphic processes in the Chemung River Valley, New York and Pennsylvania. *Assoc. Am. Geographers Annals* **56,** 24-32.

PROSSER, I. P. (1990) Fire, humans and denudation at Wangrah Creek, Southern Tablelands, NSW. *Aust. Geog. Studies* **28,** 77-95

_____ (1991) A comparison of past and present episodes of gully erosion at Wangrah Creek, Southern Tablelands, NSW. *Ibid* **29,** 139-154.

_____ & SLADE, C. J. (1994) Gully formation and the role of valley-floor vegetation, southeastern Australia. *Geology* **22,** 127-1130.

SCHUMM, S. A. (1977) "The Fluvial System" (John Wiley & Sons, New York).

_____ (1979) Geomorphic thresholds: the concept and its applications. *Institute of British Geographers* **4,** 485-515.

SHEARD, M. J. & BOWMAN, G. M. (1996) Soils, stratigraphy and engineering geology of near surface materials of the Adelaide Plains. *Mines and Energy South Australia, Report Book*, 94/9.

SHUEARD, H. & TUCKWELL, D. (1993) "Brewers and aerated water manufacturers in South Australia 1836-1936" (Swift Printing Services Pty Ltd., Stepney, South Australia).

TATE, R. (1879) The Anniversary Address of the President. *Trans. R. Soc. S. Aust.* **2,** xxxix-lxxv.

TWIDALE, C. R. (1968) "Geomorphology" (Thomas Nelson (Aust) Ltd, Melbourne)

WILLIAMS, G. E. (1969) Glacial age of the piedmont alluvial deposits in the Adelaide area, South Australia. *Aust. J. Sci.* **32,** 257.

A LATE PLEISTOCENE OCCURRENCE OF DIPROTODON AT HALLETT COVE, SOUTH AUSTRALIA

By N. S. Pledge, J. R. Prescott† & J. T. Hutton‡*

Summary

Pledge, N. S., Prescott, J. R. & Hutton, J. T. (2002) A late Pleistocene occurrence of Diprotodon at Hallett Cove, South Australia. Trans. R. Soc. S. Aust. 126(1), 39-44, 31 May, 2002.

Despite Diprotodon fossils occurring widely across Australia, until recently, few finds have been adequately dated. This is due to several reasons, primarily the inadequacies of the radiocarbon methods. New dating methods, which coincidentally increase the datable age range, have been developed in recent years. One of these is thermoluminescence (TL) dating. Yet there are still few reliably dated Diprotodon specimens because they must be found and dated in situ. A chance discovery in 1992 gave the authors an opportunity to test one of these new methods and at the same time solve a thirty year old mystery. An articulated portion of a Diprotodon skeleton found at Hallett Cove is associated with sediment TL-dated to about 55,000 years, and is also a possible source for a fossil tooth found on the nearby beach in 1971.

Key Words: Diprotodon, Hallett Cove, thermoluminescence dating, late Pleistocene.

Transactions of the Royal Society of S. Aust. (2002), **126**(1), 39–44

A LATE PLEISTOCENE OCCURRENCE OF *DIPROTODON* AT HALLETT COVE, SOUTH AUSTRALIA

by N. S. Pledge[1], J. R. Prescott[2] & J. T. Hutton[2]

Summary

Pledge, N. S., Prescott, J. R. & Hutton, J. T. (2002): A late Pleistocene occurrence of *Diprotodon* at Hallett Cove, South Australia. *Trans R. Soc. S. Aust.* **126**(1), 39–44, 31 May, 2002.

Despite *Diprotodon* fossils occurring widely across Australia, until recently, few finds have been adequately dated. This is due to several reasons, primarily the inadequacies of the radiocarbon methods. New dating methods, which coincidentally increase the datable age range, have been developed in recent years. One of these is thermoluminescence (TL) dating. Yet there are still few reliably dated *Diprotodon* specimens because they must be found and dated *in situ*. A chance discovery in 1992 gave the authors an opportunity to test one of these new methods and at the same time solve a thirty year old mystery. An articulated portion of a *Diprotodon* skeleton found at Hallett Cove is associated with sediment TL-dated to about 55 000 years, and is also a possible source for a fossil tooth found on the nearby beach in 1971.

Key Words: *Diprotodon*, Hallett Cove, thermoluminescence dating, late Pleistocene.

Introduction

Many specimens of *Diprotodon* have been found since its discovery by Major Mitchell in the Wellington Valley, NSW, in the early 19th Century, and precise ages for this, the largest known marsupial, have long been sought. Many, if not most, discoveries were made before the development of the C-14 method of radiometric dating. Others were demonstrably beyond the datable age range and radiocarbon dating of older material has been shown to be unreliable (Chappell *et al.* 1996; Roberts *et al.* 2001). Still others could not be dated for want of sufficient preserved carbon.

In 1992, Mr T. Westlake, whilst walking his dog in a newly designated council reserve at Hallett Cove (Fig. 1), 25 km south-southwest of the city of Adelaide, noticed what appeared to be a large white bone (Fig. 2) eroding out of an old exposure on a former private road. Closer examination supported this identification, and Mr Westlake subsequently informed the South Australian Museum, although he was sure that the relevant people would have known about it already. The occurrence was not known and a visit was immediately organised.

On 26 June, 1992, Mr Westlake guided the senior author and student Gavin Prideaux to the site, an old road-cutting through a spur of hillside overlooking the Field River, not far from the beach at Hallett Cove (about 35° 4′ 9″ South, 138° 29′ 8″ East). The bank was more than 2 m high, and the bone was exposed about 1.5 m below the top and about 2 m above the surface of the nearby bridge. Across the road, the hillside fell steeply to the river about 5 m below. The bone was examined *in situ* and appeared to be part of the pelvis of a large animal and, because it was fossilised and so large, probably of a diprotodontid. With some difficulty, the bone was excavated without greatly enlarging the cutting and plaster-jacketted for transport.

Materials and Methods

The jacket containing the specimen was opened in the laboratory and the sediment removed from around the bone by scraping with a small dental tool, often when the soil had been softened with water. The bone was hardened piecemeal during this process, using a dilute solution of Bedacryl® in acetone. The stratigraphic section was measured after the excavation, using a tape-measure. Other measurements were made by vernier caliper or ruler, as warranted.

Sampling for thermoluminescence (TL) dating (Aitken 1985; Wintle 1997) was carried out by Prescott and Hutton and several graduate students from the University of Adelaide Physics Department on 28 August, 1992 (Fig. 4).

Three horizontal auger holes were drilled into the bank (Fig. 5) to bracket vertically the position of the bones, which had been removed earlier. TL samples FRTS/0.9, FRTS/1.5 and FRTS/2.1 were collected for laboratory analysis, at depths below the top of the cutting of 0.9 m, 1.5 m, and 2.1 m, respectively. *In situ* gamma ray spectrometer measurements were made in the same holes from which the TL samples were collected, at about 0.5 m depth into the exposed face of the cutting.

[1] South Australian Museum, North Terrace, Adelaide S.A. 5000.

[2] Department of Physics and Mathematical Physics, The University of Adelaide SA 5005.

Dr John Hutton died during the early stages of preparation of this paper.

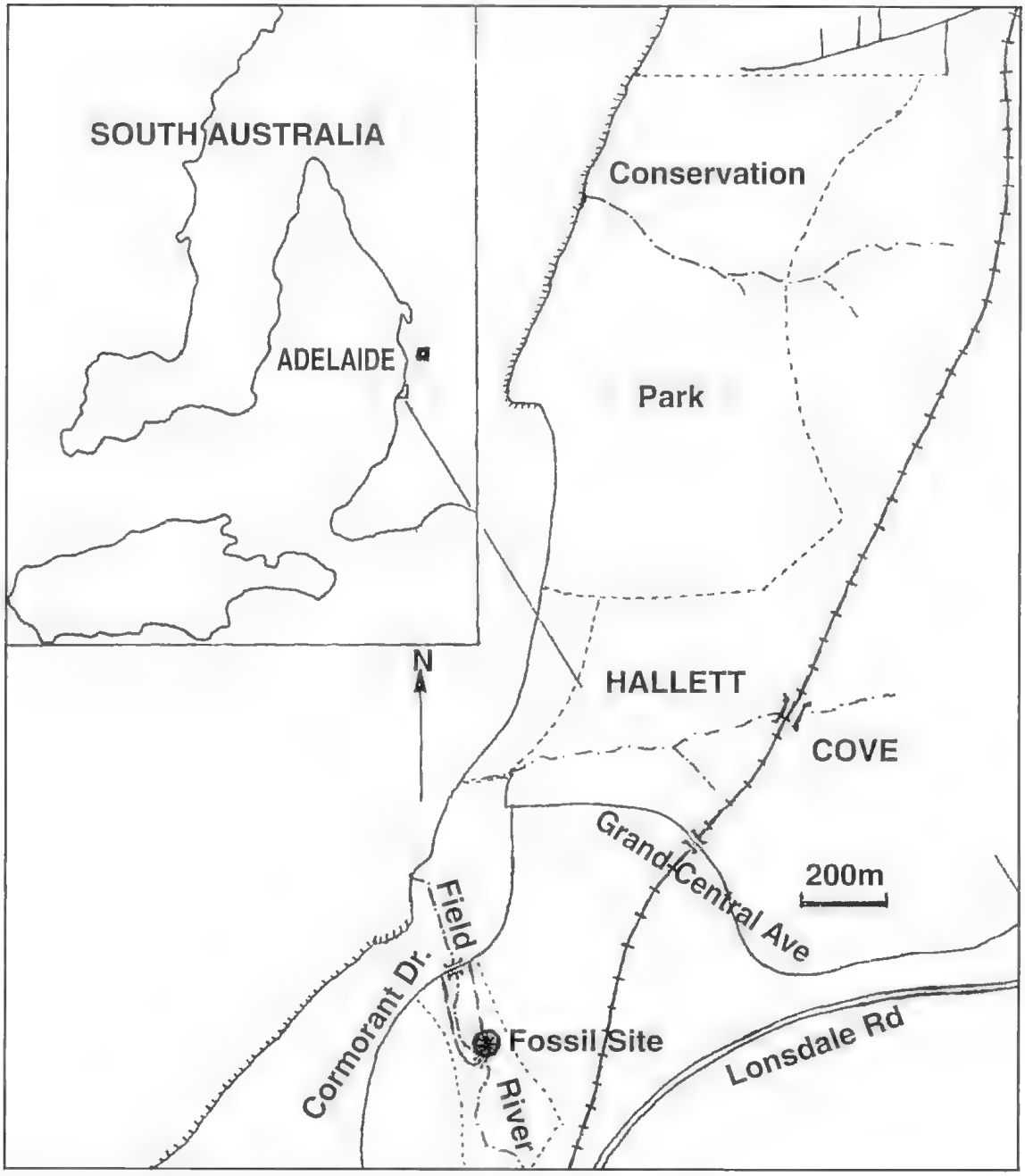

Fig. 1. Locality map; the fossil site is in a council reserve on the Field River.

Gamma ray spectrometry gives a direct measure of the radiation dose rate due to gamma radiation under prevailing field conditions and subsequent data analysis gives the concentrations of K, U and Th. These are then used for calculating the total dose rates from radiation in the environment, and for comparison with independent measurements in an assessment of the likelihood of radioactive disequilibrium in the deposits.

The age is calculated from the *age equation*:

$$\text{age (ka)} = \frac{\text{Equivalent dose (Gy)}}{\text{dose rate (Gy/ka)}}$$

where doses are measured in grays (Gy) and ages in kiloyears (ka).

Quartz grains in the 90–125 μm size range were extracted from the samples by standard procedures (Huntley *et al.* 1993).

The *selective bleach* method was used to find the

Fig. 2. The fossil bone as initially exposed in sandy lens between gravel layers. Hammer is 300 mm long.

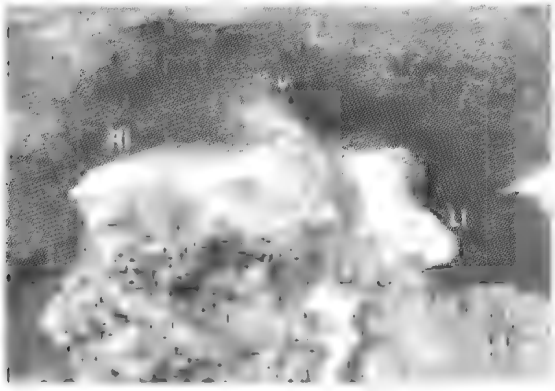

Fig. 3. The excavated *Diprotodon* pelvis, *in situ*. The skeletal fragment is upside down, anterior into the bank. The card by the hammer handle is 90 x 55 mm. IL left ischium; RI right ilium; V vertebrae.

Fig. 4. *Diprotodon* fossil site, general view, eastwards. Field River at right. Preparations being made for thermoluminescence dating by Adelaide University Physics Department staff and students; the late Dr John Hutton second from right, Prof. John Prescott at right.

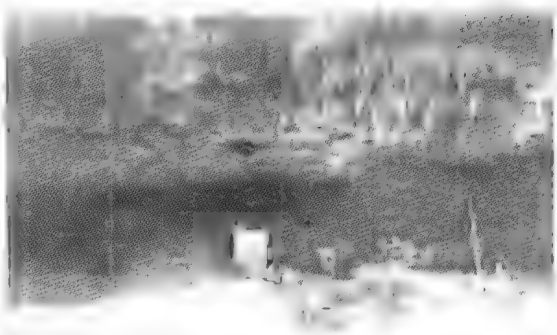

Fig. 5. Hallett Cove thermoluminescence sampling sites showing general stratigraphy, central hole is at the fossil horizon. *In situ* gamma ray scintillation counting is taking place in the lowest hole.

equivalent doses (Prescott & Mojarrabi 1993). This method was developed to reduce the uncertainty in the level of solar bleaching, which resets the TL clock. The protocol uses optical filters to select the rapidly bleached component of the TL. The equivalent dose is determined by comparing the natural TL signal with one generated in the laboratory by a standard radioactive source. The specific method is known as 'The Australian Slide' (Prescott *et al.* 1993).

Results

The fossils

The main specimen was found to comprise parts of both left and right pelves still articulated with the sacral vertebrae, plus an adjoining lumbar vertebra and a fragment of the first caudal (SAM P33487) and is considered to represent the giant marsupial *Diprotodon* Owen 1839 (Fig. 3).

The pelves form a fairly flat plate at a slight angle to the vertebral axis. The acetabulum diameter is about 100 mm, the semi inter-acetabular width (right side) is about 200 mm, the sacral length about 150 mm and the ischio-iliac length is about 440 mm. The vertebrae are not well preserved except for their neural arches; a lumbar vertebra has a centrum with a transverse diameter of about 80 mm and length of 60 mm. These measurements are within the range of specimens of *Diprotodon* spp. from Lake Callabonna in the collections of the South Australian Museum and, after comparison with the pelvis of a skeleton displayed in the South Australian Museum, the Hallett Cove specimen is considered to be a subadult or female individual. Specific identity is not possible on the material preserved.

Preservation is not good. The bones are not

petrified, being rather chalky, leached and unmineralised and held together largely by the supporting sandy loam. This circumstance proved to be both a help and a hindrance during the preparation of the specimen, as the bone was fairly easily cleaned but had to be consolidated and strengthened during the process because it would not support much weight. The specimen is consequently fragile with numerous fine cracks presumably associated with soil movement. The lower surface of the specimen in the sediment (the animal's dorsal side) is fairly complete with only some crushing of high points such as the dorsal processes of the neural arches. The opposite surface is less well-preserved with much missing bone and irregular ends, presumably where exposed, unburied parts had been eroded by the elements or incoming sediment. Although soft and susceptible to later damage, no cut marks, either from scavenger teeth or hunter's tools, were seen on any bone but no limb bones, which might have been a more attractive target, are present.

In the process of excavation, a few more bones were found in close association with the pelvis. One of these bones, a fragment of immature left mandible (SAM P35074), supported the identification of the pelvis as *Diprotodon*. This specimen, from which erupting cheek-teeth had fallen leaving only a barely worn incisor, is only 42 mm deep at the first molar alveolus, as compared to 100–110 mm or more in adult animals. Fragments of a little-worn M_1 of *Diprotodon* were also found. Another bone was of a large kangaroo, *Macropus*? sp. Several shells of small saxicolous land snails, *Succinea australis* Pérussac, 1821 (Succineidae) and *Pericharistix ardeni* Iredale, 1937 (Helicarionidae) (R. Hamilton-Bruce, pers. comm. 6 July 2001), apparently the first recorded fossil occurrence of these species in Australia), occur in the fine sediment surrounding the bones, together with fragile moulds of fine stems such as are seen in *Chara*-limestones in modern stream-pool deposits.

Geology

The fossiliferous sequence appears to be a marginal facies of the Pooraka Formation, recently redated by Bourman *et al.* (1997). Much of the *Diprotodon* skeleton had been lost, either by disarticulation or erosion before complete burial, or as a result of road-building excavations. The remaining bones lay upside-down in a shallow depression filled with poorly-sorted coarse sand, on a bed of somewhat current-imbricated pebbles of Precambrian sandstone and shale of apparently local origin (Fig. 3). The sandy horizon is lenticular and extends several metres on either side of the bones before pinching out. The pebbles, ranging up to some 5 cm in diameter, occur in beds 10 to 30 cm thick above and below the sand and are subangular to subrounded. Similar beds, alternating with sandier horizons, occur throughout the sequence exposed in the cutting. Bedrock of steeply-dipping, slightly metamorphosed Proterozoic slates and quartzites occurs within 10 m laterally, and evidently forms part of the original valley wall.

The stratigraphic sequence at the site of the bones is summarised below.

Soil – at least 0.5 m at top of cutting.

Flaggy, sheety, calcrete-cemented coarse gravel, pale brown—0.55 m.

Marly silty sand, pale pinkish buff—0.30 m. TL sample FRIS/0.9.

Fine (up to 10 mm) bedded gravel lens, becoming coarser to east and west, buff—0.10 m.

Marly silty sand, pale buff—0.20 m, pinching out laterally. Bones and saxicolous snails within this interval. TL sample FRIS/1.5.

Coarse gravelly sand, angular clasts up to 50 mm, roughly imbricated, light brown—0.20 m, thickening either side.

Brown silty clay – no base seen. Estimated depth to bridge level 1 to 2 m. TL sample FRIS/2.1 near top of this unit (see Fig.5). Height of bridge above standing water level about 3 m.

Age

Unfortunately, the quartz TL sometimes reaches dose saturation at a relatively low dose level and here, the two deepest samples, FRIS/1.5 and FRIS/2.1 were approaching this saturation. A consequence is the relatively large uncertainty in the age of FRIS/1.5. A pilot measurement on FRIS/2.1 showed that it was unlikely to yield a date for the same reason and so dating was not attempted. The pilot result is consistent with this sample being the oldest of the three.

Elemental analyses were obtained from field

TABLE 1. *Components of the age calculation and the ages for the two dated samples.*

sample	Lab. Code	equivalent Dose (Gy)	Dose-rate (Gy ka^{-1}) scint	Dose-rate (Gy ka^{-1}) XRS, NAA, alpha	averaged age (ka)
FRIS/0.9	AdTL94001	83±9	1.94±0.07	1.84±0.06	44±5
FRIS/1.5	AdTL94002	147±19	2.70±0.09	2.65±0.09	55±7
FRIS/2.1			2.75±0.11	2.94±0.15	

gamma ray scintillometry for K, U and Th; by X-ray spectrometry (XRS) for K; and by thick source alpha particle counting (TSAC) for U and Th. The thorium concentration was checked by neutron activation analysis (NAA) for FRTS/0,9 and FRTS/1,5. Good agreement among the methods indicates that, within the uncertainties of measurement, there is no radioactive disequilibrium in the samples.

Table 1 shows the components of the age calculation and the ages for the two dated samples.

Discussion and Interpretation

Comments on Table 1

The equivalent dose and its error are output from a statistical fitting programme. The errors are relatively large because the inherent variability of quartz TL and the near dose-saturation of the TL make precise curve-fitting problematic. For FRTS/0,9, the fitting programme encountered no difficulties and there was a satisfactory dose plateau. Sample FRTS/1,5 was quite close to dose saturation and has a somewhat larger uncertainty.

There are two independent values for the dose rate: (1) field gamma ray scintillometry and (2) XRS for K, NAA for Th, thick source alpha counting for U. The agreement between them is gratifying. A contribution from cosmic rays is included (Prescott & Hutton 1994). Although no equivalent dose (and no age) was measured for FRTS/2,1, the dose-rate data are included for completeness.

The error in age is determined almost exclusively by the uncertainty in the equivalent dose. The equivalent dose and age of FRTS/0,9 are well described by the quoted figures. For FRTS/1,5 the dose curve is approaching saturation. Although the error quoted for the equivalent dose is objectively found by the fitting procedures, the error limits in the age are asymmetric. This asymmetry lies within the limits shown in the table which are one standard error. At 95% confidence, with allowance for this asymmetry, the age lies within the interval 42–70 ka.

Systematic errors include variability of water content, because the dose rate depends on this. In keeping with Adelaide laboratory practice, the age is quoted for the observed water content (18% of dry weight for the whole profile). How much it may have varied in the past is a matter of professional judgement. For all levels at this site, a 1% increase in water results in a 1% decrease in dose rate. Thus, if the average water content in the past had been 1% higher, then the dose rate and the measured equivalent dose would have been lower and the present-day age estimate would be 1% low. Cosmic ray variability provides another possible source of systematic error but, at this site, it is of no consequence.

Geological history

Some 100 000 years ago, when world sea-levels were much lower and the Gulf St Vincent was a broad plain drained by the ancient River Vincent that flowed to join the River Murray to the east of the future Kangaroo Island, the ancestral Field River had a steeper gradient, and had cut a gorge back into the face of the Mt Lofty Ranges. As the sea rose from this lower level, the river's gradient decreased (and rainfall may also have decreased) and the gorge began to silt up.

It appears that, possibly during a local flash-flood some 55 thousand years ago, a *Diprotodon* died and was swept downstream with other bones that had been picked up along the way, until the stream velocity dropped and/or the carcass reached an ephemeral pool where it settled. Sand from the final flush of flood water came to rest on and around the body, which was not completely buried. The pool silted up and exposed bone disintegrated under the effects of the elements (Behrensmeyer 1978) and possibly scavengers. Later, another flood brought a layer of gravel, in a process that was to be repeated for centuries as the valley gradually filled with sediment.

The present gorge/valley was probably incised in the older sediments by a rejuvenated stream at the height of the last glacial maximum, when the gradient was again increased, or in the early Holocene, when rainfall increased. It is possible that the very tumbled and beach-rolled isolated *Diprotodon* molar, found in 1971 by nine year-old Jonathon Dicker (Anon. 1971)[1] in beach gravels at the mouth of the Field River, was washed out at this time, but it is more likely that it was uncovered during the road-building operation earlier in the 20th Century and bull-dozed into the creek, to be carried by flood-waters to the sea.

The site of the *Diprotodon* bones has since been marked with a small cairn and plaque by the Hallett Cove Progress Association.

The age of this specimen, as presented here, is close to that of the putative arrival of the first Aborigines in Australia (Thorne *et al.* 1999; but see Bowler & Magee 2000; Gillespie & Roberts 2000). A human factor has been suggested in the Australian megafaunal extinction (Flannery 1994), either by direct hunting or by environmental modification, and certain sites, e.g. Cuddie Springs, northwestern New South Wales (Field & Dodson 1999), have been claimed to show evidence of interaction between humans and megafauna; this has been challenged for Cuddie Springs (Roberts *et al.* 2001). The Hallett

[1] ANON. 1971. Boy finds ancient tooth at beach. *The Advertiser*, 31 May.

Cove specimen gives no indication of butchery, nor indeed of scavenging, with the remaining bones still articulated. It cannot therefore be used as evidence either way.

Conclusions

Fossil bones found in Quaternary sediments in the bank of the Field River, Hallett Cove, represent the partial skeleton of, probably, an immature *Diprotodon*, which was buried in an overbank deposit of the ancestral stream. Thermoluminescence dating of the sediments has given an age of between 42–70 thousand years before present at the 95% confidence level. This is close to the proposed date (Roberts *et al.* 2001) of 46 400 years BP for the megafaunal extinction event in Australia. However, there is no indication of a human factor involved in the death of this animal.

Acknowledgments

We thank the following for their help in the field and the laboratory: B. J. McHenry, J. A. McNamara, G. J. Prideaux, P. Stamatelopoulos and T. Westlake. The project was assisted by a grant to JP from the Australian Institute of Nuclear Science and Engineering.

References

AITKEN, M. J. (1985) "Thermoluminescent Dating" (Academic Press, London).

BEHRENSMEYER, A. K. (1978) Taphonomic and ecologic information from bone weathering. *Paleobiology* **4**, 150–162.

BOLTMAN, R. P., MARTINAITIS, P., PRESCOTT, J. R. & BELPERIO, A. P. (1997) The age of the Pooraka Formation and its implications, with some preliminary results from luminescence dating. *Trans. R. Soc. S. Aust.* **121**, 83–94.

BOWLER, J. M. & MAGEE, J. W. (2000) Redating Australia's oldest human remains: a sceptic's view. *J. hum. Evol.* **38**, 719–726.

CHAPPELL, J., HEAD, J. & MAGEE, J. (1996) Beyond the radiocarbon limit in Australian archaeology and Quaternary research. *Antiquity* **70**, 543–552.

FIELD, J. & DODSON, J. (1999) Late Pleistocene megafauna and archaeology from Cuddie Springs, Southeastern Australia. *Proc. Prehist. Soc.* **65**, 275–301.

FLANNERY, T. F. (1994) "The Future Eaters: an ecological history of the Australasian lands and people" (Reed, Sydney).

GILLESPIE, R. & ROBERTS, R. G. (2000) On the reliability of age estimates for human remains at Lake Mungo. *J. hum. Evol.* **38**,727–732.

HUNTLEY, D. J., HUTTON, J. T. & PRESCOTT, J. R. (1993) The stranded beach-dune sequence of south-east South Australia: a test of thermoluminescence dating, 0–800 ka. *Quat. Sci. Revs* **12**, 1–20.

PRESCOTT, J. R., HUNTLEY, D. J. & HUTTON, J. T. (1993) Estimation of equivalent dose in thermoluminescence dating—the 'Australian slide' method. *Ancient TL* **11**, 1–5.

_____ & HUTTON, J. T. (1994) Cosmic ray contribution to dose rates for luminescence and ESR dating. *Radiation Measurements* **23**, 497–500.

_____ & MOJARRABI, B. (1993) Selective Bleach—An improved 'partial bleach' method of finding equivalent doses for thermoluminescence dating of quartz. *Ancient TL* **11**, 27–30.

ROBERTS, R. G., FLANNERY, T. F., AYLIFFE, L. K., YOSHIDA, K., OLLEY, J. M., PRIDEAUX, G. J., LASLETT, G. M., BAYNES, A., SMITH, M. A., JONES, R. & SMITH, B. L. (2001) New ages for the last Australian Megafauna: continent-wide extinction about 46,000 years ago. *Science* **292**, 1888–1892.

THORNE, A., GRUN, R., MORTIMER, G., SPOONER, N. A., SIMPSON, J. J., MCCULLOCH, M., TAYLOR, L. & CURNOE, D. (1999) Australia's oldest human remains: age of the Lake Mungo 3 skeleton. *J. hum. Evol* **36**, 591–612.

WINTLE, A. G. (1997) Luminescence dating: laboratory procedures and protocols. *Radiation Measurements* **27**, 769–817.

ASPECTS OF THE SURVIVAL AND REPRODUCTION OF ANGUINA MICROLAENAE (NEMATODA: ANGUINIDAE)

By Primali de Silva & Ian T. Riley†*

Summary

De Silva, P. & Riley, I. T. (2002) Aspects of the survival and reproduction of Anguina microlaenae (Nematoda: Anguinidae). Trans. R. Soc. S. Aust. 126(1), 45-49, 31 May, 2002.

Leaf galls formed by Anguina microlaenae in Microlaena stipoides were found, upon rehydration from natural dessication, to contain adults, eggs and juveniles that had survived anhydrobiotically. The sex ratio of adults in galls, excluding a proportion of galls that contained only females, was 1:1. Females in galls containing only females were apparently sterile as eggs were not present. Rehydrated eggs hatched over a temperature range 8-25° C with an optimum of about 20° C. Only limited egg production and deposition were observed in rehydrated females incubated after removal from their galls.

Key Words: Nematoda, Anguina microlaenae, dormancy, survival, anhydrobiosis, reproduction, sex ratios.

Transactions of the Royal Society of S. Aust. (2002), **126**(1), 45-49.

ASPECTS OF THE SURVIVAL AND REPRODUCTION OF *ANGUINA MICROLAENAE* (NEMATODA: ANGUINIDAE)

by PRIMALI DE SILVA[1] & IAN T. RILEY[1]

Summary

DE SILVA, P. & RILEY, I. T. (2002) Aspects of the survival and reproduction of *Anguina microlaenae* (Nematoda: Anguinidae). *Trans. R. Soc. S. Aust.* **126**(1), 45-49, 31 May, 2002.

Leaf galls formed by *Anguina microlaenae* in *Microlaena stipoides* were found, upon rehydration from natural desiccation, to contain adults, eggs and juveniles that had survived anhydrobiotically. The sex ratio of adults in galls, excluding a proportion of galls that contained only females, was 1:1. Females in galls containing only females were apparently sterile as eggs were not present. Rehydrated eggs hatched over a temperature range 8–25° C with an optimum of about 20° C. Only limited egg production and deposition were observed in rehydrated females incubated after removal from their galls.

KEY WORDS: Nematoda, *Anguina microlaenae*, dormancy, survival, anhydrobiosis, reproduction, sex ratios.

Introduction

Among the Nematoda, members of the family Anguinidae have remarkable abilities to survive anhydrobiotically (Antoniou 1989). Second stage juveniles (J2s) of *Anguina tritici* (Steinbuch 1799) Filipjev, 1936 are known to survive for more than 30 years under dry conditions (Limber 1973). For most anguinid nematodes the survival stage is also the invasive stage and is a second, third or fourth stage juvenile, depending on the species (Chizhov & Subbotin 1985). In two leaf gall species, *Anguina australis* Steiner 1940 from *Ehrharta longiflora* Sm. (Riley *et al.* 2001) and *Anguina danthoniae* (Maggenti *et al.*) Breski 1981 (syn. *Cynipanguina danthoniae* Maggenti, Hart & Paxman 1974) from *Danthonia californica* Bol. (Maggenti *et al.* 1973), the adults are the survival stage. For these species it is not known if the invasive juvenile stage can also survive anhydrobiotically.

Anguina microlaenae (Faweett 1938) Steiner 1940, a leaf gall nematode of the Australian native grass, *Microlaena stipoides* (Labill.) R. Br., differs from most anguinid nematodes in that both eggs and J2s (although J2s were considered to be J1s at the time) are reported to survive anhydrobiotically within senescent galls (Faweett 1938). Our examination of the contents of galls formed by *A. microlaenae*, revealed that adults also survived desiccation. Given this observation and the limited details of the survival of eggs provided by Faweett (1938), further investigation of the survival of *A. microlaenae* was undertaken. The investigation included examination of (1) revival of adults and juveniles of *A. microlaenae* following rehydration of the contents of naturally desiccated galls, (2) hatching of rehydrated eggs over a range of temperatures and of different development stages and (3) egg production and deposition in rehydrated adults.

[1] Applied and Molecular Ecology, Waite Campus, The University of Adelaide, Glen Osmond SA 5064, Australia.
Corresponding author, Email: ian.riley@adelaide.edu.au

Materials and Methods

Source of galls

Galls formed by *A. microlaenae* in *M. stipoides* were obtained from two sources: (1) a field population collected in September 1999 from Toowoomba, Queensland (27° 34′ S 151° 57′ E) and stored at room temperature until used for this study (February–May, 2001); (2) a cultured population collected in February 2001 from infected *M. stipoides* grown in a shade house at the Waite Campus, Adelaide, South Australia (34° 58′ S 138° 38′ E). The cultured population was established in June 1999 from galls collected at the same site in Toowoomba; thus the two populations were of the same provenance.

Contents of galls and revival of adults and juveniles following rehydration

Twenty galls each from the field and cultured populations were dissected under water with the aid of a stereo microscope. Following incubation for 24 h at 20° C, counts were made of the adult female and male nematodes, eggs and J2s and the viability of adults and juveniles was assessed. Adults and juveniles were scored as alive if they were turgid and exhibited movement; some viable but stationary individuals may have been excluded and so the count was a conservative estimate.

Effect of temperature and egg development stage on hatching of rehydrated eggs

Eggs containing clearly developed juveniles were

incubated in shallow water (about 2.5 mm deep, adjusted for evaporation daily) in covered glass dishes at various temperatures and examined daily for hatching over 7 days. Five replicates from both field and culture populations of about 25 eggs per dish were incubated at 8, 16, 20, 25, 31° C, respectively. Observations were not continued beyond 7 days due to fungal colonisation, a problem also noted by Fawcett (1938). Also, five replicates of about 25 immature eggs were incubated at 20° C for 7 days and observed daily.

Egg production and deposition by rehydrated adult females

Adults from freshly dissected galls were placed alone or in pairs in shallow water in covered glass dishes as follows; (1) a female from a gall without males, unpaired (2) a female from a gall with no males, paired with a male, (3) a young adult female from a gall with males, paired with a male and (4) an older adult female from a gall with males, paired with a male. Young adult females were relatively more active and only slightly curved in comparison to older females, which were more obese, less active and spirally coiled. Each combination was replicated ten times and incubated at 20° C for 21 days. The females were examined every 2 days for egg development and deposition. In a separate experiment, a further 10 adult females from galls with males were incubated alone in Petri dishes on 1.5% water agar at 20° C and examined daily for egg production and deposition over 10 days.

Statistical analyses

GENSTAT 5 (Lawes Agricultural Trust, Rothamsted Experimental Station) was used for statistical analyses.

Results

The contents of the galls from the two populations are summarised in Table 1. The populations did not differ statistically (*t* test, 38 df) in any attribute other than the number of juveniles per gall. As the distributions of the eggs, juveniles and total progeny counts were not normal, these were transformed (log $e+1$) for analysis. The number of juveniles per gall in the field population was less than in the cultured population (mean log(e+1) of 0.704 v. 1.298, t = 2.16, 38 df, p = 0.037), indicating that these galls may have been collected at a slightly earlier stage of development but the contents of the galls of the two populations were otherwise equivalent in quantitative terms.

Eight galls from the two populations (20% of galls) contained females but no males (Table 2). There were no eggs or J2s in these galls. Excluding these galls with only females, the proportion of females per gall was 0.54 across both populations, which did not differ statistically from an expected ratio of 1:1. Not only was the mean ratio close to 1:1, but also all galls with both females and males contained combinations close to that ratio (Table 2).

TABLE 1. *Contents of leaf galls formed by* Anguina microlaenae *in* Microlaena stipoides *from two sources (n = 20)*

	Field Population Mean±SE (Range)	Cultured Population Mean±SE (Range)
Females	2.1±0.29 (1-6)	2.4±0.29 (1-6
Males	1.2±0.23 (0-4)	2.0±0.37 (0-6)
Adults	3.2±0.42 (1-8)	4.4±0.62 (1-12)
Female:Male	0.7±0.05 (0.5-1)	0.6±0.04 (0.4-1)
Eggs	286±64 (0-734)	74±18 (0-234)
Juveniles	151±4.3 (0-58)	81±22(0-321)
Total Progeny	301±67 (0-792)	155±37(0-555)

TABLE 2. *Number of leaf galls in* Microlaena stipoides *with various combinations of adult* Anguina microlaenae

Females per gall	Males per gall 0	1	2	3	4	5	6	Total
1	3	10	-		-	-	-	13
2	2	6	7	-	-	-	-	15
3	2	-	2	2	1	-	-	7
4	-	-			2	-	-	2
5	-	-		-	-	1	-	1
6	1	-		-	-	-	1	2
Total	8	16	9	2	3	1	1	40

- combination not found

Regression analysis (excluding galls with only females) did not reveal any significant relationships between the number of progeny per gall and the number of females, males or total adults in the gall. However, significant negative relationships were found between the number of progeny per adult (male, female or total) and the number of females, males and adults in the gall. Correlation coefficients ranged from -0.408–0.279 and probabilities of the regression coefficients from 0.02–0.03. Although only explaining a small proportion of the observed variation, these analyses indicate that the fecundity of the nematode was limited more by the resources available within the gall than the number of adults present because as the number of adults increased in the gall, the number of progeny did not increase proportionally.

All adults dissected from the galls recovered when rehydrated, were turgid and moved, albeit relatively little. Similarly, after rehydration it was estimated that 65-75% of the juveniles were alive, exhibiting the vigorous movement typical of invasive stage anguinid juveniles.

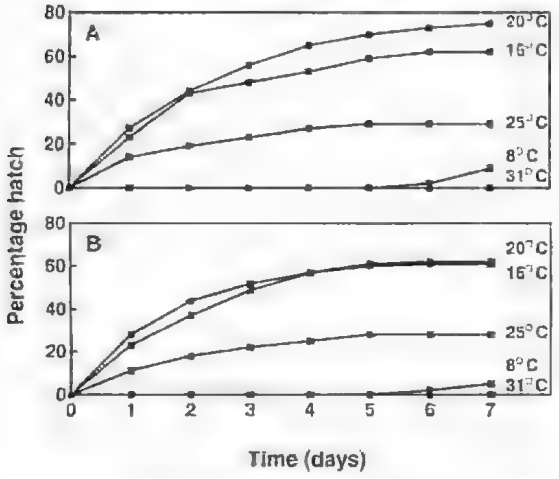

Fig. 1. Mean accumulative percentage hatch of *Anguina microlaenae* eggs (late development stage) incubated at various temperatures over a seven day period (n=5). A. Eggs from leaf galls from a field population of *Microlaena stipoides* collected at Toowoomba, Queensland ($LSD_{5\%}$ Day 7 = 9.8). B. Eggs from *M. stipoides* grown in pots at the Waite Campus, South Australia with inoculum from the same Toowoomba site ($LSD_{5\%}$ Day 7 = 12.0).

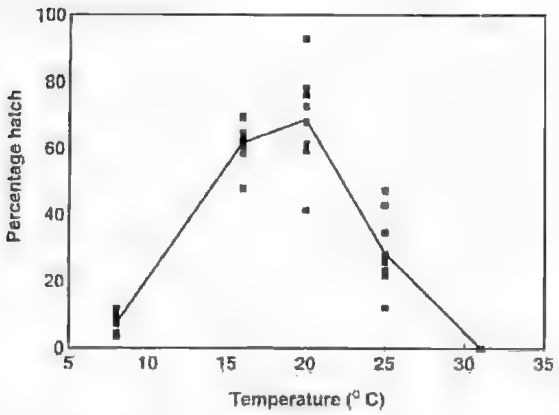

Fig. 2. Mean total percentage hatch of *Anguina microlaenae* eggs (late development stage) incubated at various temperatures for 7 days (n = 10, $LSD_{5\%}$ = 7.47).

Eggs rehydrated at a late stage of development were shown to have the ability to survive anhydrobiotically with 60–70% hatching when incubated at 16 or 20° C. Accumulative hatching of eggs over the seven day period for each temperature and population is shown in Fig. 1 and total hatching at each temperature in Fig. 2. There was no statistically significant difference between the two populations at any temperature or time. Temperature, however, had a marked effect on hatching. Maximum mean hatching of 69% occurred at 20° C but this did not differ significantly from the mean hatching rate of 62% at 16° C ($LSD_{5\%}$ = 7.5). At higher temperatures hatching was either significantly suppressed (24° C) or did not occur (31° C). At 8° C hatching was not observed until the 6th and 7th days and then only approached 10%.

Only limited hatching was observed from eggs rehydrated at an early development stage (embryonic) when incubated at 20° C. Hatching began after 5 days and was seen in four of the five replicates reaching 7–16% in 7 days.

Attempts to observe egg development and deposition in adults removed from the galls were largely unsuccessful. About half the adults were colonised by fungi (unidentified) over the three week period. Only two females, both from the group of older females taken from galls with males (combination 4), were found to have deposited any eggs; one a single egg and the other two eggs. Females incubated on agar were more prone to fungal colonisation with most females being colonised within a week.

Discussion

The study has shown that adults, eggs and J2s of *A. microlaenae* are able to survive anhydrobiotically. Although all adults survived desiccation, survival of eggs was only about 70% for those approaching maturity and considerably less for immature eggs. However, given that some immature eggs developed and hatched upon rehydration, it is possible that the lower observed survival rate of eggs reflected the incubation conditions and fungal colonisation rather than the intrinsic survival rate. Similarly, only about 70% of juveniles appeared to survive desiccation. The survival rate might have been greater if intact galls had been soaked before dissection to effect a slower uptake of water.

Our finding that adults survive desiccation differs from Fawcett's (1938) observation that adults died rapidly when galls became dry. This inconsistency may be due to the condition of the adults at the time of desiccation. If the reserves of the females had been largely exhausted by production of eggs, these adults might not have been able to survive desiccation. However, Fawcett records that the adult females had deposited 150 to 400 eggs each, which is consistent with our material, so this explanation seems unlikely. Also, we found in our material that all adults had survived, including those from galls containing large numbers of progeny. An alternative explanation may lie in differences in the rate of drying or the storage conditions. Our material either dried naturally as the host plant senesced or was air dried indoors before being stored for up to 15 months under laboratory conditions. This treatment would

not particularly favour the survival of the adults or explain the different findings. There is no obvious explanation for these contradictory findings.

Anguina microlaenae, with its capacity for adults, eggs and juveniles to survive anhydrobiotically, is unusual amongst anguinid nematodes as most have only a single survival stage. However, multiple survival stages are reported (with limited details) for *Mesoanguina amsinckia* (Steiner & Scott 1935) Chizhov & Subbotin 1985 and *Subanguina radicicola* (Greef 1872) Paramonov 1967. Womersley (1987) indicates that all stages of *M. amsinckia* survive anhydrobiotically, but cites the report of Pantone & Womersley (1968) which makes no mention of this behaviour. All stages of *S. radicicola* are said to 'hibernate' over winter in root galls (Krall 1991), although this dormancy may not be anhydrobiosis. It is conceivable that multiple survival stages, as in *A. microlaenae*, represent a transitional pattern between species with anhydrobiotic juveniles and those with anhydrobiotic adults. However, a recent molecular phylogeny of the Anguinidae (S. Subbotin pers. comm. 2001) provides no support for such a proposition.

To be of selective advantage, the survival of adult females, which have no further opportunity to feed, should facilitate continued reproductive activity. Our failure to demonstrate any significant egg production in adult females removed from galls and rehydrated may be a result of unsuitable experimental conditions. Reproductive activity is more likely to continue in rehydrated intact galls, as occurs in *A. australis* (Riley *et al.* 2001). However, given that eggs and juveniles are present in highly variable numbers before desiccation, it would be difficult to demonstrate further egg production in rehydrated intact galls.

Similarly, the survival of males points to the likelihood of further insemination after revival from anhydrobiosis, a behaviour know to occur in *A. thanthoniae* (Maggenti *et al.* 1973). Given the moderately large number of eggs deposited by anguinid females, multiple mating events are likely as male nematodes are known to produce relatively low numbers of sperm (Maggenti 1981). As noted by Fawcett (1938), and confirmed by our observation that females in galls without males did not reproduce, *A. microlaenae* only reproduces sexually, so survival of males is consistent with the possibility of reproductive activity following dormancy.

The other notable finding is the range of temperature for hatching. Although it appears that hatching is favoured by temperatures of about 16–20° C, hatching of *A. microlaenae* occurred outside this range. In contrast, reproduction of *A. australis* only occurred at about 20° C, although the temperature requirements for hatch were not separately determined (Riley *et al.* 2001). *Anguina microlaenae* has been found in sites from the temperate climate of Victoria (Fawcett 1938) with winter-dominant rainfall, through to the subtropical climate of southern Queensland with summer-dominant rainfall (this study). In contrast, *A. australis* is only known from the Mediterranean climatic zone of Western Australia. The broader temperature response of *A. microlaenae* is consistent with its wider distribution.

The occurrence of galls containing only females and the absence of galls containing only males does not appear to have been due solely to chance, as the same was found for *A. australis* (Riley 2001). It is possible that this occurrence is indicative of a mechanism such as galls only being initiated by genetically female J2s or an environmental sex determination.

Further study of the survival of immature eggs and post-dormancy reproductive behaviour of *A. microlaenae* is needed, but given the constraints imposed by fungus associated with the galls, progress in this area may require using a fungicide with no toxic or physiological effect on the nematode.

Acknowledgments

Drs K. Owen and P. Williamson are thanked for collecting infected plant material from Toowoomba. The salary of L. T. Riley is in part funded by the Grains Research and Development Corporation.

References

Andrássy, I. (1989) Arrested development in plant parasitic nematodes. *Helminthol. Abst. (Ser. B)* **58**, 1–19.

Chizhov, V. N. & Subbotin, S. A. (1987) Revision of the nematode subfamily Anguininae (Nematoda, Tylenchida) on the basis of their biological characteristic pp. 5–18 *In* Fortuner, R. (Ed.) "English translations of selected taxonomic papers in nematology Vol. 4." (California Department of Food and Agriculture, Sacramento CA, USA).

Fawcett, G. S. G. M. (1938) A disease of the Australian grass *Microlaena stipoides* R. Br. caused by a nematode *Anguillulina microlaenae* n. sp. *J. Helminth.* **16**, 17–32.

Krall, L. L. (1991) Wheat and grass nematodes: *Anguina*, *Subanguina*, and related genera pp. 721–760 *In* Nickel, W. R. (Ed.) "Manual of Agricultural Nematology." (Marcel Dekker, New York, USA).

LIMBER, D. P. (1973) Notes on the longevity of *Anguina tritici* (Steinbuch, 1799) Filipjev, 1936, and its ability to invade wheat seedlings after thirty two years of dormancy. *Proc. Helminthol. Soc. Wash.* **40**, 272-274.

MAGGENTI, A. R., HART, W. H. & PAXMAN, G. A. (1973) A new genus of gall forming nematode from *Danthonia californica* with a discussion of its life history. *Nematologica* **19**, 491-477.

_____ (1981) "General Nematology" (Springer-Verlag, New York, USA).

PANTONE D. J. & WOMERSLEY C. (1986) The distribution of flower galls caused by *Anguina amsinckiae* on the weed, common fiddleneck, *Amsinckia intermedia*. *Revue Nématol.* **9**, 185-189.

RILEY, I. T., SHEDLEY, D. & SIVASITHAMPARAM, K. (2001) anhydrobiosis and reproduction in *Anguina australis*. *Australas. Pl. Path.* **30**, 361-364.

TRIANTAPHYLLOU, A. C. & HIRSCHMANN, H. (1966) gametogenesis and reproduction in the wheat nematode, *Anguina tritici*. *Nematalogica*, **12**, 437-442.

WOMERSLEY, C. (1987) A reevaulation of strategies employed by nematode anhydrobiotes in relation to their natural environment pp. 165-173 *In* Veech, J. A. & Dickson, D. W. (Eds) "Vistas on nematology: A commemoration of the twenty-five anniversary of the Society of Nematologists" (Society of Nematologists, Hyattsville, Maryland, USA).

VOL. 126, PART 2
29 NOVEMBER, 2002

Transactions of the Royal Society of South Australia Incorporated

Contents

PUBLISHED AND SOLD AT THE SOCIETY'S ROOMS
SOUTH AUSTRALIAN MUSEUM, NORTH TERRACE, ADELAIDE, S.A. 5000

TRANSACTIONS OF THE

ROYAL SOCIETY OF SOUTH AUSTRALIA

INCORPORATED

VOL. 126, PART 2

MORPHOLOGICAL EVIDENCE FOR THE SYSTEMATIC POSITION OF THE ORDER MUSPICEIDA (NEMATODA)

By David M. Spratt & Warwick L. Nicholas†*

Summary

Spratt, D. M. & Nicholas, W. L. (2002). Morphological evidence for the systematic position of the Order Muspiceida (Nematoda). Trans. R. Soc. S. Aust. 126(2), 51-62, 29 November, 2002.

Muspiceida are tiny, highly specialised nematodes parasitic as adults in the connective and organ tissues of vertebrates. Nine genera, six monotypic, are recognised in two familes. Life cycles are unknown but modes of transmission have been widely discussed in the literature and postulated as occurring by cannibalism, cutaneous penetration or during lactation or grooming. The phylogenetic affinities and systematic rank of the Muspiceida have long been in doubt, some morphological features suggesting similarities with the Secernentea, others suggesting similarities with the Adenophorea.

Key Words: Muspiceida, Muspicea borreli, morphology, SEM, TEM, Dorylaimia, Adenophorea, Enoplea.

Transactions of the Royal Society of S. Aust. (2002), **126**(2), 51–62.

MORPHOLOGICAL EVIDENCE FOR THE SYSTEMATIC POSITION OF THE ORDER MUSPICEIDA (NEMATODA)

by David M. Spratt[1] & Warwick L. Nicholas[2]

Summary

Spratt D. M. & Nicholas W. L. (2002). Morphological evidence for the systematic position of the Order Muspiceida (Nematoda). *Trans. R. Soc. S. Aust.* **126**(2), 51–62, 29 November, 2002.

Muspiceida are tiny, highly specialised nematodes parasitic as adults in the connective and organ tissues of vertebrates. Nine genera, six monotypic, are recognised in two families. Life cycles are unknown but modes of transmission have been widely discussed in the literature and postulated as occurring by cannibalism, cutaneous penetration or during lactation or grooming. The phylogenetic affinities and systematic rank of the Muspiceida have long been in doubt, some morphological features suggesting similarities with the Secernentea, others suggesting similarities with the Adenophorea. Morphological studies using light microscopy, SEM and TEM of *Muspicea bairdi* Sambon 1925 from wild *Mus domesticus* Schwartz & Schwartz 1943 (see Figueroa *et al.* 1986) in Australia strengthen the latter proposition. Although an onchiostyle was not observed in larval or adult *M. bairdi*, evidence indicates that phasmids are absent in this species. What had previously been interpreted as "phasmidoid cells" in this and two other species in which both adult and larval forms were studied are in fact caudal glands, terminal in adults and sub-terminal in third-stage larvae, with no associated nervous tissue. This finding, together with previous evidence from other authors strengthens the view that the Muspiceida provide a link between the Mermithida and the Trichocephalida (= Trichinellida), and on morphological grounds are adenophorean, not secernentean. This conclusion accords with recent studies of phylogenetic relationships within the Nematoda and a re-classification of the phylum based on morphological and life cycle knowledge and molecular data, in particular SSU rDNA sequences from animal and plant parasitic, and free-living taxa. It accords with the placement of the vertebrate parasitic Muspiceida, Dioctophymatida and Trichinellida (=Trichocephalida) alongside the insect parasitic Mermithida and Marimermithida, the plant-parasitic Dorylaimida and the free-living Mononchida in the subclass Dorylaimia, of the class Enoplea.

Key Words: Muspiceida, *Muspicea bairdi*, morphology, SEM, TEM, Dorylaimia, Adenophorea, Enoplea.

Introduction

The nematode order Muspiceida Bain & Chabaud, 1959 is an enigmatic group of parasites occurring in the skin, eyes, brains or vascular system of vertebrates (Spratt *et al.* 1999). Its phylogenetic position within the phylum Nematoda has always been uncertain, a situation which has been further exposed by significant advances in understanding of nematode phylogeny.

Classification within the phylum Nematoda has been, until recently, based upon morphological and ecological features associated with phenotypic characters of free-living or parasitic nematodes (Chitwood 1933, 1950; Chabaud 1974; Anderson 1984, 2000; Anderson & Bain 1982; Anderson *et al.* 1974; Inglis 1983). Using these criteria, the overwhelming majority (estimated 92%) of nematode parasites of vertebrates belong to the class Secernentea and are thought to have arisen from rhabditid, free-living, microbivorous, soil nematodes (Anderson 1984). With very few exceptions, the third stage larva is infective to the definitive host (Anderson *loc. cit.*). Under unfavourable conditions, free-living rhabditids produce "dauer" larvae, third-stage larvae ensheathed in the cuticle of the second-stage. These can be induced to exsheath and resume development in the presence of food.

A minority of nematode parasites of vertebrates belongs to the class Adenophorea. However, the evolutionary origins of the Adenophorea, in contrast to the Secernentea, remain controversial (Maggenti 1983; Bain & Chabaud 1968, 1979; Inglis 1983; Anderson 1984; Adamson 1986) because many authors recognise its lack of monophyly or its homogeneity compared with the Secernentea. The adenophoreans parasitic in vertebrates are believed to have arisen from a dorylaim lineage (*sensu* Chitwood 1950) with a spear-like stylet in the buccal cavity (onchiostyle), most of which are predaceous or plant-parasitic and adapted to piercing and feeding on tissues (Anderson 1984). This may have given them a capacity to cross tissue barriers by penetration and may possibly have pre-adapted them to a parasitic way of life (Fülleborn 1929). Four parasitic groups (recognised as suborders or superfamilies) are thought to be derived from the dorylaims, three in vertebrates, Trichinellina (=Trichinelloidea), Dioctophymatina (= Dioctophymatoidea)

[1] [email above spratt@csiro.au]
[2] CSIRO Sustainable Ecosystems, GPO Box 284, Canberra ACT 2601, Australia.
[3] Department of Botany and Zoology, and The Electron Microscope Unit, Australian National University, PO Box 4, Canberra ACT 0200, Australia.

and Muspiceina (=Muspiceoidea), and one in invertebrates, primarily insects, Mermithina (=Mermithoidea) (Anderson 1984, 2000). With the exception of the Muspiceina, the affinities of the parasitic genera found in these suborders are exemplified by the presence, as in free-living dorylaims, of an onchiostyle in first-stage larvae. In contrast to the Secernentea, adenophorean nematodes do not have a "dauer" larva and infect the host in the first as well as the third or fourth larval stage. From the outset of parasitism, the Adenophorea were probably adapted to feed on tissues, hence the host's intestinal environment was probably never a trophic necessity (Filliborn 1929; Anderson 1984; Adamson 1986). Although the alimentary tract may provide an outlet for transmission stages in species of some genera (Trichinellina: *Capillaria*, *Trichuris*), thus function may be filled by the urinary system (Trichinellina: *Trichosomoides*, Dioctophymatina *Dioctophyme*) or possibly the skin (Muspiceina: *Muspicea*) in other genera. There are no lumen-dwelling, intestinal, parasitic Enoplea (Adamson 1986). Wright (1989) demonstrated that gastrointestinal inhabitants among the Trichinellina are in fact intimately associated with epithelial tissues. Modes of transmission and postembryonic development of these nematodes raise the possibility that the entire group arose as associates of earthworms and terrestrial, especially larval, insects. It was these early associates which diversified and gave rise to the parasites in both invertebrates and vertebrates (Anderson 1984).

Recently, phylogenetic relationships of adenophorean (13) and secernentean (15) nematodes have been assessed using morphological data and SSU rDNA sequence data (Kumpfer *et al.* 1998). Both data sets strongly supported the classic split into Adenophorea and Secernentea, recognizing each as monophyletic. However, subsequent analyses of a database of SSU rDNA sequences from representatives (53) of animal parasitic, plant parasitic and free living taxa resulted in a markedly different conclusion (Blaxter *et al.* 1998). The latter analyses indicated that convergent morphological evolution was common and that the Adenophorea may be paraphyletic because it includes the ancestors of the Secernentea. Five clades were recognised, all of which included parasitic species. Dorris *et al.* (1999) suggested that animal parasitism arose independently at least six times and plant parasitism at least three times. Two exclusively adenophorean clades were strongly supported. In particular, Clade I grouped the vertebrate parasitic order Trichocephalida (=Trichinellina of Anderson 2000) with the insect-parasitic Mermithida, plant-parasitic Dorylaimida and free-living Mononchida.

Subsequently, De Ley & Blaxter (2002) presented a comprehensive yet appropriately conservative treatment of the systematic position and phylogeny of the Nematoda based on the overall congruence between morphological and molecular phylogenetic analyses, notwithstanding the fact that molecular sampling of taxonomic diversity within the Nematoda remains limited, especially within Adenophorea relative to Secernentea.

This seminal work incorporates a major shift of balance in an effort to combine parasitic and non-parasitic taxa within a single phylogenetic hierarchy. They argue that such a balance stands on morphological evidence alone, following inevitably from the combination of two earlier hypotheses proposed on the basis of morphology (Lorenzen 1983, 1994) and life cycle data (Inglis 1983; Anderson 1984). These hypotheses were the paraphyly of the Adenophorea with respect to Secernentea and the assumption that all parasitic nematode taxa derived from free-living ancestors. Both hypotheses are now supported strongly by DNA sequence analysis, placing the origin of the Nematoda somewhere between chromadorids, enoplids and dorylaimids (De Ley & Blaxter 2002).

The phylogenetic affinities and systematic rank of the Muspiceida have long been in doubt (Anderson 2000). The presence of "phasmid-like" structures in three of the genera in which the larval stage has been described (Bain & Chabaud 1979) would place the Muspiceida in the Secernentea. Other morphological features would place the Muspiceida in the Adenophorea, a systematic group whose validity itself has been questioned, as outlined above. As in adult Mermithida, the intestine is replaced by a trophosome but pharyngeal gland structures suggest affinities with the Trichocephalida (=Trichinellida). The amphids have not been described. In contrast to secernenteans, adenophoreans usually have caudal and epidermal glands, lack phasmids, have a single-cell secretory-excretory system usually with a non-cuticularised terminal duct, have well-developed, usually post-labial amphids, commonly have cephalic and somatic setae and are found mostly in aquatic environments (Bird & Bird 1991). The epidermal glands are unicellular structures located in the lateral cords and open through pores in the cuticle. Each is associated with a bipolar nerve cell and constitutes a neurosecretory unit of unknown function. They are highly susceptible to isotonicity (DMS, unpub.) and so they may have an important role in water-electrolyte balance. The caudal secretory glands are usually three in number and may open through a spinneret, a valve structure at the tip of the tail thought to be used for attachment to the substratum in aquatic forms. Placement of the order Muspiceida near the Trichocephalida was strengthened with the finding by Spratt *et al.* (1999)

of lateral bacillary bands in immature female *Hoyenchnemu perplexum* Spratt, Beveridge, Andrews & Dennett, 1999. In this character, the Muspiceida appears to provide a link between the Mermithida and the Trichocephalida. Its position would be strengthened further if a true onchiostyle (i.e. an altered sub-ventral tooth and not a formation of the ventral wall of the buccal cavity – see Lorenzen 1983) were present in the adults or larval stages of at least some members of the group and if clear evidence of the absence of phasmids was found.

Muspiceu borreli Sambon, 1925 was described by Sambon (1925) based on "la filaire de Borrel" first reported by Borrell (1910). The parasite occurred naturally in the subcutaneous connective tissues, inguinal and mediastinal lymphatics and in and around cancerous tumours of mammary glands of wild populations of *Mus musculus* Linnaeus, 1758 from Strasbourg, France. It was also found in mice from London and Germany (see Brumpt 1930). Surprisingly, no new records of the parasite occurred from the work of Brumpt (1930), who erected the family Muspiceidae for the nematode, until it was reported in wild house mice, *Mus domesticus*, in Australia (Singleton 1985, Singleton and Redhead 1990).

This report provides further morphological evidence for the systematic position of the Muspiceida derived from light, scanning and transmission electron microscopical studies of *Muspiceu borreli* from wild *Mus domesticus* in Australia.

Materials and Methods

Wild *Mus domesticus* were trapped at Canberra. Mice were anaesthetised with ether vapour and killed by cervical dislocation. Carcases were skinned and skins and carcases washed in Hank's Balanced Salt Solution (HBSS) in a Petri dish, gently scraped with a blunt razor blade and rewashed. The pelt was cut into 5 pieces and suspended in HBSS in a Baermann apparatus (Thienpont *et al.* 1979) at 37°C for 3h. The immersed skin was agitated approximately every 15 min with a glass stirrer or forceps. Fluid was collected from the Baermann funnel into a test tube at 15-30 minute intervals, the tube allowed to stand for several minutes, the supernatant removed and the sediment was then removed and examined for *M. borreli* in a Petri dish. In mice known to be infected in the subcutaneous tissues, the liver, spleen, lymphatics, lungs, heart, brain, mammary glands, genitals, tongue and lips were teased apart in HBBS, allowed to stand in a test tube at 37°C for 1 h and the sediment re-examined for nematodes.

For light microscopy, some nematodes were fixed in 5% formal saline then transferred to 5% aqueous glycerol which was allowed to evaporate to anhydrous glycerol in a desiccator. They were then mounted on glass slides in anhydrous glycerol with the cover slip supported by glass beads of the appropriate size, and the cover slip ringed with Glyceel (Gurr, UK). Other specimens were fixed overnight in Berland's fixative (95% by volume glacial acetic acid, 5% concentrated formalin), transferred to 70% ethanol and cleared in lactophenol for microscopic examination. Live specimens were stained with 1% toluidine blue and with 1% acetic orcein prior to microscopic examination.

For Scanning Electron Microscopy (SEM), formalin fixed specimens were washed in saline then post-fixed in 1% osmium tetroxide for 1 h, washed in distilled water, freeze-dried, mounted on metal stubs using nail varnish as glue and coated with gold palladium under vacuum.

For Transmission Electron Microscopy (TEM), specimens were fixed overnight in cold 2.5% gluteraldehyde in phosphate buffer, pH 7.2, containing 3% sucrose, then post-fixed in 1 % osmium tetroxide for 1 h. Specimens were progressively transferred through graded ethanols and epoxypropane to Spurr epoxy resin. After hardening the resin at 60° C for 48 h, thin sections were cut, mounted on formvar coated slot grids, and stained with 6% aqueous uranyl acetate and Reynolds lead citrate. Two specimens were used for transverse sections and two for longitudinal sections.

Results

Morphology of adult (Figs 1-9, 12-24)

All *M. borreli* from wild mice were recovered from subcutaneous tissues. Adults were 1200-2300 µm long and 230-270 µm wide with a blunt cephalic end tapering posteriorly to a bifid caudal end (Figs 1-5, 8-9). The oral opening was small (1.25 µm in diameter), sub-terminal, displaced ventrally and surrounded by 6 small sensory cephalic papillae, here interpreted as 6 inner labial sensilla (Figs 2, 14, 16-17). Sixteen long cells with large nuclei and nucleoli extended from the cephalic end to the nerve ring (Figs 3, 4). The 6 inner labial sensilla passed through the cuticle to the exterior. However, external openings were not observed for the outer lateral and cephalic sensilla. A pair of pocket-like lateral amphids which stain deeply with vital dyes was observed under light microscopy but appeared, under light and scanning electron microscopy, to have no cuticular ducts opening to the exterior (Figs 3-5, 16). A variable number of cuticular cephalic nodules was present in some specimens (Fig. 17). Conspicuous transverse cuticular striae or annulations were

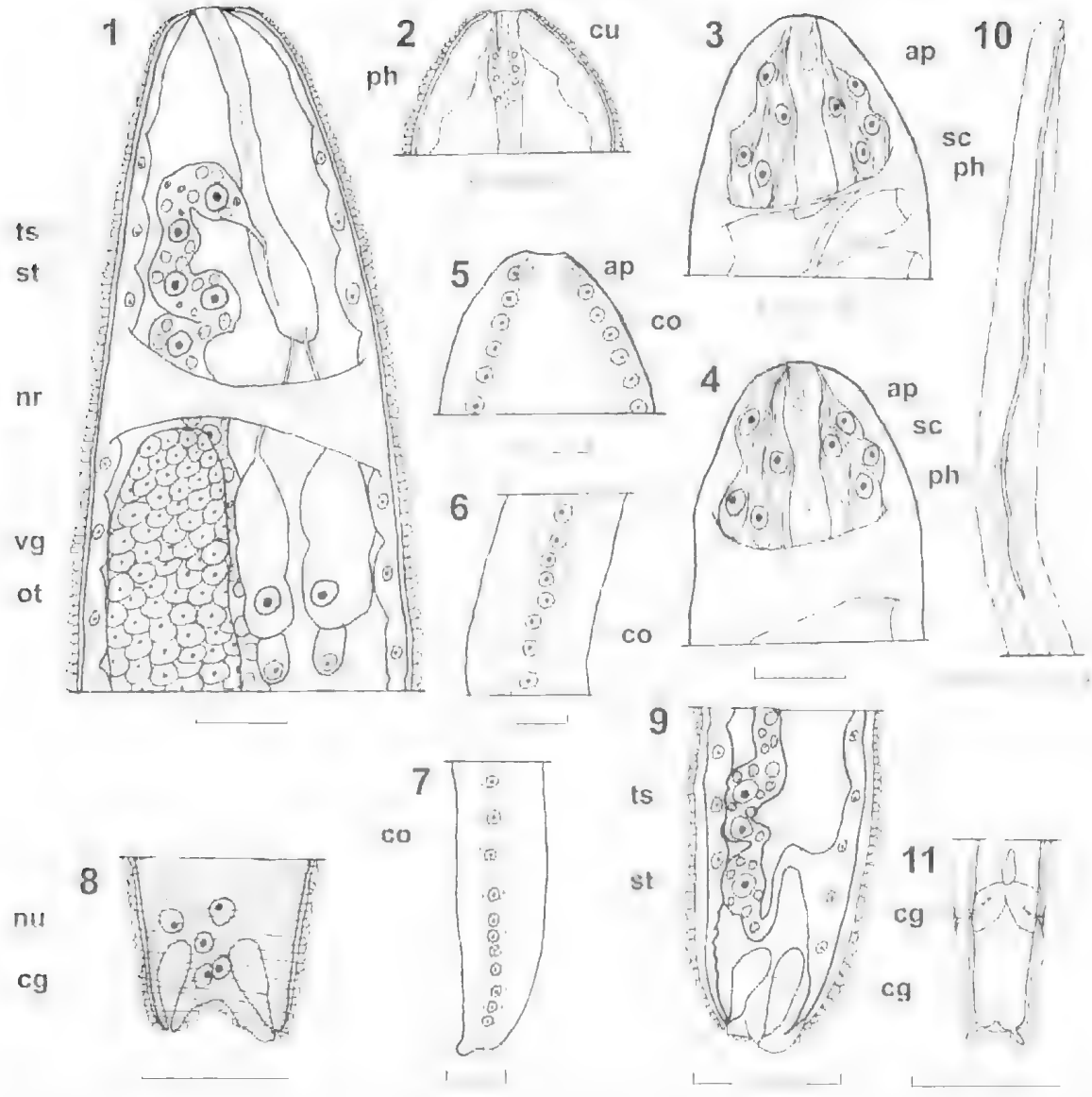

Figs 1-11. *Muspicea borrelli* from tissues of *Mus domesticus*. Fig. 1. Anterior end showing pharynx (ph), thin strand (st) of connective tissue at commencement of trophosome (ts) which contains large nuclei and numerous lipid globules, nerve ring (nr), two pairs of latero-ventral pharyngeal glands (vg) and ovi-testis (ot) containing unfertilised eggs, latero-ventral view. Fig. 2. Cephalic end showing cuticular (cu) lining of distal end of pharynx (ph) leading to ventral oral opening, lateral view (dorsal on right side). Fig. 3. Cephalic end showing pharynx (ph), suspected sheath cells (sc) of eight cephalic papillae and amphidial pouch (ap), lateral view. Fig. 4. Optical section of same showing pharynx (ph), suspected sheath cells (sc) of other eight cephalic papillae and other amphidial pouch (ap), lateral view. Fig. 5. Optical section of cephalic end showing amphidial pouches (ap) and conspicuous nuclei and nucleoli of cells of lateral cord (co), ventral view. Fig. 6. Nuclear pattern of lateral cord (co) in mid-body region, lateral view. Fig. 7. Nuclear pattern of lateral cord (co) at posterior end. Fig. 8. Caudal end showing bifid form, pair of large terminal caudal glands (cg) and associated nuclei (nu), ventral view. Fig. 9. Posterior end showing termination of trophosome (ts) in thin strand (st) of connective tissue and pair of caudal glands (cg). Fig. 10. Anterior end third-stage larva showing sub-terminal, ventral oral opening and long cuticular lining of pharynx (ph), lateral view. Fig. 11. Caudal end of third-stage larva showing conspicuous caudal glands (cg) emptying laterally, ventral view. Scale bars: Figs 1-10 = 50 μm; Fig. 11 = 20 μm.

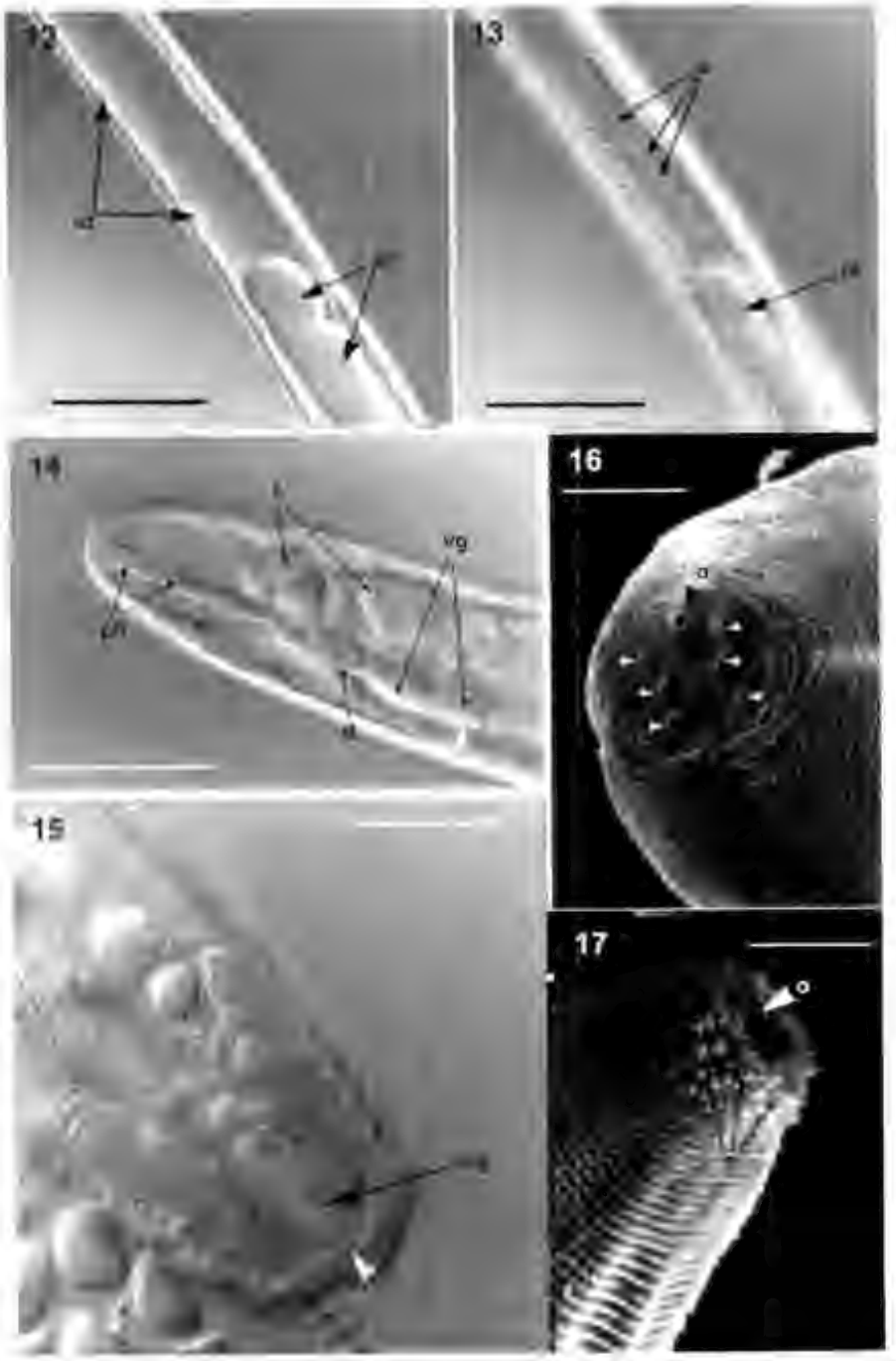

Figs 12 - 17. Adult *Muspicea borreli* - Nomarski interference micrographs and scanning electron micrographs. Fig. 12. Ovi testis (ot) containing densely packed nuclei of developing oocytes and uterus (ut), lateral view. Fig. 13. Optical section of same showing uterus containing sperm (s), lateral view. Fig. 14. Anterior end showing pharynx (ph), trophosome (ts), one of anterior ventral glands (vg) with single nucleus (arrowhead) and duct (d) from gland emptying into pharynx, lateral view. Fig. 15. Caudal extremity showing one of two large caudal glands (cg) and opening to exterior (arrow) in one lobe of bilobed tail. Fig. 16. Cephalic region illustrating oral orifice (o) located ventrally and six sub-median papillae (arrowheads), *en face* view. Fig. 17. Cephalic region showing oral orifice (o), conspicuous cuticular nodules (n) and transverse cuticular annuli, dorsal view. Scale bars: Figs 12, 13 = 150 µm; Fig. 14 = 100 µm; Fig. 15 = 50 µm; Fig. 16 10 µm; Fig. 17 = 20 µm.

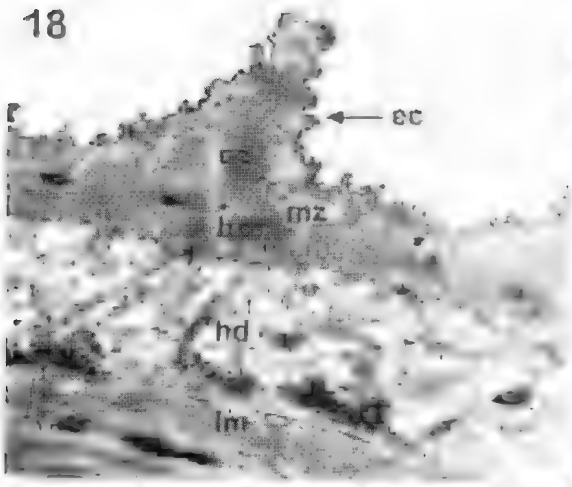
18
ec
mz
hd
lm

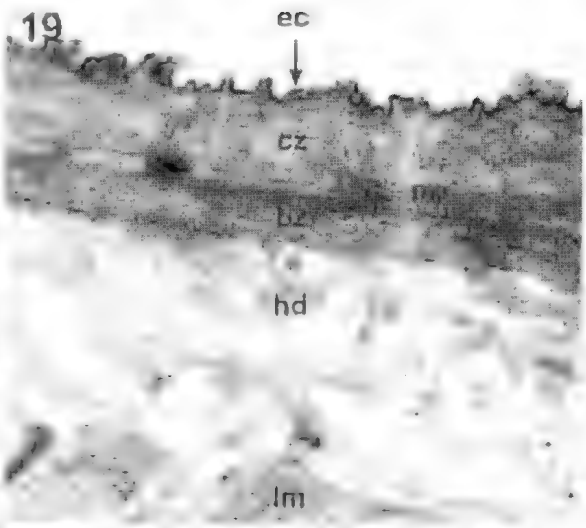
19
ec
cz
hd
lm

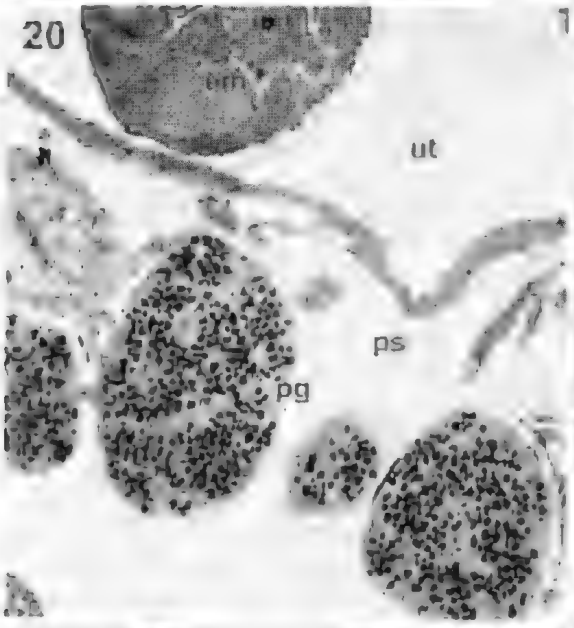
20
ut
ps
pg

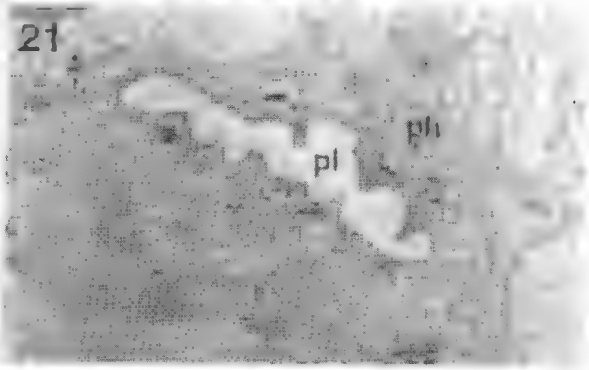
21
ph
pl


22
ut
ps

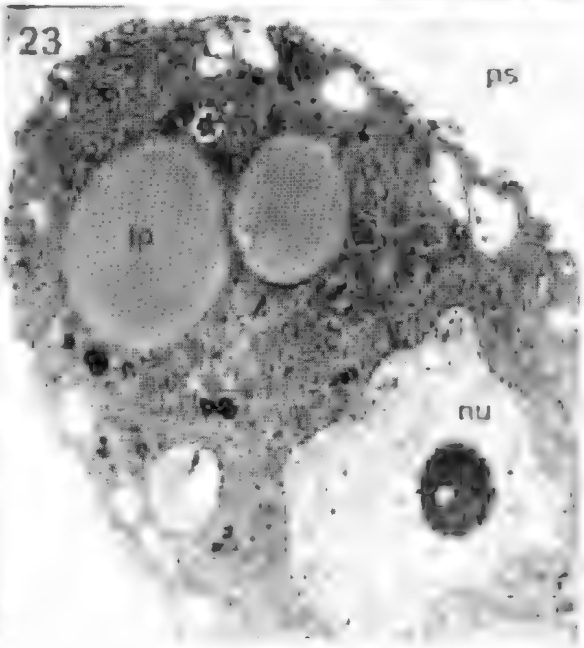
23
ps
ip
nu

present throughout the length of the adult nematode, and occasionally fused with one another (Figs 1-2, 8-9, 15-17). The lateral cords were wider and more conspicuous than the dorsal and ventral cords and had many nuclei with conspicuous nucleoli arranged regularly in a single row throughout the length of the adult (Figs 5-7). The cuticle comprised a narrow epicuticle and thicker cortical, median and basal zones (Figs 18, 19). The ventral epidermis was in contact with the endo-cuticle and formed a diffuse band of electron-dense membranes arranged radially in stacks, greatly increasing the surface area of the epidermal cell membrane in association with the endo-cuticle (Fig. 18). The cytoplasm of the ventral epidermis also contained glandular tissue with granules of protein and lipid (Figs 18-19).

A true onchiostyle was not observed in adult or larval forms of *M. borreli*. The vestigial pharynx was short, fibrous and had a narrow lumen lined with cuticle for only a short distance (Figs 1-3, 22). The pharynx contained gland cells (Fig. 21), extending as a narrow strand of tissue from the cephalic end about 150-200 µm into the pseudocoele and terminating close to the attachment of the ventral glands, near the level of the nerve ring (Figs 1, 3, 4, 14). The nerve ring occurred near the junction of the ventral pharyngeal glands and the pharynx (Figs 1, 3, 4). A pair of large, dense, distinctly bilobed, latero-ventral pharyngeal glands was suspended from the posterior portion of the pharynx by two fine ducts and a smaller pair lay immediately posteriorly (Figs 1, 14). Large stellate coelomocytes each with a voluminous nucleus, large surface area, convoluted membranes and invaginated lamellae occurred throughout the pseudocoele (Fig. 22). The trophosome extended almost the entire length of the pseudocoele as a string of large cells with prominent nuclei and nucleoli (Figs 1, 14, 23, 24). It was connected to the pharynx at the anterior end and the body wall at the posterior end by thin strands of connective tissues (Figs 1, 9). The characteristic granular appearance of the trophosome was due to the presence of lipid vacuoles (Fig. 23). The vulva was atrophied and no connection was detected between the non-functional pharynx and the uterus. The tail of the adult was bifurcate and each tip terminated in a caudal gland with a pore opening externally (Figs 8, 9, 15). The glands stained deeply with both 1% toluidine blue and with 1% acetic orcein. Five prominent nuclei with conspicuous nucleoli were associated with the glands (Fig. 8). They lacked the nerve cell connections associated with phasmids and they opened to the exterior. *Muspicea borreli* was a protandrous hermaphrodite: spermatogenesis occurred in the wall of the genital pouch and spermatozoa were released from the ovi-testes into the uterus which acted as a receptacle for self-fertilization (Fig. 13). Spermatogenesis terminated when the distal cells of the genital cord commenced division for ovogenesis (Fig. 12). Larvae developed simultaneously in the uterine pouch (Fig. 24).

Morphology of third-stage larva (Figs 10-11, 25-30)

Larvae developed to the third-stage in the uterus of the female, at which time they were 295–310 µm long and 16-17 µm wide (Figs 10, 11). Three body cuticles were detectable in living larvae escaping from female worms (Fig. 25); the inner and outer were smooth, the middle cuticle possessed conspicuous transverse striae. The oral opening was subterminal and ventral (Fig. 10). A conspicuous cuticular pharyngeal lining extended posteriorly 100-110 µm where it appeared to become surrounded by an intestinal-like structure (? trophosome) (Fig. 10) which extended to within 20-25 µm of the caudal end. A slender lumen and secretory granules were evident in this structure (Figs 26, 27). An anus was not detected. A pair of conspicuous caudal glands consisting of highly convoluted glandular tissue which stained deeply with vital dyes, emptied laterally about 20 µm from the caudal end, which terminated in two lappets (Figs 11, 28-30).

Discussion

The Muspiceida are tiny, highly specialised nematodes parasitic as adults in the tissues of vertebrates, most of them inhabiting the subcutaneous tissues of their hosts (Anderson & Bain 1982). Nine genera, six monotypic, are recognised in two families. One, the Muspiceidae Sambon, 1925, contains the genera *Muspicea* Sambon, 1925 from the subcutaneous tissues of mice (*Mus* spp.) and *Rimaggolvania* Bain & Chabaud, 1968, *Lukomeria* Chabaud & Bain, 1974, *Permisia* Bain & Chabaud, 1979 and *Maveria* Rausch & Rausch, 1983 from the subcutaneous tissues of the

Figs 18-23. Transmission electron micrographs of adult *Muspicea borreli*. Fig. 18. Longitudinal section through cuticle, epidermis and muscle. Fig. 19. Transverse section through same tissues. Fig. 20. Transverse section through pharyngeal glands. Fig. 21. Transverse section through pharynx. Fig. 22. Coelomocyte. Fig. 23. Trophosome. Scale bars 1 µm. bz cuticle basal zone, cl coelomocyte, cz cuticle cortical zone, ec epicuticle, em embryo, hd hypodermis, lm longitudinal muscle, lp lipid inclusion, mz cuticle median zone, nu nucleus, pg pharyngeal gland, ph pharynx, pl pharyngeal lumen, ps pseudocoel, ut uterus.

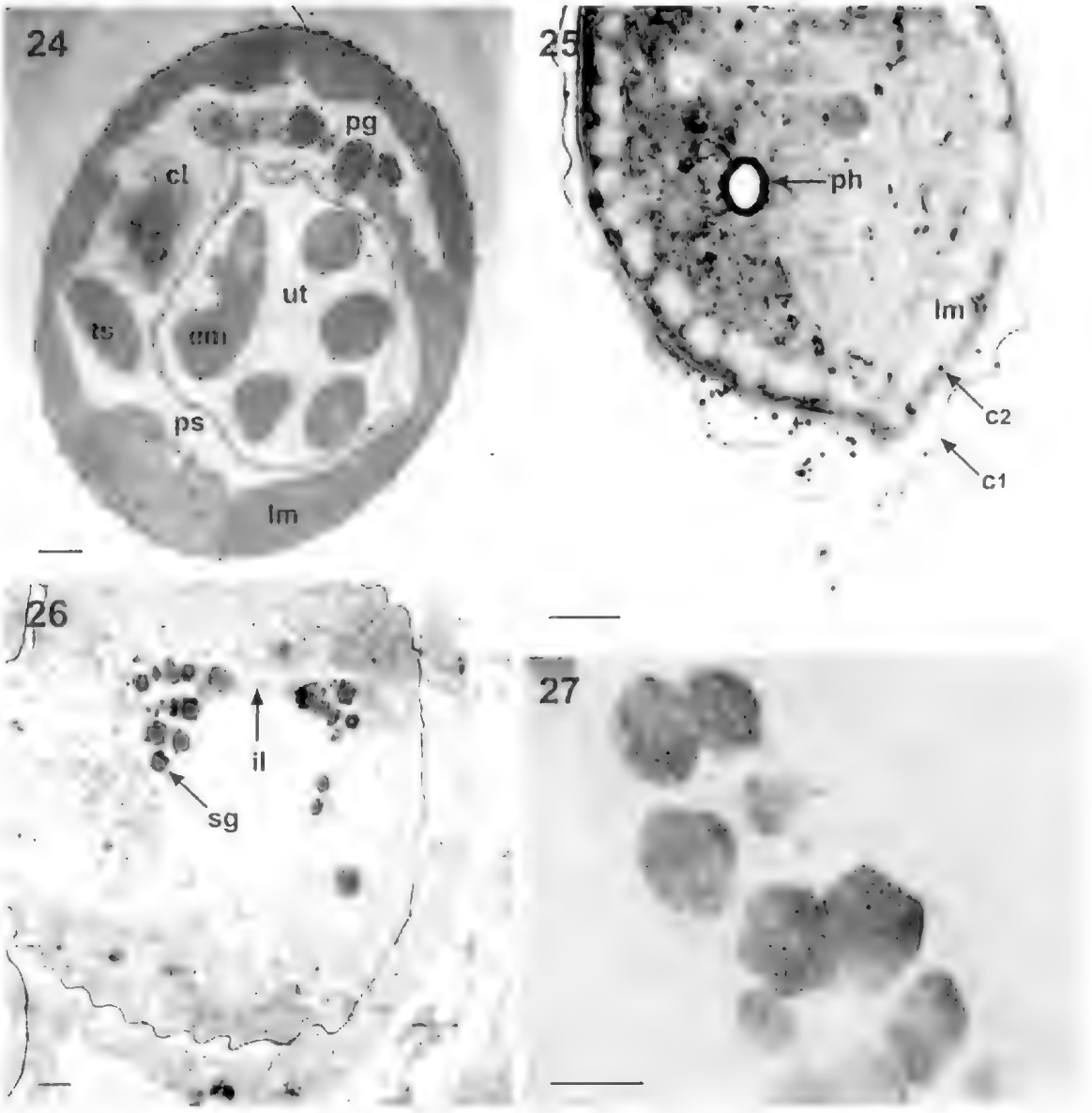

Figs 24 - 27. Transmission electron micrographs of adult and larval *Muspicea borreli*. Fig. 24. Transverse section through adult female. Fig. 25. Anterior end of juvenile from subcutaneous tissues of mouse. Scale bar = 5 µm. Fig. 26. Embryo *in utero*. Scale bar = 1 µm. Fig. 27. Secretory granules in embryonic intestine. Scale bars: Fig. 24 = 20 µm; Fig. 25 = 5 µm; Figs 26, 27 = 1 µm. cl coelomocyte, C1 outer cuticle, C2 middle and inner cuticle, em embryo, il intestinal lumen, lm longitudinal muscle, pg pharyngeal gland, ph pharynx, ps pseudocoel, sg secretory granules in embryonic intestine, ts trophosome, ut uterus.

wings and feet of bats. The second family, the Robertdollfusidae Chabaud & Campana, 1950, contains the genera *Robertdollfusa* Chabaud & Campana, 1950 from the eye of corvids and the brain of falconids, *Durikainema* Spratt & Speare, 1982 from the portal and intracardiac veins and epicardial lymphatics of kangaroos and wallabies and the pulmonary arteries of koalas and brush-tail possums, *Lappinema* Bain & Nikander, 1982 from the subcutaneous capillaries of the ears of reindeer and *Haycocknema* Spratt, Beveridge, Andrews & Dennett, 1999 from the myofibres of humans. In addition, larvae of a presumed muspiceid are known from white-tailed deer (Beaver & Burgdorfer 1984, 1987) and infective larvae of a presumed new species of Robertdollfusidae are known from the gut

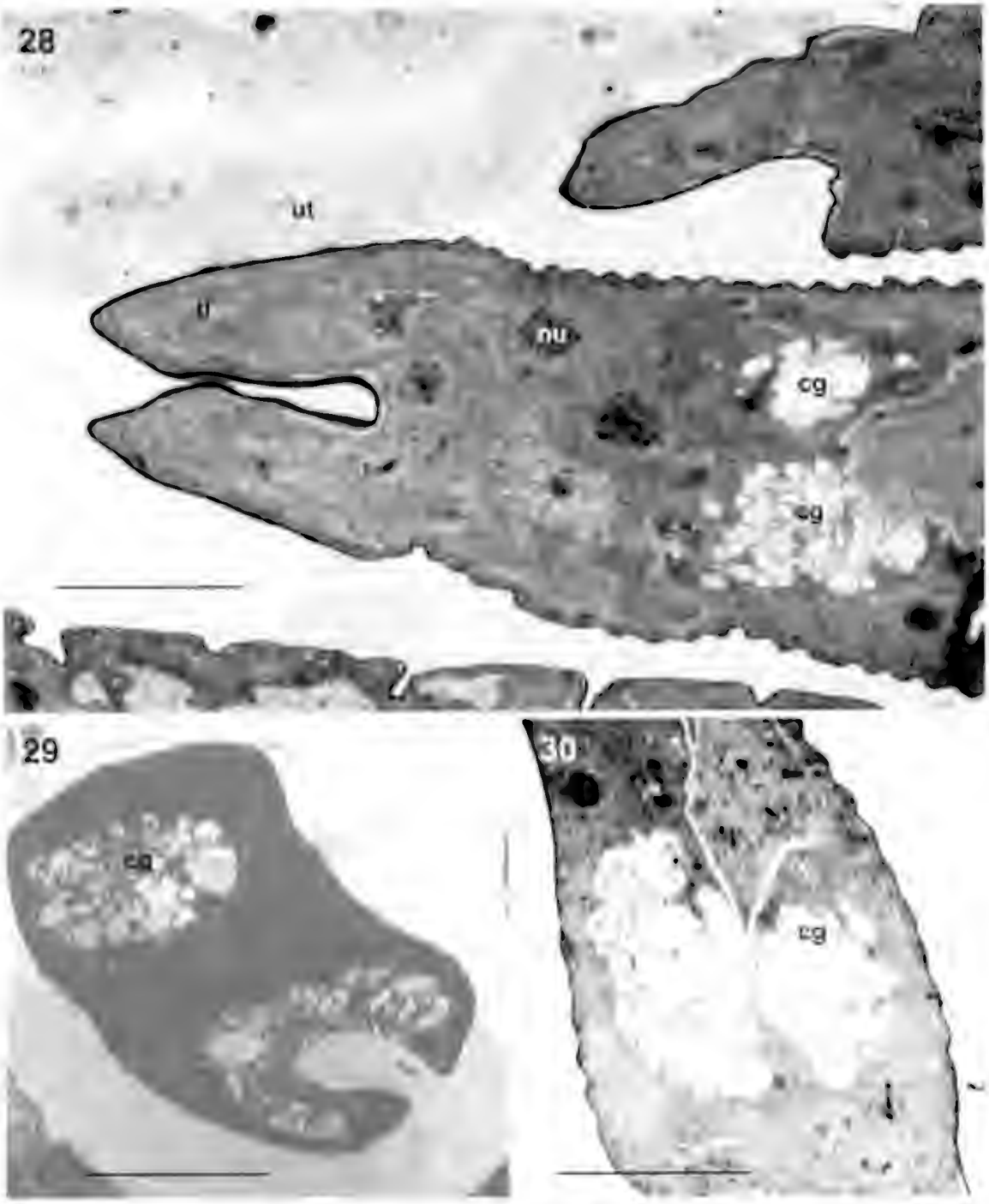

Figs 28 - 30. Transmission electron micrographs of larval *Muspicea borreli in utero* showing caudal glands, nuclei of caudal glands and terminal lappets. Fig. 28. Longitudinal section through caudal end . Fig. 29. Transverse section through caudal glands and showing pore opening of one gland (right side). Fig. 30. Longitudinal section through caudal glands. Scale bars = 5 µm. cg caudal gland, nu nucleus, tl terminal lappet, ut uterus.

of *Simulium dammosum* in Cameroon (Bain & Renz 1993). One of us (DMS) has observed larval *Durikainema* sp. in the abdomen of *Culicoides vienuiae* Macfie, 1941 (Diptera: Ceratopogonidae) near Atherton, Queensland where the tree kangaroo, *Dendrolagus lumholtzi* Collett, 1884 is known to harbour *Durikainema macropi* Spratt & Speare,1982.

Our evidence indicates that *Muspicea borreli* possesses a number of the morphological features which link it with the Adenophoren rather than the Secernentea (Bird & Bird 1991). Bain and Chabaud (1979) reported that larvae of *Lukonema*, *Muspicea* and *Rhoutgolvania* had comparable phasmids ("cellules phasmidoïdes"), i.e. a pair of large lateral cells each connected to an opening much further posterior. Our evidence from light and transmission electron microscopy indicates that in third-stage *M. borreli* at least, these large lateral cells represent caudal glands with short ducts which open laterally to the exterior (Figs 11, 28-30) rather than further posteriorly. They contain highly convoluted glandular tissue with no suggestion of nervous tissue, as occurs in phasmids (Coomans & De Grisse 1981). Bain & Chabaud (*loc. cit.*) noted that phasmids were barely perceptible in adult *Muspicea* and *Rhoutgolvania* but were particularly pronounced in the genera *Lukonema* and *Pennisia*, possibly functioning as organs of absorption. Rather than absorptive structures, phasmids are somatic sensilla with a sensillum consisting of one or more sensory neurons and excurt cells (Coomans & De Grisse, *loc. cit.*), one of the latter commonly called the phasmidial gland (Chitwood & Chitwood 1950). Consequently, these conspicuous features of *Lukonema* and *Pennisia* are more likely to represent modified caudal glands than phasmids.

We believe the sixteen long cells with large nuclei and nucleoli extending from the cephalic end to the nerve ring represent sheath cells each surrounding a sensillar canal distally (see Coomans & De Grisse 1981). The six inner labial sensilla passed through the cuticle to the exterior. However, we were unable to obtain appropriate TEM sections to confirm that the outer lateral and cephalic sensilla did not open to the exterior. Similarly, well developed, post-labial amphidial pouches are present in *M. borreli* but these did not appear, in SEM, to open to the exterior, possibly because openings were coated in gold palladium.

Features of the ventral epidermis i.e. electron dense membranes arranged radially in stacks and glandular tissue with granules of protein and lipid suggest active assimilative, secretory or excretory functions and resemble the bacillary bands found in the lateral, dorsal and/or ventral hypodermal cords of Trichocephalida (= Trichinellida) of vertebrates. However, true bacillary bands consist of glandular and non-glandular cells, the former opening to the exterior and thought to have a role in osmotic or ionic regulation, the latter not opening to the exterior and believed to function in cuticle formation and maintenance, and in storage of food materials (Sheffield 1963; Wright 1963, 1968). Similarly, the internal structure of the large stellate coelomocytes suggested an osmo-regulatory or phagocytic function. We were unable to detect the single dorsal gland cell excretory apparatus with non-cuticularized terminal duct (both features of Adenophorea) described by Bain & Chabaud (1979) and emptying into the lumen of the pharynx. As in adult Mermithida, the intestine in *M. borreli* is replaced by a trophosome. The trophosome was formed by a series of large cells with prominent nuclei and nucleoli rather than a multi-nucleated syncytium as described by Bain & Chabaud (1979). Although the caudal glands resemble those observed in other adenophoreans (Maggenti 1981), the latter normally occur as three single celled glands rather than two multicellular ones. We have found no evidence of a stylet in either the adult or larval stages of *M. borreli*.

Detailed cellular ultrastructure was not achieved in this study because by the time specimens had been extracted from the sub-dermal tissues and fixed for transmission electron microscopy, substantial degenerative changes had occurred. However, organ structure was satisfactorily preserved and observations by light and scanning electron microscopy were not impaired. We suspect that these nematodes contain substantial amounts of endonucleases and proteases, and that autolysis occurs during the post mortem examination of the host.

Some species of Muspiceida are dioecious (*Pennisia nagarseni* Bain & Chabaud, 1979, *Durikainema* spp., *Hayveckiuema perplexum*) (Bain & Chabaud 1979; Spratt & Speare 1982; Spratt & Gill 1998), others are protandrous hermaphrodites (*Muspicea borreli*, *Rhoutgolvania* spp., *Lukonema lukoschusi* Chabaud & Bain, 1974, *Maverita vespertilionis* Rausch & Rausch, 1983, possibly *Lappinema auris* Bain & Nikander, 1982) (Brumpt 1930; Bain & Chabaud 1968, 1979; Chabaud & Bain 1974; Rausch & Rausch 1983; Bain & Nikander 1982). In some species (*Robertdollfusa paradoxa* Chabaud & Campana, 1950) the vulva is functional and larvae pass through it (Chabaud & Campana 1950). In other species, the vulva is functional and larvae pass through it but then migrate between two layers of body cuticle and emerge from the head region of the adult worm (*Rhoutgolvania rhinolophi* Bain & Chabaud, 1968 (Bain & Chabaud 1968). In a third group of species (*Durikainema* spp., *Hayveckiuema perplexum*), the vulva is atrophied and

eggs hatch inside females, develop to third-stage larvae and burst from the head region killing the adult (Spratt & Speare 1982; Spratt & Gill 1998; Spratt *et al.* 1999), a developmental feature known as *endotokia matricida* (Hirschmann 1960) which offers an efficient mechanism for auto-re-infection of the host. Larvae escaping from the ruptured cephalic region of *H. perplexum* into human muscle was illustrated by Spratt *et al.* (1999). Semelparity, the death of adults upon expulsion of young, is rare in parasitic nematodes but occurs also in the Mermithida.

The genus *Maseria* is distinguished from other genera of Muspiceida by a number of morphological features, the most characteristic being the presence of a Demanian system (Chabaud *et al.* 1983; Rausch & Rausch 1983). The genus *Huyeocknema* is distinguished from other members of the order by the presence of a large amorphous "cell" supporting a granule-filled flask or gourd-shaped reservoir in the rectal region of mature and gravid females and the presence of lateral bacillary bands comprised of a single row of epidermal glands or pore cells spaced irregularly and extending posteriorly in the region of the vulva in immature females (Spratt *et al.* 1999).

The life cycles of muspiceid nematodes are unknown, but the modes of transmission have been widely discussed in the literature and postulated as occurring by cannibalism, cutaneous penetration, or during lactation or grooming (Sambon 1925; Brumpt 1930; Roman 1965; Bain & Chabaud 1968, 1979; Chabaud & Bain 1974; Bain & Nikander 1982; Spratt & Speare 1982; Anderson 1984; Adamson 1986). It has been suggested that these parasites have monoxenous life cycles and have evolved in their hosts directly from soil-dwelling ancestors (Adamson 1986). The most primitive muspiceid life cycles are thought to involve little tissue migration. Larvae are believed to penetrate the skin, develop in the subcutaneous tissues and infective stages are thought to leave through a skin lesion and seek a new host. A tissue migration becomes necessary when percutaneous transmission is replaced by oral transmission, as may occur in *Muspiceu* and possibly *Lappmema*. It is presumed that parasites of the deeper tissues, e.g. *Durikainema* spp. and *H. perplexum*, are derived from these forms.

In conclusion, although an onchiostyle was not observed in adult or larval *M. borreli*, morphological evidence presented here indicates that phasmids are absent in this species and what have previously been interpreted as phasmidoid cells are in fact caudal glands with no associated nervous tissue. This finding, together with the previous findings by Bain and Chabaud (1979) and by Spratt *et al.* (1999) strengthen the view that the Muspiceida provide a link between the Mermithida and the Trichocephalida, and on morphological grounds are adenophoreans, not secernenteans. This conclusion is in accord with Clade I of Blaxter *et al.* (1998) and Dorris *et al.* (1999) which grouped the vertebrate parasitic order Trichocephalida with the insect-parasitic Mermithida, the plant -parasitic Dorylaimida and the free-living Mononchida. It also accords with the tentative classification of the Nematoda by De Ley & Blaxter (2002) placing the vertebrate parasitic Muspiceida, Dietophymatida and Trichinellida (=Trichocephalida) alongside the insect parasitic Mermithida and Marimermithida, the plant-parasitic Dorylaimida and the free-living Mononchida in the subclass Dorylaimia, of the class Enoplea.

Acknowledgments

It is a pleasure to acknowledge the technical assistance of Dr Amand Stewart and Mr James Boyden. The late Dr Roy C. Anderson and Dr Ian Beveridge offered valuable criticism of an earlier draft of the manuscript.

References

Adamson, M. L. (1986) Phylogenetic analysis of the higher classification of the Nematoda. *Can. J. Zool.* **65**, 1478-1482.

Anderson, R. C. (1984) The origins of zooparasitic nematodes. *Can. J. Zool.* **62**, 317-328.

_____ (2000) "Nematode parasites of vertebrates, their development and transmission." Second Edn. (CAB International, Wallingford).

_____ & Bain, O. (1982) "CIH Keys to the Nematode Parasites of Vertebrates. No. 9. Keys to Genera of the Superfamilies Rhabditoidea, Dioctophymatoidea, Trichinelloidea and Muspiceoidea." (Commonwealth Agricultural Bureaux, Farnham Royal).

_____, Chabaud, A. G. & Willmott, S. (1974) "CIH Keys to the Nematode Parasites of Vertebrates, No. 1." (Commonwealth Agricultural Bureaux, Farnham Royal).

Bain, O. & Chabaud, A. G. (1968) Description de *Rhinoglyham rhinolophi* n. g., n. sp., Nématode parasite de Rhinolophe, montrant les affinités entre Muspiceoidea et Mermithoidea. *Ann. Parasitol. hum. comp.* **43**, 45-50.

_____ & _____ (1979) Sur les Muspiceidae (Nematoda-Dorylaimina). *Ibid.* **54**, 207-255.

_____ & Nikander, S. (1982) Un nématode aphasmidien dans les capillaires de l'oreille du renne, *Lappmema aurisrangiferis* n. gen., n. sp. (Robertsiellidae). *Ibid.* **58**, 383-390.

______ & Renz, A. (1993) Infective larvae of a new species of Robertdollfusidae (Adenophorea, Nematoda) in the gut of *Simulium damnosum* in Cameroon. *Ibid.* **68**, 182-184.

Beaver, P. C. & Burgdorfer, W. (1984) A microfilaria of exceptional size from the ixodid tick, *Ixodes dammini*, from Shelter Island, New York. *J. Parasitol.* **70**, 963-966.

______ & ______ (1987) Critical Comment: "Microfilaria of exceptional size is larva of muspiceoid nematode." *Ibid.* **73**, 389.

Bird, A. F. & Bird, J. (1991) "The Structure of Nematodes." Second Edn (Academic Press, San Diego, California).

Blaxter, M. L., De Ley, P., Garey, J. R., Liu, L. X., Scheldeman, P., Vierstraete, A., Vanfleteren, R., Mackey, L. Y., Dorris, M., Frisse, L. M., Vida, J. T. & Thomas, W. K. (1998) A molecular evolutionary framework for the phylum Nematoda. *Nature* **392**, 71-78.

Borrel, A. (1910) Parasitisme et tumeurs. *Ann. Inst. Pasteur, Paris.* **24**, 778-788.

Brumpt, E. (1930) *Muspicea borreli* Sambon 1925 et cancers de souris. *Ann. Parasitol. hum. comp.* **8**, 309-343.

Chabaud, A. G. (1974) "CIH Keys to the Nematode Parasites of Vertebrates. No. 1. Class Nematoda. Keys to subclasses, orders and superfamilies." (Commonwealth Agricultural Bureaux, Farnham Royal).

______ & Bain, O. (1974) Données nouvelles sur la biologie des nématodes Muspicéides fournis par l'étude d'un parasite de Chiroptères: *Lukonema lukoschusi* n. gen., n. sp. *Ann. Parasitol. hum. comp.* **48**, 819-834.

______ & Campana, Y. (1950) Nouveau parasite remarquable par l'atrophie de ses organes: *Robertdollfusa paradoxa* (Nematoda, *incertae sedis*). *Ibid.* **25**, 325-334.

______, Bain, O., Hugot, J-P., Rausch, R. L. & Rausch, V. R. (1983) Organe de Monsieur de Man et insémination traumatique. *Revue Nématol.* **6**, 127-131.

Chitwood, B. G. (1933) A revised classification of the Nematoda. *J. Parasitol.* **20**, 131.

______ (1950) An outline classification of the Nematoda pp. 12-25 *In* Chitwood, B. G. & Chitwood, M. B. (Eds) "Introduction to Nematology" (University Park Press, Baltimore).

Coomans, A. & De Grisse, A. (1981) Sensory structures pp. 127-174 *In* Zuckerman, B. M., Rohde, R. A. (Eds) "Plant Parasitic Nematodes. Volume III" (Academic Press, London and New York).

De Ley, P. & Blaxter, M. (2002). Systematic position and phylogeny pp. 1-30 *In* Lee D. L. (Ed.) "The Biology of Nematodes" (Taylor & Francis, London).

Dorris, M., De Ley, P. & Blaxter, M. L. (1999) Molecular analysis of nematode diversity and the evolution of parasitism. *Parasitol. Today* **15**, 188-193.

Figueroa, F., Tichy, H., McKenzie, I., Hammerling, U. & Klein J. (1986) Polymorphism of lymphocyte antigens-encoding loci in wild mice. *Curr. Top. Microbiol. Immunol.* **127**, 229-235.

Fulleborn, F. (1929) On the larval migration of some parasitic nematodes in the body of the host and its significance. *J. Helminthol.* **7**, 15-26.

Hirschmann, H. (1960) Reproduction of Nematodes pp. 140-167 *In* Sasser, J. & Jenkins, W. R. (Eds) "Nematology. Fundamentals and Recent Advances with Emphasis on Plant Parasitic and Soil Forms" (University of North Carolina Press, North Carolina).

Inglis, W. G. (1983) An outline classification of the phylum Nematoda. *Aust. J. Zool.* **31**, 243-255.

Kampfer, S., Sturmbauer, C. & Ott, J. (1998) Phylogenetic analysis of rDNA from adenophorean nematodes and implications for the Adenophorea-Secernentea controversy. *Invert. Biol.* **117**, 29-36.

Lorenzen, S. (1983) Phylogenetic systematics: problems, achievements and its application to the Nematoda pp. 11-23 *In* Stone, A. R., Platt, H. M. & Khalil, L. F. (Eds) "Concepts in nematode systematics" (Academic Press, London & New York).

______ (1994) "The phylogenetic systematics of free living nematodes". (The Ray Society, London).

Maggenti, A. (1981) "General Nematology" (Springer-Verlag, New York, Heidelberg, Berlin).

______ (1983) Nematode higher classification as influenced by species and family concepts pp. 25-40 *In* Stone, A. R., Platt, H. M. & Khalil, L. F. (Ed.) "Concepts in nematode systematics" (Academic Press, London & New York).

Rausch, R. L. & Rausch, V. R. (1983) *Maseria vespertilionis* n. g., n. sp. (Dorylaimina: Muspiceidae), a nematode from Nearctic bats (Vespertilionidae). *Ann. Parasitol. hum. comp.* **58**, 361-376.

Roman, E. (1965) Super-famille des Muspicéoïdes (Muspiceoidea) pp. 721-726 *In* Grassé, P.-P. (Ed.) "Traité de Zoologie, Anatomie, Systematique, Biologie" Vol 4 Pt 2 Némathelminthes (Masson, Paris).

Sambon, L. W. (1925) Researches on the epidemiology of cancer made in Iceland and Italy (July-October 1924). *J. trop. Med. Hyg.* **28**, 39-71.

Sheffield, H. G. (1963) Electron microscopy of the bacillary band and stichosome of *Trichuris muris* and *T. vulpis*. *J. Parasitol.* **49**, 998-1009.

Singleton, G. R. (1985) Population dynamics of *Mus musculus* and its parasites in Mallee wheatlands in Victoria during and after a drought. *Aust. Wildlife Res.* **12**, 437-445.

______ & Redhead, T. D. (1990) Structure and biology of house mouse populations that plague irregularly: an evolutionary perspective. *Biol. J. Linn. Soc.* **41**, 285-300.

Spratt, D. M. & Speare, R. (1982) *Durikainema macropi* gen. et sp. nov. (Muspiceoidea: Robertdollfusidae), a remarkable nematode from Macropodidae (Marsupialia). *Ann. Parasitol. hum. comp.* **57**, 53-62.

______ & Gill, P.A. (1998) *Durikainema phascolarcti* n. sp. (Nematoda: Muspiceoidea: Robertdollfusidae) from the pulmonary arteries of the koala *Phascolarctos cinereus* with associated pathological changes. *Syst. Parasitol.* **39**, 101-106.

______, Beveridge, I., Andrews, J. R. H. & Dennett, X. (1999) *Haycocknema perplexum* n.g., n.sp. (Nematoda: Robertdollfusidae): an intramyofibre parasite in man. *Ibid.* **43**, 123-131.

Thienpont, D., Rochette, F. & Vanparijs, O. F. J. (1979) "Diagnosing helminthiasis through coprological examination" (Janssen Research Foundation, Beerse, Belgium).

Wright, K. A. (1963) Cytology of the bacillary bands of *Capillaria hepatica*. *J. Morphol.* **112**, 233-259.

______ (1968) Structure of the bacillary bands of *Trichuris myocastoris*. *J. Parasitol.* **54**, 1106-1110.

______ (1989) Parasites in peril - the trichuroid nematodes pp. 65-80 *In* Ko, R. (Ed.) "Current Concepts in Parasitology" (Hong Kong University Press, Hong Kong).

A TAXONOMIC REVISION OF THE CAMPONOTUS WIEDERKEHRI AND PERJURUS SPECIES-GROUPS (HYMENOPTERA: FORMICIDAE)

By S. O. Shattuck & A. J. McArthur***

Summary

Shattuck, S. O. & McArthur, A. J. (2002) A taxonomic revision of the Camponotus wiederkehri and perjurus species-groups (Hymenoptera: Formicidae). Transactions of the Royal Society of S. Aust. (2002), 126(2), 63-90, 29 November, 2002.

The Camponotus wiederkehri and perjurus species groups are defined for the first time and revised at species level. Thirteen species are included in the wiederkehri species group, six of which are newly described while four previously valid species are synonymised. These species include arenatus sp. nov., aurocinctus (Smith) (and its new synonym midas Froggatt), ceriseipes Clark, donnellani sp. nov., gouldianus Forel, owenae sp. nov., postcornutus Clark, prosseri sp. nov., rufonigrus sp. nov., setosus sp. nov., terebrans (Lowne) (including its synonyms testaceipes Smith, latrunculus victoriensis Santschi and myoporus Clark), versicolor Clark and wiederkehri Forel (with its new synonyms denticulatus Kirby, latrunculus Wheeler and wiederkehri lucidior Forel). The perjurus species group contains the single rare species perjurus sp. nov.

Key Words: Hymenoptera, Formicidae, Formicinae, species-group, Camponotus.

Transactions of the Royal Society of S. Aust. (2002), **126** (2), 63-90.

A TAXONOMIC REVISION OF THE *CAMPONOTUS WIEDERKEHRI* AND *PERJURUS* SPECIES-GROUPS (HYMENOPTERA: FORMICIDAE)

by S. O. Shattuck* & A. J. McArthur**

Summary

Shattuck, S. O. & McArthur, A. J. (2002) A taxonomic revision of the *Camponotus wiederkehri* and *perjurus* species-groups (Hymenoptera: Formicidae). *Transactions of the Royal Society of S. Aust.* (2002), **126** (2), 63-90, 29 November, 2002.

The *Camponotus wiederkehri* and *perjurus* species groups are defined for the first time and revised at species level. Thirteen species are included in the *wiederkehri* species group, six of which are newly described while four previously valid species are synonymised. These species include *arenarius* sp. nov., *aurochiceus* (Smith) (and its new synonym *mulus* Froggatt), *cerviceps* Clark, *domethani* sp. nov., *gouldianus* Forel, *owenae* sp. nov., *postcornutus* Clark, *prosseri* sp. nov., *rufonigrus* sp. nov., *setosus* sp. nov., *terebrans* (Lowne) (including its synonyms *testaceipes* Smith, *laticeps* Wheeler and *myoporus* Clark), *versicolor* Clark and *wiederkehri* Forel (with its new synonyms *denticulatus* Kirby, *laticeps* Wheeler and *wiederkehri lucidior* Forel). The *perjurus* species group contains the single rare species *perjurus* sp. nov.

Key Words. Hymenoptera, Formicidae, Formicinae, species-group, *Camponotus*.

Introduction

In this paper we revise species of ants in the newly defined *wiederkehri* and *perjurus* species groups of the genus *Camponotus*. Fourteen species are recognised, seven of which are described for the first time; four previously valid species are treated as synonyms. These groups are restricted to Australia and contain species which range from common to rare and from widespread to restricted in distribution. They are most abundant and species rich in semi-arid regions and all are apparently ground nesting. Taxonomically, the species treated here were previously placed in the subgenera *Myrmophyma*, *Myrmosaulus*, *Myrmotarba* and *Tanaemyrmex*, placements which were made when the species were originally described and have not been discussed since. During this study it has become quite clear that the current subgeneric classification within *Camponotus* is chaotic and near-worthless. Species here placed in the *wiederkehri* species group share similarities in overall body shape and size including the placement of the compound eyes and the configuration of the mesosoma and petiole. In addition, all share a cluster of elongate hairs on the base of the mentum. This cluster is unique in the genus and strongly suggests they are monophyletic. At present, the higher-level classification within *Camponotus* is poorly understood and until the entire genus is examined more closely, it is inappropriate to speculate on relationships among species. *Camponotus gouldianus* is associated with a leafhopper and *C. terebrans* is associated with a butterfly. For an overview of the subfamily (Formicinae) and genus (*Camponotus*) in Australia see Shattuck (1999).

* CSIRO Entomology, G. P. O. Box 1700, Canberra, A.C.T. 2601, Australia.

** South Australian Museum, North Terrace, Adelaide, South Australia, 5000, Australia.

Methods

Measurements

Size and shape characters were quantified and are reported as lengths or indices. Measurements were made with a stereo microscope using a dual-axis stage micrometer wired to digital readouts. The following measurements and indices are reported.

- CI Cephalic index: HW/HL.
- HL Maximum head length in full face view, measured from the anterior-most point of the clypeal margin to the midpoint of a line drawn across the posterior margin of the head.
- HW Maximum head width in full face view excluding the eyes.
- ML Mesosomal length measured from the anterior margin of the pronotal collar to the posterior extension of the propodeum lobes.
- MTI Maximum length of mid tibia, excluding the proximal part of the articulation which is received into the distal end of the femur.
- SI Scape index: SL/HW.
- SL Length of the scape (first antennal segment) excluding the basal neck and condyle.

Location of material examined

AMSA, Australian Museum, Sydney, New South Wales; ANIC, Australian National Insect Collection, Canberra, ACT; BMNH, The Natural History Museum, London, UK; MCZC, Museum of

Comparative Zoology, Harvard University, Cambridge, Massachusetts, USA; MHNG, Muséum d'Histoire Naturelle, Geneva, Switzerland; MVMA, Museum of Victoria, Abbotsford, Victoria; SAMA, South Australian Museum, Adelaide, South Australia; WAMP, Western Australian Museum, Perth, Western Australia.

Most of the non-type material is in ANIC and SAMA.

Collectors of material examined.

AAS, A. A. Simpson; ACK, A. C. Kistner; AHB, A. H. Burbidge; AJM, A. J. McArthur; AJO, A. Johnson; AKN, A. K. Nousala; ALY, A. L. Yen; AMD, A. M. Douglas; AML, A. M. Lea; AMM, A. M. Morgan; ARP, A. R. Peilié; AWF, A. W. Forbes; AZE, A. Zeitz; BBL, B. B. Lowery; BHO, B. Hölldobler; BPI, B. Pike; BRH, B. R. Hutchins; CBA, C. Barrett; CHW, C. H. Watts; CNI, C. Nilson; CTM, C. T. Mercovich; CWA, C. Warner.; DCT, D. C. T. Rentz; DCO, D. Cox; DDA, D. Davidson; DHI, D. Hirst; DHK, D. H. Kistner; DSC, D. Schultz; EBB, E. B. Britton; EBR, E. Broomhead; EDE, E. D. Edwards; FFR, F. F. Riek; EGM, E. G. Mathews; FLO, F. Locke; FTR, F. Troughton; EXP, South Australian Museum Expedition; EYF, E. Yeatman; FAC, F. A. Cudmore; FSC, F. Schaefer; FSH, F. Shepherd; GCA, G. Campbell; GCM, G. C. Medlin; GFG, G. F. Gross; GFR, G. Friend; GJM, G. J. Mulze; GLH, G. L. Howie; GPB, G. P. Browning; GRI, Griffith Collection South Australian Museum; HBW, H. B. White; HCS, Horn Centenary Survey NVMA; HFR, H. Frahn; HHE, H. Heatwole; HMC, H. M. Cane; HOF, B. O. Fletcher; HOW, H. Owens; HRL, H. Reynolds; HWE, H. Wesselman; IAR, I. Archibald; IFB, I. F. B. Common; IGE, I. Gee; IVA, I. Valentine; JAF, J. A. Forrest; JAH, J. A. Herridge; JAR, J. Archibald; JBA, J. Balderson; JBS, J. B. Stuckey; JCG, J. C. Goudie; JCM, J. C. Myers; JDL, J. D. Erskine; JDI, J. E. Dixon; JDM, J. D. Majer; JED, J. E. Dowse; JLF, J. E. Feehan; JFF, J. F. Field; JFI, J. Findley; JGO, J. G. O. Tepper; JHA, J. Hawkins; JLA, J. Lawrence; JMC, J. McAreavey; JRB, J. R. B. Low; JRE, J. Reid; JRU, J. Ruhle; JSH, J. Shaw; JSM, J. Smith; JTH, J. Thurmer; JWI, J. Wilkinson; KCA, K. Casparson; KDA, K. Davey; KMA, K. Martin; KMC, K. McKelson; KRO, K. Roth; KRP, K. R. Pullen; KTR, K. T. Richards; LHI, L. Hitch; LPK, L. P. Kelsey; LQU, L. Queale; MAA, M. A. Adams; MDA, M. Davies; MIT, Mitchell; MJD, M. J. Douglas; MLS, M. L. Simpson; MMA, M. Mulpital; MPE, M. Peterson; MSU, M. S. Upton; NBT, N. B. Tindale; NCS, Nature Conservation Society of South Australia Inc.; NLA, N. Lawrence; PAI, P. Aitken; PCO, P. Copley; PGE, P. Gee; PGR, P. Greenslade; PHU, P. Hudson; PJF, P. J. Fargher; PJM, P. J. M. Greenslade; PPL, P. Plym; PRB, P. R. Birks; PSW, P. S. Ward; RBH, R. B. Halliday; RBR, R. Brandle; RCC, R. C. Chandler; RDN, R. D. Nutting; REL, R. Elder; RFO, R. Foster; RHC, R. H. Crozier; RHM, R. H. Mew; RJB, R. J. Bartell; RJK, R. J. Kohout; RJW, R. J. White; RRA, R. Raven; RSI, R. Smith; RSM, R. S. McInnes; RVS, R. V. Southcott; RWT, R. W. Taylor; SAH, S. A. Harrington; SANPGLS, S. Aust. National Parks and Wildlife, Goyders Lagoon Survey; SANPNOPS, South Australian National Parks and Wildlife, North Olary Plains Survey; SANPNS, South Australian National Parks and Wildlife, Nullarbor Survey; SANPPITJ, South Australian National Parks and Wildlife, Pitantjatjara Lands Survey; SANPSDS, South Australian National Parks and Wildlife, Stoney Desert Survey; SANPSOPS, South Australian National Parks and Wildlife, South Olary Plains Survey; SANPVS, South Australian National Parks and Wildlife, Vertebrate Survey; SANPWTRS, South Australian National Parks and Wildlife, Western Flinders Ranges Survey; SANPYS, South Australian National Parks and Wildlife, Yeltabinna Survey; SBA, S. Barker; SDO, S. Donnellan; SLE, S. Lewer; SMO, S. Morrison; SOS, S. O. Shattuck; SRM, S. R. Morton; TAW, T. A. Weir; TGR, T. Greaves; TGW, T. G. Wood; TRO, T. Robinson; WAL, W. A. Low; WBH, W. B. Hitchcock; WCC, W. C. Crawley; WDD, W. D. Dodd; WHC, Waterhouse Club, South Australian Museum; WKH, W. K. Head; WLB, W. L. Brown; WLN, W. L. Nutting; WMC, Western Mining & Royal Geographical Society Expedition; WMW, W. M. Wheeler; YCC, Y. C. Crozier.

Genus *Camponotus* Mayr 1861

Definition of the C. wiederkehri *species group*

Members of the *C. wiederkehri* species group can be separated from other Australian *Camponotus* by the presence of a cluster of four or more distinct elongate curved or "J"-shaped hairs on the base of the mentum (near the posterior region of the buccal cavity) in all worker castes (Fig. 1). In a few species related to *C. ephippium* similar hairs are present but these are scattered along the length of the mentum rather than being present as a posterior cluster.

Complexes within the C. wiederkehri *species group*

The *C. wiederkehri* species group can be divided into four complexes as follows. While it is likely that these complexes represent monophyletic groups (and there is no evidence that they do not) synapomorphies supporting these groupings have not been sought in this study. It is more appropriate for these studies to be developed as a holistic study of the genus.

1. *aureopilus* complex: Includes *C. arenatus*, *aureopilus*, *owenae*, *setosus* and *versiculor*. This complex is defined by the presence of a distinct and angular metanotal groove in minor workers which is depressed (sometimes only slightly) below the anterior region of the propodeum (Figs 3, 8, 9).
2. *cerisecipes* complex: Includes *C. cerisecipes*, *donnellani*, *prasseri* and *rufonigrus*. In this complex the posterior section of the mesonotum is weakly but distinctly convex immediately anterior of the metanotal groove (more so in minors, less so in majors) and the metanotal groove in minors varies from a distinct angle to a shallow concavity (Figs 12, 14, 18, 34, 36).
3. *posticornatus* complex: Includes *C. posticornatus*. In this complex the entire mesosoma in minor workers is strongly arched, lacks a metanotal groove and the posterior face of the propodeum is only weakly differentiated from the dorsal face (Fig. 31); in major workers the posterior corners of the head taper rearwards into blunt protuberances (Figs 28, 29).
4. *terebrans* complex: Includes *C. gouldianus*, *terebrans* and *wiederkehri*. In this complex the posterior section of the mesonotum is flat (or nearly so) immediately anterior of the metanotal groove and the metanotal groove in minor workers is absent or weakly developed (Figs 23, 47, 58).

Definition of the C. perjurus *species group*

This species group is recognised by having the head produced upwards so that its attachment to the pronotum is well below its upper margin (Fig. 61). It has a reduced number of hairs on the mentum compared to species of the *wiederkehri* group, approaching the arrangement found in relatives of *C. ephippium*. This group contains a single species, *C. perjurus* described below.

Key to workers of the *Camponotus wiederkehri* species group

1. Erect hairs present on all surfaces of tibiae 2
   Erect hairs absent from outer surfaces of tibiae, inner surface with a double-row (although appressed pubescence may be present).....4
2. Metanotal groove in minor worker a distinct but sometimes shallow trough (Fig. 42); known only from the Kimberley region of northern Western Australia (Fig. 43)..... *setosus*
   Metanotal groove in minor worker weakly developed (Fig. 23) or absent (Fig. 47); known only from southern Australia (Figs 24, 48).....3
3. Number of erect hairs on propodeum greater than 40; pubescence on head and gaster abundant and with individual hairs overlapping; summit of petiolar node in profile rounded in minor workers (Fig. 23), a blunt angle in major workers (Fig. 21)..... *gouldianus*
   Number of erect hairs on propodeum less than 25; pubescence on head and gaster sparse and with individual hairs generally non-overlapping or at most only slightly overlapping; summit of petiolar node in profile angular in both minor and major workers (Figs 45, 47)..... *terebrans*
4. Entire mesosoma in lateral view strongly arched, lacking a metanotal groove and with the posterior face of the propodeum only weakly differentiated from the dorsal face (Figs 29, 31); posterior corners of head of major worker tapering rearward into blunt protuberances (Figs 28, 29)..... *posticornatus*
   Mesosoma in lateral view flat or at most with the pronotum and mesonotum weakly arched and separated from the propodeum by a weak angle (Fig. 14) or a distinct, angular or concave metanotal groove (Fig. 9), the posterior face of the propodeum always separated from the dorsal face by a rounded angle (Fig. 14); posterolateral corners of head rounded in majors (Figs 33, 34)..... 5
5. Metanotal groove in minors depressed below the anterior region of propodeum (Figs 8, 9); metanotal groove in majors angular (Fig. 6); dorsum of petiolar node in minors broadly or weakly convex, flat or weakly concave, the anterior face much shorter than the posterior face (Figs 8, 9); petiolar node in majors broadly rounded above (Fig. 6)..... 6
   Metanotal groove in minors absent (Fig. 58) or angular (Fig. 14) and always even with the anterior region of propodeum; metanotal groove in majors a broad, shallow angle (Fig. 12); dorsum of petiolar node in minors angular or broadly rounded, the anterior face at most only slightly shorter than the posterior face (Fig. 14); petiolar node in majors angular above (Fig. 12) 9
6. Dorsal and anterior regions of pronotum dark red-black, distinctly darker than the yellow-red mesonotum and propodeum ..... *arenatus*
   Entire mesosoma uniform in colour, varying from dark red-black to black 7
7. Elongate (overlapping) and dense pubescence present on dorsum of head, mesosoma, gaster and tibiae..... *aureopilus*
   Short (non-overlapping) and scattered pubescence present on dorsum of head, mesosoma, gaster and tibiae 8
8. Anterior region of first gastral tergite dark reddish black or black; similar in colour to propodeum; metanotal groove in minors distinct

and depressed well below the anterior region of propodeum (Figs 8, 9) ..... *aurochetus*
First and second gastral tergites red, distinctly lighter in colour than the reddish black propodeum; metanotal groove in minors weakly to moderately depressed below the anterior region of the propodeum (Figs 52, 53) ..... *versicolor*

9.. Posterior section of mesonotum flat (or nearly so) immediately anterior of metanotal groove, metanotal groove absent or weakly developed in minors (Fig. 58); anterior clypeal margin in majors projecting with a straight central region separated from lateral regions by distinct angles (Fig. 55)..... *wiederkehri*
Posterior section of mesonotum weakly but distinctly convex immediately anterior of metanotal groove (more so in minors, less so in majors); metanotal groove varying from a distinct angle to a shallow concavity in minors (Figs 14, 18, 36); anterior clypeal margin in majors broadly convex across entire width (Fig. 11) 10

10. Propodeum with at most 4 elongate erect hairs which are limited to the angle between the dorsal and posterior faces..... *donnellani*
Propodeum generally with more than 10 erect hairs which are always scattered along the entire dorsal surface 11

11.. Metanotal groove well defined and angular (Fig 39); black head contrasting with red mesonotum ..... *rufonigrus*
Metanotal groove a weakly defined concavity (Figs 14, 36); head same colour as mesonotum (both either red or black)..... 12

12. Scapes relatively short (in minors, SI < 1.5) (Fig. 15); petiolar node of minors generally more upright and narrower (Fig. 14)..... *vertiscapes*
Scapes relatively long (in minors, SI > 1.4) (Fig. 15); petiolar node of minors generally lower and broader (Fig. 36)..... *prosseri*

Species of the C. wiederkehri *species group*

Camponotus arenatus sp. nov
(FIGS 2-4)

Material Examined

Holotype. Minor worker from **South Australia:** Hambidge [labelled as Hambridge] National Park, 17 December 1970, E. B. Britton (ANIC)

Paratypes. Two minor workers, same data as holotype (ANIC, SAMA).

Other material examined

Northern Territory: 15km S Alice Springs (PJM). **South Australia:** Cowell (BBL); Maralinga (GFG); Yumbarra CP, 26km N Inila Rock Waters (HOW) **Western Australia:** 20mi. W Sandstone on Mt Magnet Rd. (AMD & MJD).

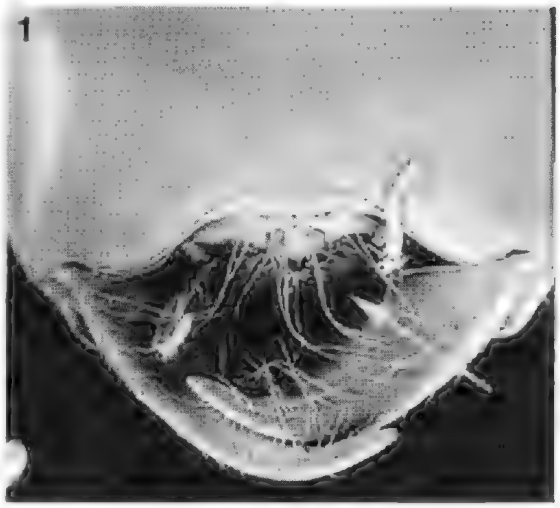

Fig. 1. Underside of the head showing distinctive cluster of elongate curved or "J"-shaped hairs (indicated by arrow) on the mentum.

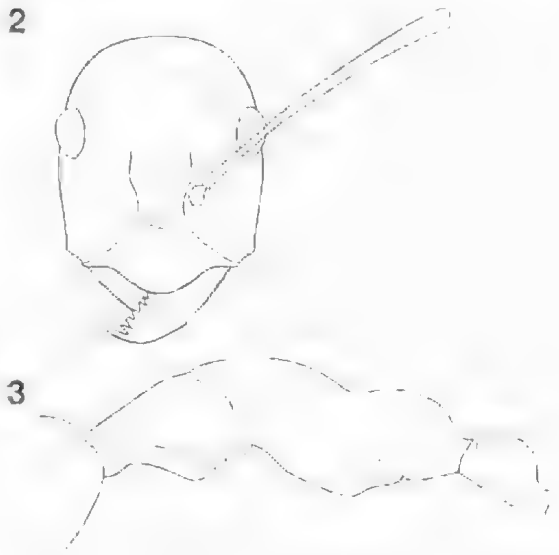

Figs 2-3. *C. arenatus* workers. Fig. 2. Head of minor worker. Figs 3. Mesosoma and petiole of minor worker

Worker diagnosis (minor worker)

Tibiae and scapes lacking erect hairs. In minor workers metanotal groove depressed below level of the anterior region of the propodeum; dorsal surface of node broadly convex, its anterior face much shorter than the posterior face (Fig. 3). Dorsal and anterior regions of the pronotum dark red-black, distinctly darker than the yellow-red mesonotum and

Fig. 4. Distribution of *C. arenatus* material examined during this study

propodeum. This species is superficially similar to *C. donnellani* in overall colour pattern but differs in the larger size of the minor worker and the depressed metanotal groove.

Description (minor worker)

Anterior clypeal margin broadly convex (Fig. 2). Dorsal surface of pronotum weakly convex and separated from the weakly convex mesonotum by a shallow angle; metanotal groove slightly but distinctly depressed below the level of the anterior propodeum; propodeum uniformly and weakly convex and without a distinct angle, ratio of dorsum to declivity about 1.5 (Fig. 3). Petiolar node with a short anterior face which is weakly differentiated from the broadly convex upper surface, the rear face indistinguishable from the upper surface (Fig. 3). Erect hairs moderately abundant on all surfaces of the head and dorsal surfaces of the mesosoma, petiolar node and gaster, absent from scapes and tibiae. Head and anterior regions of pronotum black, posterolateral pronotum (immediately above the fore coxae), mesonotum, propodeum, petiole and legs yellow-red; gaster varying from entirely yellow-red to a combination of the yellow-red anteriorly and red-black posteriorly.

Measurements

Minor worker (n=5). CI 0.77 – 0.79; HL 1.94mm – 2.20mm; HW 1.50mm – 1.74mm; ML 3.45mm – 3.81mm; MTL 2.26mm – 2.47mm; SI 1.49 – 1.59; SL 2.38mm – 2.59mm.

Comments

This uncommon species is known from a limited number of minor workers. It ranges from south-central South Australia, north to southern Northern Territory and west-central Western Australia (Fig. 4). The only biological information is provided by the single worker collected by B. B. Lowery. It was swept from mallee on red sand.

Etymology

From *arena*, alluding to the sandy nature of the known collection sites of this species.

Camponotus auriscinctus (F. Smith)
(FIGS 5-10)

Formica auriscincta Smith, 1858: 39.

Camponotus auriscinctus – Mayr, 1886: 355.

Camponotus midas Froggatt, 1896: 390; Clark, 1930*a*: 22 (queen described, worker redescribed). New synonymy.

Camponotus sp. 8 – Imai *et al.*, 1977: 369.

Material examined

Camponotus auriscinctus. Worker holotype or syntypes from Adelaide, South Australia. A single specimen (minor worker) in BMNH is labelled as the type of this species. However, this specimen was acquired in 1870, several years after the original description was published. It is currently not known whether the acquisition date is in error or the type specimen is lost. For the purposes of this study this specimen is considered a type specimen for this name.

Camponotus midas. Syntypes from Illamurta, Northern Territory (1 worker (missing from point) and 1 queen in AMSA; 7 workers, 1 queen and 1 male in MCZC; 1 worker in MVMA; 3 workers in BMNH (with an additional 6 workers labelled as "C. Australia. Hom Coll., 96-37" and bearing a Type label).

Other material examined.

New South Wales: 12km S Coombah (PSW); 45km N Balranald (SOS); Ascot Vale (RSM); Black Hill Creek (RHM); Broken Hill (FSH); Broken Hill Airport (RSM); Matakana RS (BBL); Mount Gipps (RHM); Mundi Mundi, nr. Broken Hill (PJM & IVA); Pinnacles, 12mi. W Broken Hill (BBL); Pooncarie, W. Smith property (RHC & YCC & AKN); Silverton (PJM). **Northern Territory:** 15km S Alice Springs (PJM); 23mi. N Narwietooma HS (RSM & JED); 33km E Ayers Rock (JEF); 7km W Curtin Springs (SOS); Andado (HOF); Kings Creek Stn (SDO); nr. Ayers Rock (BBL); Old Andado, c.15km EbyN Andado HS (JEF); Uluru NP 15 km ESE (HCS). **Queensland:** Muncoonie Lake (RRA); Cunnamulla (BBL); Foxes Ck. (GCA); Sandringham (PJM). **South Australia:** 10km NW Emu Junction (JAH); 10km WSW Mt. Playford, Murnpeowie (JRE); 10mi. S Loxton (BBL); 11km ENE Arabana Hill, Murnpeowie (JRE); 14 km SW Taplan (SANPWS); 14km SbyW Beltana (JEF); 14km

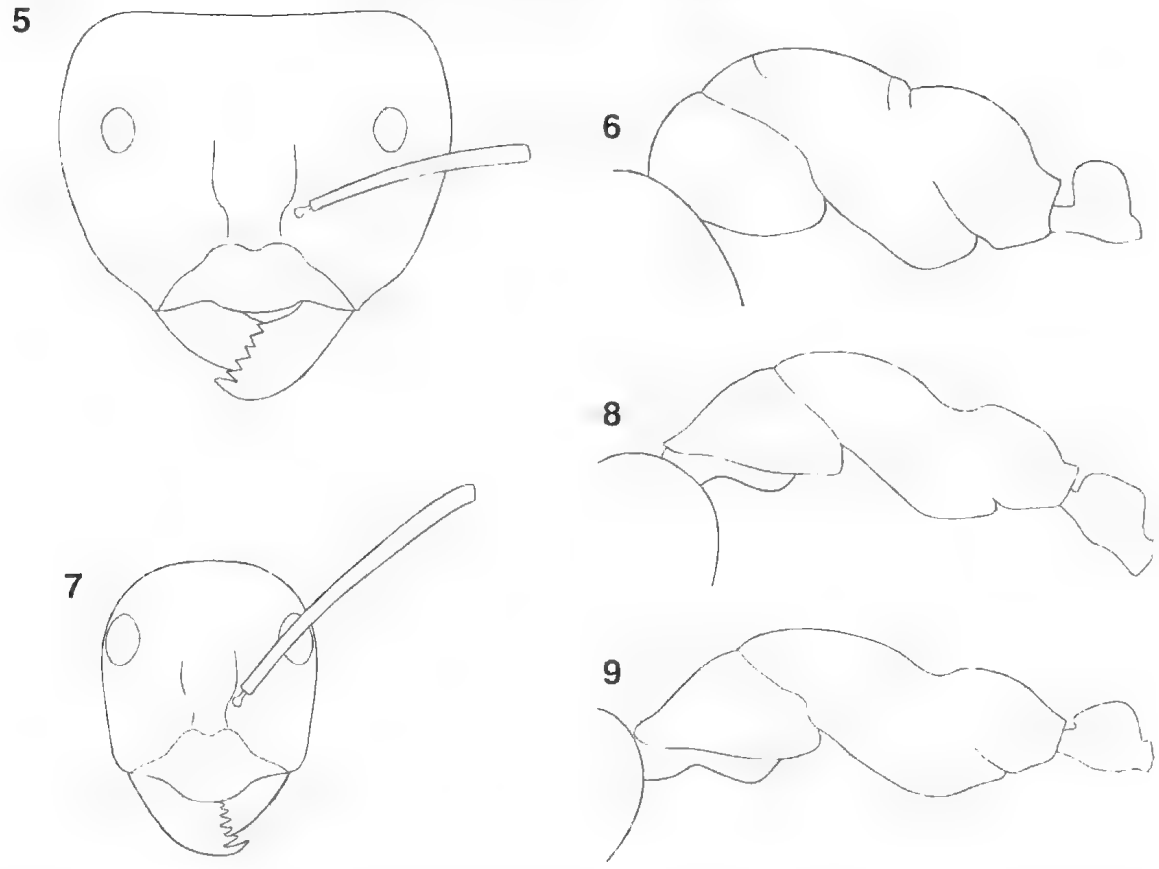

Figs 5-9. *C. aurocinctus* workers. Fig. 5. Head of major worker. Fig. 6. Mesosoma and petiole of major worker. Fig. 7. Head of minor worker, Figs 8-9. Mesosoma and petiole of minor worker.

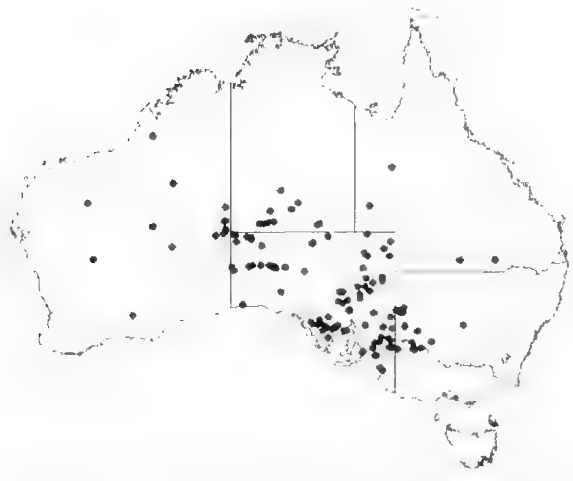

Fig. 10. Distribution of *C. aurocinctus* material examined during this study.

WNW Renmark (KRP); 1km N Vokes Hill junction (JAF); 1km W Emu Camp, Victoria Desert (PJM); 2.5km N Limestone dam (SANPSOPS); 26km SSE Illintjitja (SANPPITJ); 30mi E Farina, Mt. Lyndhurst (ETR); 31km NW Renmark (KRP); 3km W Emu Camp, Victoria Desert (PJM); 4.8km SE Coongie, Coongie Lakes Study site 10E (JRE); 40km W Vokes Hill Junct. (JAF); 40km WNW Emu, Victoria Desert (PJM); 40mi. SW Iron Knob (JRE); 45km WNW Emu, Victoria Desert (PJM); 4km NE Marroo Hill, Cowarie (PRB); 5 km SW Farina (SANPSOPS); 60km E Vokes Hill, Victoria Desert (PJM); 6km W Koonchera, Birdsville Track (PJM & JAF); 70km E Emu, Victoria Desert (PJM); 9km ESE Wapalanchie Tank, Cowarie (TRO); Adelaide (GRI); Adelaide (JGO); Alton Downs old HS, c.48km SW Birdsville (JEF); Ampeinna Hills 10.5 km E (SANPPITJ); Andamooka Ranges (MIT & GFG); Approdinna Attora Knolls 86.3 km SW (SANPSDS); Barton Siding (AML); Beda Hill (JAF); Bimbowrie 2 km NE (SANPNOPS); Brookfield Conservation Park (Site No. 1) (SOS);

c.18km SSE Poochera (RWT & RJB); c.22km N Beltana (JEF); Calperum NE Boundary (AJM); Cambrai (PJM); Cheesman Peak 13.2 km NW (SANPPITJ); Clifton Hills Outstation (JAF & DHJ); Coongee Lakes (JRE); Coongie Lake (DHJ); Coongie Lakes (JRE); Cordillo Downs Stn (SANPSDS); Cordillo Downs Stn (SANPSOPS); Corrobinnie Hill, Eyre Penin. (KCA); Danggali CP, Red Tank Dam (AJM); Darke Reske, Eyre Pen (BBL); E Purni Bore at junction of French Track and Rig Rd., Simpson Desert (JAF); Emu Camp, Victoria Desert (PJM); Emu Junction 10 km NW (JAF); Etadunna Stn. (JTH); Farina 5 km SW (SANPSDS); Gammon Ra. NP, Balcanoona area (AJM); Gawler Ranges (PJM); Glenelg (WBH); Gum Lagoon (EGM & JAF); Hamilton Ck. (RBR); Hamilton Stn. (WKH); Hincks NP (EBB); Illintjitja 23 km WSW (SANPPITJ); Iron Knob 40 miles SW (EFR); Kendal (AWF); Killiparu CP (SLE); Kimba (PJM & IVA); Kimba, edge of Pinkawillinie C.P. (FSC); Koonamore (PJM); Koonamore 9 km E (SANPNOPS); Koonamore, Nillinghoo (PJM); Koonchera Waterhole 6.25 km S (SANPGLS); Koonchera: Birdsville Track (PJM & JAF); Kopi, Eyre Pen. (PJM); Kunytjanu 25 km NW (SANPPITJ); L. Meramangye, Victoria Deser: (PJM); L. Torrens, nr. Beda Hill (JAF); Lake Appadare 2.4km S (WHC); Lake Callabonna (AZE); Lake Gilles CP (BPI); Lake Palankarinna (JTH); Little Pine Hill c. 32mi. SW Whyalla (EBB); Mabel Creek (PGR); Marpoo Waterhole (PGE & IGE); Marsella Hill 3.6 km SE (SANPSDS); Maryinna Hill 21.5 km ESE (SANPPITJ); May Hill 9.3 km WNW (SANPSDS); Montecollina Bore (JSH); Morgan vale, Danggali CP (AJM); Mount Lindsay 3.1 km WNW (SANPPITJ); Mt. Gunson, SE Woomera (PJM); Mt. Sturt, nr. salt lake, N. Eyre Pen. (JAF); Munyaroo CP, 7km SSW Moonable HS, 37km fr. Whyalla (WKH); NW Yaninee, Eyre Penin. (KCA); Olympic Dam (EGM & CWA); Paney, nr. Pink Lake, Gawler Ranges (WHC); Pinkawillinie CP, Eyre Pen. (JAF); Pinnacles Mine (RHM); Pipalyatjara 27.5 km NE (SANPPITJ); Poochera (BHO); Purni Bore 77 km E (SANPSDS); Purni Bore, SW Simpson Desert (PJM); Radium Hill (PAI); S end of L. Windabout (BBL); S Koonchera, Birdsville Track (PJM & JAF); S of Mann Ra. 8.5km NW Mt. Kintore (SANPPITJ); Serpentine L., Great Victoria Desert (PJM); Serpentine Lakes (JAF); Simpson Desert (DSC); Sinclair Gap (PHD); Stockyard Plain (AJM); Taplan 14 Km SW (SANPVS); Thirty Thousand Tank (GCM); Tomahawk Dam (JAF); Trinity Well (as 'Trinity') (EXP); Ungarinna Rockhole (SANPPITJ); Vokes Hill 1 km N (JAF); Wallatinna 16 km W (SANPPITJ); Yelpawaralinna Waterhole 7.6 km NNW (SANPGLS). **Victoria:** 9km ESE Hattah (ALY); Bannerton (CNI); Hattah (ALY); Lake Mournpall, Hattah-Kulkyne Nat. Park (SOS); Millewa South Bore (ALY); Halls Creek (KMA); Mungilli Claypan (KDA). **Western Australia:** 11km W Terhan W-H (PJM & HHE); 11mi, N Mt. Aloysius (RSM & JED); 163km SlibyE Broome (IFB); 16km W Mt. Aloysius (JEF); 16km W Mt. Aloysius (JEF & TWF); 19mi. N Mt. Aloysius (RSM & JED); 20mi. W Sandstone on Mt. Magnet Rd (AM & MJD); 22mi. WSW Mt. Forrest (RSM & JED); 24km SSW Turee Creek HS (MPE); 28mi. NE Carnegie HS (RSM & JED); 66km SWbyW Docker River, Northern Territory (JEF & TWE); Canning Stock Route (EXP); Cavenagh Ra. (KTR); Koonalda Cave (WHC); Meekatharra-Billiluna Pool Canning Stock Route (EXP); Norseman (BBL); Norseman Area (AM & MJD); Sir Fredrick Ra. (KTR)

Worker diagnosis

Tibiae lacking erect hairs. In minors, metanotal groove depressed below the level of the anterior region of the propodeum; dorsal surface of petiolar node relatively long and flat, its anterior face much shorter than the posterior face (Figs 8, 9). Mesosoma uniform in colour, varying from dark red-black to black, anterior region of first gastral tergite similar in colour to propodeum, gastral tergites often with the trailing edge golden yellow, the golden colour (when present) varying in width from a narrow band to involving most of the tergite.

Description (major worker)

Anterior clypeal margin weakly convex (Fig. 5). Dorsal surfaces of pronotum and mesonotum convex and separated by a shallow angle; propodeum uniformly convex and without a distinct angle; petiolar node with distinct anterior and posterior faces, its upper surface varying from a broad, blunt angle to uniformly convex and sometimes with the medial section nearly flat (Fig. 6). Erect hairs absent from scapes, petiole and tibiae, absent or a few scattered hairs on the outline of head and dorsum of mesosoma and gaster; underside of head with none to about 30. Body varying from dark red to red-black, the head and dorsal surfaces of pronotum and mesonotum sometimes darker than the lateral mesonotum, propodeum, legs and petiole; gaster reddish black with yellow-gold banding along the posterior edge of each segment which varies from being absent to involving the entire visible portion of the segment.

Description (minor worker)

Anterior clypeal margin convex to broadly angular (Fig. 7). Dorsal surfaces of pronotum and mesonotum convex and separated by a shallow, broad angle, the posterior metanotum ending in the

metanotal groove; metanotal groove distinct, separated from the anterior propodeum by a short face which varies from steep (Fig. 8) to gentle (Fig. 9); dorsal and posterior faces of propodeum flat to weakly concave and separated by a broad, gentle angle. Anterior face of petiolar node short and separated from the dorsal face by a sharp angle, dorsal face elongate and flat to weakly concave and separated from the posterior face by a broad, rounded angle, posterior face flat (Figs 8, 9). Erect hairs absent from scapes and legs, absent or with a few scattered hairs on the outline of head, mesosoma, petiole and gaster; underside of head with up to about 30 hairs. Body varying from red to red-black, head and sometimes propodeum, petiole and middle and hind legs usually slightly lighter than the pronotum; gaster dark reddish black and sometimes with yellow-gold banding along the posterior margin of each segment which varies from narrow to involving the entire visible segment, in which case the gaster is completely yellow-gold.

Measurements

Workers (n 20). CI 0.80 (minors) – 1.22 (majors); HL 2.04mm – 4.05mm; HW 1.63mm – 4.94mm; ML 3.68mm – 5.14mm; MTL 2.58mm – 3.14mm; SI 0.63 (majors) – 1.53 (minors); SL 2.50mm – 3.00mm.

Comments

Camponotus midas, established by Froggatt (1896), is here considered a synonym of *C. aurocinctus*. Froggatt made no mention of *C. aurocinctus* in his description of *C. midas* and it is unclear if he was aware of *aurocinctus*, and if so, how it differed from his species. Clark (1930a) redescribed *C. midas* and separated it from *C. aurocinctus* "by the shape of the thorax and node, and the colour of the gaster. In *C. aurocincta* the posterior margin of the segments is narrowly yellow. In *midas* the whole of the segments, except the base of the first, are entirely bright golden yellow." Unfortunately, the currently available material shows that all of these characters are highly variable. Many show an east-west clinal pattern, with several changing rapidly across central South Australia. For example, *C. aurocinctus* specimens from Western Australia are generally darker and hairier (especially on the underside of the head) compared to those from eastern South Australia eastward. The western populations also tend to have broader bands of golden yellow on the gaster with completely black gasters essentially unknown. In contrast, eastern populations often have narrow bands or lack banding completely, the gasters being uniformly black. Other characters, such as the depth of the metanotal groove and the relative length of the petiolar node, vary considerably within local areas or within single nest series. This variation suggests that a single widespread and variable species is involved rather than two (or more) separate species.

Camponotus aurocinctus is known from south-central Queensland, western New South Wales and north-western Victoria west through South Australia and southern Northern Territory to west-central Western Australia (Fig. 10). It is ground nesting, shows a strong preference for sandy soils and is most often found as foragers during daylight hours. One of us (AJM) has observed this species at Stockyard Plain and Danggali Conservation Park, South Australia, foraging in the vicinity of *Camponotus terebrans*. The karyotype of this species was discussed by Imai *et al.* (1977) (as *Camponotus* sp. 8).

Camponotus veriseipes Clark
(FIGS 11–16)

Camponotus (*Myrmophyma*) *veriseipes* Clark, 1938: 378.

Material examined

Syntypes. Six workers from N. end of Reevesby Island, South Australia, December, 1936, J. Clark (3 in ANIC, 3 in MVMA).

Other material examined

Northern Territory: 15km S Alice Springs (PJM); NW Alice Springs, Atartinga (PJM). **South Australia:** 10km WSW Lameroo (PJM); 6km NW Mt. Pleasant (PJM); Banff, Coorong (PJM); Belair (PJM); Bridgewater (PJM); Calca (BBL); Calca, 30km SE Streaky Bay (BBL); Cape Bauer (RWT & RJB & BBL); Clifton Hills Outstation (JAF & DHI); Coorong, Coolatoo (PJM); Coorong, 5km WNW Pitiochry HS (PJM); Eyre Pen., 6km W Wanilla (PJM); Innes Natl. Pk., York Peninsula (PJM); Kangaroo Is., 1km N Breakneck Ck. (PJM); Kangaroo Is., N Breakneck R. (PJM); Mt. Compass (BBL); Mt. Lofty (BBL); Mt. Rescue CP, Jimmy's Well (JAF); Port Parham (BBL); Sandy Creek, Mt. Lofty Ranges (EYE); Poochera (PSW); Streaky Bay (BBL); Victor Harbour (PJM). **Western Australia:** 20km S Condingup (SOS); 53mi. EbyS Ravensthorpe (RWT); Cape Arid NP, Yokinup Bay (AHB); Coalmine Beach, Walpole-Nornalup Natl. Pk. (JLA & NLA); Esperance area (BBL); Green's Pool, William Bay Natl Pk (SOS); Junana Rock, 9km NW Mt. Ragged (RWT); Ocean Beach, Denmark (BBL); Redgate Beach, Leeuwin-Naturaliste Natl Pk (SOS); Waterfall Beach, William Bay Natl Pk (SOS); William Bay Rd., Denmark (BBL); William Bay, Denmark (BBL).

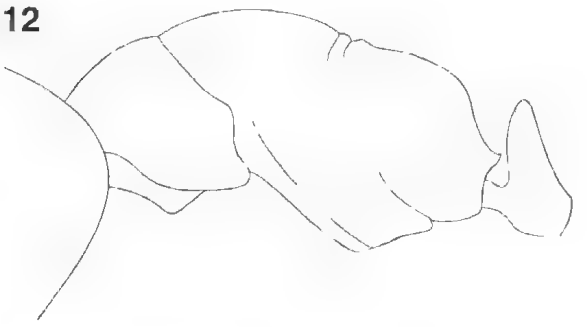

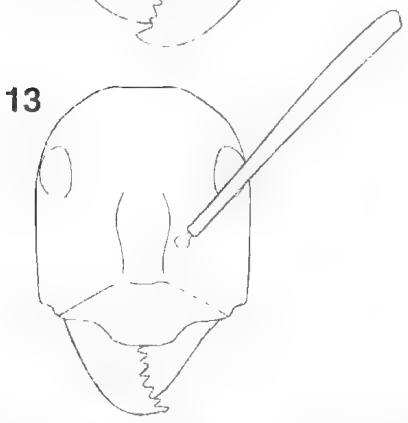

Figs 11-14. *C. ceriseipes* workers. Fig. 11. Head of major worker. Fig. 12. Mesosoma and petiole of major worker. Fig. 13. Head of minor worker. Fig. 14. Mesosoma and petiole of minor worker.

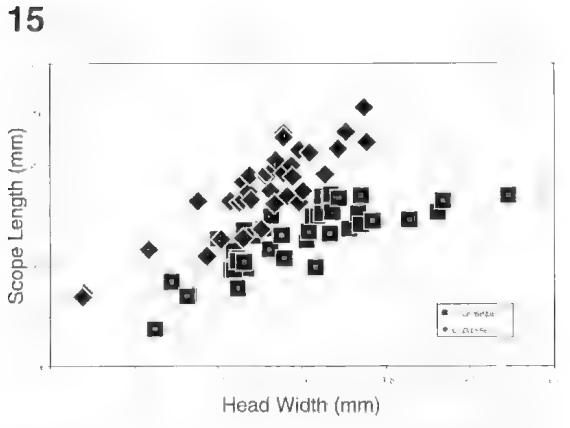

Fig. 15. Distribution of scape length versus head width for *C. ceriseipes* and *C. prosseri* minor workers.

Fig. 16. Distribution of *C. ceriseipes* material examined during this study.

Worker diagnosis

Scapes relatively short (in minors, SI < 1.5) (Fig. 15). Posterior section of mesonotum weakly but distinctly convex immediately anterior of the metanotal groove (more so in minors, less so in majors); metanotal groove a shallow, weakly defined concavity in minors (Figs 12, 14). Petiolar node angular or broadly rounded above, the anterior face at most only slightly shorter than the posterior face (Figs 12, 14). Tibiae and scapes lacking erect hairs, propodeum with more than 10 erect hairs (occasionally with fewer) which are scattered along the entire dorsal surface (never limited to near the propodeal angle as in *C. donnellani*). Anterior

clypeal margin in majors broadly convex across its entire width. Head same colour as mesonotum (both either red or black).

This species is most often confused with the morphologically similar *C. prosseri*. The surest way to separate these species is based on scape length. In larger minor workers of *C. ceriseipes* the scape is relatively short compared with similar sized *C. prosseri* workers (Fig. 15). Note, however, that this difference is minimal or non-existent in smaller workers due to allometry in this character. Other characters useful in separating minor workers of these taxa are the generally higher and narrower petiolar node (Fig. 14) and shiny integument in *C. ceriseipes* compared to the lower and broader node (Fig. 36) and duller integument in *C. prosseri*. The shape of the node works well for the majority of minor workers while the shininess of the integument is more problematic due to the highly qualitative nature of, and greater variation in, this character.

Description (major worker)

Pronotum and mesonotum gently convex, metanotum distinct, propodeal dorsum weakly convex, sometimes a little stronger near metanotum; angle well rounded and indistinct, anterior face of petiolar node straight, summit narrowly rounded, posterior face straight, feebly concave near summit (Fig. 12). Anterior margin of clypeus weakly convex, scarcely projecting, with a weak carina (Fig. 11). Posterior margin of head, underside of head, mesosoma, node and gaster with scattered long setae, tibiae and scapes lacking erect hairs. Head red to black, scape red to black, funiculus dark brown; pronotum red to dark brown; mesonotum red to dark brown; petiole red to black; gaster very dark brown to black; legs red to black.

Description (minor worker)

Anterior clypeal margin convex, carina distinct (Fig. 13). Pronotum and mesonotum an even, broad convexity; metanotum indistinct; anterior region of propodeum feebly concave, posterior region straight, angle distinct and widely rounded, ratio of dorsum to declivity near 2 (Fig. 14). Anterior face of petiolar node straight, inclined forward, summit rounded, posterior face straight (Fig. 14). Posterior margin of head, underside of head, mesosoma, petiole and gaster with scattered long setae, tibiae and scapes lacking erect hairs. Head red to black, scape red to black, funiculus dark brown; pronotum, mesonotum, propodeum and petiole each red to black; gaster very dark brown to black; legs red to black.

Measurements

Workers (n=94) CI 0.82 (minor) – 1.23 (major); HL 1.42mm – 3.31mm; HW 1.25mm – 4.06mm; ML 2.36mm – 4.28mm; MTL 1.59mm – 2.58mm; PnW 1.07mm – 2.45mm; SI 0.68 (major) – 1.42 (minor); SL 1.75mm – 2.58mm.

Remarks

The specimens here treated as belonging to this species show considerable variation in body colour. The head and mesosoma range from uniform red to uniform black with essentially all intermediate combinations displayed among the available material. There is a weak trend for the Western Australian specimens to be darker and a distinct trend for the Northern Territory specimens to be lighter. However, numerous specimens bridge the gaps between these colour forms, especially within Western Australia, and specimens nearly identical to those from the Northern Territory occur in South Australia along with more typical workers.

Camponotus ceriseipes ranges from eastern South Australia west along the coast through Western Australia, with two known collections from southern Northern Territory. It has been found in coastal sand-plain heath, coastal scrub, limestone mallee, low scrub on a dry ridge and on vegetated coastal sand dunes. Nests have been found under rocks and in open sand and workers have been collected from pitfall traps and while beating vegetation. The species has been found with myrmecophilides (Orthoptera) at Mount Compass, South Australia, by B. B. Lowery.

Camponotus donnellani sp. nov.
(FIGS 17-19)

Material examined

Holotype. Minor worker from Kings Creek Station, Northern Territory, 23 August, 1992, S. Donnellan sandhill (ANIC).

Paratypes. Two minor workers, same data as holotype (ANIC, SAMA).

Other material examined

Northern Territory: 29km ESE Uluru, Uluru Kata Tjuta (JWA); 15km ESE Uluru, Uluru-Kata Tjuta (JWA). **South Australia**: 3.1km WNW Mt Lindsay (SANPPTJ); E shore Serpentine Lakes (JAF).

Worker diagnosis

Propodeum with at most 4 elongate erect hairs near the angle between the dorsal and posterior faces. Pronotum and mesonotum flatly convex, metanotal grove indistinct, anterior region of propodeal dorsum feebly concave, straight posterior. Petiolar node broadly rounded above, its anterior face at most only

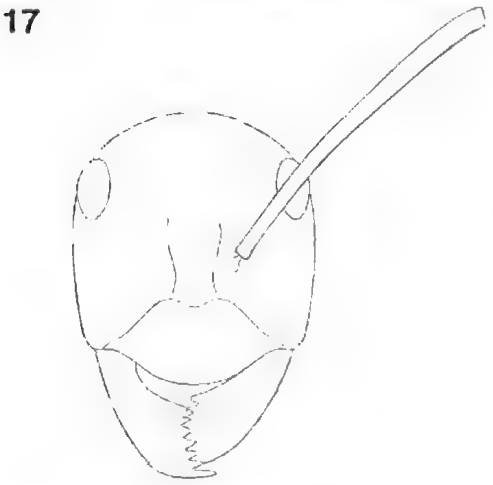

Figs 17-18. *C. donnellani* worker. Fig. 17. Head of minor worker. Fig. 18. Mesosoma and petiole of minor worker.

Fig. 19. Distribution of *C. donnellani* material examined during this study.

slightly shorter than the posterior face (Fig. 18). Tibiae and scapes lacking erect setae. Anterior clypeal margin feebly projecting, broadly convex across its whole width.

Camponotus donnellani is similar to *C. arenatus* in overall colour pattern but differs in the smaller size of the minors and the flatter mesosomal dorsum with a less distinct metanotal groove. It may also be confused with smaller, paler workers of *C. cerisetpes*, but differs in having fewer erect hairs on the propodeal dorsum.

Description (minor worker)

Pronotum and mesonotum gently convex, metanotal grove indistinct; anterior region of propodeum feebly concave then straight, lacking an angle between the dorsal and posterior faces, ratio dorsum to declivity about 3 (Fig. 18). Anterior face of petiolar node about as long as dorsal face and separated from it by a moderate convexity; dorsal face weakly convex and separated from the posterior face by a broad, rounded angle; posterior face flat (Fig. 18). Elongate erect hairs scattered on all surfaces of head (including underside), mesosoma, node and gaster, absent from scapes and tibiae. Anterior clypeal margin convex broadly angular (Fig. 17). Head, mesosoma and petiole red with upper surfaces of head, pronotum and sometimes mesonotum infuscated with dark red-black, legs red-black basally, red distally; gaster dark red-black.

Measurements

Holotype, CI 0.89; HL 1.58mm; HW 1.40mm; ML 2.58mm; MTL 1.78mm; SI 1.32; SL 1.85mm.

Remarks

Camponotus donnellani has been encountered a limited number of times in north-western South Australia and south-western Northern Territory. It has been collected from a sand hill in association with *Triodia* spp. in the Great Victorian Desert of southern Northern Territory. Little else is known of its biology.

Etymology

Named after Dr Steve Donnellan of the South Australian Museum, the collector of this species.

Camponotus gouldianus Forel
(FIGS 20-24)

Camponotus gouldianus Forel, 1922: 100.

Material examined

Syntypes. Two medium workers from Sea Lake, Victoria, both badly damaged (MHNG).

Other material examined

New South Wales: Balranald (JWI); c. 26km E Euston (RJK). **Northern Territory:** Illamurta Spr CP (JAF & DHI). **South Australia:** 10km NE Chilpuddie, Gawler Ranges (PJM); 10km NW Ceduna (RFO); 11km E Poochera (RWT & RJB &

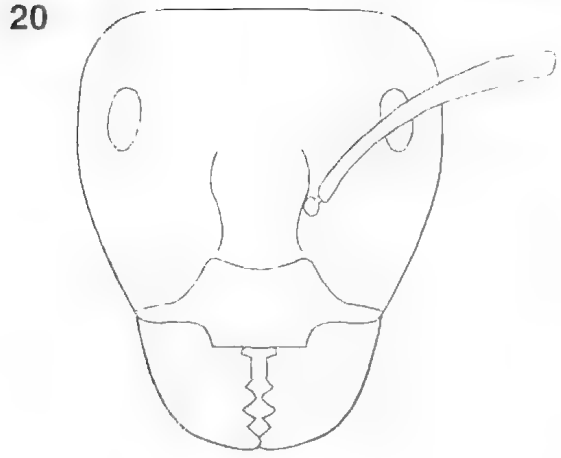

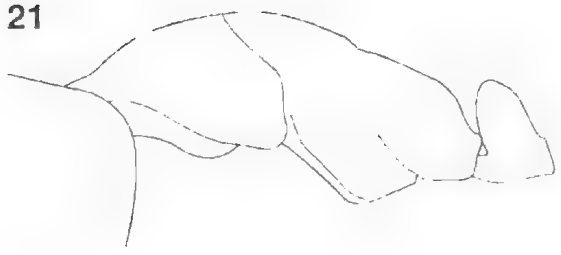

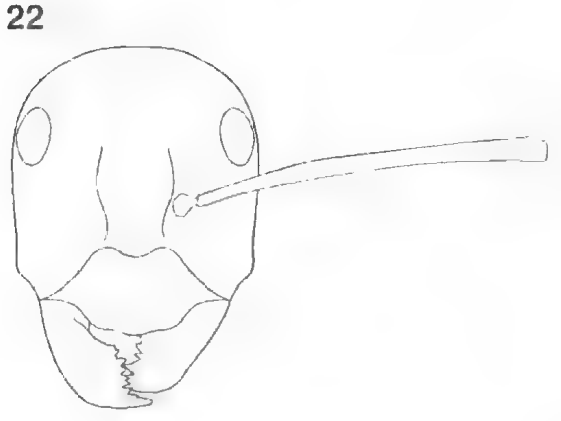

Figs 20-23. *C. gouldianus* workers. Fig. 20. Head of major worker. Fig. 21. Mesosoma and petiole of major worker. Fig. 22. Head of minor worker. Fig. 23. Mesosoma and petiole of minor worker.

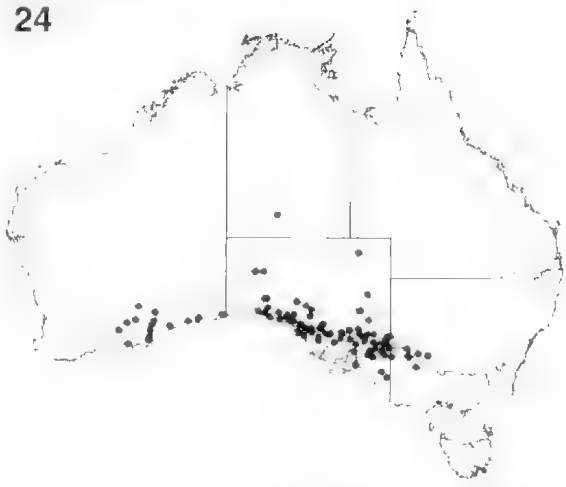

Fig. 24. Distribution of *C. gouldianus* material examined during this study.

ELO); 11mi. E Kimba (PJM); 12km E Ceduna (RFO); 12km E Warramboo, Eyre Pen. (PJM); 13km E Ooldea (JAF); 13mi. SE Streaky Bay (TGR); 15km NW Renmark (SOS); 18km E Ceduna (RFO); 20km E Ceduna (JAF); 20km E Paney HS, Gawler Ranges (PJM); 20km E Ulooloo (PJM); 20km ENE Umberatana (PJM); 20km NW Minnipa (AJM); 23km NbyW Renmark (SOS); 32km N Renmark (SOS); 3mi. W Penong (TGR); 41km EbyN Nullarbor (RWT); 45km WNW Emu, Victoria Desert (PJM); 4km W Wirrula (JAF); 4mi. E Oraparinna (GFG); 53km E Vokes Hill, Victoria Desert (PJM); 53km NbyW Renmark (SOS); 58km E Vokes Hill, Victoria Desert (PJM); 5km N Poochera (RWT & RJB & ELO); 60km N Colona (EXP); 60km NNE Ceduna (JAF & PJM); 6km W Nundroo (RFO); 7.4km SW Poochera on Port Kenny Rd (RWT & RJB & ELO); 7.5km NW Venus Bay (SANPNS); 79km NNW Renmark (AJM); 7km NE Pumong (SANPVS); 7km SE Belah (SANPSOPS); 7km SSW Munyaroo CP (WKH); 7km W Inila Rock Waters (SANPYS); 9km N Atkindale HS (SANPSOPS); Aldinga Scrub (SMO); Allendale HS 9 km N (SANPSOPS); Baratta 6 km NW (SANPSOPS); Belah 7 km SE (SANPSOPS); Blyth (BBL); Brookfield Conservation Park, 0.5km S Camp area (SOS); Brookfield Conservation Park, Camp area (SOS); Buckleboo (EBR); Calpatanna CP, Eyre Pen. (JAF); Calpatanna Waterhole (JAF); Calperum Amalia (AJM); Calperum Murphys (AJM); Calperum NE corner (AJM); Cambrai (PJM); Canopus Dam (AJM); Canopus HS, Danggali CP (TWE & KRP); Ceduna (KCA); Ceduna 10 km NW (RFO); Ceduna 18 km E (RFO); Chadee (LQU); Chowilla (TGW & PJM); Clements Gap CP (DHI); Colona 60 km N (EXP); Cooltong (GLH); Coultong

(AJA & MAA); Cowell (BRH); Danggali Tipperary Dam (AJM); Danggali, NE corner (AJM); Flash Jack Dam (SANPSOPS); Gawler Ra Lake Everard Stn (GFG); Gawler Ra Scrubby Peak (JAF); Gawler Ranges (PJM); Hideaway Hut (SANPSOPS); Inila Rock Waters 7 km W (SANPYS); Kataropko Creek (AJM), Kimba (PAI); Kokatha, Gawler Ranges (PJM); Kooma, Eyre Peninsula (PJM); Koonamore (PJM); Koonamore HS (JAF); Kychering Soak (RCC); Lake Everard Stn, Gawler Ranges (GFG); Lake Gilles (JAF); Lock (AJM); Loxton Paynes Farm (AJM); Loxton Snodgrass Farm (AJM); Mambray Creek, Port Augusta (PJM); Middle Dam (SANPSOPS); Middleback Stn. (AJO); Minnipa 20 km NW (AJM); Mitcherie Rockhole (SANPYS); Mongolata (SANPSOPS); Moorowie Plain (PJM); Morgan vale, Danggali CP (AJM), Mount Arooma (SANPNWFRS); Mount Ive (AJA & PJF); Mount Rescue CP (JAF); Mundoora NP (PJM); Munyaroo CP 7 km SSW (W.K.Head); N.S.W. Coombah (PSW); Nundroo (AJA & SBA); Nundroo 6 km W (RFO); Nundroo Roadhouse (RFO); Oak Bore (GCM); Oodlea (AML); Oodlea 13 km E (JAF); Oraparinna 4 mi E (GFG); Oraparinna, Flinders Ranges (PJM); Orroroo (GFG); Pandappa (SANPSOPS); Paringa (SANPVS); Poochera (BHO); Poochera (GFG); Poochera (RWT & RJB & ELO); Poochera (AJM); Poochera area (RWT); Poochera area (RWT & PSW); Poochera Cemetery (AJM & CHW); Poochera Hotel (SOS); Poochera, "Freightline site" just S of village (RWT & RJB); Pooginook Flat (GLH); Port Kenny (SANPVS); Purnong 7 km NE (SANPVS); Rockwater Rockhole (SANPVS); Salt Lake (PHU); Scrubby Peak, Gawler Ranges (JAF & WKH); Stockyard Plain (GLH); Streaky Bay (BBL); Streaky Bay (JMC); Streaky Bay (PGR); Thirty Thousand Tank (GCM); Tinda Catch (SANPSOPS); Tipperary Dam, Danggali CP (AJM); Venus Bay (SEG); Waikerie (BBL); Wedina Well, Calpatanna CP, Eyre Pen. (JAF); Weebubbie (PAI); Whyalla (PJM & RBH); Windsor (HBW); Wingoonie Hill (SANPSOPS); Wirrula 4 km W (JAF); Wirrulla (KCA); Yalata (SANPNS); Yaninee (CWA); Yelpawaralinna Creek (JAH & DHI); Yookamurra (WHC); Yumbarra CP (JAH); Yumbarra dog fence (JAF); Yumbarra Rockhole (SANPYS). **Victoria:** 3.3km N Millewa South Bore (ALY); Hattah 6.3 km N (ALY); Lake Hattah (JDI); Mildura (JCM); Millewa South Bore 3.3 km N (ALY); Sea Lake (JCG). **Western Australia:** 10-25km N Junana Rock, on Balladonia Rd (RWT); 10km NE Peak Charles, Peak Charles Natl Pk (SOS); 10km S Balladonia (SOS); 10mi. SE Karonie (RWT); 12km SE Mt Ragged, Cape Arid Natl Pk (SOS); 160km ENE Esperance (PSW); 23km ESE of Cocklebiddy (RWT); 23mi. W Fraser Rge, HS (RWT); 25mi. NbyW Balladonia HS (RWT); 36mi. SE by E Zanthus (RWT); 3km SW Mt Ragged, Cape Arid Natl Pk (SOS); 55km S Balladonia (SOS); 60mi E Balladonia Stn. (JGR); 6km S Norseman (JEF); Balladonia 80 km E (AJM & SBA); Border Village (KMA); Cape Arid National Park (AJM & SBA); Cape Arid NP (RPF); Esperance (BBL); Eucla (SOS); Gora [as Goora] Hill (TGR); Jarrahsend (AJM & WMA); Junana Rock, 9km NW Mt. Ragged (RWT); Kambalda31.30S 115.41E (JDM); Madura (AJM); Madura (IFB & MSU); Mt. Ragged (BBL); Mundrabilla Motel (AJM & SBA); Weebubbie (PAI); Worsley (JDM).

Worker diagnosis

Erect hairs present on tibiae and scapes. Metanotal groove absent in minor workers. Propodeum with more than 40 erect short and long setae. Pubescence on head and gaster abundant, with individual hairs overlapping. In profile, dorsum of petiolar node rounded in minor workers, a blunt angle in major workers. The relatively elongate body with abundant erect hairs will separate this species from close relatives.

Description (major worker)

Anterior clypeal margin with a nearly straight but crenulate medial projection with angular corners (Fig. 20). Pronotum weakly convex; posterior mesonotum, metanotum and dorsum of propodeum flat and long; propodeal angle rounded, declivity straight, ratio dorsum to declivity about 2 (Fig. 21). Anterior face of petiolar node convex, summit blunt, posterior face mostly convex (Fig. 21). Except for funiculus, entire body covered with plentiful erect setae. Head red to dark brown, scape dark brown to black, funiculus dark brown, pronotum red-brown; propodeum red-brown; gaster black; legs lighter than mesosoma.

Description (minor worker)

Anterior clypeal margin feebly convex, strongly projecting, crenulate, anterior corners with wide angles; medial carina blunt (Fig. 22). Pronotum feebly convex; mesonotum and dorsum of propodeum flat and long, sometimes feebly concave, angle rounded, posterior face straight, ratio of dorsum to declivity about 3 (Fig. 23). Anterior face of petiolar node convex, summit bluntly rounded, posterior face convex (Fig. 23). Except for funiculus, entire body covered with plentiful erect setae. Head red to dark brown, scape dark brown to black, funiculus dark brown, mesosoma, node, and gaster darker; legs lighter than mesosoma.

Measurements

Workers (n =20). CI 0.86 (minor) – 1.11 (major); HL 1.83mm – 4.24mm; HW 1.59mm –4.71mm; ML

2.87mm – 4.91mm; MTL 2.22mm – 3.04mm; PnW 1.18mm – 2.66mm; SI 0.65 (major) – 1.60 (minor); SL 2.46mm – 3.08mm.

Remarks

This is one of the most commonly encountered species in this group. It occurs from western New South Wales and Victoria west to south-central Western Australia and can be found in a range of habitats including mallee on a number of soil types. In sandy soils nest entrances are at ground level generally close to the trunks of mallee or other tall vegetation. In heavier soils nest entrances are constructed of soil formed into a column about 30 mm diameter and 100 mm tall with an entrance hole in the side near the rounded summit. The purpose of this turret is not known but is likely to be related to predator avoidance and/or to prevent water entering the nest during flooding. A nuptial flight was observed at Waikerie, South Australia on 15 May 1998 at 3 pm when the temperature was 25°C. This ant is known to be the host for an unusual group of leafhoppers, members of the Eurymelidae (Hemipera). These leafhoppers live in the ants' nests and forage nocturnally along with the ants (Day & Pullen 1999).

Camponotus owensae sp. nov.
(FIGS 25–27)

Material examined
Holotype. Minor worker from 32km NNE Inila Rock Waters, Yumbarra Conservation Park, 31° 44′ 01″ S 133° 26′ 59″ E, South Australia, 20-24 March. 1995, H. Owens (SAMA).

Paratypes. Three minor workers, same data as holotype (1 in SAMA, 2 in ANIC).

Worker diagnosis
Tibiae with abundant suberect hairs. In minors, metanotal groove depressed below the level of the anterior region of the propodeum; dorsal surface of petiolar node relatively long and flat, its anterior face much shorter than the posterior face. Elongate (overlapping) and dense pubescence present on head, mesosoma, gaster and tibiae. Body colour black. The configuration of the metanotal groove and the abundant pilosity will separate this species from others in this species group.

Description (minor worker)
Anterior clypeal margin projecting, median portion nearly straight and feebly crenulate with rounded angles laterally (Fig. 25). Pronotum, mesonotum, metanotum and the anterior one-fifth of

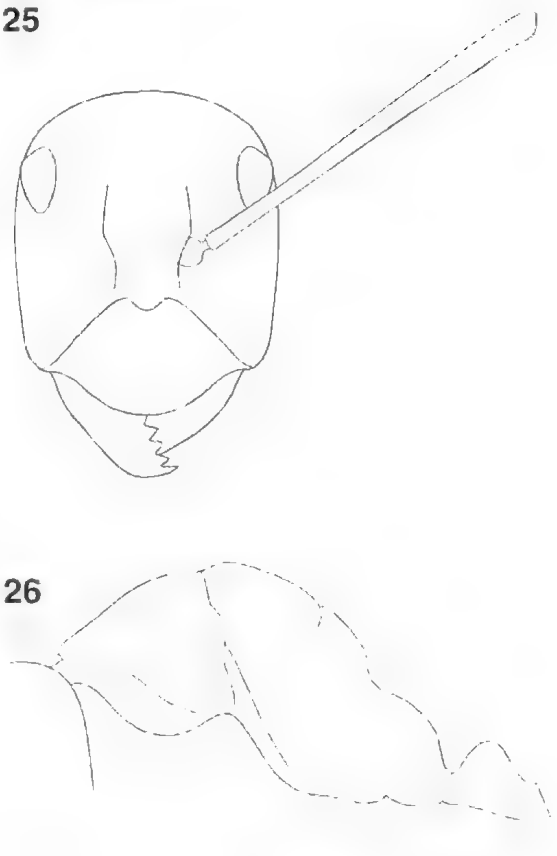

Figs 25-26. *C. owensae* workers. Fig. 25. Head of minor worker. Fig. 26. Mesosoma and petiole of minor worker.

Fig. 27. Distribution of *C. owensae* material examined during this study.

propodeum a strong, even domed convexity distorted only by the two feeble, well separated sutures of the metanotum, the posterior four-fifths of propodeum rise from a wide concavity to a posterior hump which includes the rounded angle and the mostly straight posterior propodeal face (Fig. 26). Anterior face of petiolar node straight, shorter than posterior face, summit narrowing upwards to a rounded angle (Fig. 26). Entire body black and covered with plentiful erect and flat lying white setae except antennae where setae are flat lying to suberect.

Measurements

Minor worker (n=2). CI 0.80 – 0.83; HL 2.04mm – 2.35mm; HW 1.63mm – 1.95mm; ML 3.33mm – 3.89mm; MTL 2.98mm – 3.08mm; PnW 1.42mm – 1.60mm; SI 1.50 – 1.71; SL 2.79mm – 2.92mm.

Etymology

Named after Helen Owens of the South Australian Department of Environment, Heritage and Aboriginal Affairs, who found this species during a faunal survey.

Remarks

This rare species has been collected only once from south-western South Australia (Fig. 27). Specimens were collected in pitfall traps in mallee. Nothing else is known of its biology.

Camponotus postcornutus Clark
(FIGS 28–32)

Camponotus (*Tanaemyrmex*) *postcornutus* Clark, 1930*b*: 121.

Material examined

Syntypes, 10 workers from Bungulla and Tammin, Western Australia (1 in AMSA, 5 in MCZC, 4 in MVMA).

Other material examined

South Australia: Blythe (BBL). **Western Australia:** 26mi. NWbyW Norseman (RWT); 32km W Salmon Gums (GPB); 35km S Kambalda (JAF); 38.8km ex Murchism R-Billabong (DHK & ACK & WLN & RDN); 53mi SSW Coolgardie (RWT); 71km S Payne's Find (GPB); 9mi SW Grass Patch (RWT); Binneringie Road, 6km ESE Widgiemooltha (JAF); Bungulla (TGR); Frenchman Bay, S Albany (LPK); Kalbarri Natl Pk (BBL); Mullewa (WMW); Norseman Area (AMD & MJD); Parker Ra. [as Parkers] (TGR); Salmon Gums, 70mi. N Esperance (BBL); Tammin (TGR); Tardun (CTM).

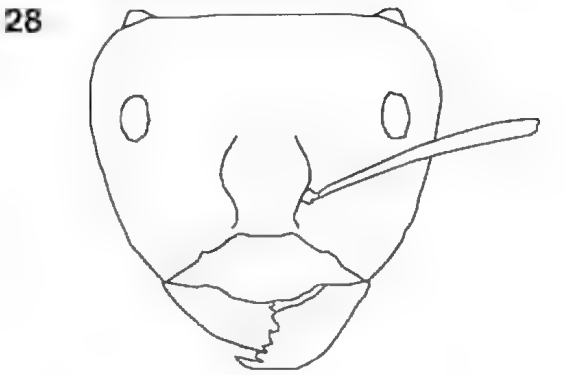

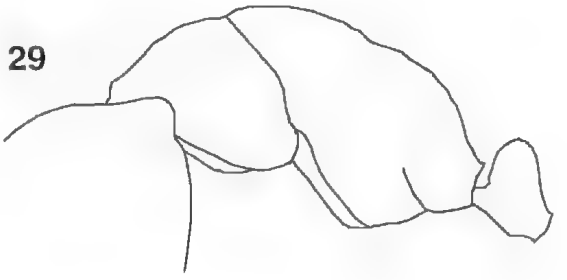

Figs 28-31, *C. postcornutus* workers. Fig. 28. Head of major worker. Fig. 29. Mesosoma and petiole of major worker. Fig. 30. Head of minor worker. Fig. 31 Mesosoma and petiole of minor worker.

Fig. 32. Distribution of *C. postcornutus* material examined during this study.

Worker diagnosis

In minor workers, the pronotum, mesonotum and dorsum of propodeum form a strong, even convexity, the metanotal groove is absent and the posterior face of the propodeum is only weakly differentiated from the dorsal face. The posterior corners of the head in major workers taper rearward into blunt protuberances. The shape of the mesosoma and the cephalic protuberances in major workers will separate this species from close relatives.

Description (major worker)

Medial section of anterior clypeal margin weakly projecting anteriorly with broad lateral angles and a feeble medial concavity; carina distinct (Fig. 28). Posterior corners of head produced as blunt horns in major and medium workers (Figs 28, 29). Pronotum, mesonotum and metanotum form an even convexity, propodeal dorsum and posterior face form a separate even convexity without angle (Fig. 29). Anterior face of petiolar node convex, summit moderately sharp, posterior face straight (Fig. 29). Dorsal and undersides of head, mesosoma, petiole, gaster and coxa with sparse reddish, long erect setae. Entire body dark red-brown with the gaster darker.

Description (minor worker)

Anterior clypeal margin projecting weakly, carina sharp (Fig. 30). Pronotum, mesonotum and dorsum of propodeum form a reasonably even convexity; propodeal angle broadly rounded, posterior face straight, ratio of dorsum to declivity about 2 (Fig. 31). Anterior face of petiolar node convex, summit bluntly rounded, posterior face convex (Fig. 31). Dorsal and undersides of head, mesosoma, petiole, gaster and coxa with sparse reddish long erect setae. Entire body dark red-brown with the gaster darker.

Measurements

Workers (n=8). CI 1.06 – 1.18; HL 1.95mm – 4.16mm; HW 2.06mm – 4.89mm; ML 3.28mm – 4.90mm; MTL 2.16mm – 2.84mm; PnW 1.71mm – 3.13mm; SI 0.57 – 1.14; SL 2.35mm – 2.77mm.

Remarks

This species is ground nesting with a simple entrance hole. It is most common in south-western Western Australia with a single collection from South Australia which is lighter in colour than those from Western Australia. Material is mostly from relatively dry areas such as mallee.

Camponotus prosseri sp. nov.
(FIGS 15, 33-37)

Material examined

Holotype. Minor worker from Streaky Bay, South Australia, 30 August 1974, B. B. Lowery, mallee, in sand (ANIC).

Paratypes. 25 workers, 10 queens and 1 male, same data as holotype (2 workers and 1 male in SAMA, remainder in ANIC).

Other material examined

New South Wales: 1mi. S Hillston (BBL); 4mi. N Condobolin (BBL); 62.8km N Coonabarabran (LPK); 7mi. S Hillston (BBL); Berrigan SF (BBL); Pooncarie (RHC & YCC & AKN). **South Australia:** 20km E Ulooloo (PJM); 32km N Renmark (KRP); 7km SE Balah (SANPSOPS); Aldinga (BBL); Innes Natl. Pk., York Peninsula (PJM); Innes Natl. Pk., York Peninsula (PJM); Koonamore (PJM); Loxton Payne's Farm (AMA); Loxton Snodgrass (AMA); Marion Bay, Yorke Pen. (RSI); Poochera (PSW); Poochera (RWT & RJB); Port Lincoln, 2km N Cape Tournefort (PJM); Port Lincoln, Eyre Pen., F Horse Rock (PJM); Port Lincoln, Horse Rock (PJM); Port Lincoln, Spalding Cove (PJM); Port Parham, 50mi. N Adelaide (BBL); Streaky Bay (BBL); Streaky Bay (BBL); Yumbarra CP, 6km NNE Inlia Rock Waters (HOW). **Western Australia:** 28km WSW Israelite Bay, Cape Arid Natl Pk (SOS); 30km W Israelite Bay (GPB & GJM); 53mi SSW Coolgardie (RWT); 53mi. SSW Coolgardie (RWT); 62km NE Albany, Hassell Natl Pk (SOS); 72km SW Norseman (SOS); 80km, West Talbot Rd, Beverley (AMD & MJD); Albany (TGR); Balladonia and Madura (BBL); Eucla (SOS); Gora [as Goora] Rock (TGR); Kings Park (BBL); Mt Ragged, Cape Arid NP (ABB); Norseman (BBL); Salmon Gums (BBL); Stirling Ra. (GFR); Stirling Ra. NP (GPB)

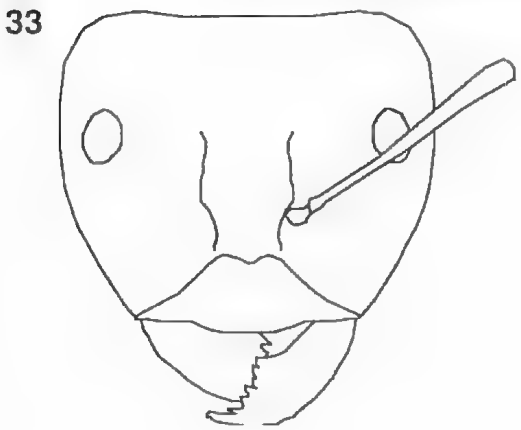

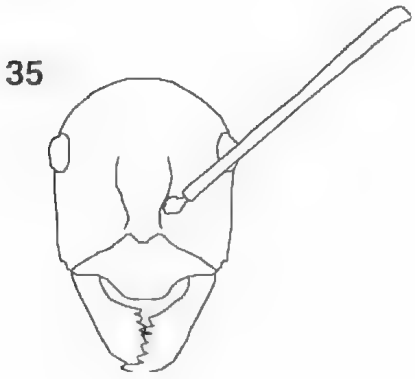

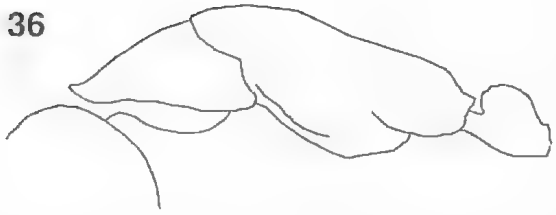

Figs 33-36. *C. prosseri* workers. Fig. 33. Head of major worker. Fig. 34. Mesosoma and petiole of major worker. Fig. 35. Head of minor worker. Fig. 36. Mesosoma and petiole of minor worker.

Fig. 37. Distribution of *C. prosseri* material examined during this study.

Worker diagnosis

Anterior clypeal margin in major workers broadly convex across its entire width (Fig. 33). Scapes relatively long (in minor workers, SI > 1.4) (Fig. 15). Tibiae lacking erect hairs, propodeum with more than 10 erect hairs which are scattered along the entire dorsal surface. Posterior section of mesonotum weakly but distinctly convex immediately anterior of the metanotal groove (more so in minors, less so in majors); metanotal groove a shallow, weakly defined concavity in minors (Figs 34, 36). Petiolar node angular or broadly rounded above, the anterior face at most only slightly shorter than the posterior face (Figs 34, 36). Head same colour as mesonotum (both either red or black).

This species is morphologically similar to *C. cerisciipes* and is easily confused with it. The difference is outlined under *C. cerisciipes* above.

Description (major worker)

Anterior clypeal margin weakly convex, scarcely projecting, with a weak carina (Fig. 33). Pronotum and mesonotum gently convex, metanotum distinct, dorsal propodeal face weakly convex, sometimes a little stronger near metanotum; angle well rounded (Fig. 34). Anterior face of petiolar node straight, summit rounded, posterior face straight, often feebly concave near summit in dorsal view (Fig. 34). Posterior margin and underside of head, mesosoma, petiole and gaster with scattered long setae, tibiae and scapes lacking erect setae. Head red to black, scape red to black, funiculus dark brown; pronotum red to dark brown; mesonotum red to dark brown; petiole red to black; gaster very dark brown to black; legs red to black.

Description (minor worker)

Anterior clypeal margin convex, carina distinct (Fig. 35). Pronotum and mesonotum an even, wide convexity, metanotum indistinct, propodeal dorsum feebly concave anteriorly, straight posteriorly, angle widely rounded, ratio of dorsum to declivity near 2 (Fig. 36). Anterior face of petiolar node short, flat, inclined forward, summit rounded, about as high as long, posterior face short, flat (Fig. 36). Posterior margin and underside of head, mesosoma, petiole and gaster with scattered long setae, tibiae and scapes lacking erect hairs. Head and mesosoma clothed in fine flat-lying pubescence sufficiently dense in places to hide the integument. Head red to black, scape red to black, funiculus dark brown; pronotum, mesonotum, propodeum and petiole each red to black; gaster very dark brown to black; legs red to black.

Measurements

Workers (n=94). CI 0.72 (minor) – 1.21 (major); HL 1.50mm – 3.21mm; HW 1.08mm – 3.88mm; ML 2.41mm – 4.13mm; MTL 2.14mm – 2.66mm; PnW 0.98mm – 2.42mm; SI 0.70 (major) – 1.76 (minor); SL 1.90mm – 2.71mm.

Etymology

Named after Dr Ian Prosser, Canberra, Australia.

Remarks

The specimens considered here as belonging to this species show consistency in overall head, mesosomal and petiolar shape as well as overall size. The length of the scape varies but this variation is highly correlated with head width (Fig. 15) as would be expected for a single taxon. However, these specimens do show considerable variation in colour and to a lesser extent pilosity. Allowing for a few apparently callow or faded individuals, all specimens have the head and gaster black. The mesosoma, petiole and legs, however, vary from black to yellow-red. These colours show considerable variation in intensity with essentially all shades between the extremes present. In general most nest series are fairly consistent in colour pattern with the exception of the petiole and legs, which can vary among individuals. However, the variation between series shows a more interesting pattern. The pronotum is generally black but is partially to completely red in a few collections from Western Australia. The mesosoma and propodeum vary from black to red but this variation occurs throughout the range of the species and the lighter colour is much more common, especially for the propodeum where red is more common than black. It should be noted that the development of the red colour follows a distinct pattern. The propodeum must be red for the mesonotum to be red, and the mesonotum must be red for the pronotum to be red. This means that the most common colour pattern is black with a red propodeum followed by black pronotum with red mesonotum and propodeum and finally individuals with a completely red mesosoma. The colours of the petiole and legs vary independently of the mesosoma.

The variation in pilosity is substantial but generally less obvious than that found in body colour. Both the erect hairs and appressed pubescence vary from sparse to abundant on all major body regions. And as with colour, most variation occurs between nest series rather than within nest series. However, no significant geographic pattern was detected regarding the development of pilosity, and there was no obvious correlation between colour patterns and pilosity. The only exception to this is a set of specimens from south-western Western Australia which had abundant long erect setae. In spite of this one group, it proved difficult to segregate the available material into subsets for which diagnoses could be developed. There were distinct sets of individuals which shared colour or pilosity patterns but there remained a number of specimens which were either intermediate between these sets or which could not be placed comfortably within these sets. As a result, all of these specimens are here treated as belonging to a single, wide-ranging taxon which shows considerable variation in a number of characters, with a note that some of these may well represent distinct species which are not diagnosable with the material currently available.

Biologically, these ants have been found in mallee, *Callitris* woodlands and coastal scrub. They are known to nest under stones as well as in open soil without covering, especially in sand, and they have been taken in pitfall traps. They are known to forage on low vegetation including mallee and yellow box.

Camponotus rufonigrus sp. nov.
(FIGS 38-40)

Material examined

Holotype. Minor worker from Cambrai, South Australia, 4-7 February 1972, P. J. M. Greenslade, dune IIb. (ANIC).

Paratypes. 8 workers, same data as holotype except: 1 collected 21-25 February, 1972, dune III; 2 collected 7-10 February, 1972, dune III; 1 collected 25-29 February, 1972, dune Ib; 2 collected 28 January, 1972, dune; 2 collected 18-21 February, 1972, dune III (ANIC).

38

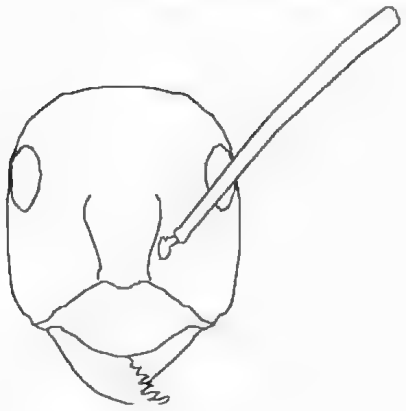

39

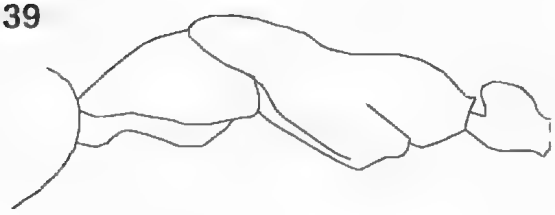

Figs 38-39. *C. rufonigrus* workers. Fig. 38. Head of minor worker. Fig. 39. Mesosoma and petiole of minor worker.

40

Fig. 40. Distribution of *C. rufonigrus* material examined during this study.

Other material examined

South Australia: Gawler Ra. (PJM); Yumbarra CP, 23.5 km NW Inila Rock Waters (HOW).

Worker diagnosis

Anterior clypeal margin broadly convex across its entire width (Fig. 38). Tibiae and scapes lacking erect hairs; propodeum with more than 10 erect hairs which are scattered along the entire dorsal surface. Petiolar node angular or broadly rounded above, the anterior face at most only slightly shorter than the posterior face (Fig. 39). Black head contrasting with red mesonotum.

Description (minor worker)

Anterior clypeal margin evenly convex, carina strong (Fig. 38). Pronotum and mesonotum forming an even convexity, metanotum indistinct, propodeal dorsum concave anteriorly and flat posteriorly, angle rounded, declivity straight, ratio of dorsum to declivity about 1.5 (Fig. 39). Anterior face of petiolar node flat, short, summit widely rounded, posterior face convex (Fig. 39). Dorsal and under surfaces of head, mesosoma, petiole, gaster and coxa with sparse long erect setae. Entire body clothed in fine short indistinct flat lying pubescence. Head, anterior of mesosoma, most of node and gaster dark brown to black, otherwise red-brown.

Measurements

Minor worker (n=3). CI 0.85 – 0.86; HL 1.37mm 1.60mm; HW 1.16mm – 1.38mm; ML 2.19mm – 2.59mm; MTL 1.53mm 1.96mm; PnW 0.98mm – 1.20mm; SI 1.44 1.55; SL 1.75mm – 2.14mm.

Etymology

Named after its red and black body colour.

Remarks

This species is known from three localities in southern South Australia (Fig. 40). Two collections consists of single minor workers, while one (from Cambrai) contains nine minor workers collected at six different times during January and February, 1972. Thus this species has been rarely collected and then generally in small numbers. The limited biological information suggests that this species occurs on sand.

Camponotus setosus sp. nov.
(FIGS 41-43)

Material examined

Holotype. Minor worker from Manning River Gorge, 16°39'S 125°55'E, Western Australia, 1 June 1992, S. O. Shattuck (ANIC).

Paratypes. 21 minor workers, same data as holotype (3 in SAMA, 18 in ANIC).

Other material examined

Western Australia: 1.5km W King Edward River crossing (SOS).

41

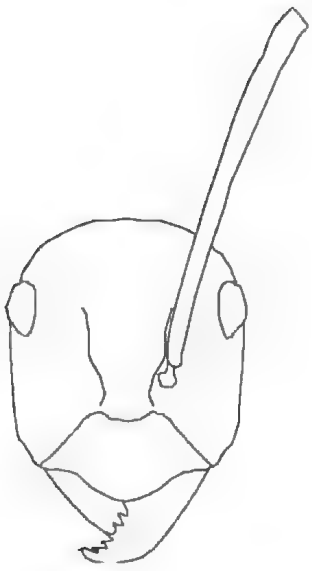

42

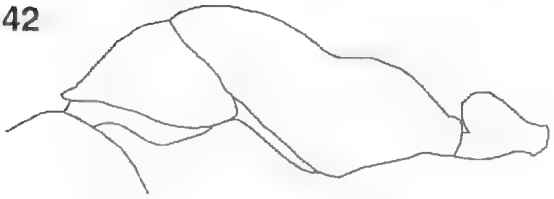

Figs 41-42. *C. setosus* workers. Fig. 41. Head of minor worker. Fig. 42. Mesosoma and petiole of minor worker.

43

Fig. 43. Distribution of *C. setosus* material examined during this study.

Worker diagnosis

Erect hairs present on tibiae. Metanotal groove a distinct, shallow trough. These two characters will separate this distinctive species from others in this group.

Description (minor worker)

Pronotum and mesonotum form together an even, raised convexity followed by the angular trough of the metanotum, the weakly convex dorsal surface of the propodeum, a widely rounded angle and the straight posterior face (Fig. 42). Entire body covered with dense flat lying pubescence, erect setae absent from antennae. Pubescence on posterior of gaster yellow, elsewhere white. Gaster black, most of head, mesosoma and node black, the remainder with red patches; antennae dark brown; coxa and femora red, tibiae and tarsi brown.

Measurements

Workers (n=4). CI 0.85 – 0.88; HL 1.88mm – 1.96mm; HW 1.64mm – 1.69mm; ML 3.08mm – 3.20mm; MTL 2.34mm – 2.54mm; PnW 1.50mm – 1.54mm; SI 1.45 – 1.57; SL 2.45mm – 2.62mm.

Etymology

Named after the abundant long setae present on most regions of its body.

Remarks

This apparently uncommon species is restricted to the Kimberley region of Western Australia (Fig. 43). All known collections consist of ground-foraging workers in open *Eucalyptus* woodlands.

Camponotus terebrans (Lowne)
(FIGS 44-48)

Formica testaceipes Smith, 1858: 39 (preoccupied by Leach, 1825: 290).

Camponotus testaceipes – Mayr, 1862: 662.

Formica terebrans Lowne, 1865: 278 (first available replacement name for *Formica testaceipes* Smith) – Mayr, 1876: 65.

Camponotus (*Myrmoturba*) *latruncelus victoriensis* Santschi, 1928: 479 – McArthur *et al.*, 1998: 587.

Camponotus (*Tanaemyrmex*) *myoporus* Clark 1938:379 McArthur et al., 1998: 587.

Material examined

Formica testaceipes: Syntype workers from King George Sound, Western Australia (BMNH - see McArthur *et al.* (1998)).

Formica terebrans: Syntype workers and queens from Sydney, New South Wales (see McArthur *et al.* (1998)).

Camponotus (*Myrmoturba*) *latruncelus victoriensis*: Syntype workers and males from Elsternwick and Belgrave, Victoria (see McArthur *et al.* (1998)).

Camponotus (*Tanaemyrmex*) *myoporus*: Syntype

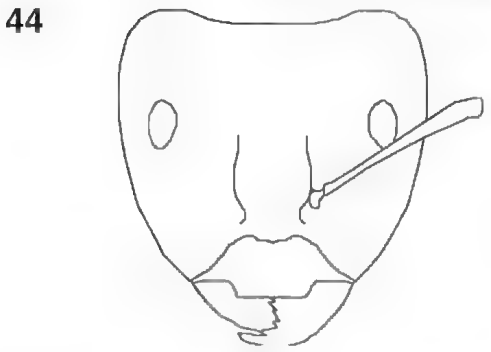

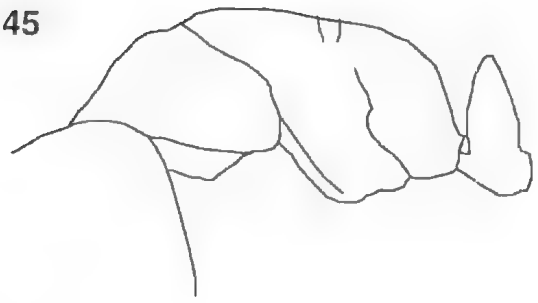

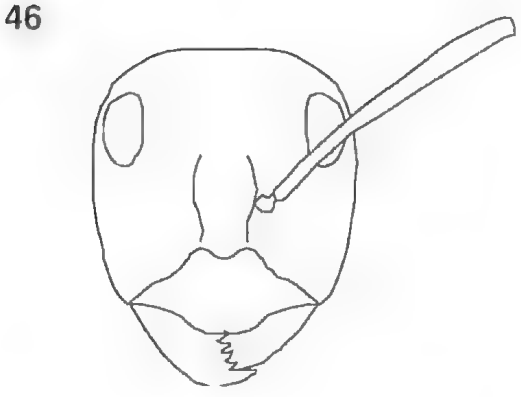

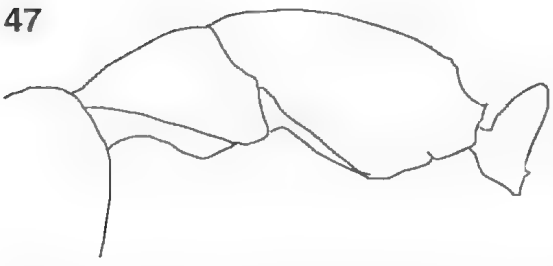

Figs 44-47. *C. terebrans* workers. Fig. 44. Head of major worker. Fig. 45. Mesosoma and petiole of major worker. Fig. 46. Head of minor worker. Fig. 47. Mesosoma and petiole of minor worker.

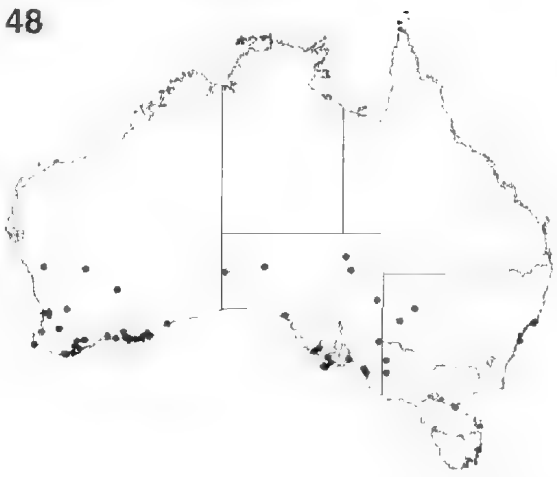

Fig. 48. Distribution of *C. terebrans* material examined during this study. For additional material see McArthur *et al.*, (1998).

workers from Reevesby Island, South Australia (3 in MVMA, 6 in ANIC - see McArthur *et al.* (1998)).

Other material examined
See McArthur *et al.* (1998).

Worker diagnosis
Erect hairs present on scapes and tibiae. Metanotal groove weakly developed and essentially absent (Figs 45, 47). Propodeum with 10 to 25 erect hairs. Pubescence on head and gaster sparse, with individual hairs generally non-overlapping or at most only slightly overlapping. In profile, dorsum of petiolar node angular in both minor and major workers (Fig. 45, 47). These characters will separate this taxon from close relatives, especially the morphologically similar *C. gouldianus*.

Description (major worker)
Medial section of anterior clypeal margin straight, projecting anteriorly with rectangular lateral corners, crenulate; carina indistinct (Fig. 44). Pronotum and mesonotum weakly convex; metanotum distinct as two parallel, transverse grooves; dorsal surface of propodeum straight, angle well rounded, posterior face mostly straight, length of dorsal and declining faces about equal (Fig. 45). Anterior face of petiolar node convex, summit sharp, posterior face mostly straight (Fig. 45). Entire body with plentiful long erect setae tending to suberect on tibiae and scape, absent from funiculi. Head red-brown to black, funiculi lighter, mesosoma and node yellow to brown, gaster darker than mesosoma, legs lighter.

Description (minor worker)
Anterior clypeal margin with median section

convex and strongly projecting, carina distinct (Fig. 46). Pronotum and mesonotum mostly weakly convex; the smallest workers without a metanotal groove; dorsal propodeal surface straight, angle well rounded, posterior face straight, ratio dorsum to declivity exceeds 2 in smallest workers (Fig. 47). Anterior and posterior faces of petiolar node generally parallel, summit bluntly convex (Fig. 47). Entire body with plentiful long and short erect setae tending to suberect on tibiae and scape, absent from funiculi. Head brown, funiculi lighter, mesosoma and node yellow to brown, gaster darker than mesosoma, limbs lighter.

Measurements

Workers (n=20). CI 0.85 (minors) – 1.11 (majors); HL 1.36mm – 3.28mm; HW 1.15mm – 3.64mm; ML 2.07mm – 3.64mm; MTL 1.56mm – 2.39mm; PnW 0.91mm – 2.02mm; SI 0.66 (majors) – 1.54 (minors); SL 1.77mm – 2.39mm.

Remarks

Camponotus terebrans is common in sandy soil or disturbed sites across much of southern Australia (Fig. 48). Nests are sometimes located adjacent to the trunks of trees or shrubs with abundant excavated soil deposited around the numerous entrances. In some cases excavations have been observed to apparently damage or kill nearby shrubs. In other cases nests and their entrances are in open areas and lack mounds. Colonies may be very large and sometimes have "highways" leading to trees and other colonies. This species is often found in association with *Ogyris* spp. butterflies (Braby 2000). For additional details see McArthur *et al.* (1998).

Camponotus versicolor Clark
(FIGS 49-54)

Camponotus (*Myrmosaulus*) *versicolor* Clark, 1930*b*: 122.

Material examined

Syntypes. Workers from Emu Rocks, east of Ongerup, Western Australia (6 in ANIC, 3 in MCZC, 3 in WAMP, 5 in MVMA, 3 in BMNH).

Other material examined

Western Australia: 33mi. SbyE Karonie (RWT); 9mi. E Newdegate (TGR); Bungulla (TGR); Emu Rock (HRE); Newdegate (HMC & TGR); Norseman (BBL).

Worker diagnosis

Tibiae and scapes lacking erect hairs. In minor workers, metanotal groove angular to slightly

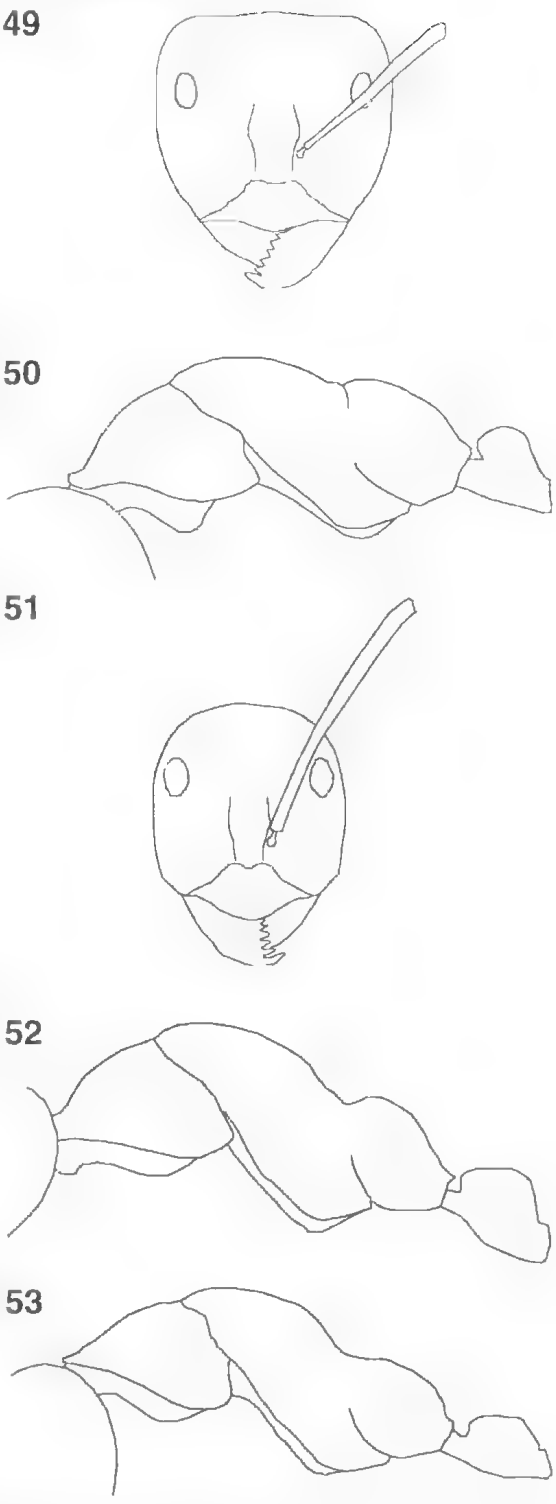

Figs 49-53. *C. versicolor* workers. Fig. 49. Head of major worker. Fig. 50. Mesosoma and petiole of major worker. Fig. 51. Head of minor worker. Figs 52-53. Mesosoma and petiole of minor worker.

Fig. 54. Distribution of *C. versicolor* material examined during this study.

depressed below the anterior region of the propodeum (Figs 52, 53); dorsal surface of petiolar node in minors relatively long and flat to weakly convex, its anterior face much shorter than the posterior face (Figs 52, 53). Mesosoma black and with at least the first two gastral tergites red and distinctly lighter in colour than the propodeum, gastral tergites never with golden-yellow bands. The configuration of the metanotal groove combined with the distinctively coloured gaster will separate this species from close relatives.

Description (major worker)

Dorsal surfaces of pronotum and mesonotum convex and separated by a shallow angle; propodeum uniformly convex without a distinct angle; petiolar node with parallel anterior and posterior faces, its upper surface slightly elongated flat to weakly convex (Fig. 50). Erect hairs sparse on outline of head including underside, scattered on mesosoma, petiole, coxa and gaster, absent from tibiae and scapes. Anterior clypeal margin weakly convex (Fig. 49). Body red-black, head and petiole slightly lighter than mesosoma; gaster with the first two tergites red, the remainder red-black.

Description (minor worker)

Anterior clypeal margin convex (Fig. 51). Dorsal surfaces of pronotum and mesonotum convex and separated by a shallow, broad angle; metanotal groove either a broad angle (Fig. 53) or a shallow trough (Fig. 52); dorsal and posterior faces of propodeum flat to weakly convex and separated by at most a gentle angle. Anterior face of petiolar node short and separated from the dorsal face by a distinct angle, dorsal face elongate and flat to weakly convex and separated from the posterior face by a broad, rounded angle, posterior face flat (Figs 52, 53). Erect hairs abundant on outline and underside of head, mesosoma, petiole, coxa and gaster; erect hairs absent from scapes and tibiae. Body dark red-black or black with the head sometimes slightly lighter; gaster with at least the first two tergites red and the remainder dark red-black, or sometimes entirely red.

Measurements

Workers (n=7). CI 0.82 (minors) – 1.06 (majors); HL 2.23mm – 3.20mm; HW 1.83mm – 3.42mm; ML 3.96mm – 4.86mm; MTL 2.72mm – 3.00mm; SI 1.45 (majors) – 1.60 (minors); SL 2.93mm – 4.95mm.

Remarks

Camponotus versicolor is an uncommon species which is limited to a narrow band across southern Western Australia (Fig. 54). It is most similar to *C. aurocinctus* and can be separated from it by the darker body colour and red gastral tergites. Minor workers of *C. aurocinctus* also have larger numbers of erect hairs on the head and mesosoma compared to this species. Essentially nothing is known concerning the biology of *C. versicolor*.

Camponotus wiederkehri Forel
(FIGS 55-59)

Camponotus wiederkehri Forel, 1894: 232.

Camponotus denticulatus Kirby, 1896: 204 – Clark, 1930*a*: 19 (worker redescribed). New synonymy.

Camponotus (*Myrmotarba*) *laruneulus* Wheeler, 1915: 814. New synonymy.

Camponotus wiederkehri lucidior Forel, 1910: 81 – Crawley, 1915: 136 (queen description). New synonymy.

Material examined

Camponotus wiederkehri: Syntype workers from Charters Towers, Queensland (MHNG).

Camponotus denticulatus: Syntype workers from MacDonell (as McDonell) Ranges, Northern Territory (2 in MCZC, 1 in MVMA).

Camponotus (*Myrmotarba*) *laruneulus*: Syntype workers from Todmorden, South Australia (1 in SAMA).

Camponotus wiederkehri lucidior: Syntype workers and males from Tennant Creek, Northern Territory (3 workers in MCZC, 2 workers in MHNG).

Other material examined

New South Wales: Waukeroo (RHM): 10 mi. N

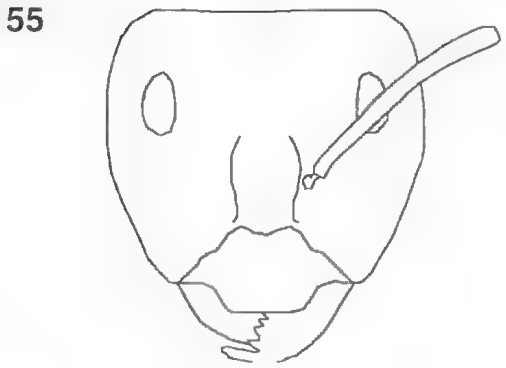

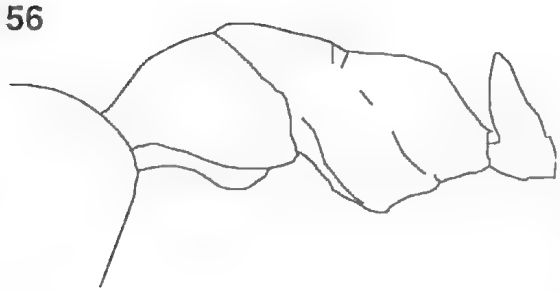

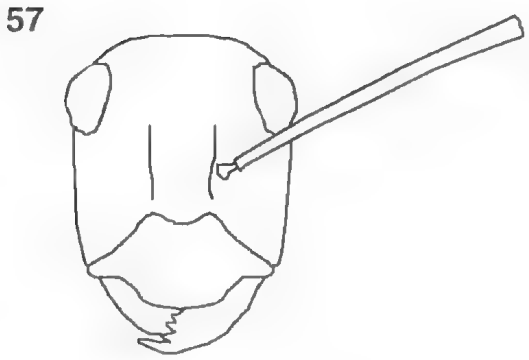

Figs 55-58. *C. wiederkehri* workers. Fig. 55. Head of major worker. Fig. 56. Mesosoma and petiole of major worker. Fig. 57. Head of minor worker. Fig. 58. Mesosoma and petiole of minor worker.

Fig. 59. Distribution of *C. wiederkehri* material examined during this study.

Broken Hill (RHM). **Northern Territory:** 1.5km N Alice Springs (PJM & RJW); 12km SW Katherine (PJM); 15km S Tea Tree (MMA & JHA); 20mi. SE Anthonys Lagoon (TGR); 25km S Andado Stn Rodinga Ra (JAF & DHI); 35km S Darwin (LHI); 37km E Wallara Ranch (SOS); 3km E Serpentine Gorge (SOS); 50km WNW Hermannsburg (SOS); 7km W Timber Creek (MMA); Alice Springs (CBA); Alice Springs (WLB); Alice Springs (WCC); Alice Springs (LHI); Alice Springs (PPL); Alice Springs (KRO); Batten Ck., 30km WSW Borroloola (JEF); Bing Bong HS (JEF); Bitter Springs Creek (JAF & DHI); Bullita Outstation (MMA); Camfield (IAR); Colyer Creek, 8km N Alice Springs (SOS); Corroboree Rock, 2(km E Alice Springs (SOS); Darwin (SMO); Darwin (HWE); Doyles Ridge nr. Birdum (TGR); Flying Fox Creek (SMO); Glen Helen (SOS); Helen's Ck., Banka Banka Rd. (TGR); Illamurta Spring (JAF & DHI); Jasper Gorge (IAR); Katherine (RVS); Kings Canyon Nat. Pk. (SOS); Kings Creek Caravan Park (SDO); Kulgera (JBS); Kunoth Paddock, 30km NW Alice Springs (WAL); Kunoth Park nr. Alice Springs (PJM & WLO); Macdonnel Downs (SAMA Exped.); McArthur R., 48km SWbyS Borroloola (JEF); Narwietooma (AWF); NW Brunette Downs (TGR); Phillip's River (TGR); Port Darwin (WDD); Rimbija Is., Wessel Islands (EDE); Rimbija Is., Wessel Islands (TAW); Roderick Creek (IAR); Ruby Gap Gorge (JAF & DHI); Tennant Creek (JFF); Trephina Gorge Nature Park (JBS); Trephina Gorge, 55km ENE Alice Springs (SOS); Turnoff into Ormiston Gorge (SOS); Umbrawarra Gorge (JAR & IAR); Valley of Winds, The Olgas (JEF & TAW); Victoria River (BRH); Yulara, campground (SOS). **Queensland:** 1.5km WNW Riversleigh HS, nr. Gregory R. (JAF); 106mi.

NW Mt. Isa (TGR); 10mi. W Mt. Garnet (BBL); 16mi. ESE Gilbert R. Crossing, E of Croydon (JED); 18mi. ESE Emerald (JED); 1mi. S Carpentaria Downs HS, SE Emasleigh (JED); 1mi. SE Lorraine HS (JED); 25km S Woodstock (PJM); 28mi. N Thorntonia HS, NE of Camooweal (JED); 2mi. SE Camel Ck. HS, W of Ingham (JED); 2mi. SE Mary Kathleen (JED); 4mi. NE Oorindi (JED); 50mi. N Julia Creek (REL), 52km S Woodstock (PJM); 5mi. W Lotus Vale HS, N of Normanton (JED); 7km E Charters Towers (PJM); 9mi. NE Camooweal (JED); Barcaldine (GEG); Blackall (JBS); Carpentaria Downs (JED); Charters Towers; Clermont (BBL); Cooktown (BHO); Dalgonally, nr. Cloncurry R. (JED); Doomadgee Mission Station (PAI & NBT); Emerald (FAC); Emerald (JHA); Emerald District (SAH); Greenvale (JED); Greenvale Station area (SAH); Helenslee (TGR); Homestead (FHI); Jericho (FAC); Mareeba (BBL); Mornington Mission (PAI & NBT); Mt. Isa (JRU); nr. Dimbulah (RWT & JEF); Quilpie (JSM); St. George (BBL); Star R. Crossing (SAH); Surbiton (FAC); Townsville Charters Towers Rd. (TGR); Undilla HS, NE of Camooweal (JED); Winton (FAC). **South Australia:** 10km W Mabel Ck. (PJM); 11km N Maryinna Hill (SANPPITJ); 155km N Cook (JAF); 20km ENE Pipalyatjara (SANPPITJ); 26mi S Kunytjanu (SANPPITJ); 53km E Vokes Hill, Victoria Desert (PJM); 60km S Pimba (MAA); 7mi. E Wilgena (TGR); 80km E Ernu Junction, Victoria Desert (PJM); Andamooka (JAH); Arltunga (DCO); Arnoma Dam (AJM & JDE); Beltah (SANPSOPS); Birthday Hill, N Tarcoola (PJM); Blood Ck. (CBA); Box Creek (AJM & JDE); 22km N Beltana (JEF); Clifton Hills Outstation (JAF & DHI); Coober Pedy (BBL); Copper Hill (HFR); Curdimurka, L. Eyre (BBL); Davenport Range (AJM & MAA); Douglas Creek (MAA); Dulkaninna (PCO); Ernabella Mission (NBT); Ernabella Mission Stn. (BBL); Everard Park (JFI); Farina (PJM); Gawler Ranges (PJM); Hideaway Hut (SANPSOPS); Lake Eyre (BBL); Lake Gairdner (AAS & MLS); Mabel Ck (TGR); Mimili (SANPPITJ); Mitchell Nob (SANPPITJ); Mt. Cooperina (SANPPITJ); Mt. Finke (PJM & JAF); Musgrave Ranges (BBL); Ngaruitjara (SANPPITJ); Ooldea (AML); River Diamentina (AMM); Robertstown (SANPSOPS); Ronald Well (SANPPITJ); S end of L. Windabout (BBL); Sereech Owl Creek (WMC); The Twins HS (RSM); Vokes Hill (JAF); Vokes Hill (GEG); Vokes Hill, Victoria Desert (PJM); Womikata Bore, Musgrave Ra. (SANPPITJ); Woocalla (RSM); Yardea (AJM & PJF). **Western Australia:** 100km E Southern Cross (PJM); 100km SEbyE Broome (JFB); 11km N Wiluna (DDA & SRM); 163km SEbyE Broome (JFB); 45mi. S Onslow (GCA); 50km N Kalgoorlie (PJM); 53mi. SSW Coolgardie (RWT); 70km E Kalgoorlie (JEF); 7km W Kununurra, Bandicoot Ra. (DCF & JBA); Ashburton River (RHM & GCA); Balgo Mission (ARP); Balladonia (BBL); Black Stone Range (KTR); Canegrass, NNE Kalgoorlie (JED); Derby (WDD); Jigalong (JHI); Kalgoorlie (PAI); Kalgoorlie [as Kalgoolie] (TGR); Kalumburu Mission (MDA); Kimberley area nr. Kalumburu Mission (<5 mi.) (WLE); Kununurra boat ramp (RHM & GCA); LaGrange Mission, 120km S Broome (KMC); Lyndon R., Carnarvon (RHM), Lyndon River, Carvarvon (RHM); Meekatharra, Mt. Newman mid. Gascoyne R. (PJM); Mitchell Plateau (mining camp) (DCF & JBA); Mooka Bulla (NBT); Onslow (RHM); Ord R. (SAH); Pilgangoora Mining Centre (NBT); Pindar (CTM); Port George iv (JRB); Roebourne (WDD); Windjana Gorge NP (PSW).

Worker diagnosis

Anterior clypeal margin in major workers projecting, the central region straight with rectangular sides joining the lateral regions (Fig. 55). Posterior section of mesonotum flat (or nearly so) immediately anterior of the metanotal groove, metanotal groove essentially absent or weakly developed in minors (Fig. 58), a broad, shallow angle in majors (Fig. 56). Petiolar node angular or broadly rounded above, the anterior face at most only slightly shorter than the posterior face (Figs 56, 58). Tibiae and scapes lacking erect hairs.

Description (major worker)

Medial section of anterior clypeus strongly projecting, its margin straight and lateral corners broadly angular, carina weak (Fig. 55). Pronotum and mesonotum a slightly raised even convexity; metanotum with two distinct groves, the anterior section of the propodeal dorsum feebly concave anteriorly and feebly convex posteriorly, propodeal angle widely rounded, posterior face mostly straight, ratio of dorsum to declivity about 1 (Fig. 56). Anterior and posterior faces of petiolar node straight; summit flat, narrow and sharp, sometimes bidentate, its posterior margin feebly concave (Fig. 56). Dorsum and underside of head, mesosoma, petiole, coxa and gaster with plentiful scattered erect setae, reduced numbers on propodeal angle and declivity, absent from scapes, flat lying on tibiae. Head yellow-red to dark brown, antennae red to red-brown, mesosoma and node yellow-red to brown; gaster darker, legs lighter.

Description (minor worker)

Medial section of anterior clypeus strongly projecting, its margin convex, crenulate; carina distinct (Fig. 57). Pronotum weakly convex, anterior section of mesonotum weakly convex, the remainder

joins with propodeal dorsum to form a long flat surface ending in a widely rounded propodeal angle and short posterior face, ratio of dorsum to declivity about 3 (Fig. 58). Anterior face of petiolar node mostly convex, summit sharp (in front view pointed), posterior face mostly flat (Fig. 58). Dorsum and underside of head, mesosoma, petiole, coxa and gaster with scattered long setae; reduced numbers on propodeal angle and declivity; absent from tibiae and scapes. Entire body clothed with fine pubescence. Mesosoma yellow-red to dark red-brown, sometimes with darker or lighter patches; head, node and gaster generally darker, legs lighter.

Measurements

Workers (n= 20) CI 0.80 (minors) – 1.08 (majors); HL 1.51mm – 3.33mm; HW 1.21mm – 3.61mm; ML 2.51mm – 3.83mm; MTL 1.92mm – 2.62mm; PnW 0.97mm – 2.13mm; SI 0.68 (majors) – 1.60 (minors); SL 1.94mm – 2.45mm.

Remarks

This is one of the most commonly encountered and widespread species in this group (Fig. 59). In southern Australia nests are generally mounds approximately 150 to 200mm in diameter with steeply sloping sides and a flat summit with the entrance in a slight depression in the centre. These mounds are often decorated with small stones. Nests are often in heavy soil in open areas and are less common or are absent from areas of high rainfall. Often several mounds may be seen within a few metres of each other.

Morphologically, this species (as conceived here) shows minimal variation in body shape and pilosity (other than that expected for a polymorphic taxon) but does show considerable variation in colour. The colour ranges from clear yellow-red to black with essentially all grades of colour in between. In most cases the colour is uniform within an individual but various degrees of infuscation on the mesosoma are common. Also, most variation occurs between rather than within nest series although the development of infuscation does vary within nest series. Finally, this colour variation shows little geographic pattern with essentially all colour forms being found in all regions, the only exception being northern regions of the Northern Territory where light forms predominate.

The types of *C. wiederkehri* and *C. wiederkehri luteldior* represent the more lightly coloured forms of this taxon. These two taxa were separated based on trivial and non-significant differences in size, sculpturing and the shape of the anterior clypeal margin (Forel 1910) and they clearly represent the same taxon. *Camponotus latrunculus* represents an intermediately coloured form and compares well with the types of *C. wiederkehri*. Wheeler (1915) was apparently unaware of *C. wiederkehri* as he made no mention of it in his description of *C. latrunculus* and this is likely the cause of this synonymy. The final previously proposed name, *C. denticulatus*, represents the dark form of this taxon. However, it is morphologically very similar to the other forms placed here and no justification could be found for treating it as a separate taxon.

Species of the C. perjurus *species group*

Camponotus perjurus sp. nov.
(FIGS 60-62)

Material examined

Holotype: Minor worker from 74 km E by N Cosmo Newberry, Western Australia, 13 November 1977, J. E. Feehan (ANIC).

Other material examined. **South Australia**: 80km NNE Ceduna (JAF); Emu Camp, Victoria Desert (PJM); Mt. Gunson, SE Woomera (PJM). **Western Australia**: 40km SE Ravensthorpe (RWT); Borden (EFR).

Worker diagnosis

Head of minor worker produced upwards so that its attachment to the pronotum is well below its upper margin (Fig. 61). Often with weak purple or green iridescent hue on head and body. The attachment of the head is unique to this species group, if not the genus, and will readily separate this species from others.

Description (minor worker)

Anterior clypeal margin wide, projecting, evenly convex and feebly crenulate, with a feeble medial carina (Fig. 60). Pronotum and mesonotum a raised convexity which smoothly joins the feebly concave dorsal surface of the propodeum, the propodeal angle rounded, its posterior face short and straight, the ratio of dorsum to declivity about 4 (Fig. 61). Metanotal spiracles high, near the dorsal mesosomal surface. Petiolar node leaning forward, parallel anteriorly and posteriorly, with a long, weakly convex summit (Fig. 61). Body red-brown except for gaster and parts of legs which are darker, sometimes with a weak purple or green iridescent hue. Entire body clothed in fine white indistinct pubescence with sparse long setae on the anterior and posterior of head, mesosoma, petiolar node and gaster, absent on the underside of head.

Measurements

Minor worker (n= 5). CI 0.79 – 0.95; HL 1.89mm

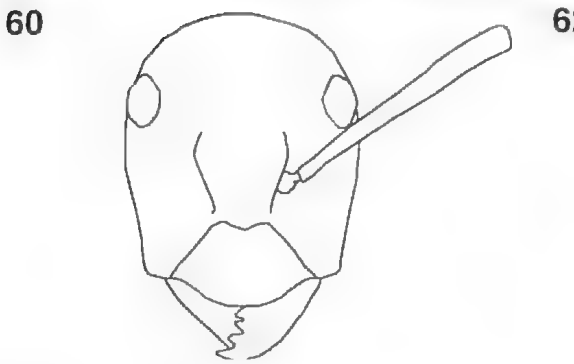

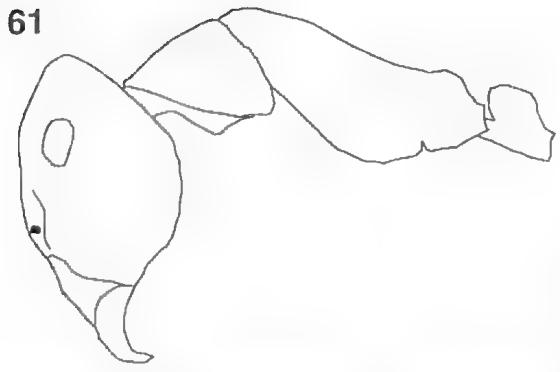

Figs 60-61. *C. perjurus* workers. Fig. 60. Head of minor worker. Fig. 61. Mesosoma and petiole of minor worker.

2.31mm; HW 1.72mm – 1.84mm; ML 2.84mm – 3.11mm; MTL 2.32mm – 2.43mm; PnW 1.41mm – 1.54mm; SI 1.22 – 1.28; SL 2.14mm – 2.30mm.

Etymology

From *perjurus*, to lie about one's true nature.

Remarks

This species appears to be a mimic of members of the *Iridomyrmex purpureus* species group (subfamily Dolichoderinae). This is based on the purple or green iridescent colour which is similar to *Iridomyrmex viridiaeneus* Viehmeyer (Shattuck 1993). Also, only single foragers have been found and most of these have been collected in association with *Iridomyrmex spodipilus* Shattuck and *Camponotus prosseri* Shattuck and McArthur. They have been found from central South Australia west into south-central Western Australia (Fig. 62).

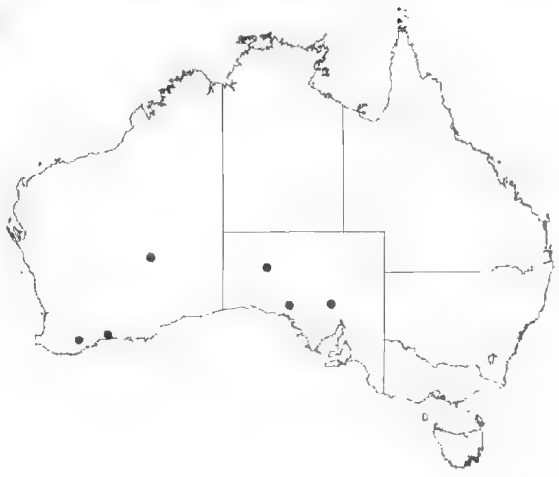

Fig. 62. Distribution of *C. perjurus* material examined during this study.

Acknowledgments

We would like to thank the following for providing comments on earlier versions of this manuscript: A. Andersen, B. Halliday and two anonymous reviewers. The illustrations were prepared by N. Barnett. Financial support was provided by the Australian Biological Resources Study, CSIRO Entomology and the South Australian Museum.

References

Brady, M. F. (2000) "Butterflies of Australia, their identification, biology and distribution". Melbourne: CSIRO Publishing. 1008 pp.

Clark, J. (1930a) New Formicidae, with notes on some little-known species. *Proc. R. Soc. Vic.* **43**, 2-25.

_____ (1930b). Some new Australian Formicidae. *Proc. R. Soc. Vic.* **42**, 116–128.

_____ (1938) Reports of the McCoy Society for Field Investigation, and Research. No. 2. Sir Joseph Bank Islands. Part I. Formicidae (Hymenoptera). *Proc. R. Soc. Vic.* **50**, 356–382.

Crawley, W. C. (1915) Ants from north and central Australia, collected by G. F. Hill. Part I. *Ann. Mag. Nat Hist.* **(8)15**, 130–136.

Day, M. F. and Pullen, K. R. (1999) Leafhoppers in ant nests: some aspects of the behaviour of Pogonoscopini (Hemiptera: Eurymelidae). *The Victorian Naturalist* **116**, 12-15.

Forel, A. (1894) Quelques fourmis de Madagascar (récoltées par M. le Dr. Völtzkow); de Nouvelle Zélande (récoltées par M. W. W. Smith); de Nouvelle Calédonie (récoltées par M. Sommer); de Queensland (Australie) récoltées par M. Wiederkehr; et de Perth (Australie occidentale) récoltées par M. Chase. *Ann. Soc. Entomol. Belg.* **38**, 226-237.

_____ (1910) Formicides australiens reçus de M. M. Froggatt et Rowland Turner. *Rev. Suisse Zool.* **18**, 1–94

_____ (1922) Glanures myrmécologiques en 1922. *Rev. Suisse Zool.* **30**, 87–102.

FROGGATT, W. W. (1896) Honey ants. pp. 385 392 *In* Spencer, B. (Ed.) "Report on the work of the Horn Scientific Expedition to Central Australia, Pt. 2 Zoology", Melville, Mullen & Slade, Melbourne.

IMAI, H. T., Crozier, R. H. and Taylor, R. W. (1977) Karyotype evolution in Australian ants. *Chromosoma* **59**, 341–393.

KIRBY, W. F. (1896) Hymenoptera. pp 203 209 *In* Spencer, B. (ed.) "Report on the work of the Horn Scientific Expedition to Central Australia, Pt. 1 supplement", Melville, Mullen & Slade, Melbourne.

LEACH, W. E. (1825) Descriptions of thirteen species of *Formica* and three species of *Culex*, found in the environs of Nice. *Zoological Journal* **2**, 289–293.

LOWNE, B. T. (1865) Contributions to the natural history of Australian ants. *Entomologist* **2**, 275–280.

MAYR, G. L. (1862) Myrmecologische Studien. *Verh. Zool.-Bot. Ges. Wien* **12**, 649–776.

_____ (1876) Die australischen Formiciden. *Journal des Museum Godeffroy* **5**, 56–115.

_____ (1886) Notizen über die Formiciden-sammlung des British Museum in London. *Verh. Zool.-Bot. Ges. Wien* **36**, 353–368.

MCARTHUR, A. J., ADAMS, M. & SHATTUCK, S. O. (1998) A morphological and molecular review of *Camponotus terebrans* (Lowne) (Hymenoptera: Formicidae). *Aust. J. Zool.* **45**, 579–598.

SANTSCHI, F. (1928) Nouvelles fourmis d'Australie. *Bull. Soc. Vaudoise Sci. Nat.* **56**, 465–483.

SHATTUCK, S. O. (1993) Revision of the *Iridomyrmex purpureus* species group (Hymenoptera: Formicidae). *Invertebr. Taxon.* **7**, 113-149.

_____ (1999) Australian ants: their biology and identification. *Monographs on Invertebrate Taxonomy* **3**, 1–226.

SMITH, F. (1858) "Catalogue of hymenopterous insects in the collection of the British Museum. Part 6. Formicidae". London: British Museum. 216 pp.

WHEELER, W. M. (1915) Hymenoptera. *Trans. R. Soc. S Aust.* **39**, 805–823.

STRATIGRAPHY OF THE LAKE MALATA PLAYA BASIN, SOUTH AUSTRALIA

By A. Dutkiewicz & C. C. von der Borch†*

Summary

Dutkiewicz, A. & von der Borch, C. C. (2002). Stratigraphy of the Lake Malata Playa Basin, South Australia. Trans. R. Soc. S. Aust. 126(2), 91-102, 29 November, 2002.

The 19 m-thick Late Quaternary stratigraphic sequence within Lake Malata, Eyre Peninsula is dominated by autochthonous gypsum, present as relatively mud-free gypsarenites and gypsum-clay laminae overlying a skeletal peloidal grainstone of the Bridgewater Formation near the base of the lacustrine succession. Calcite and dolomite mud are minor components of the column and several metres of these deposits appear to have been deflated into marginal lunettes. The skeletal peloidal grainstone has been severely modified by dissolution and formation of phreatic calcite, dolomite and gypsum cements under alternating pluvial and arid conditions. Discrete units are separated by disconformities and attest to rapid changes in climatic and hydrologic conditions over the lower Eyre Peninsula, commencing with emplacement of the Bridgewater Formation ca. 400 ka.

Key Words: Quaternary palaeoclimate, salt lakes, Lake Malata, Bridgewater Formation, carbonate mud, gypsum, dolomite, Eyre Peninsula.

Transactions of the Royal Society of S. Aust. (2002), **126**(2), 91-102.

STRATIGRAPHY OF THE LAKE MALATA PLAYA BASIN, SOUTH AUSTRALIA

by A. DUTKIEWICZ* & C. C. VON DER BORCH†

Summary

DUTKIEWICZ, A. & VON DER BORCH, C. C., (2002). Stratigraphy of the Lake Malata Playa Basin, South Australia. *Trans. R. Soc. S. Aust.* **126**(2), 91-102, 29 November, 2002.

The 19 m-thick Late Quaternary stratigraphic sequence within Lake Malata, Eyre Peninsula is dominated by autochthonous gypsum, present as relatively mud-free gypsarenites and gypsum-clay laminae overlying a skeletetal peloidal grainstone of the Bridgewater Formation near the base of the lacustrine succession. Calcite and dolomite mud are minor components of the column and several metres of these deposits appear to have been deflated into marginal lunettes. The skeletal peloidal grainstone has been severely modified by dissolution and formation of phreatic calcite, dolomite and gypsum cements under alternating pluvial and arid conditions. Discrete units are separated by disconformities and attest to rapid changes in climatic and hydrologic conditions over the lower Eyre Peninsula, commencing with emplacement of the Bridgewater Formation ca. 400 ka.

KEY WORDS: Quaternary palaeoclimate, salt lakes, Lake Malata, Bridgewater Formation, carbonate mud, gypsum, dolomite, Eyre Peninsula.

Introduction

Lake Malata is an ephemeral salt lake situated 33 m above mean sea level in a mid-latitude region on lower Eyre Peninsula, South Australia (Fig. 1). It covers a total surface area of around 21 km^2, which excludes numerous small deflationary playa lakes to the east of the main basin. Lake Greenly, 10 km south-west of Lake Malata, forms another major playa lake in the region but appears not to have been connected to Lake Malata in the relatively recent past (Dutkiewicz 1996)[1] and indeed has a different stratigraphic sequence (Dutkiewicz & von der Borch 1995). Notably, Lake Malata is dominated by autochtonous evaporite deposits which are interbedded with carbonate mud, whereas Lake Greenly is dominated by carbonate muds interbedded with minor evaporites. Lake levels in Lake Malata fluctuate rapidly and seasonally as a consequence of surficial hydrological closure and rapid changes in the inflow-evaporation balance, which relies heavily on regional rainfall. During the wet winter season the lake retains < 0.5 m water, which evaporates in summer leaving behind a cm-thick halite crust. Although there is little direct evidence for the origin of the lake, geomorphologically its formation appears to have coincided with the emplacement of the Bridgewater Formation sub-parabolic dunes during late Quaternary sea-level high stands. These dunes, which consist of skeletal peloidal sands, may have effectively dammed the pre-Pleistocene drainage channel thus forming local depocentres. Also, as the Bridgewater Formation forms the main recharge aquifer in the region, groundwater seepage along the dune lobes would have invariably enhanced lake basin formation within interdunal corridors and in

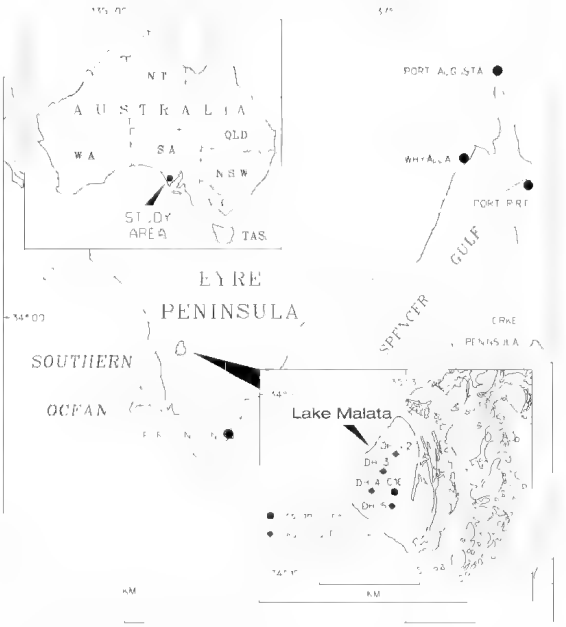

Fig. 1. Map of Eyre Peninsula showing Lake Malata and location of sediment cores.

* School of Geosciences, Building F05, The University of Sydney NSW 2006, Australia

† School of Chemistry, Physics and Earth Sciences, Flinders University, GPO Box 2100, SA 5001, Australia

[1] DUTKIEWICZ, A. (1996) "Quaternary Palaeoclimate from Lake Malata-Lake Greenly Playa Complex, South Australia" PhD thesis, The Flinders University of South Australia (Unpubl.).

areas of low relief. Prominent geomorphological features include clay pellet lunettes, gypsum lunettes and beach deposits along the eastern margins of most playa basins (Dutkiewicz *et al.* 2002) some of which reach 9 m in height. Apart from the sub-parabolic dunes, pisolitic red soils and calcrete of possible Tertiary age dominate the geomorphology to the south and west of the main basin (Dutkiewicz *et al.* 2002).

This paper focuses on the sedimentary succession within Lake Malata, which provides evidence of past fluctuations in lake level, groundwater chemistry, and Quaternary climates. The carbonate-evaporite cycles reflect hydrologic and geomorphologic settings of the basin, detrital influx, groundwater seepage and recharge, and wind shear, which often redistributes surface water and wet sediment across the entire lake surface and deflates dry sediment into marginal lunettes. Post-depositional diagenesis of primary and clastic carbonates and evaporites will be discussed briefly as these also have been influenced by climatic oscillations.

Methods

The stratigraphic sequence is based chiefly on five diamond drill cores taken from the main basin in 1987 by Gilfillan and Associates Pty. Ltd. to determine the viability of gypsum mining (Fig. 1). The cores sampled the lake sequence to basement and are available for viewing at the South Australian Department of Mines and Energy core library in Glenside, Adelaide. Despite their deteriorated state, compaction of up 60% and 80% recovery, careful sampling and detailed petrographic study of about 50 thin sections allowed a stratigraphic succession and palaeoenvironmental reconstruction to be established for Lake Malata. Unfortunately, sediments from the drill cores were unsuitable for radiocarbon and thermoluminescence dating due to contamination, exposure to sunlight, and paucity of suitable material available for dating. Consequently, a piston coring method was used to sample 1.8 m of fresh sediment from the center of Lake Malata (Fig. 1). AMS dating of the sequence, however, was unsatisfactory due to high concentrations of Na, Mg and K salts and low organic carbon contents (Dutkiewicz 1996)[1].

All cores were logged and the mineralogy of selected horizons analysed in some detail. The colour was determined using the Munsell colour chart. Unconsolidated material was wet sieved; the coarse fraction was examined under a binocular microscope, and the composition of the fine fraction determined using X-ray diffraction. Consolidated material was cut perpendicular to bedding, impregnated and used for thin sectioning. The thin sections were partly stained with Alizarin red-S, and

Fig. 2. Correlation of cores through the Lake Malata basin

studied with a polarising microscope. Textures and cements were further examined using Scanning Electron Microscopy at CEMMSA at Adelaide University.

Gypsum samples in hand specimen are described using a grain-size classification scheme of Warren (1982) while primary and secondary gypsum petrofabric descriptions are based on criteria outlined by Bowler & Teller (1986) and Magee (1991). The skeletal peloidal sands and grainstones in Lake Malata have been correlated with calcareous aeolianites from the Bridgewater Formation using detrital, mollusean, foraminiferal, echinoderm, algal, bryozoal and peloidal compositional classes.

Stratigraphy

Gypsum constitutes at least 70% of the bulk sediment within the Lake Malata basin. Carbonate (calcite and dolomite) and detrital clays form a relatively minor component and occur as fine laminations or interbeds rather than discrete units. However, strandline deposits, which include several phases of carbonate pellet lunette and gypsum foredune deposition (Dutkiewicz *et al.* 2002), suggest that at least 5 m of carbonate mud and at

least 10 m of gypsum sand have been removed from the lake basin during periods of deflation and lunette-building spanning ca. 115-6 ka (Dutkiewicz *et al.* 2002). Individual units comprising the most completely sampled succession from diamond drill core DH-5, which appears to have been taken from the palaeo-lake centre, are discussed in detail. A cross-section through the Lake Malata basin using all available diamond drill cores is shown in Figure 2. Contacts between the individual units are sharp with disconformities between units 6, 5 and 4, and 6, 4 and 3.

Unit 7: Basement (Weathered Gneiss)

The basement consists of yellowish grey, very soft and highly weathered gneiss which contains abundant pebble and sand-sized grains of clear and grey quartz, sericite and iron oxides. The gneiss is exposed around the southern and eastern margin of Lake Malata where it forms a graben-type structure.

Unit 6: Gypsum-Rich Sericite

This unit consists of very light grey to light grey, heavy and very dense sericite clay containing randomly-oriented, displacive pyramidal gypsum. The gypsum is lenticular in thin section and displays a diversity of grain-size with crystals ranging from less than 1 mm up to 5 mm in length. The crystals are isolated and lack contact with each other. The poor sorting of the crystals reflects the variable porosity and permeability of the sericite matrix, which together determine the *in situ* growth of the pyramidal gypsum. The centres of the crystals frequently display polycrystalline overgrowths, seen as distinct crystal zoning under polarised light. Iron oxides are commonly incorporated along the cleavage planes of gypsum. The sericite matrix displays a high birefringence under crossed polars and is clearly the weathering product of the underlying unit. Unit 6 is approximately 70 cm in thickness in DH-5 and 3 m in thickness in DH-3, reflecting the irregularity in basement and variable depth of the weathering zone.

Unit 5: Laminated Gypsarenite

Unit 5 consists of finely laminated gypsarenite, which reaches approximately 1 m in thickness in DH-5 and disconformably overlies Unit 6 (Figs 2, 3a). The unit has not been recognised elsewhere in the basin and possibly represents local deposition within a deeper, central part of the basin. In fact, Unit 4 directly overlies Unit 6 in all cores with the exception of core DH-5. The gypsarenite comprises alternating wavy mm-thick laminae of very light grey fine to medium-grained, moderately to well-sorted sugary gypsum, coarser gypsum in a matrix of clay and dolomite, and medium light grey clay which drapes the underlying gypsum-rich laminae. Most of the gypsum crystals are prismatic and appear as equant polygons in thin section (Fig. 3a). The finer-grained gypsum is closely-packed, matrix-free, with only minor to trace amounts of fine-grained iron oxides. Prismatic gypsum comprising the coarser layers, on the other hand, occurs in a matrix of non-oriented clay and carbonate, predominantly kaolinite and saccharoidal dolomite, and displays concentrations of iron oxides along cleavage planes (Fig. 3b). Matrix-free, coarse-grained gypsum is also common but represents grading of the finer crystals rather than discrete laminae. Displacive, lenticular or pyramidal gypsum forms are rare but occasionally occur within the coarser gypsarenite layers, where they are oriented randomly or sub-vertically to bedding. Unlike the clay laminae comprising a more recent and better-preserved Unit 3, the clay in Unit 5 lacks optical orientation. A possible explanation for this is the relative abundance of coarse grains such as gypsum, quartz and iron oxides, which are incorporated in these laminae and prevent the clay particles from becoming aligned. Clay orientation may also be disrupted by post-depositional growth of gypsum within overlying and underlying layers.

Unit 4: Skeletal Peloidal Grainstone

Unit 4 consists of a strongly cemented skeletal peloidal grainstone, which disconformably overlies Unit 5 in DH-5 and Unit 6 in DH-1 to DH-4. The grainstone attains only 50 cm in thickness in DH-5 but reaches a maximum thickness of 3.5 m in the easternmost basin core DH-4, where it forms a unique and complex sequence of diagenetic carbonate-evaporite fabrics. These include moldic porosity filled by poikilotopic gypsum and dolomicrospar (Figs 4a, b), dolomicrospar and microspar cements containing displacive gypsum discoids (Fig. 4c) and dolomicrospar-coated allochems with a late pore-filling gypsum cement (Fig. 4d). A possible explanation for the difference in unit thickness between DH-4 and DH-5 is that DH-4 is relatively proximal to the margin of the lake and is better suited for the deposition of sandy near-shore facies, in particular calcareous sands derived from surrounding sub-parabolic dunes. In DH-5, the grainstone is essentially a light olive grey, well-lithified gypsiferous wackestone with approximately 40-60% fabric-selective (moldic) porosity and displacive, poorly-sorted pyramidal gypsum within a micrite matrix (Figs 3c, d). The gypsum crystals occur as isolated laths, characterised by sharp crystal faces indicating minimal dissolution. Although the gypsum is generally randomly or sub-vertically oriented to bedding, individual crystals show a tendency for displacive

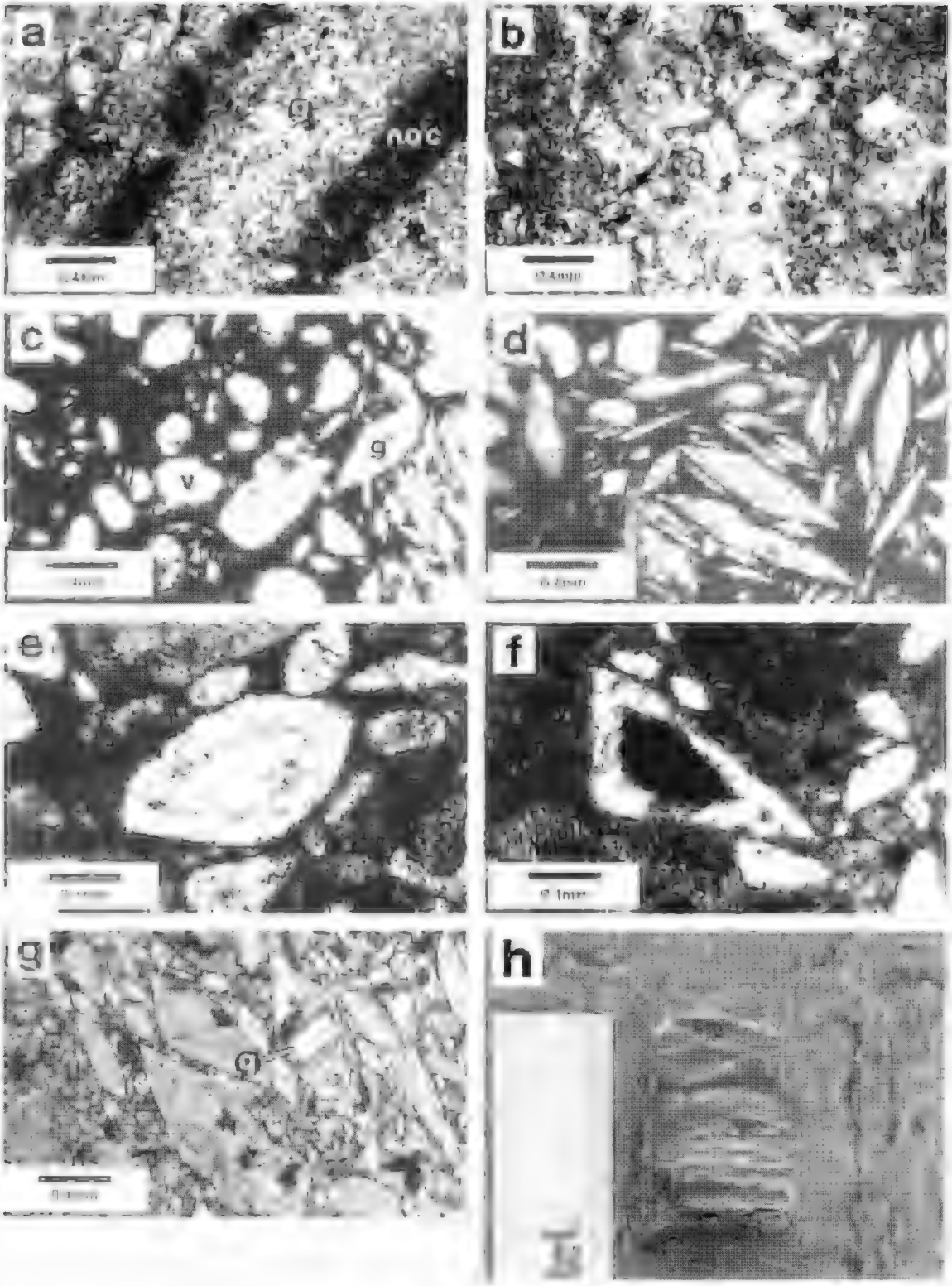
a
g
noc
b
c
v
g
d
e
f
g
g
h

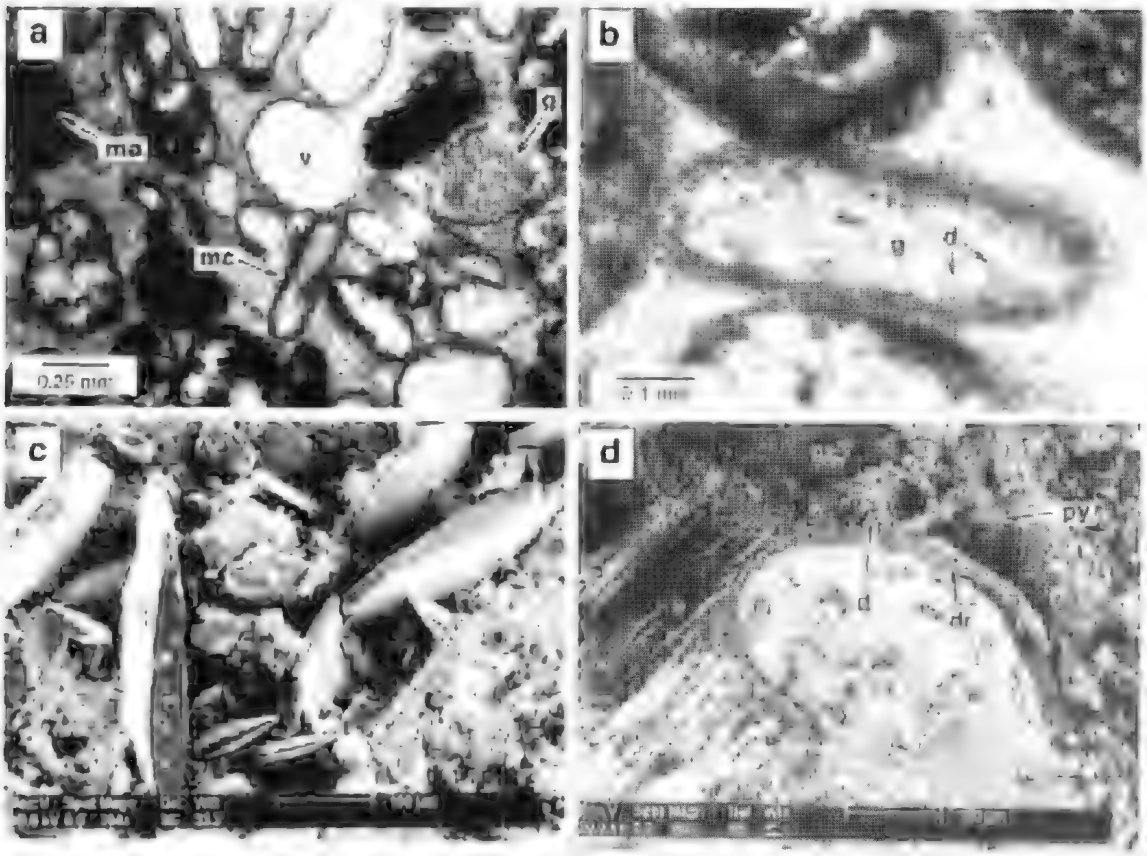

Fig. 4. Photomicrographs of the skeletal peloidal grainstone in Unit 5. Thin section images (a-b) taken under plain light. a) Moldic porosity partially filled by poikilotopic gypsum. Note micrite coatings (mc), micritised allochems (ma), empty allochemical voids (v) occasionally filled by gypsum (g). Intergranular cement consists almost entirely of poikilotopic gypsum (g). b) Allochemical void partially filled by anhedral dolomicrospar (d) and gypsum (g). Intergranular porosity is filled by poikilotopic gypsum and minor anhedral dolomicrospar. c) SEM image showing displacive gypsum discoids within a dolomicrospar/calcite microspar cement. d) SEM image showing a dolomicrospar rind (dr) around a micritised allochem. The rind forms contact sutures with neighbouring dolomicrospar rinds surrounding allochemical voids which are partially filled by dolomicrospar (d). Intergranular cement consists of poikilotopic gypsum and sparse dolomicrospar. Note the presence of intergranular pyrite (py).

Fig. 3. Photomicrographs of Units 3, 4 and 5 from the Lake Malata basin taken under plain light. (a) Gypsum-clay couplets in Unit 5. The thicker laminae consist of fine to coarse-grained equant (prismatic) gypsum (g) and the thinner laminae consists of non oriented clay (noc) dominated by kaolinite. (b) Prismatic equant gypsum crystals in Unit 5. The matrix consists of kaolinite and dolomite. Iron oxides are commonly incorporated along the cleavage planes of gypsum. (c) Completely leached portion of the skeletal peloidal grainstone comprising Unit 4. Allochemical voids (v) are present within a dolomicrite matrix. Displacive discoidal (pyramidal) gypsum (g) is common and often forms clusters. (d) Abundant gypsum discoids in Unit 4. The discoids are randomly oriented to bedding and are rarely in contact with each other. (e) Pyramidal gypsum in Unit 3. Note zoning within the centre of the crystal caused by the inclusion of iron oxides around a pre-existing detrital core or gypsum nucleus. (f) Poorly-formed discoidal (pyramidal) gypsum crystal from the base of Unit 3. The centre of the crystal is occupied by a quartz core (q). (g) Gypsum discoids comprising the basal gypsarenite in Unit 3. The crystals are oriented sub-vertically to bedding and show zoning near the crystal edges related to dissolution and re-precipitation of the gypsum or variable growth rates of the single crystal. Quartz (?) (q) cores are occasionally present. (h) Core section showing regularly alternating laminae of gypsum (light) and clay (dark) comprising the gypsum-clay laminite in Unit 3 in DH-5

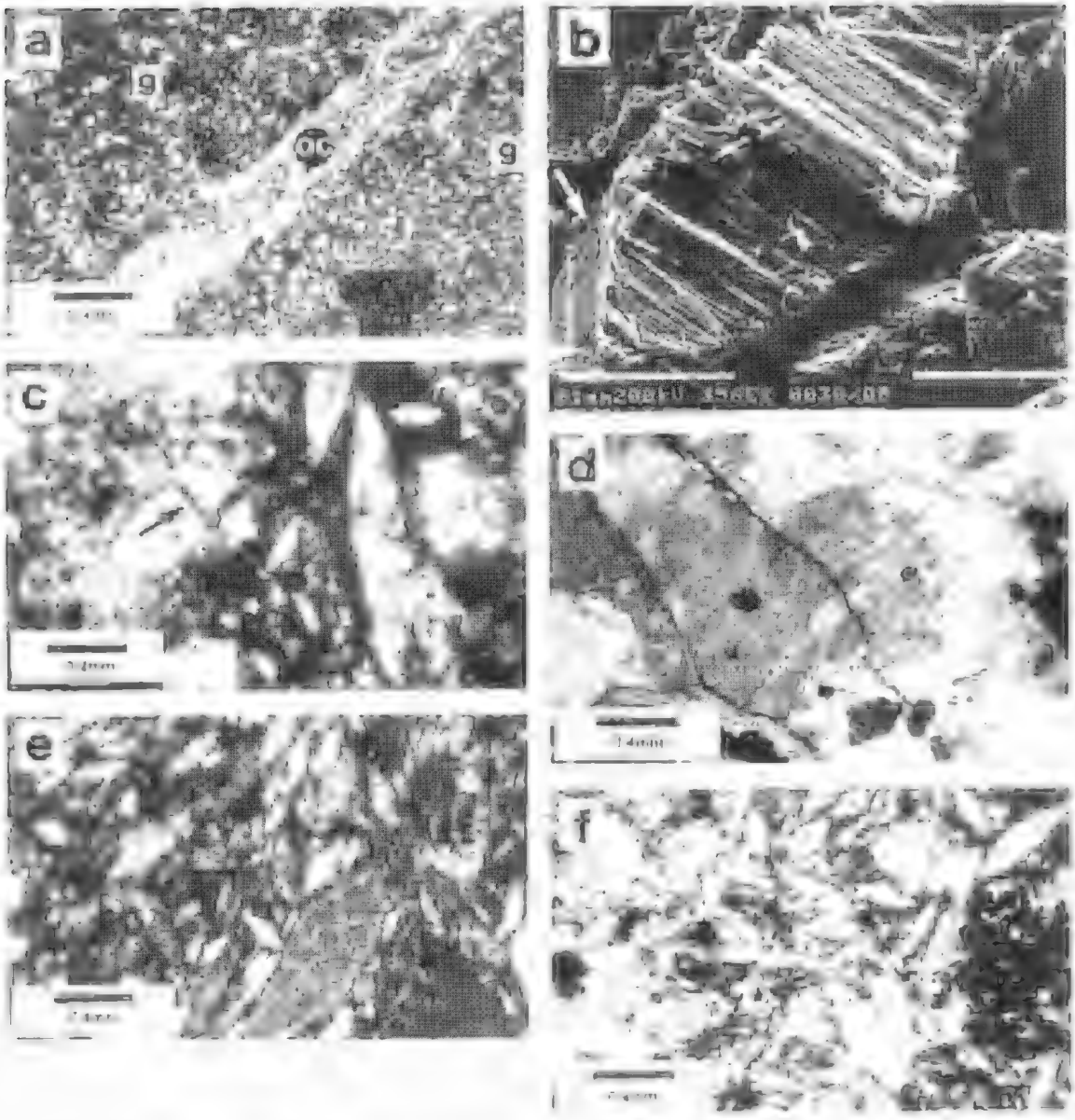

Fig. 5. Thin section (a, c–f) and SEM (b) photomicrographs showing the gypsum habits in Units 3 and 2. Polarised light (a) plain light (c–f). a) Gypsum-clay couplets comprising the gypsum-clay laminite in Unit 3. The laminae consist of highly oriented clay (oc) dominated by kaolinite, overlain and underlain by thicker layers of extremely fine-grained, equant prismatic gypsum crystals (g). b) Gypsum discoid (pyramidal gypsum) from the upper gypsarenite layer in Unit 3. The face of the crystal is the {011} cleavage plane which shows considerable recrystallisation. Note the presence of fine-grained sub-spherular dolomite (arrow). c) Fracturing and minor reworking of a gypsum crystal (arrow) near the base of the upper gypsarenite horizon in Unit 3. Displacive (pyramidal) gypsum is the most common crystal morphology in this unit. The matrix consists of a mixture of kaolinite and dolomite. The gypsum is very poorly sorted. d) Coarse, intergrown bladed (pyramidal) gypsum near the base of Unit 2 showing the presence of fibrous kaolinite (?) along the cleavage planes. Plain light. e) Sub-vertically to randomly oriented discoidal (pyramidal) gypsum within a calcite-dolomite matrix comprising gypsarenite in Unit 2. Recrystallisation and zoning are particularly common in this zone. f) Abundant iron oxides forming clusters within Unit 2.

sub-circular cluster arrangement (Fig. 3c) reminiscent of gypsite nodules. Preserved allochemical components in DH-4, as well as the general shape and size of the voids in DH-5, suggest that the porosity has resulted from a complete dissolution of skeletal and peloidal allochems sourced by the Bridgewater Formation. Detrital grains include fine-grained quartz, plagioclase and iron oxides, which have not been affected by dissolution. Grain counting and cluster analysis, although restricted to a small unleached portion of the unit in DH-4, show good correlation with the Bridgewater Formation and the 9 m beach ridge along the eastern margin of Lake Malata (Dulkiewicz *et al.* 2002). Although textures and fabrics described for DH-5 are consistent with pedogenesis, in DH-4 the skeletal peloidal grainstone has undergone extensive phreatic diagenesis which is reflected in fabric-selective moldic porosity; isopachous dolomicrospar rinds; intergranular and intragranular void-filling dolomicrospar; and poikilotopic and void-filling gypsum cement (Fig. 4).

Unit 3: Laminated Gypsarenite

Unit 3 disconformably overlies Unit 4 and attains a thickness of 6 m. It consists of a medium light grey to light grey gypsarenite containing variable amounts of interdispersed dolomite mud and kaolinite, fine-grained gypsarenite, and displacive gypsite nodules. The unit is interbedded with a finely laminated gypsarenite over the 9.5-10.5 m and 11.5-12 m depth intervals (Fig. 3h). The laminated sequences consist of alternating mm-thick wavy laminae of very light grey, sugary, fine to medium-grained, well-sorted gypsum, finer (~ 1 mm thick) laminae of medium dark grey, optically oriented kaolinite, and light grey mm-thick laminae of medium-grained gypsarenite in a matrix of clay and dolomite mud. Clay draping is common. A metre-thick layer of fine to medium-grained, moderately-sorted gypsarenite separates the laminated intervals.

The gypsum-clay laminae overlie a gypsarenite layer which consists of randomly and sub-vertically oriented pyramidal gypsum crystals within a matrix of saccharoidal dolomite (Fig. 3e). The gypsum crystals are relatively wide across the c-axis and show variable grain-size and degree of sorting. A cm-thick layer of pyramidal crystals oriented parallel to bedding, and showing little variability in grain-size, is also present. Zoning of crystals is common and may be attributed to: 1) the incorporation of iron oxides along cleavage planes and crystal boundaries during a change in the growth rate or during selective dissolution of the crystal (Fig. 3e); 2) crystal growth around a detrital core (Figs. 3f, g); 3) the development of gypsum overgrowths at the margins of gypsum crystals which lack optical continuity with the rest of the crystal. In this sense, the pre-existing gypsum crystals provide a nucleus for subsequent gypsum growth; and 4) selective dissolution followed by re-precipitation of central and marginal parts of crystals. All of these features have been observed in this part of the unit.

The repetitious nature of the clay and gypsum laminae bears a striking resemblance to similarly varved sequences from Lake Tyrrell (Bowler & Teller 1986), Prungle Lakes (Magee 1991) and Lake Eyre (Magee *et al.* 1995). In Lake Malata, the individual laminae consist of: 1) fine to coarse-grained, reversely graded, closely-packed, matrix-free, horizontally oriented prismatic gypsum; 2) relatively coarse-grained, frequently reversely graded, horizontally oriented, prismatic gypsum in a matrix of non-oriented clay (Fig. 3a). Here, the clay contains abundant iron oxides and minor fine-grained, displacive, vertically oriented pyramidal gypsum; and 3) optically oriented clay (kaolinite) with minor iron oxides and minor coarse-grained prismatic gypsum (Fig. 5a). The laminae are equally spaced and cyclic.

The gypsarenite overlying the gypsum-clay laminae consists of medium to coarse-grained, poorly-sorted, pyramidal gypsum in a matrix of non-oriented clay and saccharoidal dolomite with abundant gypsite nodules. The gypsum is randomly orientated to bedding and displays perfectly formed polycrystalline discoids under the SEM (Fig. 5b). A small number of the crystals, however, are prismatic and oriented parallel to bedding. The gypsite nodules are several mm in diameter, displacive and consist of silt-sized pyramidal gypsum forming matrix-free, cumulus-shaped clusters. Iron oxides are abundant and occur along cleavage planes of the pyramidal gypsum crystals. Fracturing and apparent reworking of a number of crystals are evident (Fig. 5c).

Unit 2: Gypsarenite

Unit 2 consists of yellowish grey to light olive grey, slightly muddy, medium to coarse-grained and poorly-sorted gypsarenite. The unit is approximately 5 m in thickness and sharply overlies Unit 3. The mud fraction consists of dolomite with minor amounts of detrital kaolinite, becoming increasingly calcite-rich (low-Mg calcite) towards the top of the unit where dolomite and kaolinite are present only in trace amounts. Kaolinite is occasionally incorporated within gypsum cleavage planes (Fig. 5d). Centimetre-thick laminations of relatively muddy gypsarenite alternating with less muddy gypsarenite are common between 4.5-5 m and 3.5-4 m. A decimetre-thick layer of greyish yellow green

kaolinite is present between 5 and 5.4 m overlying a dm-thick layer of coarse-grained displacive discoids of pyramidal gypsum measuring about 1 cm in length. White, irregular and displacive gypsite nodules and gypsite layers are common between 5.5 and 6 m. In thin section, the gypsarenite consists of pyramidal crystals oriented randomly and sub-vertically to bedding dispersed within a carbonate (calcite and dolomite) matrix (Fig. 5e). Gypsum grain size is variable, with individual crystals ranging from less than 1 mm to 1 cm in length. Gypsite nodules also consist of randomly oriented pyramidal gypsum crystals. However, the crystals occur as poorly-developed discoids and form dense, displacive, matrix-free nodules within slightly muddy gypsarenite. Although detrital cores contribute to crystal zoning, the majority of the gypsum laths are zoned due to dissolution and rapid re-precipitation of gypsum (Fig. 5e). Large, bladed, occasionally fractured and intergrown, prismatic gypsum up to 1 cm in length is common near the base of the unit, where it shows replacement by low-Mg calcite (?) along the cleavage planes. Minor amounts of horizontally oriented prismatic crystals and clusters of iron oxide minerals (Fig. 5f) are also associated with this layer.

Unit 1 – Gypsarenite

Unit 1 consists of olive grey, muddy, medium to coarse-grained, poorly-sorted gypsarenite interbedded with cm-thick layers of gypsite and a dm-thick layer of organic-rich, olive black low magnesian calcite mud near the base. The unit is approximately 70 cm thick and sharply overlies Unit 2. The gypsum is pyramidal, with individual long c-axes oriented randomly or sub-vertically to bedding. The crystals occasionally show inclusions of mud, indicative of fast growth rates within a mud matrix (Kastner 1970). Clusters of iron oxides are present locally. Only Unit 1 is represented within the piston core (C16; Fig. 1).

Interpretation of depositional environments

The stratigraphic sequence reflects largely groundwater controlled oscillations in lake levels associated with humid and arid climatic episodes, which in a vertical sequence are marked by the presence of saline lacustrine facies (carbonates and evaporites), intermittent aeolian deposition of skeletal peloidal sand, lunette-building and pedogenesis of marginal regions.

Laminated clay-rich gypsarenite (Unit 5), which disconformably overlies weathered basement gneiss in the region, forms the base of the lacustrine sequence. The clay was most likely deposited in topographic lows as channel runoff during a relatively pluvial period, with flow and erosion initiated during and after heavy rains. Deposition may have occurred in the early Pleistocene prior to the initial emplacement of the sub-parabolic dunes ca. 700 ka (Wilson 1991)[2], which buried vast areas of the land surface and played a key role in the formation of the lake basins and the regional aquifer. This is supported by the absence of skeletal peloidal allochems within the clay which would otherwise be expected to be transported with the flow, with calcareous sand and grainstone occurring higher in the stratigraphic sequence. Lamination of clays, in DH-5 in association with gypsarenite, suggests intermittent, possibly annual deposition controlled by the duration and frequency of the pluvial episodes. Regionally, the clay probably represents a relatively low flow regime, where only clay-sized particles with a very fine sand fraction are deposited in the centre of the basin.

Deposition of skeletal peloidal sands (Unit 4) is most likely related to Wilson's (1991)[2] phase I (ca. 400 ka) or early phase II (ca. 220 ka) emplacement of the Bridgewater Formation sub-parabolic dunes. The skeletal peloidal sand disconformably overlies basement clay and shows intense diagenesis and strong cementation in the centre of the Lake Malata basin. It is disconformably overlain by lacustrine gypsarenites in Lake Malata as indicated by sharp lithological discontinuities and the presence of indurated horizons above and below the unit, which are the result of subaerial exposure and pedogenesis. Deposition of Unit 4 is closely related to the Lake Malata foredune ridge, deposited during a prolonged pluvial phase ca. 319 ka (Dutkiewicz *et al.* 2002). The skeletal peloidal sand has undergone induration and cementation partly due to subaerial exposure and partly due to precipitation of phreatic intergranular cement, which reflects alternating groundwater fluctuations. The indurated (pedogenic) horizons indicate minor breaks in deposition of the sand, which is controlled largely by sediment supply and the intensity of the westerly winds. Relatively minor amounts of lacustrine carbonate have been deposited intermittently within the sand, forming discontinuous interbeds, as conditions became more pluvial for short-lived periods of time.

Vast amounts of the mobile skeletal peloidal sand would have been transported into the basin prior to dune stabilisation, during the landward migration of the dunefield and during subsequent episodes of dune re-activation. The sand was transported into the lake basin mostly by the strong prevailing westerlies

Wilson, C. C. (1991). Geology of the Quaternary Bridgewater Formation of the Southwest and Central South Australia." PhD thesis, The Flinders University of South Australia (Unpubl.)

and partly by local runoff which drained the sub-parabolic dunes. Emplacement of the first phase of skeletal peloidal sand initiated the formation of a major unconfined aquifer and the onset of lacustrine carbonate deposition. The lake at this time was relatively fresh, and the recharge rates high. The ca. 319 ka Lake Malata ridge and abundant dissolution features in the recharge aquifer and within the Lake Malata basin indicate evidence for high groundwater tables. Dissolution of allochems, particularly during the freshening recharge episodes, was essential in providing sufficient ions for the subsequent chemical precipitation of low-Mg calcite.

The skeletal peloidal sand experienced some reworking within the basin, as indicated by the presence of a relatively thin layer of the sand overlying laminated gypsarenite in DH-5. In this part of Lake Malata, the sand experienced induration and pedogenesis as reflected in the presence of a cryptocrystalline micrite cement and displacive pyramidal gypsum associated with a fluctuating water table. Pedogenesis appears to have been particularly effective in areas of lateral thinning of the sand/grainstone and may be related to the role of the grainstone as a recharge conduit and preferential drying of low recharge parts of the lake. Thick beds of skeletal peloidal grainstone, on the other hand, experienced intense diagenesis in the form of carbonate-evaporite fabrics related to oscillations in groundwater and the phreatic diagenetic environment (e.g., DH-4). In particular, carbonate cements formed during periods of increased pluviality, relatively low evaporation/inflow ratios associated with relatively high lake levels and low salinities. The dolomite represents a combination of replacive and void-filling cements linked with fabric-selective dissolution of allochems. Gypsum cements are void-filling and post-date carbonate cementation. They were formed during arid periods characterised by high evaporation/inflow ratios and low lake levels.

Following the first phase of dune migration (and formation of the calcareous recharge aquifer), the lakes were inundated with carbonate-enriched ground and surface water, with solutes derived largely through the dissolution of skeletal and peloidal allochems. This is evident in the first cycle of diagenesis in the skeletal peloidal grainstone within the basin, which is marked by the precipitation of carbonate cement, and in the considerable thickness of chemically-precipitated carbonate mud in regions of former lake extent overlying the first phase of skeletal peloidal sand deposition (Dutkiewicz 1996)[1]. The thickness and the relatively homogeneous nature of the carbonate units in marginal areas (Dutkiewicz 1996)[1] indicate that precipitation occurred under relatively long-lived hydrologically and climatically uniform conditions in a low energy, open-lake environment. The carbonate mud units correlate with laminated gypsarenite in Lake Malata (DH-5) from which several metres of carbonate have been removed by deflation during the construction of carbonate pellet lunettes over a period spanning ca. 96 to 15 ka (Dutkiewicz *et al.* 2002). It is possible that the indurated horizons separated by unlithified carbonate mud within these deposits are related to lunette pedogenesis associated with major falls in groundwater levels (Dutkiewicz *et al.* 2002). Possibly due to burial and moisture content, carbonate and clay pellets associated with lunette-building have not been detected at depth within the mud sequences.

Deposition of the skeletal peloidal grainstone in Lake Malata was followed by the onset of alternating shallow and relatively deep saline conditions associated with frequent groundwater fluctuations. This is illustrated by the presence of a distinct, finely laminated gypsarenite sequence (Unit 3) comprising alternating laminae of clay and prismatic gypsum, which overlies the skeletal peloidal grainstone towards the basin centre. In Lake Malata, carbonate sedimentation was restricted to marginal areas, proximal to the recharge aquifer, with gypsum deposition confined to central, deeper parts of the basin. The repetitive nature and constant thickness of the laminae in this unit suggest an alternating wet-dry, seasonal depositional cycle. Clays which comprise the thin (< 1 mm) laminae and represent the fine-grained clastic component, were transported into the basin during the wet winter season as runoff which drained the eastern and western clay-rich slopes surrounding the lake. While the finer clastics were transported into the deeper, central parts of the basin, coarser clastics, including skeletal peloidal sand which is currently eroded from the sub-parabolic dunes bordering the southern lake margin, were deposited in the near-shore regions. Magee (1991) suggested that a density difference between the dilute inflow and concentrated lake brines would allow the fresh floodwater carrying a suspended clay to glide over the brine for considerable distances prior to the clay flocculating and settling to the lake bottom. Evaporation, combined with reduced inflow into the lake during the dry months, would subsequently concentrate the surface brine and allow prismatic gypsum to precipitate within the brine body or at the brine-air interface.

In Lake Malata, primary, subaqueous precipitation of gypsum is supported by: 1) the absence of reworking features such as fracturing and rounding, which are indicative of abrasion during transport, thus consistent with crystals growing at the

sediment-water interface (Magee 1991); 2) the absence of variable grain size within a single gypsum laminae, which is indicative of diagenetic growth of crystals following deposition; and 3) the presence of wavy laminae, suggesting the presence shallow water. Therefore, gypsum comprising the laminae is of the "settled" variety of Magee (1991) having formed at the brine-air interface and then settled to the lake sediments as described by Schreiber *et al.* (1982). Coarsening-upwards of the gypsum crystals suggests that the surface brines became increasingly saline and supersaturated towards the end of the dry season, producing larger and fewer crystals (Schreiber 1978; Magee 1991). In order for subaqueous gypsum to precipitate and accumulate in significant amounts, the basin must be groundwater controlled and contain permanent saline water which is maintained only when the basin receives a constant supply of water and experiences high evaporation rates (Rosen 1994). The presence of clay within a number of the gypsum layers is related to brief flooding episodes during the dry phase, which apart from supplying fine-grained clastics to the lake, are insufficient to dilute the brine below the level of gypsum saturation. Iron oxides are supplied either during the flooding of the basin or are the product of sulphate-reducing bacteria oxidising iron sulphides. The cycle is repeated with the next wet episode, during which clay drapes the underlying gypsum. This provides an impervious layer which seals the gypsum and prevents it from undergoing dissolution, as the brine freshens by mixing with the dilute inflow.

Mechanisms involved in orientation of clay particles are not completely understood. A number of proposed mechanisms have been reviewed by Magee (1991), although to date very little work has been done on highly oriented clay particles. Most noteworthy contributions by Mead (1964) and Somerfield (1984) suggested compaction, de-watering of clays and flocculation as possible controlling factors in particle alignment. Bowler and Teller (1986) suggested that formation and preservation of oriented clays in saline lacustrine environments is dependent on salinity and the activity of benthic micro-organisms. They proposed that deep water, aerated, low salinity environments would support scavenging organisms which are likely to disturb oriented clay particles. On the other hand, organisms cannot become established under conditions of extreme salinity and transported clays are able to flocculate and settle undisturbed. Since microfauna is relatively rare (or rarely preserved) in Lake Malata, the explanation of Bowler and Teller (1986) provides a likely mechanism for clay particle alignment in the laminae documented here.

Conditions following the seasonal deposition of the gypsum-clay laminite changed dramatically within the Lake Malata basin as lake levels dropped. This was due to an overall increase in the evaporation/inflow ratio caused by a decrease in precipitation, which is the main source of recharge into the lake, and/or a decrease in the fraction of groundwater lost due to leakage through an increasing impermeable skeletal peloidal grainstone (Dutkiewicz *et al.* 2000). Sediments directly overlying the laminated sequence are no longer varved and are dominated by pyramidal rather than prismatic gypsum (units 2 and 3). In fact, pyramidal gypsum is the most common form of gypsum within the evaporite beds and comprises thick units within Lake Malata and Lake Greenly. Pyramidal gypsum has been found in many coastal settings such as Hutt and Leeman Lagoons in Western Australia (Arakel 1980), Trucial Coast (Shearman 1966) and more recently in Lake Tyrrell (Bowler & Teller 1986) and Prungle Lakes (Magee 1991). Unlike prismatic gypsum, which forms within a standing brine body, pyramidal gypsum precipitates interstitially from saturated pore waters immediately below the sediment surface within the capillary zone under the influence of high evaporation rates (Bowler & Teller 1986). In Lake Malata, it is commonly found within a carbonate/clay matrix, where it either completely displaces the surrounding matrix forming mud-free gypsarenite, or undergoes diagenetic growth with gypsarenites becoming coarse-grained and poorly-sorted while isolated crystals become massive and reach several centimetres in length. Absence of solid inclusions within the massive gypsum indicates slow growth under uniform conditions (Kastner 1970). Pyramidal gypsum comprising gypsarenites, on the other hand, is generally cloudy due to the incorporation of impurities, suggesting fast growth under uniform conditions where the gypsarenites are moderately to well-sorted, and non-uniform conditions where the gypsarenite is poorly-sorted.

Bowler & Teller (1986) suggested that sediment layers containing abundant pyramidal gypsum crystals may be good indicators of past fluctuations in groundwater. The fact that pyramidal or discoidal gypsum comprises gypsum lunettes/foredunes along the eastern margin of Lake Malata in itself suggests seasonally oscillating hydrological conditions (Dutkiewicz *et al.* 2002). Since the gypsum lunettes/foredunes contain only traces of carbonate or clay pellets, it is the generally mud-free thick gypsarenite beds such as Units 3 and 2 which are the most likely source of the gypsum. In this scenario, gypsum is reworked by wave action during a relatively wet episode and deposited at the eastern lake margin, where it is subsequently deflated into a lunette or foredune during the next dry episode. The

seasonal deposition of the gypsum foredune mimics the earlier deposition of the gypsum-clay laminae, which are no longer forming due to an overall drop in lake level and a shift from a throughflow to a relatively closed discharge basin. As advocated by Bowler (1983), near-surface precipitation of gypsum and other salts assists in pelletisation of lacustrine mud and clay. This process is required for deflation of mud and clay from the lake surface and is possible only under a groundwater discharge regime. The general absence of gypsum within carbonate pellet lunettes indicates that most of the gypsum precipitated as groundwaters rose slightly and the capillary fringe reached the lake surface, following a period of deflation and oscillating low water tables.

Units 1 and 2, which comprise the Lake Malata sequence, correlate well with the alternating carbonate-evaporite beds in Lake Greenly (Dutkiewicz & von der Borch 1995). However, correlation of individual beds is impossible, partly due to deflation of several metres of carbonate and its subsequent deposition along the north-eastern margin of Lake Malata (Dutkiewicz *et al.* 2002), and partly due to local hydrology, geomorphology and aquifer characteristics which control the deposition of carbonates in one basin and evaporites within the other basin. However, within a single vertical sequence, the carbonate beds are associated with humid conditions and relatively low evaporation/inflow ratios, whereas the gypsum is associated with arid conditions and relatively high evaporation/inflow ratios. Thermoluminescence dating of carbonate-pellet lunettes suggest that these humid-arid oscillations may have been operating since ca. 16 ka, which post-dates the majority of carbonate pellet lunette deposition and overlaps with formation of the gypsum lunette/foredune ca. 5.6 ka cal BP (Dutkiewicz *et al.* 2002).

Acknowledgments

A. Dutkiewicz gratefully acknowledges the financial support of Flinders University. We thank Joe Lorenzin for the preparation of thin sections and staff at the DME core library and the CEMMSA at Adelaide University for their help with accessing and analysing the Lake Malata sediments. Core C16 was sampled with the help of fellow Flinders University post-graduate and honours students. We are indebted to the Modra Family for their hospitality and help during our prolonged stays in the field. Chris von der Borch acknowledges the continuing support of the School of Physics, Chemistry and Earth Sciences at Flinders University. We thank Martin Williams for a thorough review of the manuscript.

References

Arakel, A. V. (1980) Genesis and diagenesis of Holocene evaporitic sediments in Hutt and Leeman lagoons, Western Australia. *J. Sed. Pet.* **50**, 1305-1326.

Bowler, J. M. (1983) Lunettes as indices of hydrologic change: a review of Australian evidence. *Proc. Royal Soc. Vic.* **95**, 147-168.

_____ & Teller, J. F. (1986) Quaternary evaporites and hydrologic changes, Lake Tyrrell, north-west Victoria. *Aust. J. Earth Sci.* **33**, 43-63.

Dutkiewicz, A., Herczeg, A. L. & Dighton, J. C. (2000) Past changes in isotopic and solute balances in a continental playa: clues from stable isotopes of lacustrine carbonates. *Chem. Geol.* **165**, 309-329.

_____ & von der Borch, C. C. (1995) Lake Greenly, Eyre Peninsula, South Australia: sedimentology, palaeoclimatic and palaeohydrologic cycles. *Palaeogeog. Palaeoclim. Palaeoecol.* **113**, 43-56.

_____, _____ & Prescott, J. R. (2002) Geomorphology of the Lake Malata-Lake Greenly Complex, South Australia, and its implications for Late Quaternary Palaeoclimate. *Trans. R. Soc. S. Aust.* **126**, 103-115.

Kasner, M. (1970) An inclusion hourglass pattern in synthetic gypsum. *Am. Mineral.* **55**, 2128-2130.

Magee, J. W. (1991) Late Quaternary lacustrine, groundwater, aeolian and pedogenic gypsum in the Prungle Lakes, southeastern Australia. *Palaeogeog., Palaeoclim., Palaeoecol.* **84**, 3-42.

_____, Bowler, J. M., Miller, G. H., & Williams, D. L. G. (1995) Stratigraphy, sedimentology, chronology and palaeohydrology of Quaternary lacustrine deposits at Madigan Gulf, Lake Eyre, South Australia. *Palaeogeog Palaeoclim., Palaeoecol* **113**, 3-42.

Milne, R. H. (1964) Removal of water and rearrangement of particles during the compaction of clayey sediments - review. *U.S. Geological Survey Professional Paper*, No. 497-B, 23 pp.

Rosen, M. R. (1994). The importance of groundwaters in playas: A review of playa classifications and the sedimentology and hydrology of playas. *In* Rosen, M.R. (Ed.) "Paleoclimate and Basin Evolution of Playa Systems" Geol. Soc. Am. Special Paper No. 289

SCHREIBER, B. C. (1978) Environments of subaqueous gypsum deposition. pp. 43-73 *In* Dean, W. E. & Schreiber, B. C. (Eds) "Marine Evaporites" SEMP Short Course No. 4. Soc. Econ. Min. Palaeont., Tulsa, U.S.A.

_____, ROTH, M. S. & HELMAN, M. L. (1982) Recognition of primary facies characteristics of evaporites and the differentiation of those forms from diagenetic overprints pp. 1-32 *In* Hanaford, C. R., Loucks, R. G. & Davies, G. R. (Eds) "Depositional and Diagenetic Spectra of Evaporites - A Core Workshop" SEMP Core Workshop 3, Calgary.

SHEARMAN, D. J. (1966). Origin of marine evaporites by diagenesis. *Inst. Min. Met. Trans.* **75**, 208-215.

SONNENFELD, P. (1984). Brines and Evaporites. (Academic Press, New York, U.S.A.).

WARREN, J. K. (1982) The hydrological setting, occurrence and significance of gypsum in late Quaternary salt lakes in Australia. *Sedimentology*, **29**, 609-637.

GEOMORPHOLOGY OF THE LAKE MALATA-LAKE GREENLY COMPLEX, SOUTH AUSTRALIA, AND ITS IMPLICATIONS FOR LATE QUATERNARY PALAEOCLIMATE

By A. Dutkiewicz, C. C. von der Borch† & J. R. Prescott‡*

Summary

Dutkiewicz, A. von der Borch, C. C. and Prescott, J. R. (2002) Geomorphology of the Lake Malata-Lake Greenly complex, South Australia, and its implications for late Quaternary palaeoclimate. Trans. R. Soc. S. Aust. 126(2), 103-115, 29 November, 2002.

Lunettes, foredunes and beach ridges from the Lake Malata-Lake Greenly playa complex on the Eyre Peninsula attest to major changes in lake level and palaeoclimate over the last 320,000 years. These have been dated by a combination of thermoluminescence and radiocarbon techniques, thus allowing correlation with Late Quaternary Oxygen Isotope stages. The lakes experienced a major wet phase ca. 320 ka followed by multiple arid episodes linked to relatively cool periods and low eustatic sea-levels between 115-16 ka. Aeolian activity and aridity wre particularly intense during the Last Glacial Maximum with the onset of a dry climate and carbonate pellet lunette-building commencing as early as 26 ka. The Holocene palaeoclimate is marked by seasonally oscillating wet and dry periods reflected in the intermittent deposition of gypsum lunettes, carbonate ridges and quartz foredunes around the eastern margins of lakes Malata and Greenly.

Key Words: Quaternary palaeoclimate, salt lakes, Lake Malata, Lake Greenly, lunettes, thermoluminescence dating, Bridgewater Formation, carbonate, gypsum.

Transactions of the Royal Society of S. Aust. (2002), **126**(2), 103-115.

GEOMORPHOLOGY OF THE LAKE MALATA-LAKE GREENLY COMPLEX, SOUTH AUSTRALIA, AND ITS IMPLICATIONS FOR LATE QUATERNARY PALAEOCLIMATE

by A. Dutkiewicz[1], C.C. Von Der Borch[2] & J.R. Prescott[3]

Summary

Dutkiewicz, A. von der Borch, C. C. and Prescott, J. R., (2002). Geomorphology of the Lake Malata-Lake Greenly complex, South Australia, and its implications for late Quaternary palaeoclimate. *Trans. R. Soc. S. Aust.* **126**(2), 103-115, 29 November, 2002.

Lunettes, foredunes and beach ridges from the Lake Malata-Lake Greenly playa complex on the Eyre Peninsula attest to major changes in lake level and palaeoclimate over the last 320,000 years. These have been dated by a combination of thermoluminescence and radiocarbon techniques, thus allowing correlation with Late Quaternary Oxygen Isotope stages. The lakes experienced a major wet phase ca. 320 ka followed by multiple arid episodes linked to relatively cool periods and low eustatic sea-levels between 115-16 ka. Aeolian activity and aridity were particularly intense during the Last Glacial Maximum with the onset of a dry climate and carbonate pellet lunette-building commencing as early as 26 ka. The Holocene palaeoclimate is marked by seasonally oscillating wet and dry periods reflected in the intermittent deposition of gypsum lunettes, carbonate ridges and quartz foredunes around the eastern margins of lakes Malata and Greenly.

Key Words: Quaternary palaeoclimate, salt lakes, Lake Malata, Lake Greenly, lunettes, thermoluminescence dating, Bridgewater Formation, carbonate, gypsum.

Introduction

Lake basins are one of the richest archives of terrestrial palaeoclimate data (e.g., Williams *et al.* 1998; Mason *et al.* 1994; Rodó *et al.* 2002). In particular, surficially-closed basins such as salt lakes are extremely sensitive to changes in climate and respond accordingly by adjusting their lake and groundwater levels. They are widespread in south-western, south-eastern and northern parts of Australia where they often represent the termini of large endoreic basins (e.g., Bowler & Magee 1988; Magee *et al.* 1995; Macumber 1991; Bowler 1971). As salt lakes are susceptible to drying and erosion, one of the most challenging aspects associated with their study is resolving the problem of discontinuous stratigraphic records. This, however, can be achieved by examining and dating not only the sedimentary succession in the basin itself, but also the geomorphologic features such as beach ridges and lunettes, as these invariably formed during major changes in lake levels and climate. In this study we describe strandline features of the Lake Malata-Lake Greenly Complex (Fig. 1), which contain a rich record of major climate change exposed along its eastern shores. Most of these features have been dated by thermoluminescence and radiocarbon dating and provide a framework for late Quaternary climate change in South Australia. These are discussed in detail in this paper.

Fig. 1. Map of Eyre Peninsula showing the location of the Lake Malata-Lake Greenly Complex.

School of Geosciences, Building 1435, The University of Sydney, NSW 2006, Australia
School of Chemistry, Physics and Earth Sciences, Flinders University, GPO Box 2100, SA 5001
Department of Physics and Mathematical Physics, University of Adelaide, 5005, Australia

General Setting

The Lake Malata-Lake Greenly Complex consists of a chain of north north-east trending Quaternary carbonate-evaporite playa lakes, situated approximately 33 m above mean sea level in a mid-latitude region on lower Eyre Peninsula, South Australia (Fig. 1). The main basins, Lake Malata and Lake Greenly, are separated by an extensive easterly trending calcareous, sub-parabolic dune system, which forms the main regional aquifer. Emplacement of these dunes during the late Quaternary sea-level highstands (Wilson 1991)[1] most likely caused the damming of a pre-Pleistocene drainage channel, with subsequent groundwater seepage along the dune lobes facilitating formation of lakes Malata and Greenly. Both basins are eroded along their south-west margins with adjacent basement rocks up to 5 metres above the present-day lake floor suggesting a graben-type depression. Numerous smaller playas, located exclusively to the east of the main basins, appear to have formed much later, via the interactive processes of deflation and groundwater discharge. Hydrologic, stratigraphic and geomorphologic evidence collected to date indicates that the main basins have never been surficially connected.

At present, all lakes in the Lake Malata-Lake Greenly Complex are ephemeral groundwater-discharge playas characterised by a cm-thick halite crust during the dry summer months. Depths of up to 0.5 m of water, partly due to direct precipitation and partly due to reduced evaporation exist during the wet winter months. The solutes are derived from marine salt accession via aerosols and by evaporation of inflow (surface and groundwater), which delivers chemical weathering products from surrounding sedimentary and basement rocks and syndepositional recycling of evaporites. The hydrology and geochemistry of the main basins have been discussed elsewhere (Dutkiewicz *et al.* 2000). Although defined by the same mineralogical suite, basin sediments from Lake Greenly and Lake Malata are distinctly different. Lake Greenly sediments are dominated by carbonate mud (calcite and dolomite) measuring several metres to decimetres in thickness, with the uppermost 3 m of the basin sequence interbedded with dm-thick layers of gypsarenite (Dutkiewicz & von der Borch 1995). In contrast, Lake Malata is dominated by gypsum, which occurs in the form of relatively mud-free, m-thick gypsarenites, and mm-thick gypsum-clay laminae which overlie a cemented skeletal peloidal grainstone near the base of the succession. The skeletal peloidal grainstone overlies weathered basement. The difference in the relative abundance of carbonate and gypsum over the lake complex is related to the local hydrologic setting of each basin and rainfall/recharge distribution over the region.

Geomorphology

The morphology of the playa lakes depends on the nature of the pre-existing surface, the angle of the long basin axis to the direction of the prevailing wind, the presence and depth of surface water, the proximity of the groundwater to the lake surface and playa-groundwater chemistry. Aeolian reworking, ground and surface water fluctuations and interactions play a secondary role in modifying the lake geomorphology, which ultimately reflects major changes in climate. A number of geomorphologic features directly associated with the Lake Malata-Lake Greenly Complex include islands, spits, lunettes, irregular sub-parabolic dunes, beach ridges, sandy beaches, marginal seepage-spring zones and surface drainage channels (Fig. 2). In this

Fig. 2. Geomorphologic map of the Lake Malata-Lake Greenly Complex showing the location of TL and AMS dated samples.

[1] Wilson, C. C. (1991). 'Geology of the Quaternary Bridgewater Formation of the Southwest and Central South Australia.' PhD thesis, The Flinders University of South Australia (Unpubl.)

Table 1. Thermoluminescence and ^{14}C ages of key geomorphologic features.

Sample Name	Geomorphologic Feature	Description	Dating Method	Age
LM1	Gypsum lunette/Gypsum dune	Coarse-grained, moderately-sorted gypsarenite overlain by a gypsite capping.	AMS	4.81 ± 0.09 ka B.P. 5.59 (2s = 5.32-5.72) ka cal B.P.[1]
ML4	Carbonate pellet lunette	Slightly pelletal, clayey carbonate overlain by an indurated carbonate layer.	TL	16.1 ± 1.2 ka
ML5	Carbonate pellet lunette	Slightly gypsiferous and pelletal clayey carbonate overlain by an indurated carbonate layer.	TL	53.9 ± 4.4 ka
ML7	Foredune ridge (Lake Malata ridge)	Strongly cemented, well-sorted, medium to coarse-grained skeletal peloidal grainstone.	TL	319 ± 52 ka
ML9	Carbonate pellet lunette	Gypsiferous, slightly clayey, pelletal carbonate.	TL	115 ± 14 ka
ML10	Carbonate pellet lunette	Slightly pelletal carbonate overlying an indurated nodular carbonate layer. Abundant iron-stained quartz.	TL	84.5 ± 9.3 ka
ML11.1	Carbonate pellet lunette	Clayey carbonate overlain by an indurated carbonate layer.	TL	43.4 ± 3 ka
ML11.2	Carbonate pellet lunette	Pelletal carbonate overlying an indurated carbonate layer.	TL	15.6 ± 0.7 ka
ML12	Carbonate pellet lunette	Slightly gypsiferous pelletal carbonate overlying a moderately indurated chalky carbonate layer.	TL	17.5 ± 1.1 ka
ML13	Carbonate pellet lunette	Strongly indurated nodular carbonate layer.	TL	75.1 ± 5.4 ka
ML14	Carbonate pellet lunette	Pelletal carbonate mud overlying Coxiella sand.	TL	1.17 ± 0.1 ka
ML15	Carbonate pellet lunette	Pelletal carbonate mud overlain by cobbles of weakly to moderately indurated chalky carbonate.	TL	17.3 ± 0.8 ka
ML17	Sub-parabolic dune	Moderately cemented, well-sorted, medium-grained skeletal peloidal grainstone.	TL	70.6 ± 3.2 ka
ML18	Quartz foredune	Moderately-sorted, medium to coarse-grained quartz sand. Abundant Coxiella, ostracode and foraminifer fragments.	TL	1 ± 0.09 ka 0.26 ± 1.93 ka[3]
GL4	Carbonate pellet lunette	Pelletal carbonate overlain by cobbles of weakly to moderately indurated chalky carbonate.	TL	26 ± 1.7 ka
GL8	Carbonate pellet lunette	Slightly pelletal and clayey carbonate mud.	TL	96.3 ± 13.9 ka

[1] dated by accelerator mass spectrometry (AMS); Lab No. OZB152U; conventional (uncalibrated) age

[2] calibration based on Stuiver and Reimer (1993) and Stuiver et al. (1998)

[3] average of two ages (312 ± 67 ka and 325 ± 77 ka; Dutkiewicz & Prescott 1997)

[4] the younger age indicates remobilisation of the foredune obtained using the double plateau on the plateau test (Dutkiewicz & Prescott 1997)

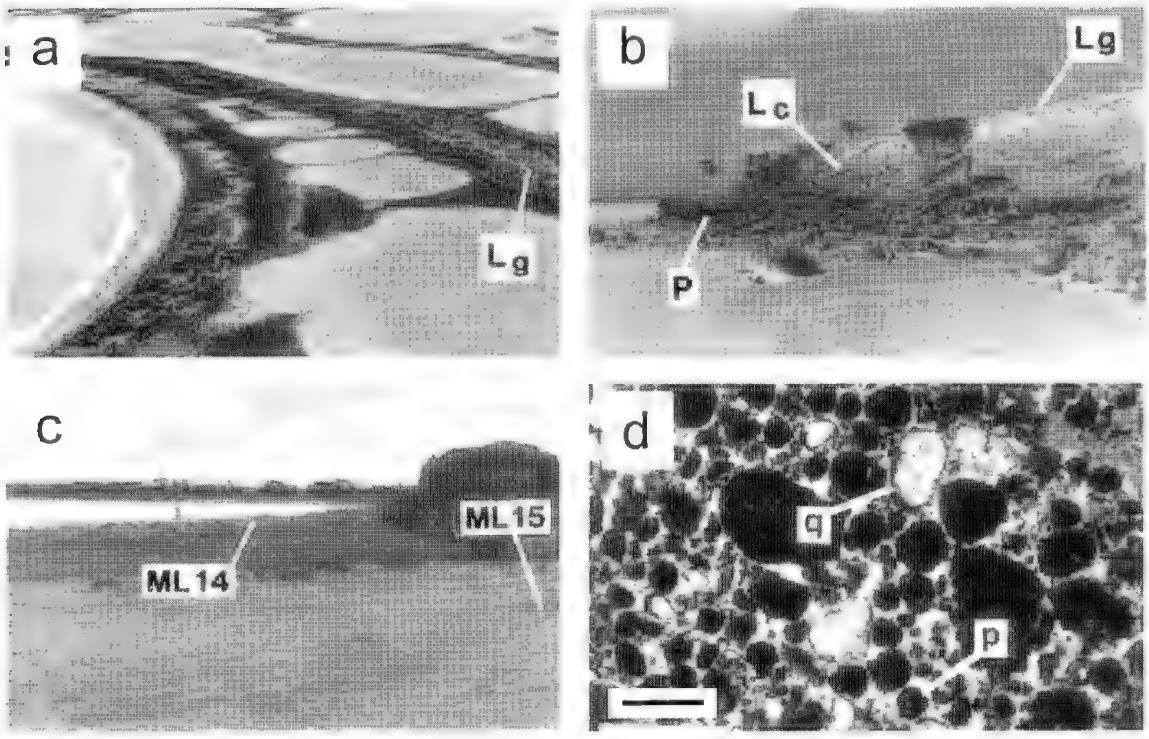

Fig. 3. (a) A chain of playa lakes that have previously deflated into a gypsum lunette (L_g). View is towards the north. Centre of photograph spans approximately 600 m. (b) A 5 to 6 m-high, truncated lunette profile at the south-western margin of Lake Greenly. Basement is unconformably overlain by an indurated pedogenic horizon (P), which is in turn overlain by an altered carbonate pellet lunette (L_c). Gypsite layer (L_g) overlies L_c with a gradational contact. (c) Lee side of two carbonate pellet lunettes (~1.17 ka ML14 and ~17.3 ka ML15) along the eastern margin of a small playa lake north of Lake Malata, forming a prograding lunette sequence separated by a samphire-vegetated mud flat. These represent Phase III and Phase I deposition events in Fig. 4. (d) Thin-section photomicrograph showing bimodal carbonate pellets (p) with a minor amount of well-rounded carbonate-coated quartz (q) of similar grain-size. Plain light. Scale is 0.25 mm.

paper we describe some of the key geomorphological features ranging in age from 319 ± 72 ka to 1 ± 0.9 ka (Dutkiewicz & Prescott 1997; Fig. 2, Table 1) which formed as a result of major climate change.

Lunettes

Although clay, quartz and gypsum are the most common minerals comprising lunettes (crescentic dunes associated exclusively with playa lakes; e.g., Bowler 1983; Warren 1982; Williams *et al.* 1991; Chen *et al.* 1991; Macumber 1991), those in the Lake Malata-Lake Greenly Complex consist either of gypsum sand or sand-sized carbonate pellets. In general, the gypsum and carbonate pellet lunettes are part of a prograding sequence, which rises 2 to 3 m above the present-day lake floor. They are characterised by at least two disconformities in the form of pedogenic layers or erosional scarps and younger deflation basins (Figs 3a, b, c). The lunettes occur along the eastern margins of most playas in the complex and provide a partial indication of the amount of material that has been deflated from the lake basins. Their associated pedogenic horizons (disconformities) are potential time-stratigraphic markers for strandline-basin correlations.

Four discrete units representing four major phases of lunette deposition have been recognised from exposed sections and dated by TL between 115 ± 14 ka and 1.17 ± 1.1 ka (Dutkiewicz & Prescott 1997; Fig. 4). The distinction is based largely on the degree and style of pedogenic alteration of the indurated carbonate layer (disconformity) overlying the soft lunette material, and field relationships of lunette deposits. Notably, progressive pedogenesis and loss of original pelletal texture are a function of increasing age while the composition and colour of the lunettes and pedogenic horizons reflect the immediate source area. Internal structures, such as low-angle planar beds normally expected from seasonal accumulation, are very diffuse or non-existent and are attributed to the breakdown of pellets by moisture and pedogenesis. Individual deposits may reflect multiple phases of lunette deposition and stabilisation, although the general

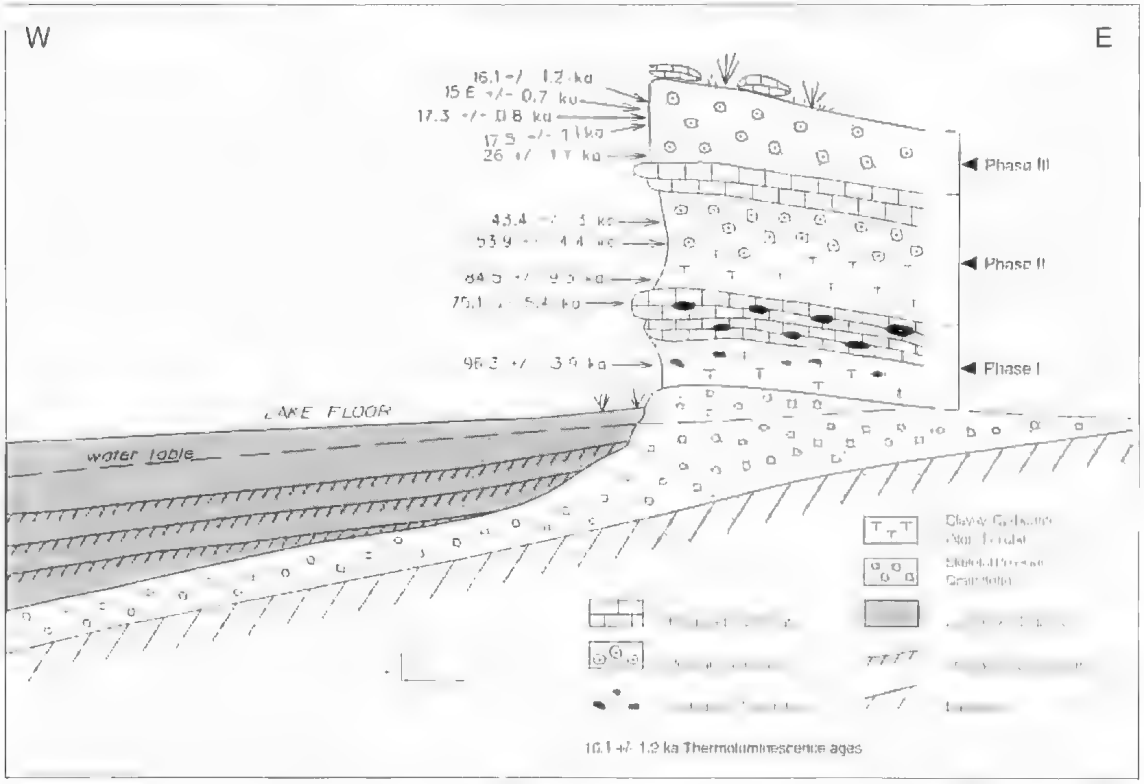

Fig. 4. Idealised schematic west-east section of Lake Malata showing three major phases of carbonate pellet lunette deposition in a single onlapping sequence. Thermoluminescence dates are also shown.

homogeneity of the deposits makes differentiation of these difficult.

The pelletal fraction consists almost exclusively of low-Mg calcite and minor clay minerals dominated by montmorillonite. The coarse, non-pelletal fraction usually contains minor amounts of abraded gypsum discoids or prisms, quartz, iron oxides, peloids, foraminifera, ostracode carapaces and *Coxiella* fragments, and trace amounts of lithoclasts, pyrite and remnants of algal mats including rare charophyte oogonia. In thin-section and under the scanning electron microscope (SEM), the carbonate lunettes consist of bimodal sand-sized carbonate pellets and minor sand-sized quartz (Fig. 3d). Quartz grains tend to be well-rounded and carbonate-coated, while gypsum is discoidal, poorly-sorted, shows effects of dissolution and abrasion and frequently occurs as semi-cemented aggregates. Gypsite nodules are common in the gypsiferous lunettes.

In general, the degree of pedogenic alteration corresponds with the age of the lunette and conforms with Netterberg's (1967) calcrete classification. For example, the oldest lunettes show intense pedal development in the form of cavernous, nodular calcrete and complete loss of the original pelletal structure in the underlying deposit. Younger lunettes, on the other hand, are capped by a chalky, powdery calcrete or more massive and strongly indurated hardpan calcrete, both of which are nodule-free and frequently comprise several undulose sheet layers which themselves reflect multiple phases of pedogenesis. These are overlain either by thin veneers of pelletal soil or younger, onlapping lunette deposits. The youngest lunettes display a strong pelletal fabric with samphire vegetation acting as the main post-depositional stabiliser.

Three major phases of gypsum lunette formation have been identified in this study. The best examples occur virtually along the entire lengths of the inner and outer margins of eastern Lake Malata (Fig. 2) where the lunettes form a prograding, cross-bedded sequence measuring up to 7 m above the present-day lake (Fig. 5a). An organic-rich layer within the core of the main lunette has been dated by AMS at 5.59 ka cal B.P. and is currently being mined for gypsum for agricultural purposes. The cliffed sections of the Lake Malata lunettes are onlapped by clean, well-sorted gypsarenite which forms the present-day beach. The lunette sequences are stabilised by a weakly indurated 40 cm to 3 m-thick capping of gypsite which is colonised by abundant salt-tolerant shrubs and samphire vegetation. The relationship

Fig. 5. (a) Two phases of gypsum lunette deposition along the inner eastern margin of Lake Malata. Beach sand (B_s) consists of coarse-grained gypsarenite. Younger Phase III gypsum lunettes are stabilised entirely by vegetation. Distance from the Lake Malata margin to playa lake immediately behind Phase III lunette is 400 m. (b) Gypsum lunette (L_g) representing Phase II gypsum lunette deposition overlying a clayey carbonate pellet lunette (L_c) along the inner eastern margin of Lake Malata. Poorly-sorted, coarse-grained beach sand (B_s) comprising basement and skeletal peloidal grainstone lithoclasts forms the present-day beach. Note presence of coarse-grained white gypsum sand (g) onlapping L_c.

between the gypsum and carbonate lunettes is not always clear, as the gypsum lunettes are generally larger and more extensive, completely obscuring underlying units which essentially become barriers for their development. Along the outer south-eastern margin of Lake Malata and the south-western margin of Lake Greenly, exposed sections clearly show a gypsum lunette overlying a carbonate pellet unit (Fig. 5b). However, farther north and along the inner margin of Lake Malata, the gypsum lunettes appear to extend in a southerly direction away from the flanks of the carbonate lunettes without directly overlying the carbonate pellet units in exposed sections. Field relationships and a single AMS date suggest that the gypsum lunettes are generally younger than the carbonate pellet lunettes.

The gypsum lunettes consist almost entirely of medium to coarse-grained, moderately to well-sorted gypsarenite with small amounts of carbonate (low Mg calcite) and trace amounts of fine-grained quartz and iron oxides. Consequently, the gypsum lunettes were unsuitable for TL dating and only in one case contained sufficient organic carbon for ^{14}C dating. The carbonate content may be attributed either to the presence of carbonate pellets, carbonate coating the gypsum crystals during their growth in the lake basin, or to biogenic components. Fragments of ostracodes, *Cyprella* and the foraminifer *Elphidium* are common within the uppermost 65 cm of the most recent gypsum lunettes. The gypsarenite consists of 1–4 mm long, slightly abraded anhedral lensoids, marked by dissolution kinks. The thickness of the gypsite capping varies between 40 cm to 3 m and is a function of the size and the age of the lunette. The thicker and the more indurated the gypsite horizon, the older the lunette. The gypsite consists entirely of 10 μm long acicular crystals under the SEM. Gypsite also occurs as cm-thick interbeds within the gypsum lunette where it most likely represents stabilisation of individual, possibly annual, aeolian layers. In the same manner that the indurated carbonate layers represent disconformities within the carbonate pellet lunettes sequence, the gypsite units represent periods of non-deposition within the gypsum lunettes. Low angle aeolian bedding is well-developed within the gypsum lunettes and reflects grain-size variations and general sorting of the gypsarenite within the individual laminae.

Beach Ridges and Foredunes

The most distinct geomorphologic feature associated with the Lake Malata-Lake Greenly Complex is a 9 m-high, arcuate, indurated skeletal peloidal grainstone beach ridge dated by TL at 319 ± 52 ka (Dutkiewicz & Prescott 1997: Table 1), which is present along the eastern margin of Lake Malata ("Lake Malata Ridge" in Figs 2 and 6). The ridge has

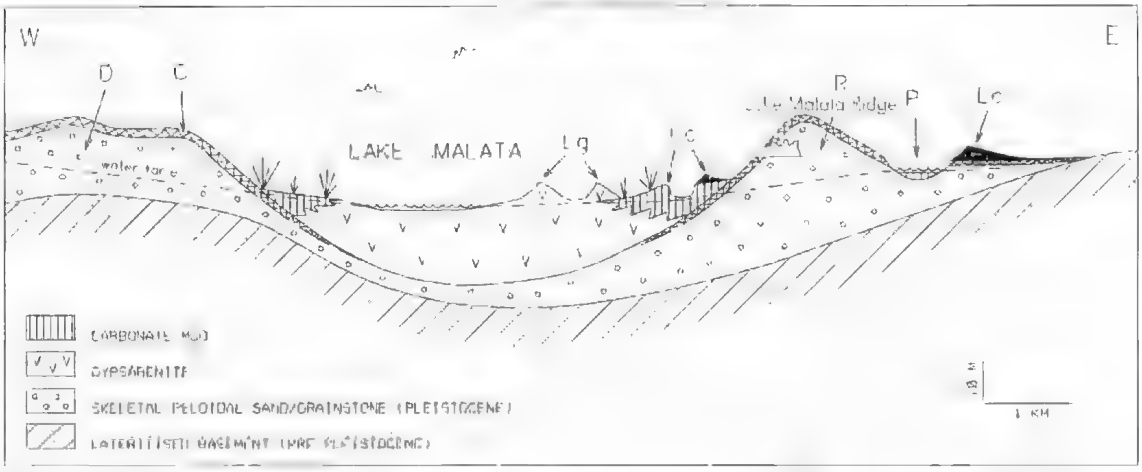

Fig. 6. Schematic west-east section across Lake Malata showing the western margin of the lake basin bordered by calcretised (C) sub-parabolic dunes (D), and the eastern margin by a major arcuate ridge (R) and a series of transverse gypsum lunettes (L_g) and carbonate pellet lunettes (L_c), and small playa lakes (P).

been correlated with a similar grainstone sampled by drilling, which overlies the basement in the Lake Malata basin (Dutkiewicz 1996)[2] and represents the largest and quite possibly the oldest geomorphologic feature associated with the lake complex. The ridge is cavernous and has an up to 10 cm-thick capping of calcrete, which is locally overlain by a thin red soil containing abundant ferruginous pisolites. The ridge sediments outcrop sporadically along the south-western margin of Lake Malata where they are overlain unconformably by a gypsum lunette. Sedimentary structures were not observed, possibly due to calcretisation and a general lack of outcrop and exposure. The beach ridge consists of a locally tufaceous, medium-grained, well-sorted skeletal peloidal grainstone comprising sub-rounded to well-rounded micritised peloids, abundant mollusk fragments, coralline red algae, foraminifera, minor echinoid fragments, rare bryozoa and varying amounts of lithoclasts and angular quartz grains (Fig. 7a). Its composition correlates well with the Bridgewater Formation, which comprises surrounding sub-parabolic dunes and spectacular cliffs on the west coast of the Eyre Peninsula (Wilson 1991).

More recent but pervasive beach deposits are found around the shorelines of Lake Malata and Lake Greenly and associated playa lakes. The composition of the beach sand depends largely on the source and its thickness on the sediment supply and the proximity of the source to the lake margin, the water depth, and the fetch of the lake. For example, poorly-sorted, very coarse sands and gravels are associated with basement outcrops. Thick (up to 3.5 m), localised accumulations of beach sand are common along the south-western margin of Lake Greenly and southern Lake Malata, where they consist of very coarse angular quartz, lithoclasts of basement rock, calcrete, and skeletal peloidal grainstones, iron oxides, feldspar, mica, and skeletal peloidal allochems derived from surrounding sub-parabolic dunes. Fragments of *Coxiella* sp., ostracodes, foraminifera and charophyte oogonia are occasionally incorporated. Medium to coarse-grained, moderately-sorted, skeletal peloidal sand, on the other hand, forms a beach along the southern margin of Lake Greenly where the source is a set of parabolic dunes proximal to the lake basin. In contrast, carbonate playa lakes associated with Lake Greenly are characterised by shorelines dominated by biogenic fragments including ostracode valves, *Coxiella* sp., foraminifera and minor charophyte oogonia. These are occasionally very weakly indurated. Beaches associated with Lake Malata, on the other hand, are dominated by coarse-grained gypsarenite and fragments of *Coxiella* sp.

A 3 m-high foredune along at the south-eastern margin of Lake Malata situated less than 200 m west of the Lake Malata ridge is of particular interest (Fig. 7b) and has a maximum TL age of 1 ± 0.09 ka (Dutkiewicz & Prescott 1997; Table 1). It also hosts an undisturbed Aboriginal campsite comprising a stone grinding plate and scraping tools. The beach consists of medium to coarse-grained, moderately-sorted sand dominated by coarse to fine-grained, angular to well-rounded quartz, moderate amounts of

[2] Dutkiewicz, A. (1996) "Quaternary Palaeoclimate from Lake Malata Lake Greenly Playa Complex, South Australia" PhD thesis, The Flinders University of South Australia (Unpubl.)

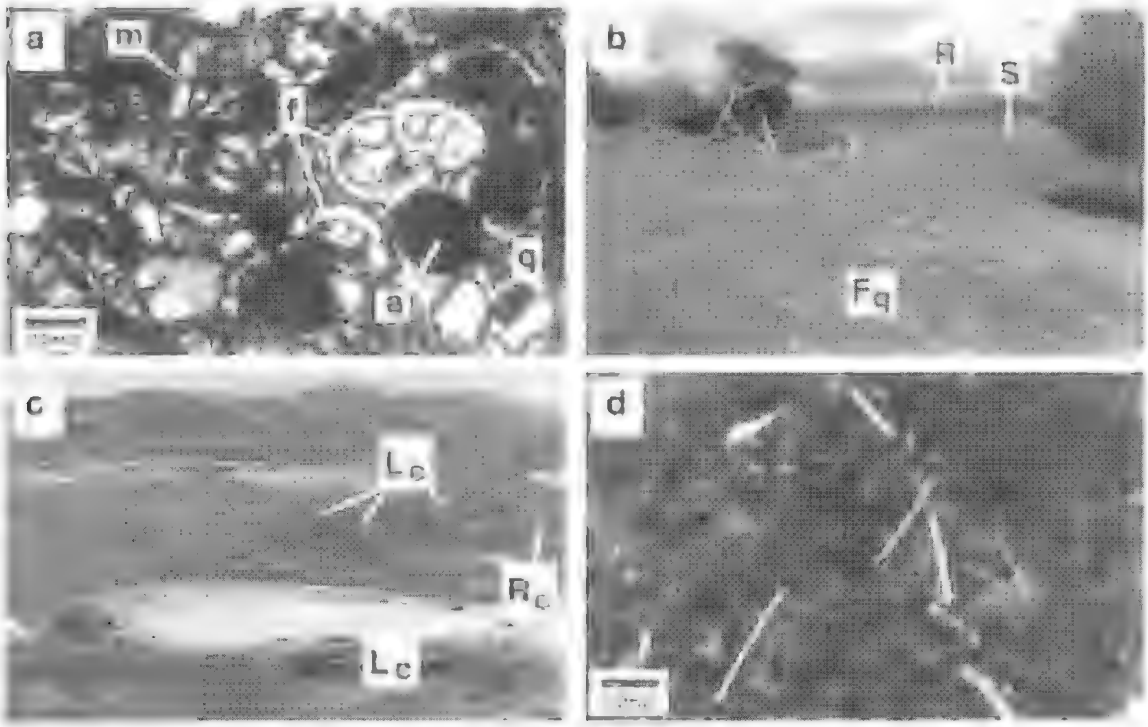

Fig. 7. (a) Thin-section photomicrographs of the skeletal peloidal grainstone comprising the Lake Malata Pleistocene ridge. The grainstone is composed of abundant fragmented (f), mollusc shell (m), calcareous red algal (a) and peloidal allochems. Quartz (q) is also present. The grainstone is strongly cemented by micrite. Polarised light. (b) 3 m-high quartz foredune (F_q) separated from the Lake Malata ridge (R) by an ephemeral seepage-spring zone (S) measuring approximately 150 m in width. The foredune has a maximum TL age of ~1 ka. Trees are approximately 2 m tall. (c) Aerial view of the eastern margin of Lake Greenly characterised by a prograding sequence of low lying carbonate pellet lunettes (L_c) and carbonate ridges (R_c). Centre of photograph spans 750 m. (d) Thin section photomicrograph of sediment comprising R_c (c). Composed of abundant ostracode fragments within a micritic matrix. Plane light.

medium-grained peloids, and fragments of *Cerithia* sp., ostracodes and foraminifera. Carbonate pellets with approximately 10% fine to medium-grained quartz sand are present at a depth of 1 m below the surface. Further south, the deposit grades into very coarse-grained and poorly sorted beach sand approximately 1 m above the present day lake level. The sand is dominated by fine to coarse-grained angular and occasionally iron-stained quartz and fragments of *Coxiella* sp. Moderate amounts of lithoclasts derived from skeletal peloidal grainstones and calcretes, minor amounts of peloids and feldspar, and trace amounts of charophyte oogonia and mica are also present. Here, the sand overlies a 1m-thick humic coquina layer dominated by fragments of *Coxiella* sp., minor amounts of quartz, and trace amounts of foraminifera, ostracodes, charophyte oogonia, peloids, mica and recent vegetation. This layer, in turn, overlies a strongly indurated skeletal peloidal grainstone which outcrops thinly along the margin of the lake.

The geomorphologic features along the eastern margin of Lake Greenly are strikingly different from those of Lake Malata. This is attributed mainly to the differences in basin morphologies, particularly the orientation of the long basin axis to the direction of the prevailing wind, the nature of the basin sediments, and the groundwater chemistry. The associated lunette-ridge system is low in relief and difficult to map but unmistakable when seen from air (Fig. 7c). In fact, mapping of the individual lunettes and ridges could only be achieved using aerial photography. In addition, exposed lunette sections are rare and lunettes appear to have formed a prograding sequence, sourced by episodic deflation within Lake Greenly. Unlike the prograding lunette sequence at Lake Malata, where individual lunettes are separated by deflationary basins, the Lake Greenly lunettes appear to be separated by a series of carbonate ridges. The ridges are very similar in hand specimen and in outcrop style to the indurated carbonate horizons associated with lunettes which makes the distinction of these features extremely difficult in the field.

The most easily recognised carbonate ridges occur proximal to the present-day northeastern lake margin, where four ridges representing four phases of lake regression have been recognised. The ridges are approximately 2 to 3 m above the present-day floor of Lake Greenly and form fractured and rubbly carbonate sheets. They lack the smooth and continuous arcuate outcrop style common to indurated carbonate horizons associated with lunettes. The crusts consist of low-Mg calcite and are chalky and friable, with a mm-thick coating of laminar calcrete. Tubular voids are abundant more so than in the indurated carbonate horizons associated with carbonate pellet lunettes and appear to be related to plant growth in relatively soft sediment. However, no fossil plant remains were found. Scanning electron microscope analysis of these crusts shows the presence of abundant, straight or gently curved, occasionally branching, ~ 5 μm-thick calcite encrusted endolithic fragments. The morphology and size of these filaments are consistent with fungal structures described by Klappa (1979) and indicate pedogenesis in the subaerial vadose environment. In thin-section, the crusts consist of micrite, which occasionally displays a globular texture and abundant, generally randomly-oriented, calcitic shell fragments which comprise 5 to 15% of the total sediment (Fig. 7d). The shell fragments consist of low-Mg calcite and are generally straight or gently curved, approximately 10 μm in diameter and generally 1 to 2 mm in length and most likely represent disarticulated ostracode valves. Foraminiferal fragments are rare. The deposits have not been dated due to the paucity of suitable materials such as organic matter and quartz.

Discussion

The Late Quaternary geomorphology in the Lake Malata-Lake Greenly Complex is represented by a complex suite of ridges, lunettes and foredunes which have been dated between 320 ka and 1 ka. The period covers a time of dramatic climatic oscillations during which the formation of the lake complex was initiated and the lakes experienced a major lacustral (wet) phase followed by a series of drying and deflationary episodes punctuated by periods of pedogenesis and relatively minor lacustral events. Oscillations between these climatic extremes culminated in the present-day status of the lakes as groundwater-discharge playas.

Wet phase ca. 320 ka

The main lacustral phase is represented by the *ca* 320 ka (Oxygen Isotope Stage 9; Fig. 8) Lake Malata beach ridge (Figs 2 and 6) deposited during a phase of high lake level. Its morphology is consistent with foredune deposition and we envisage that it formed by deflation of sand from wave-nourished lakeshore beaches in very much the same manner that coastal foredunes and foredune ridges are built immediately behind zones of beach swash. Prior to stabilisation of the surrounding sub-parabolic dunes, a large amount of the skeletal peloidal sand was blown and washed into the lake basin and subsequently reworked by wind-generated waves during a pluvial climatic phase. A combination of relatively lower than present evaporation rates, highly effective precipitation, increased runoff and recharge and high water tables, associated with an interglacial sea-level highstand, would have resulted in the accumulation of relatively fresh water within the lake basin. The size of the ridge suggests that at least 1 m of water was present in the lake basin during the wet winter months, which would have been characterised by higher rainfall and lower evaporation relative to present. Such a relatively high lake level, combined with strong north-westerly winds associated with the winter months, would have initiated wave-generated currents capable of moving large volumes of the skeletal peloidal sand as bedload towards the eastern, and particularly the south-eastern lake margin where the ridge attains its maximum width. Under these conditions the sand accreted on the eastern lakeshore of Lake Malata as a beach deposit and was subsequently deflated by strong south-westerly winds into a foredune immediately behind this high-energy beach. The height of the beach ridge attests to the fact that this period was relatively long-lived, characterised by enhanced seasonality and a large and continuous sediment supply. The ridge was eventually stabilised by pedogenesis and vegetation during an extended period of non-deposition. That only one such feature is present within the Lake Malata-Lake Greenly Complex indicates a unique depositional episode. The absence of a similar foredune ridge along the eastern margin of Lake Greenly may be attributed not only to a lack of sediment supply, but also to the basin morphology, particularly the orientation of the long axis to the direction of the prevailing westerly wind. The Lake Greenly basin is oriented approximately at 45° to the direction of the prevailing westerly wind, while the Lake Malata axis lies at 90°.

Consequently, the ridge represents a Pleistocene "megalake" or "lacustral" stage (*sensu* Bowler 1980, 1981; De Deckker 1988) in the evolution of the lake basin and overlaps with Wilson's (1991) Phase III deposition of Bridgewater Formation dunes during mid to late Pleistocene interglacial sea-level highstands. Megalake shorelines, such as a 13.5 m high beach at Lake Tyrrell, contain abundant shells of *Coxiella* sp. (Macumber 1980; Bowler &

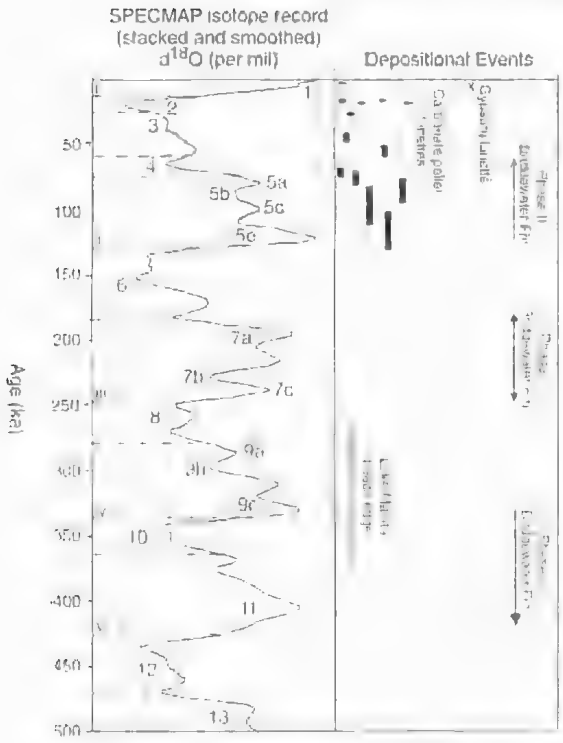

Fig. 8. Ages of major geomorphologic features in the Lake Greenly-Lake Malata complex plotted against the SPECMAP curve (Imbrie *et al.* 1989; McIntyre *et al.* 1989). Ages of the isotope stages 1 to 6 after Martinson et al. (1987). Ages for the deposition of the Bridgewater Formation after Wilson (1991). Roman numerals denote glacial terminations. The length of each bar indicates uncertainty in measurement of the age of lunette/ridge (see Table 1 for detail).

Teller 1986). Curiously, there is a lack of lacustrine fauna (fresh and saline water-tolerant) within the beach ridge grainstone and equivalent sediments in the basin. Possible explanations for this are: 1) post-depositional dissolution of organisms caused by a change in the physical and chemical environments; 2) destruction of shells during high energy transport rendering them unrecognisable in the sediment record; and 3) the high-energy, sandy lake basin may have been unsuitable for lacustrine organisms.

Formation of the ridge may have commenced considerably earlier than 320 ka, which marks the waning stages of deposition from the lee side of the ridge. Wilson (1991)[1] proposed that the emplacement of the Bridgewater Formation dunes along the west coast of the Eyre Peninsula occurred during sea-level highstands as early as 700 ka (onset of Oxygen Isotope Stage 17). Therefore, it is likely that ridge accretion also occurred episodically throughout Oxygen Isotope Stages 17 to 7 and Stage 5 interglacials (Fig. 8), until the sediment supply was exhausted and recharge rates decreased due to a fall in eustatic sea-level, giving rise to a new depositional regime in the Lake Malata-Lake Greenly Complex. A comprehensively dated sequence through the Lake Malata ridge could potentially provide palaeoclimatic information prior to 320 ka.

Palaeoclimate ca. 320-115 ka

We have no direct record of sedimentation and evolution of the lake system for the period 320-115 ka. As mentioned earlier, the Lake Malata ridge may have continued accreting intermittently during pluvial episodes, particularly during Oxygen Isotope Stage 7 until ~ 180 ka, when the emplacement of Phase II dunes along the west coast of the Eyre Peninsula was most intense (Wilson 1991)[1]. The morphology and pedogenic alteration of sub-parabolic dunes overlying thick carbonate sequences south of Lake Greenly (Dutkiewicz 1996)[2] are consistent with a later episode of Wilson's (1991)[1] Phase II dune emplacement during the last interglacial (Stage 5; Fig. 8). This suggests that deposition of lacustrine carbonates most likely occurred prior to and intermittently during the warm interstadials of Oxygen Isotope Stage 6 and during the warm intervals of the last interglacial (Oxygen Isotope Sub-stage 5e). Landward migrating sub-parabolic dunes would have buried regions relatively close to the coast, whereas more distal areas, such as Lake Malata, would have been subject to continued carbonate precipitation. Large volumes of this mud are likely to have been deflated into lunettes during Oxygen Isotope Stage 6, which is broadly similar to stages 4, 3 and 2 during which lunette deposition was pervasive. Further sampling and dating is required to decipher the palaeoclimate record during this period.

Multiple Arid Episodes ca. 115-10 ka

Lunettes form by deflation of sand-sized material, which commonly includes pelletised clays derived from a drying lake floor by uni-directional wind (Bowler 1973; 1980; 1983). Factors involved in the construction of clay pellet lunettes (fluctuating groundwater levels, uni-directional wind, aridity) have been discussed extensively by Bowler (1973) and the same explanation can be applied to the carbonate pellet lunettes from the Lake Malata-Lake Greenly Complex. The ages of the lunettes indicate that seasonally arid climates and intense prevailing westerly winds in southern Australia occurred several times since the last interglacial. Although the TL ages are not sufficiently precise to date the exact onset of each arid episode, at the very least they indicate the time when lunette building was in full

swing. In general, these correlate with periods of relatively low eustatic sea-level and oscillations to cold intervals, many of which had not previously been associated with continental aridity and lunette building. The oldest lunette horizon dated *ca.* 115 ka corresponds to the last glacial inception and termination of the last interglacial (Oxygen Isotope Sub-stage 5d). Aeolian activity increased again at *ca.* 96 ka (Oxygen Isotope Sub-stage 5c), 85 ka (cold Sub-stage 5b), and 75 ka and 70 ka (Sub-stages 5a/4). Significantly, a strongly-indurated pedogenic horizon dated at *ca.* 75 ka suggests that the lunette material was most likely modified soon after the shift from stage 5 to 4 which globally marks the main glacial transition. Similar periods of deflation and pedogenesis are estimated to have occurred around 90 ka and before about 70 ka in the Madigan Gulf at Lake Eyre (Magee *et al.* 1995). Lunette-building in the Lake Malata-Lake Greenly complex occurred twice during the interstadial of stage 3 with maximum aeolian activity centred around the two cold stadials ca. 54 ka and 43 ka immediately following the end of the main glacial transition. These ages likely correspond to the 60-50 ka playa deflation phase and dune building at Lake Eyre (Magee & Miller 1998). Unlike Lake Eyre, however, there is no evidence at Lake Malata or Lake Greenly for a major lacustral phase in the period 50-35 ka (Magee & Miller 1998). However, further excavation work is required to test whether a beach deposit of this age might be buried beneath younger aeolian sediments.

Several lunettes in the lake system dated at *ca.* 18 ka, 17 ka and 16 ka, cluster on Oxygen Isotope Stage 2, which marks the peak of the last glaciation for the Australian continent around 20 and 17 ka (e.g., Bowler 1986; Colhoun 1991). The age of the oldest lunette near this cluster dated at ca. 26 ka corresponds to the transition between Oxygen Isotope Stage 3 and Stage 2, indicating that the onset of arid conditions and lunette-building during the last glacial maximum commenced as early as 26 ka in this part of Australia. This corresponds to a general decrease in the number of high and intermediate lakes in Australia after 26 ka (Harrison 1993) and the onset of a dry-lake phase around 30 ka at Lake Eyre (Magee & Miller 1998). Aeolian activity appears to have peaked ca. 17.5-16 ka, which correlates well with the Last Glacial Maximum at 17.9 ka (Martinson *et al.* 1987). During this glacial period the sea level was at its lowest and the climate experienced intensified aridity and high westerly wind speeds (Bowler & Wasson 1984; Petit *et al.* 1990) conducive to pervasive dune-building over arid and semi-arid regions of Australia (Bowler & Wasson 1984; Wasson 1986). Lunette-building was in its waning stages ca. 16-15 ka, with local deposition still occurring locally until ca. 15.6 ka and was restricted to northern parts of the lake complex. Based on records from approximately 35 Australian lakes, Harrison and Dodson (1993) suggest a brief interval to wetter conditions during 15-13 ka, which is consistent with absence of lunette sequences at Lake Malata. These authors further propose that arid conditions persisted after the last glacial maximum culminating in maximum aridity at 12 ka, by which time most Australian lakes were dry. This would correspond to pedogenesis of Last Glacial Maximum lunettes in the lake complex.

Wet-arid cycles in the Holocene

Gypsum lunettes in the Lake Malata-Lake Greenly Complex have formed in two stages, in a slightly different manner to carbonate pellet lunettes. The gypsum first precipitated within the lake basin in association with groundwater oscillations and evaporation at the capillary fringe (Teller *et al.* 1982; Bowler & Teller 1986; Magee 1991). Although sand-sized discoids exposed during a dry period when the lake levels are low are easily deflated by prevailing winds, the similarity in grain-size and morphology of gypsum forming present-day beaches and the youngest lunettes at Lake Malata suggests that the most recent gypsum lunettes most likely formed by deflation of reworked material deposited at the lake margin during an earlier relatively higher lake level. Since surficial sediments in the Lake Malata basin are dominated by hemi-pyramidal gypsarenite, a combination of a thin skin of water and strong wind would provide an efficient mechanism for transporting and depositing the gypsum at the lake margin. Transportation by wave action is further supported by the presence of ripple marks on gypsarenite-dominated playa surfaces and by the abundance of biogenic fragments within the most recent deposits. The gypsum is subsequently deflated and sorted during a more arid period. Therefore, the gypsum lunettes most likely represent foredunes deposited under seasonally oscillating relatively high lake levels and relatively low lake levels in response to changing evaporation/inflow. Strong winds dominanted by a westerly component are required throughout the entire cycle of deposition and reworking. A single AMS-dated horizon from the middle of the lunette indicates that this process was well underway ca. 5,6 ka cal B.P. most likely coinciding with the Holocene sea-level highstand *ca.* 6.4 ka (Belperio *et al.* 2002). The mean annual precipitation at this time is estimated to have increased by 20-50% (Wasson & Donnelly 1991) with maximum lake levels recorded at most sites in Australia (Bowler 1981; Wasson & Donnelly 1991; Harrison 1993; Harrison & Dodson 1993).

Although gypsum lunettes have formed in the

relatively recent past at Lake Malata, this has not been the case at Lake Greenly. The reason for this is that at Lake Greenly gypsum occurs several decimetres below the lake surface beneath dolomitic carbonate muds (Dutkiewicz & von der Borch 1995). In this scenario, surficial carbonate would first have to be pelletised and deflated before interstitial gypsarenites are exposed to undergo reworking. Therefore, while gypsum lunettes were forming in the relatively recent past at Lake Malata, carbonate ridges were more likely to form concurrently at Lake Greenly. The complex system of lunettes and ridges at the eastern margin of Lake Greenly suggests that this may have been the case. The fragmented nature of the ostracode valves in the Lake Greenly ridges serves as an indication of reworking by wave action during relatively higher lake levels. The ridges constitute a prograding sequence formed by exposure of lacustrine carbonate mud under gradually regressing lake shorelines. The carbonate mud has undergone subsequent stabilisation by vegetation followed by pedogenesis and induration in the subaerial vadose environment. Consequently, these beach ridges are excellent indicators of the former lake extent and although undated may be concurrent with the formation of gypsum lunettes at Lake Malata.

The recent 3 m-high beach deposit (ML18, Fig. 2) at Lake Malata the remobilisation of which has been dated at ca. 1 1.93 ka (Dutkiewicz & Prescott 1997), represents a foredune formed by aeolian reworking of coarse beach sand. Aeolian deposition is supported by the finer grain-size and better sorting of the sand compared to other beach deposits of broadly similar composition, and by the presence of carbonate peloids. In particular, the coquina layer within the deposit is indicative of a lacustral period during which relatively high lake levels and lower salinities caused by increased precipitation and/or decreased evaporation rates would have allowed large numbers of *Coxiella* gastropods to inhabit Lake Malata. The orientation of the foredune along the south-eastern shoreline is consistent with the orientation of prevailing south-westerly winds, which operate during the dry summer months. Aeolian activity was generally high at this time and is further supported by the most recent lunette building episode in the Lake Malata region dated at ca. 1.2 ka (Dutkiewicz & Prescott 1997).

Acknowledgments

The Flinders University and the archaeometry special fund of the Physics Department, University of Adelaide, provided financial support for this study, which is based on PhD research carried out by A. Dutkiewicz. AMS dating was funded by AINSE Grants 93/127 AMS and 94/176 AMS. Chris von der Borch acknowledges the continuing support of the School of Physics, Chemistry and Earth Sciences at Flinders University. We are grateful to Martin Williams for his constructive comments on the manuscript.

References

BELPERIO, A. P., HARVEY, N. & BOURMAN, R. P. (2002) Spatial and temporal variability in the Holocene sea-level records of the South Australian coastline. *Sed. Geol.* **150**, 153-169.

BOWLER, J. M. (1971) Pleistocene salinities and climatic change: evidence from lakes and lunettes in southeastern Australia pp. 47-65 *In* Mulvaney, D. J. & Golson, J. (Eds) "Aboriginal Man and Environment in Australia" (ANU Press, Canberra).

_____ (1973) Clay dunes: their occurrence, formation and environmental significance. *Earth Sci. Rev.* **9**, 315-338.

_____ (1980) Quaternary chronology and palaeohydrology in the evolution of Mallee landscapes pp. 17-36. *In* Storrier, R. R. & Stennard, M. E. (Eds) "Aeolian Landscapes in the Semi-Arid Zone of South Eastern Australia" *Proceedings of the Australian Society of Soil Science Incorporated Conference, Riverina Branch, Mildura.*

_____ (1981) Australian salt lakes: a palaeohydrological approach. *Hydrobiologia* **82**, 431-444.

_____ (1983) Lunettes as indices of hydrologic change: a review of Australian evidence. *Proc. R. Soc. Vic.* **95**, 147-168.

_____ (1986) Spatial variability and hydrologic evolution of Australian lake basins: Analogue for Pleistocene hydrologic change and evaporite formation. *Palaeogeog. Palaeoclim. Palaeoecol.* **54**, 21-41.

_____ & MAGEE, J. W. (1988) Lake Frome: stratigraphy, facies analysis and evaluation of a giant playa pp. 4-6 *In* SLEADS Conference 88, "Salt Lakes in Arid Australia" Australian National University, Canberra.

_____ & TELLER, J. T. (1986) Quaternary evaporites and hydrologic changes, Lake Tyrrell, north-west Victoria. *Aust. J. Earth Sci.* **33**, 43-63.

_____ & WASSON, R. J. (1984) Glacial age environments of inland Australia pp. 183-208 *In* Vogel J. C. (Ed.) "Late Cainozoic Palaeoclimates of the Southern Hemisphere" (Balkema, Rotterdam).

CHEN, X.Y., BOWLER, J. M. & MAGEE, J. W. (1991) Aeolian landscapes in central Australia: Gypsiferous and quartz dune environments from Lake Amadeus, *Sedimentology* **38**, 519-538.

COLHOUN, E. A. (1991) Climate during the Last Glacial maximum in Australia and New Guinea. Australian and New Zealand Geomorphologic Group Special Publication No. 2.

DE DECKKER, P. (1988) Large Australian lakes during the last 20 million years: sites for petroleum source rock or metal ore deposition, or both? pp. 45-58 *In* Kelts, A.J. & Talbot, M.R. (Eds) "Lacustrine Petroleum Source Rocks" Geological Society Special Publication, No. 40.

DULKIEWICZ, A. & PRESCOTT, J. R. (1997) Thermoluminescence ages and palaeoclimate from the Lake Malata-Lake Greenly Complex, Eyre Peninsula, South Australia. *Quat. Sci. Rev.* **16**, 367-385.

_____, HERCZEG, A. L. & DIGHTON, J. C. (2000) Past changes in isotopic and solute balances in a continental playa: clues from stable isotopes of lacustrine carbonates. *Chem. Geol.* **165**, 309-329.

_____ & VON DER BORCH (1995) Lake Greenly, Eyre Peninsula, South Australia: sedimentology, palaeoclimatic and palaeohydrologic cycles. *Palaeogeog., Palaeoclim., Palaeoecol.* **113**, 43-56.

HARRISON, S. P., 1993. Late Quaternary lake-level changes and climates of Australia. *Quat. Sci. Rev.* **12**, 211-231.

_____ & DODSON, J. (1993) Climates of Australia and New Guinea since 18,000 yr B.P. pp. 265-293 *In* Wright H. E., Kutzbach, J. E., Jr., Webb III, T., Ruddiman, W. F. Street-Perrott, F. A. & Bartlein, P. J. (Eds) "Global Climates Since the Last Glacial Maximum" (University of Minnesota Press, Minnesota Minneapolis).

IMBRIE, J., MCINTYRE, A. & MIX, A. (1989) Oceanic Response to Orbital Forcing in the Late Quaternary: Observational and Experimental Strategies. pp. 121-164 *In* Berger, A., Schneider, S. H. & Duplessy, J.-C. (Eds) "Climate and the Geosciences" (Kluwer Academic Publishers, Boston, Massachusetts)

KLAPPA, C. F. (1979) Lichen stromatolites: criterion for subaerial exposure and a mechanism for the formation of laminar calcretes (caliche). *J. Sed. Pet.* **49**, 387-400.

MCINTYRE, A., RUDDIMAN, W. F., KARLIN, K. & MIX, A. C. (1989) Surface water response of the Equatorial Atlantic Ocean to orbital forcing. *Paleocean.* **4**, 19-55.

MACUMBER, P. G. (1980) The influence of groundwater discharge on the mallee landscape pp. 67-84 *In* Storrier, R.R. & Stennard, M.E. (Eds) "Aeolian Landscapes in the Semi-Arid Zone of South Eastern Australia" Proceedings of the Australian Society of Soil Science Incorporated, Conference, Mildura, Riverina Branch.

_____ (1991) Interactions Between Ground-water and Surface Systems in Northern Victoria. Department of Conservation and Environment, Australia.

MAGEE, J. W. (1991) Late Quaternary lacustrine, groundwater, aeolian and pedogenic gypsum in the Prungle Lakes, southeastern Australia. *Palaeogeog., Palaeoclim., Palaeoecol.* **84**, 3-42.

_____ & MILLER, G. H. (1995) Lake Eyre palaeohydrology from 60 ka to the present: beach ridges and glacial maximum aridity. *Ibid.* **144**, 307-329.

_____, BOWLER, J. M., MILLER, G. H., & WILLIAMS, D. L. G. (1995) Stratigraphy, sedimentology, chronology and palaeohydrology of Quaternary lacustrine deposits at Madigan Gulf, Lake Eyre, South Australia. *Ibid.* **113**, 3-12.

MARTINSON, D. G., PISIAS, N. G., HAYS, J. D., IMBRIE, J., MOORE, T. C. JR. & SHACKLETON, N. J. (1987) Age dating and orbital theory of ice ages: development of a high-resolution 0 to 300,000 years chronostratigraphy *Quat. Res.* **27**, 1-29.

MASON, I. M., GOZKOWSKA, M. A. J., RAPLEY, C. G. & STREET-PERROT, F. A. (1994) The response of lake levels and areas to climatic change. *Clim. Change* **27**, 161-197.

NETTERBERG, F. (1967) Some roadmaking properties of South African calcretes pp. 77-81 *In* Proceedings of 4th Regional Conference on Soil Mechanics and Foundation Engineering.

PETIT, J. R., MOLNIER, L., JOUZEL, J., KOROTKEVICH, Y. S., KOTLYAKOV., V. I. & LORIUS, C. (1990). Palaeoclimatological and chronological implications of the Vostok core dust record. *Nature* **343**, 56-58.

ROBO, X., GIRAFT, S., BURJACHS, E., COMPS, F. A., TENORIO, R. G. & JOLLY, R. (2002) High-resolution saline lake sediments as enhanced tools for relating proxy palaeolake records to recent climatic data series. *Sed. Geol.* **148**, 203-220.

STUIVER, M. & REIMER, P. J. (1993) Extended ^{14}C database and revised CALIB radiocarbon calibrating program. *Radiocarbon* **35**, 215-230.

_____, _____, BARD, E., BECK, J. W., BURR, G. S., HUGHEN, K. A., KROMER, B., MCCORMAC, F. G., v. d. PLICHT, J. & SPURK, M. (1989) INTCAL98 Radiocarbon age calibration 24,000-0 cal BP. *Radiocarbon* **40**, 1041-1083.

TELLER, J. T., BOWLER, J. M. & MACUMBER, P. G. (1982). Modern sedimentation in Lake Tyrrell, Victoria, Australia. *J. Geol. Soc. Aust.* **29**, 159-175.

WARREN, J. K. (1982) The hydrological setting, occurrence and significance of gypsum in late Quaternary salt lakes in Australia. *Sedimentology*, **29**, 609-637.

WASSON, R. J. (1986) Geomorphology and Quaternary history of the Australian continental dunefields. *Geog. Rev. Japan*, **59**, 55-67.

_____ & DONNELLY, T. H. (1991) Palaeoclimatic reconstructions for the last 30,000 years in Australia - A contribution to the prediction of future climate. CSIRO Division of Water Resources, Technical Memoir No 91/3, CSIRO, Canberra.

WILLIAMS, M. A. J., DE DECKKER, P., ADAMSON, D. A. & TALBOT, M. R. (1991). Episodic fluviatile and aeolian sedimentation in a late Quaternary desert margin system, central western New South Wales pp. 258-287 *In* Williams, M. A. J., De Deckker, P. & Kershaw, A. P. (Eds) "The Cainozoic of Australia: A Re-Appraisal of the Evidence" Geological Society of Australia Special Publication No.18.

WILLIAMS, M., DUNKERLEY, D., DE DECKKER, P., KERSHAW, P. & CHAPPELL, J. (1998) "Quaternary Environments" (Arnold, London)

SMALL SCALE SPATIAL DISTRIBUTION PATTERNS AND MONITORING STRATEGIES FOR THE INTRODUCED MARINE WORM, SABELLA SPALLANZANII (POLYCHAETA: SABELLIDAE)

By Craig A. Styan[*1] *& Joanna Strzelecki*[*2]

Summary

Styan, C. A. & Strzelecki, J. (2002) Small scale spatial distribution patterns and monitoring strategies for the introduced marine worm, Sabella spallanzanii (Polychaeta: Sabellidae). Trans. R. Soc. S. Aust. 126(2), 117-124, 29 November, 2002.

Spatial distribution patterns were determined for the introduced marine worm, Sabella spallanzanii (Gmelin), at Largs Bay, South Australia, as part of a study to determine the most efficient methods to survey these worms living on soft sediment habitats. Worms were patchy and, across a range of spatial scales, more likely to be found together than if they were randomly distributed. Average density varied among sites between 0 and nearly 10 worms m^{-2}.

Key Words: Sabella spallanzanii, introduced species, marine pest, survey, spatial pattern, distribution.

Transactions of the Royal Society of S. Aust. (2002), **126**(2), 117–124.

SMALL SCALE SPATIAL DISTRIBUTION PATTERNS AND MONITORING STRATEGIES FOR THE INTRODUCED MARINE WORM, *SABELLA SPALLANZANII* (POLYCHAETA: SABELLIDAE)

by Craig A. Styan[1] & Joanna Strzelecki[2]

Summary

Styan, C. A. & Strzelecki, J. (2002) Small scale spatial distribution patterns and monitoring strategies for the introduced marine worm, *Sabella spallanzanii* (Polychaeta: Sabellidae). *Trans. R. Soc. S. Aust.* **126**(2), 117–124, 29 November 2002.

Spatial distribution patterns were determined for the introduced marine worm, *Sabella spallanzanii* (Gmelin), at Largs Bay, South Australia, as part of a study to determine the most efficient methods to survey these worms living on soft-sediment habitats. Worms were patchy and, across a range of spatial scales, more likely to be found together than if they were randomly distributed. Average density varied among sites between 0 and nearly 10 worms m^{-2}. Four different sampling units were trialled to determine the most efficient for ongoing monitoring. We did not find strong evidence of counting bias among divers of different experience, but at some sites all divers may have underestimated the number of worms when using 0.25m^2 quadrats. Larger sampling units (25m x 1m and 5m x 1m transects) sampled area more quickly on a per m^2 basis, but 1m^2 quadrats were the most efficient sampling unit to survey worms within a site. At a larger (bay) scale, sampling unit size had little effect on the effort needed to reliably detect an increase in worm numbers; the number of sites sampled had a much greater influence on power once more than about 10 to 15 minutes were spent underwater at each site. A cost-effective plan for detecting (α=β=0.05) moderate increases (50%) in the abundance of *S. spallanzanii* at Largs Bay involves diver pairs sampling randomly within sites for 20 minutes per site, using 5m transects (6 per diver) or 25m transects (3 per diver), at ≥ 15 randomly located sites each time. A similar time underwater, sampling with 1m^2 quadrats (31 per diver), would have only slightly less power (0.91).

Key Words: *Sabella spallanzanii*, introduced species, marine pest, survey, spatial pattern, distribution.

Introduction

During mid 1990s, the European feather duster worm, *Sabella spallanzanii*, was detected in a number of marine areas across southern Australia. Presumably, its presence is the result of a recent introduction of the worm into Australian waters, perhaps inadvertently imported in the ballast water of trans-oceanic container ships (Andrew & Ward 1997; Patti & Gambi 2001). The large, up to 50 cm long, *S. spallanzanii* tends to form dense aggregations and, at least on small scales, can have serious impacts on subtidal sessile flora and fauna (Holloway & Keough 2002). Few known predators and life history traits including fast growth, extended spawning time and high fecundity (Currie *et al.* 2000; Giangrande *et al.* 2000) make plausible the possibility of large increases in local population sizes and rapid geographic spread of this marine pest.

In South Australia, *S. spallanzanii* have been found at West Lakes and the North Haven/Largs Bay areas off metropolitan Adelaide since at least 1993, and the worm now seems to be firmly established at these sites (C. Styan pers. obs.). They may have been in the Port River for several years longer (N. Holmes, Kinhill Engineers, pers. comm.). In South Australia and elsewhere, the worms are known to colonise a range of habitats, from reefs and man-made structures such as piers and marinas, to soft sediment habitats, including seagrass beds. Given the potential threat these worms pose, large scale monitoring programmes are needed, together with small scale manipulative experiments across a range of habitats, to understand properly the ecological effects of the worm as they spread. Before any monitoring programme can proceed, however, methods need to be developed to estimate accurately the abundance *S. spallanzanii* in the field. We focus here on determining efficient methods for monitoring worms on soft sediment habitats. These habitats are the most common in South Australian gulfs and so, because of their extent, could potentially harbour large numbers of worms. Other work will be needed to determine the most efficient methods for surveying worms in other habitats such as rocky reefs or marinas.

Determining the abundance of organisms underwater is not always a trivial task, even for relatively large, sessile organisms (e.g. Inglis & Lincoln Smith 1995; Benedetti-Cecchi *et al.* 1996).

Department of Environmental Biology, University of Adelaide, South Australia 5005, Australia.
[1] Present address: Centre for Research on Ecological Impacts of Coastal Cities, University of Sydney, NSW 2006, Australia.
Present address: Present address: CSIRO Marine Research, GPO Box 20, North Beach, WA 6020, Australia.

Workers have a wide range of survey techniques and sampling to choose from, but, unfortunately, often arbitrary choice about which methods are used can commonly lead to wasted effort and resources (Downing & Downing 1992). Obviously, planning is necessary for any underwater survey to ensure that, whilst effort and costs are minimised, surveys retain sufficient accuracy and statistical precision to allow confident interpretation of data (Andrew & Mapstone 1987; Underwood 1997). Such planning requires information about the relative cost and effort required per sample (and perhaps an evaluation of different sampling units), and information about the appropriate number of samples that need to be taken to generate desired levels of statistical precision and power. The number of samples required, in turn, depends on the way organisms are distributed spatially.

Information necessary for survey planning can sometimes be obtained from previous work, but no information was available about the distribution of *S. spallanzanii* on soft sediment habitats, typical of the gulfs in South Australia. So, in 1996 we conducted pilot surveys of *S. spallanzanii* in these habitats at a number of sites within Largs Bay, Gulf St Vincent. Our study had two specific aims. First, we wanted to determine how worms were distributed, on a range of spatial scales, and how this varied with abundance. Second, we wanted to determine the time taken to count worms, the relative magnitude of variance components between replicate samples at different spatial scales, and the differences in these found using a range of standard underwater sampling units (0.25m^2 and 1.0m^2 quadrats, 5m x 1m transects and 25m x 1m transects).

Counting even large organisms underwater is not always done equally well by divers with different experience (Inglis & Lincoln Smith 1995). Thus, there is a potential to bias results and/or increase variance estimates if multiple divers are used in surveys, making changes in abundance even more difficult to detect. We used a range of divers conducting these surveys, so we needed to determine whether having different divers involved surveying affected counts of worms. So before including data from each diver in the planning analyses, we also tested whether there was any evidence of bias in the total number of worms experienced and inexperienced divers counted in a survey, using randomization tests.

The overall aim of our work then, was to determine the most efficient technique to use for regular monitoring of the abundance of *S. spallanzanii* on soft sediment habitats.

Styan C.A. (1998) The reproductive ecology of the scallops *Chlamys tatiana* in South Australia. PhD Thesis. Department of Environmental Biology, University of Adelaide, South Australia (Unpubl.).

Methods

Location of surveys

We sampled at 6 sites within Largs Bay between February and November 1996. Largs Bay was chosen as our main field location for this work because we knew from previous work[1] that reasonable densities of *S. spallanzanii* were present. We also conducted some preliminary searching for *S. spallanzanii* at other locations; specifically, the areas surrounding jetties at Edithburgh and Ardrossan (Gulf St Vincent) and Wallaroo (Spencer Gulf). Those areas were searched because we considered that they were likely to be anchorage points for boating and shipping from Port Adelaide, and thus possible destinations of worms spread through hull fouling. Although a few individuals of the similar looking native feather duster worm, *Sabellastarte* sp. were found at all locations, no *S. spallanzanii* was found in 2 x 40 minute dives at any of these other locations.

Largs Bay is a shallow bay (4 to 8m deep), close to the Port River and several marinas, areas known to also support high numbers of *S. spallanzanii* on pylons and moorings (C.A. Styan pers. obs.). The substrate in Largs Bay is predominantly soft sediment, consisting of a mosaic of seagrass (*Posidonia* spp.) meadows; sand patches and patches of degraded seagrass, characterised by silty sediments. Common, large invertebrates in the area include razor fish (*Phaxas bicolor*), scallops (*Chlamys bifrons*), starfish (*Uniophora granifera*), whelks (*Pleuroploca australis*) and sea tulips (*Pyura spinifera*). General underwater visibility during the study was good and ranged between 5 and 15m.

Survey methods

Six sites within Largs Bay were haphazardly selected between 500m and 1500m offshore. At each site, two sets of tape measures were set out by divers to act as survey base lines. The direction of these base lines was haphazardly chosen (there was little current flow), with divers laying out the line as they swam in opposite directions from the anchor. One pair of divers worked along one each base line, with each diver independently placing randomly selected quadrat or transect starting points at pre-determined places along the line. Square quadrats and transects had one edge lying along, and transects ran perpendicular to, the base line. Divers used a 1m stick to define the transect width and counted worms as they rolled out a tape measure for the set distance. Each diver was based on opposite sides of the base line to minimise interference between divers.

On the first day of sampling (14/2/96), we set out only two 50m base lines at site 1. Four divers each measured ten 0.5 x 0.5m quadrats, then ten 1m x 1m

quadrats, then three to five 5m x 1m transects and then one to three 25m x 1m transects. The time taken to measure each of these sets of units (separately) was recorded for each diver. On subsequent days (at sites 2-5), two 200m base lines were laid out, and quadrats and transects were conducted as divers moved along the base line (i.e. sampling with different units was both spatially and temporally interspersed). On these days each diver counted ten 0.25m² quadrats, ten 1m² quadrats, five 5m transects and one 25m transect. The exception to this was on the final day of sampling (26/11/96; site 6) when only one 200m base line was laid and a single pair of divers conducted surveys.

Testing for diver bias

At each site our survey teams consisted of 3 experienced scientific divers (each with hundreds of hours of underwater work logged) and one inexperienced scientific diver (<15 hours underwater work). Before pooling divers' data, we tested whether divers might count worms differently. Individual divers changed between days/sites, but the mix (1 inexperienced: 3 experienced) did not change. Pairs of divers worked on separate base lines within sites, principally to prevent divers getting in each other's way, but also to increase the spatial spread of the sampling within a site. As a result, for each site there was the potential to make 2 sorts of dive experience comparisons between divers who were sampling the same area; between an experienced and an inexperienced diver on one base line, and between 2 experienced divers working on the other line (each for 0.25m², 1.0m² quadrats and 5m transects). However, we could not make these comparisons for a number of base lines where worms were absent or found in only a few samples.

We used a series of randomisation tests to compare the difference in total number of worms counted by the two divers on a base line with the distribution of differences between divers if the counts had instead been allocated randomly. This distribution was constructed with a simple macro in Excel, using the inbuilt random number generator to allocate the counts to divers in 1000 simulations. We tested the hypothesis that if there were a counting bias, one diver would count more worms in total than the other diver on the same base line, and differences as large as this (or larger) would be infrequent when counts were randomly allocated. We chose to run the randomisation tests rather than t-tests because the data were very skewed in most cases. The randomisation tests allowed us to make the comparison about sampling worms without first transforming the data or modifying the hypothesis accordingly.

Spatial distributions

To describe the spatial distribution of *S. spallanzanii* at a range of scales, and how it changed with population density we calculated Morisita's Indices at each site, for each of the different sized sampling units. Morisita's Index (I_M) describes how much more likely it is that two individuals drawn at random will have come from the same sampling unit than if the population had been randomly dispersed. For example, an index of 1.5 means that individuals are 50% more likely to have come from the same quadrat or transect than if the population had been randomly dispersed (Hurlburt 1990).

The formula for I_M is:

$$I_M = \left(\frac{\sum X}{\sum X - 1}\right)\left(\frac{1}{\mu^2}\right)\left(\frac{\sigma^2}{\mu} + \mu - 1\right)$$

(Morisita 1971)

Where X is the number of samples, μ is the sample mean and σ^2 is the sample variance. Because I_M is essentially a variance to mean ratio, the null hypothesis that $I_M = 1.0$ can be tested, based on the χ^2 distribution with (n-1) degrees of freedom (Hurlburt 1990). We calculated I_M for each of the sample unit sizes at each site, pooling data from divers and baselines within each.

Power calculations & cost-efficiency

Power calculations were done in Excel (using the PiFace add-in to calculate non-central F-distributions; R. Lenth, University of Iowa) for a simple sampling design where equal time was spent by two divers working underwater, before or after a time interval over which worm numbers might have changed. Time (before and after) was treated as a fixed factor in our analyses. Using measured estimates of the average time taken per sample unit to determine the number of samples that could be taken for a given time underwater, and expected variance associated with each sample unit, we calculated either the size of an increase in mean abundance that pairs of divers could detect, or the time taken for pairs to detect a given sized change, both with $\alpha=\beta=0.05$ (Underwood 1997). These calculations were done with respect to monitoring designed to detect changes on 2 spatial scales: 1) within a single, fixed site and 2) across the entire Largs Bay area. We set $\alpha=\beta=0.05$ because we were equally concerned about type I and II errors, and wanted a low probability of incurring either (Mapstone 1995).

Within a single fixed site, statistical power to detect a change through time will be determined by the variance among sample units within that site (and the number of samples taken). Using the variances

associated with each site, we did the power calculations for each site and sample unit combination separately. Times needed at a site per period to detect a 50% increase in worm abundance (with $\alpha=\beta=0.05$) were log-transformed before averaging and back-transformation. Similarly, we did the power calculations for each sample unit using two other estimates of the variance within sites, each averaged across sites (but both calculated slightly differently). The first mean variance estimate was generated from an hierarchical ANOVA across sites 2-5 (see below), the second calculated after averaging the coefficients of variation from all 6 sites.

On a larger (bay) scale, statistical power to detect a change through time will be determined by the variance in the mean abundance of worms among sites, and the number of sites sampled in each time period; i.e. the test denominator MS will be a combination of variance within sites (among sampling units) and variance among sites in the mean density of worms. The magnitude of these variance components can be determined from the mean square estimates in an hierarchical ANOVA (Underwood 1997; see also Table 1). Our sites were in effect randomly chosen within Largs Bay and, despite data not really meeting assumptions (they were very skewed), we ran ANOVAs on the raw data to determine the magnitude of the among and within site mean squares estimates, and hence the size of the individual variance components. We did the ANOVA only on the 4 sites where we had balanced data and equal numbers of samples in each site (sites 2-5). Using these variance component estimates, we were able to generate the expected denominator MS for the test of an increase between times across Largs Bay, under a range of scenarios (varying the number of sites sampled and time spent sampling per site), and for each of the different size sampling units.

Results

At Largs Bay *S. spallanzanii* were patchy on a number of spatial scales. We found quite large differences among sites in the abundance of worms (Fig. 1). Worms were quite common at some sites, for example average density was nearly 10 worms m^{-2} at site 2, but worms were virtually absent at others (e.g. site 3). The highest densities measured in single sample units were 52 and 49 worms m^{-2} at site 2, in a 5m transect and a $1m^2$ quadrat, respectively. Within each site, and across each sample unit size, the distribution of worms within sampling units was very skewed, with many units not containing any worms at all (Fig. 2).

We found little evidence of bias in the numbers of worms that different divers counted within baselines. For $0.25m^2$ quadrats, none of the four randomisation tests between experienced divers, nor the test between an inexperienced and an experienced diver was significant at the $p=0.05$ level. Similarly, none of the four randomisation tests between experienced divers, or the one test between an inexperienced and an experienced divers was significant for the $1m^2$ quadrats. None of the four tests between experienced divers was significant for the 5m transects, but one of two tests between inexperienced/experienced divers was significant ($p=0.035$) for the 5m transects. However, we might expect nearly one significant test (at $\alpha=0.05$), even if the null hypothesis was true, given the overall number (16) of these tests we conducted.

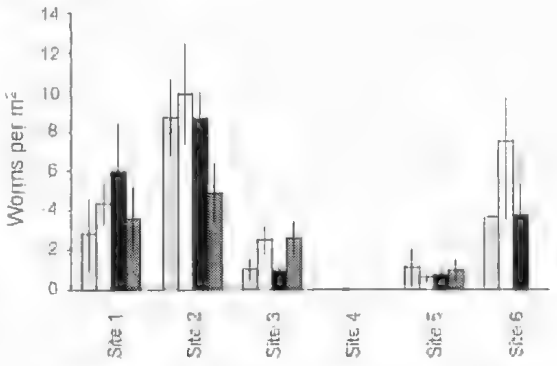

Fig. 1. Mean density (±S.E.) of *S. spallanzani* at anchoring sites within Largs Bay. At each site, density estimates using different sampling units are shown separately, pooling estimates from divers: 25m transects (grey bars); 5m transects (white bars); $1m^2$ quadrats (black bars); $0.25m^2$ quadrats (diagonal striped bars).

TABLE 1. *Estimates of variance components within and among anchoring sites (2-5) at Largs Bay following ANOVA, using 3 different sized sampling units.*

Sampling unit	Source	d.f.	Mean Square	
25m transect	Among Sites	3	$39929 = \sigma^2_{within} + 4\sigma^2_{among}$	($\sigma^2_{among} = 9187.4$)
($\mu = 70.0$)	Within Sites	12	$3179.3 = \sigma^2_{within}$	
5m transect	Among Sites	3	$10302 = \sigma^2_{within} + 20\sigma^2_{among}$	($\sigma^2_{among} = 468.3$)
($\mu = 16.4$)	Within Sites	76	$936.6 = \sigma^2_{within}$	
1m² quadrat	Among Sites	3	$656.71 = \sigma^2_{within} + 40\sigma^2_{among}$	($\sigma^2_{among} = 15.65$)
($\mu = 2.60$)	Within Sites	156	$30.64 = \sigma^2_{within}$	

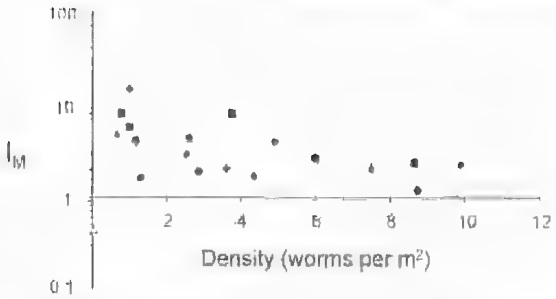

Fig. 2. Spatial distribution of *S. spallanzanii* at a range of spatial scales within anchoring sites, and how this varies with population density. 25m transects (circles); 5m transects (triangles); 1m² quadrats (squares); 0.25m² quadrats (diamonds). Morisita's (1971) index (I_M) values significantly different from 1.0 (at $p = 0.05$) are shown as filled symbols; the one non significant value is shown unfilled.

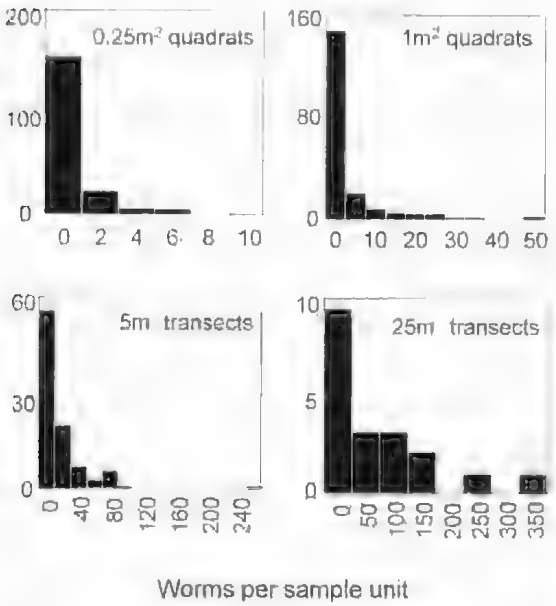

Fig. 3. Frequency histograms of the number of *S. spallanzanii* per sampling unit, pooling across anchoring sites.

We did not compare estimates of density among sites or sampling units because of very unequal numbers of samples, very heterogeneous variances among sample unit sizes (and sites), and skewed distributions, with large numbers of zeros in the data (Fig. 2). However, we did note that at two sites (2 and 6) where worms were relatively abundant, estimates of average density made with the 0.25m² quadrat seemed to be less than those made with the other sampling units (Fig. 1), perhaps indicating bias (across all divers). For this reason, we did not consider 0.25 m² quadrats in the power calculations. Variance component estimates following the ANOVA are shown in Table 1.

Figure 3 also illustrates the patchiness of worms, but at a range of intermediate (within site) scales. As worms became more abundant, there appeared to be some decrease in patchiness across all of the (within site) scales, but worms nonetheless were still significantly more likely to be found together than if they had been randomly distributed. Worms were quite patchy on larger (within site) scales, with I_M values significantly greater than 1.0 at the 5m and 25m transect scales (Fig. 3). Additional patchiness at smaller scales was reflected in the even higher I_M values for the 0.25m² and 1.0m² quadrats, which incorporated variation at larger scales and variation at small scales. Only one I_M index (for 0.25 m² quadrats, at very low density) was detected as not being significantly greater than 1.0. At small scales, *S. spallanzanii* were clearly arranged in distinct clumps, with 10s of worms sometimes attached to the same small piece of (rare) hard substratum such as a *Pinna* shell. Quite often, however, we also found clumps of worms that did not appear to be attached to any hard substrata, and which appeared to be firmly rooted in the soft sediments.

Fig. 4 shows the average time taken to sample each unit at the first site, for the range of sampling units we tested. As expected, 25m transects took much longer (mean time=363 sec) than 5m transects (173.4 sec), that took longer than 1m (37.8 sec) and 0.5m quadrats (33 sec). Clearly, larger sampling units took less long to count on a per m² basis than smaller sampling units. Error bars on Fig. 4 illustrate the range of per unit times we found among the divers that conducted our surveys. For each sample unit, the slowest diver was the inexperienced one, but the fastest varied among the experienced divers (one was faster at quadrats, another at transects). Fig. 4 also illustrates the decrease in the average coefficient of variation with increasing sample unit area.

Within a site, power calculations based on the average coefficient of variation across sites found that for a given time sampling underwater, 1m² quadrats provided a more powerful sampling technique than the other sampling units (Fig. 5). The finding that 1m² quadrats were more powerful than 5m or 25m transects was also found when we used the (overall) within sites variance estimates (i.e. from the ANOVA of sites 2-5; see Table 1 and below). When the power calculations were done separately for each site (i.e. across the range of population densities illustrated in Fig. 2), using the specific variance estimate found for each site, we generally found the same result. Whilst the level and the difference in power between units varied with site, in four out of five cases, the 1m² quadrats were the most powerful technique. In the fifth, 5m transects

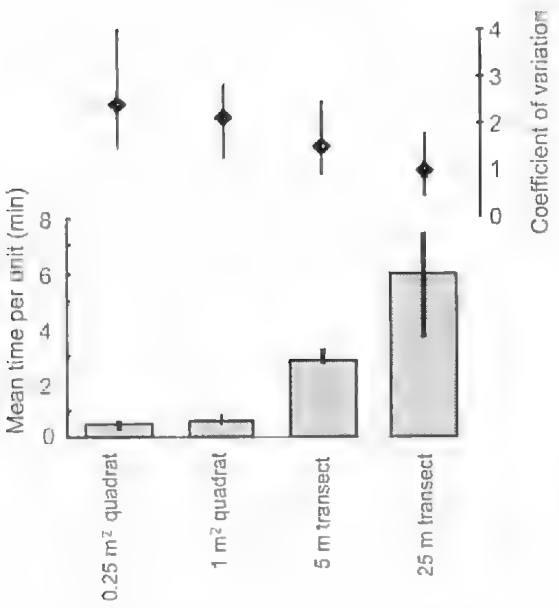

Fig. 4. Average of mean time taken to count *S. spallanzanii* per unit (averaged across n=4 divers), contrasted with the average coefficient of variation within anchoring sites (across 6 sites), for the 4 different sized sampling units. Vertical lines indicate the range of values (maximum to minimum) for both measures.

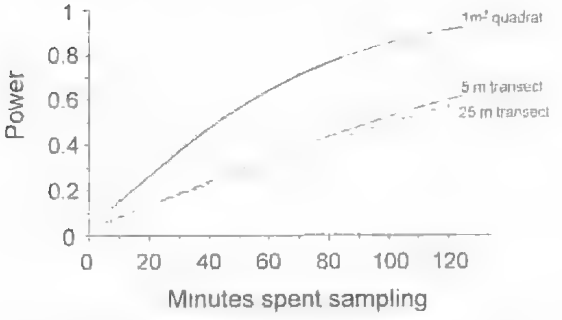

Fig. 5. Statistical power of different sampling units to measure a 50% increase in the mean abundance of *S. spallanzanii* within an anchoring site between 2 periods, given the effort (time) 2 divers spend sampling underwater in each period. The calculation of each power curve takes into account the number of samples that can be sampled by 2 divers in each period using a particular sample unit, and the mean coefficient of variation using that unit. (α=0.05).

were more powerful, but 1m² quadrats were very nearly as powerful for any given effort and the C.V. for 5m transects was based on only four samples. Across all the locations we sampled, we estimated that a pair of divers using 1m² quadrats would, on average, need to sample a site for 128 min (range=50 - 266 min), at both times, to detect a 50% increase in abundance through time (α=β=0.05) at that site. Equally powerful surveys using 5m or 25m transects would, on average, necessitate nearly twice as much time underwater (averages=240 or 248 min respectively).

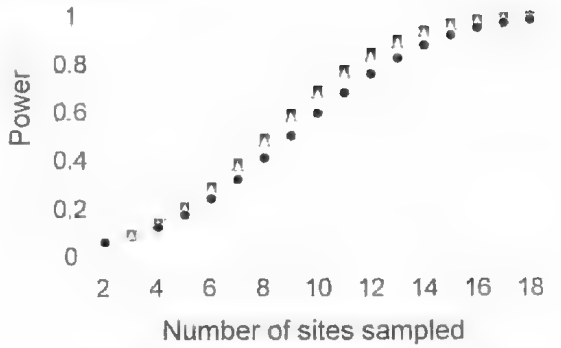

Fig. 6. Effect of sample unit on the statistical power to detect a 50% increase in the mean abundance of *S. spallanzanii* within Largs Bay, between 2 periods, with the number of randomly located sites visited per period. A pair of divers spend 20 min sampling in each site using either 1m² quadrats (circles), 5m transects (squares) or 25m transects (triangles). (α=0.05).

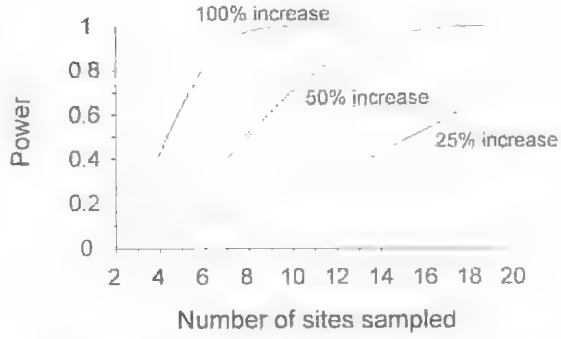

Fig. 7. Power to detect varying increases in the mean abundance of *S. spallanzanii* within Largs Bay, between 2 periods, with the number of randomly located sites visited per period. A pair of divers spend 20 min sampling in each site using 5m transects. (α=0.05).

At the scale of across Largs Bay, sampling unit size had little effect on the number of sites required to reliably detect an increase in worm abundance (Fig. 6). Moreover, the time spent in each site had very little effect on power, once 10-15 minutes had been spent in each site (i.e. once the number of sample units for each diver was >two). We did not illustrate the effect of time per site here, because the results for even short dives (e.g. 20 minutes sampling) were trivial. Our calculations found that the best way to detect a moderate (50%) increase in the abundance

of *S. spallanzanii* across Largs Bay would be to have diver pairs sampling randomly within sites for a minimal time greater than 15 minutes (say, about 20 min per site), using 5m transects (6 per diver) or 25m transects (3 per diver), at ≥ 15 randomly located sites each time. A similar sampling scheme using 1m² quadrats (31 per diver) would have only slightly less power (0.91). The power to detect increases, given the number of sites each sampled by a pair of divers for 20 minutes per period, is illustrated in Fig. 7. Increases of 25% or less are difficult to detect without very large numbers of sites being sampled. More moderate increases (>50%) should be much easier to detect.

Discussion

Sabella spallanzanii living on soft sediment habitats at Largs Bay were patchy on a range of spatial scales. Worms were found in small, tight clumps, and then there were patches of these at larger scales within sites, and large variation in overall abundance between sites separated by 100s to 1000s of metres. Whatever the underlying biological or physical causes of the distribution of *S. spallanzanii* on soft sediment habitats, our work has illustrated that, depending on the spatial scale of monitoring, this spatial patchiness can influence the decision about which sort of sampling unit should be used to measure changes in worm abundance.

We found that 1m² quadrats were clearly the most efficient sampling unit for estimating worm abundance within a site. This was despite our finding that 25m transects (and 5m transects) were much faster to conduct per m² of seafloor surveyed. Essentially, the trade-off here between sampling fewer places along a base line with larger sampling units (but sampling each of these places more precisely) and sampling more places (but each less precisely) with a smaller unit, favoured the latter. Whilst transects cover more area on a small scale relatively quickly, the extra effort expended counting along a transect would be better expended sampling more, randomly determined, positions within a site (10s to 100s of metres away), with a smaller sampling unit. Thus, we conclude that if precise estimates of worm abundance are needed on smaller, site scales, then 1m² quadrats should be used as a sampling unit. If estimates of worm abundance are needed on this scale then the use of 1m² quadrats can lead to substantial savings in effort and/or increases in precision, relative to monitoring with 5m or 25m transects.

In contrast, we found that when monitoring for changes at larger scales, statistical power will depend essentially only on how many sites are sampled. For monitoring across Largs Bay, the choice of sampling unit between quadrats or transects will be unimportant because, for a given sampling effort, the differences in power between different sized sampling units were less than the increase (or decrease) in power if one more (or less) site were sampled. We also found that, provided a reasonable amount of time was spent at each site (at least 15 minutes), the time spent per site had only a small effect on the overall power of a monitoring programme. Thus, the power of any monitoring programme for these worms can effectively only increase through sampling more sites. Consequently, we recommend that time spent per site is minimised to about 20 minutes per site (=15 minutes, plus a few extra to ensure at least several counts are taken within a site) and that effort is put into sampling more sites (at least 15) rather than sampling sites more intensively.

We did not find strong evidence of differences in the number of worms counted among divers, but divers' experience did influence the time it took them to count worms. Having more experienced divers in a survey team might speed up monitoring, but including inexperienced divers in surveys as well should not seriously bias abundance estimates or make surveys less powerful. We did uncover some evidence that, at least on soft sediment habitats and for moderate worm densities, all divers may underestimate worm abundance with 0.25m² quadrats. As a result, we would recommend against the use of 0.25m² quadrats as a sampling unit in future monitoring programmes, at least on soft sediment habitats. Of course, recommendations about optimal sampling units and strategies depend on the habitat being surveyed, and the spatial distribution of worms at a range of scales within the scale of interest. So, on hard substrata where worms are often found at much higher densities and perhaps not as patchy, we predict that smaller (<0.25m²) quadrats may be more effective, though this will need further testing.

Our finding that using a particular sampling unit to sample worms can, in some situations, lead to much more powerful surveys for a given effort is not particularly novel. Indeed, an expectation that we might find this was the basis for doing this work in the first place (e.g. Andrew & Mapstone 1987; Underwood 1997). Nor is our finding that broader scale surveys here are more influenced by the number of sites sampled, rather than the precision of sampling within each site, very surprising: especially given the large inter-site variation in worm abundance. We note that these specific results are, however, entirely dependent on the spatial distributions of *S. spallanzanii* at Largs Bay, and the trade-off between precision and effort required for various sampling units. For other species or even

S. spallanzanii in other habitats such as on piers or marinas, the spatial distribution patterns and trade-offs may be different and so, consequentially, might the recommendations for surveys (Andrew & Mapstone 1987; Underwood 1997). The only real way to find out how to best survey for other circumstances is to conduct a preliminary study (similar to this one) for those circumstances; this is an often repeated, but apparently seldom heeded, call (Underwood 1997).

Acknowledgments

We wish to thank Andrew Melville, Emma Cronin, Rebecca Fisher and Ian Magraith for help with field sampling. Alan Butler, David Williams and Piers Brissenden helped with the logistics of this work. We gratefully acknowledge the support of the South Australian Department of Environment and Natural Resources, through the Marine Environment Protection Fund programme.

References

Andrew, J. & Ward, R. D. (1997) Allozyme variation in the marine fanworm *Sabella spallanzanii*: comparison of native European and introduced Australian populations. *Mar. Ecol. Prog. Ser.* **152**, 131-143.

Andrew, N. L. & Mapstone, B. D. (1987) Sampling and the description of spatial pattern in marine ecology. *Oceanogr. Mar. Biol. Ann. Rev.* **25**, 39-90.

Benedetti-Cecchi, L., Airoldi, L., Abbiati, M. & Cinelli, F. (1996) Estimating abundance of benthic invertebrates: a comparison of procedures and variability between observers. *Mar. Ecol. Prog. Ser.* **138**, 93-101.

Currie, D. R., McArthur, M. A. & Cohen, B. F. (2000) Reproduction and distribution of the invasive European fanworm *Sabella spallanzanii* (Polychaeta: Sabellidae) in Port Phillip Bay, Victoria, Australia. *Mar. Biol.* **136**, 645-656.

Downing, J. A. & Downing, W. L. (1992) Spatial aggregation, precision, and power in surveys of freshwater mussel populations. *Can. J. Fish. Aquat. Sci.* **49**, 985-991.

Giangrande, A., Licciano, M. & Pagliara, P. (2000) Gametogenesis and larval development in *Sabella spallanzanii* (Polychaeta: Sabellidae) from the Mediterranean Sea. *Mar. Biol.* **136**, 847-861.

Holloway, M. G. & Keough M. J. (2002) Effects of an introduced polychaete, *Sabella spallanzanii* on the development of epifaunal assemblages. *Mar. Ecol. Prog. Ser.* **236**, 137-154.

Hurlburt, S. H. (1990) Spatial distribution of the montane unicorn. *Oikos* **58**, 257-271.

Inglis, G. J. & Lincoln Smith, M. P. (1995) An examination of observer bias as a source of error in surveys of seagrass shoots. *Aust. J. Ecol.* **20**, 273-281.

Mapstone, B. D. (1995) Scalable decision rules for environmental-impact studies - effect size, type-I, and type-II errors. *Ecol. Appl.* **5**, 401-410.

Morisita, M. (1971) Composition of the I-index. *Res. Pop. Ecol.* **13**, 1-27.

Patti, F. P. & Gambi, M. C. (2001) Phylogeography of the invasive polychaete *Sabella spallanzanii* (Sabellidae) based on the nucleotide sequence of internal transcribed spacer 2 (ITS2) of nuclear DNA. *Mar. Ecol. Prog. Ser.* **215**, 169-177.

Underwood, A. J. (1987) "Experiments in ecology. Their logical design and interpretation using analysis of variance" (Cambridge University Press, Cambridge, UK).

FIRST RECORDS OF TWO FAMILIES OF FRESHWATER AMPHIPODA (COROPHIIDAE, PERTHIIDAE) FROM SOUTH AUSTRALIA

BRIEF COMMUNICATION

Summary

Since 1994, extensive sampling of streams in South Australia (SA) has occurred as part of the Monitoring River Health (MRH) Program, the AusRivAS project and local monitoring for the Onkaparinga Catchment Water Management Board and other agencies. This work has revealed many macroinvertebrate taxa not previously reported from SA, including specimens of the amphipod families Corophiidae and Perthiidae. Freshwater corophiids previously have been recorded only from the Brisbane River in Queensland[1,2], and perthiids have been recorded only from Western Australia[2,3].

Transactions of the Royal Society of South Australia (2002), **126**(2), 125–126.

BRIEF COMMUNICATION

FIRST RECORDS OF TWO FAMILIES OF FRESHWATER AMPHIPODA (COROPHIIDAE, PERTHIIDAE) FROM SOUTH AUSTRALIA

Since 1994, extensive sampling of streams in South Australia (SA) has occurred as part of the Monitoring River Health (MRH) Program, the AusRivAS project and local monitoring for the Onkaparinga Catchment Water Management Board and other agencies. This work has revealed many macroinvertebrate taxa not previously reported from SA, including specimens of the amphipod families Corophiidae and Perthiidae. Freshwater corophiids previously have been recorded only from the Brisbane River in Queensland[1–3] and perthiids have been recorded only from Western Australia[4,5].

The Corophiidae is a speciose family found in marine and freshwater habitats around the world. In Australia, the only known freshwater species is *Paracorophium excavatum*, found also in New Zealand[1]. Specimens recently found in SA appear to be *P. excavatum*, but as the original description of the species in Australia is dubious (J.H. Bradbury, Univ. Adelaide, pers. comm.), they are identified here as Corophiidae SAsp1. The body is slightly flattened dorsoventrally, and the urosome is markedly so. There is no accessory flagellum on the antennules. The merus of the second gnathopod is elongate and all pereopods are heavily setose. The third uropod is small, with an outer ramus that is twice as long as the inner ramus, and is partly hidden by a rounded, entire (not cleft), fleshy telson.

Sites where Corophiidae SAsp1 occurs in SA are widespread but disjunct. They include the Tod River on Eyre Peninsula (34° 35′ E, 135° 53′ S), the Bremer River near Hartley (35° 10′ E, 139° 01′ S), Gorge Ck (34° 56′ E, 139° 09′ S) and Reedy Ck (34° 56′ E, 139° 13′ S), both of which are tributaries of the Murray River; and Lake Bonney (37° 39′ E, 140° 19′ S) and the Lake Frome outlet drain (37° 34′ E, 140° 07′ S) in the south east. It occurs in still and flowing water habitats with conductivities of 2890–25700 µS/cm. It is abundant at all these sites, and often cohabits with *Austrochiltonia australis* (Ceinidae), the most common freshwater amphipod in SA.

The distribution of Corophiidae SAsp1 in SA suggests marine influences. Two records are from watercourses that empty into the sea (Lake Frome outlet, Tod River), and the others drain to the Murray River or Lake Alexandrina, both of which were connected to the ocean before construction of river-mouth barrages in 1940. According to Chilton[1], who first identified *P. excavatum* from Queensland (Brisbane River), this species prefers running waters near the coast. All New Zealand records are from brackish waters[3].

The family Perthiidae previously was known only from south-western Western Australia (WA)[4,5]. It contains a single genus, *Perthia* and two species, *P. acutitelson* and *P. branchialis*. The antennules are not significantly longer than the antennae, and the accessory flagellum of each antennule is 2-segmented. Thoracic segments carry dendritic sternal gills. The gnathopods are large and cumlevered. Pereopod 6 is longer than pereopod 7. In *P. branchialis* the inner ramus of uropod 3 is one quarter the length of the outer ramus; in *P. acutitelson* it is about two thirds as long as the outer ramus. Although specimens from SA fit the descriptions of both WA species, the distance between the two regions suggests that there may be taxonomic differences (J. H. Bradbury, pers. comm.).

Most specimens of *Perthia* spp. from SA are from a small area of the Mount Lofty Ranges, in the Onkaparinga catchment near Adelaide, but they have also been collected from the Murray River at Woods Point. The latter site has a chemical composition like other sites where *Perthia* spp. have been collected, but it is a lowland river rather than an upland stream. SA Water uses the Onkaparinga River as a conduit for Murray water, and it is possible that translocation of species has occurred.

From the physicochemical characteristics of sites in WA and SA where *Perthia* spp. have been collected, it would appear that the group prefers slow-flowing or still habitats, cool temperatures and fresh water (<1500 mS/cm) with low nutrient levels (total phosphorus <0.1 mg/L, total Kjeldahl nitrogen <1 mg/L) and neutral to acidic pH. They generally occur in catchments with relatively high rainfall and native vegetation. The most likely factors to restrict the distribution of *Perthia* spp. in SA are conductivity and rainfall.

Higher rainfall generally means greater permanency of water bodies. In the MRH survey of WA (1994-2000), *Perthia* spp. were found at 550 sites. All have average annual rainfall of 600-1400 mm/yr (S. Halse, Dept Conservation & Land Management, Perth, pers. comm.). In SA, all sites other than Woods Point have annual rainfall >600 mm/yr. Only a small area of SA receives rainfall in this range (i.e. Kangaroo Island, Mt Lofty Ranges, Mt Gambier region). Woods Point does not receive high rainfall, but nonetheless has a high degree of permanency.

The average conductivity of WA and SA MRH sites where *Perthia* spp. were found was around 850 µS/cm (S. Halse, pers. comm.; AWQC, unpubl.). The conductivity of SA MRH sites was 150-100 000 µS/cm, and most were >1500 µS/cm. Therefore 850 µS/cm is "fresh" and uncommon by SA standards. Conductivity may limit the distribution of *Perthia* spp. in SA.

These new records add to the known biodiversity of SA and may also contribute to evolutionary and ecological studies. Amphipods are potentially useful as environmental indicators, due to their ecological importance, numerical abundance and sensitivity to toxicants and pollutants[6–8], but their use is limited to the few regions where comprehensive taxonomic and natural history investigations have been undertaken[9]. These new records may extend their use in this way.

These data are from programs funded by Land and Water Australia, Environment Australia, the Environment Protection Agency of South Australia, the Onkaparinga Catchment Water Management Board and the Murray-Darling Basin Commission. Thanks to John Bradbury for taxonomic advice, Stuart Halse and Ivor Growns for

unpublished data, Beth Hughes and Chris Madden, Paul McEvoy, Tracy Venus, Vlad Tsymbal, Peter Schultz, Amber Lang and Darren Hicks for collection and identification of samples.

[1] **Chilton, C.** (1920) The occurrence in the Brisbane River of the New Zealand amphipod, *Paracorophium excavatum* (G. M. Thomson). *Memoirs of the Queensland Museum* **7**, 1-8.

[2] **Bradbury, J. H. & Williams, W. D.** (1999) Key to and checklist of the inland aquatic amphipods of Australia. *Technical Reports of the Australian Museum* **14**, 1-21.

[3] **Stráskraba, M.** (1964) *Perthia* n.g. (Amphipoda, Gammaridae) from freshwater of Western Australia, with remarks on the genera *Neoniphargus* and *Uroctena*. *Crustaceana* **7**, 125–139.

[4] **Chapman, M. A. & Lewis, M. H.** (1976) "An Introduction to the Freshwater Crustacea of New Zealand" (William Collins (New Zealand) Ltd., Auckland).

[5] **Hart, B. H. & Fuller S. L. H.** (1979) "Pollution Ecology of Estuarine Invertebrates" (Academic Press, New York).

[6] **Thomas, J. D.** (1993) Biological monitoring and tropical biodiversity in marine environments: a critique with recommendations, and comments on the use of amphipods as bioindicators. *Journal of Natural History* **27**, 795-80.

D. J. TAYLOR, Australian Water Quality Centre, PMB 3 Salisbury, South Australia 5108. E-mail: daria.taylor@sawater.com.au

ROYAL SOCIETY OF SOUTH AUSTRALIA INCORPORATED

Patron:

HER EXCELLENCY MARJORIE JACKSON-NELSON, AC, MBE
GOVERNOR OF SOUTH AUSTRALIA

OFFICERS FOR 2002-2003

President:

O. W. WIEBKIN, BSc, PhD

Vice-Presidents:

R. W. FITZPATRICK, Bsc Agric, MSc Agric, PhD
N. F. ALLEY, BA(Hons), MA, PhD

Secretary:

J. H. LOVE, BA, BD

Treasurer:

J. T. JENNINGS, BSc(Hons), PhD

Editor:

N. F. MORCOM, BSc(Hons), PhD

Assistant Editor:

Librarian:

Programme Secretary:

N. J. SOUTER, BSc(Hons)

Minutes Secretary:

Membership Secretary:

A. J. McARTHUR, BE

Members of Council:

J. E. PATTISON, MA, BSc, MSc, Grad Cert Ed
P. A. PARSONS, BAgSc, PhD, ScD, FLS
R. D. SHARRAD, BSc(Hons), PhD, DipT(Sec)
M. IQBAL, BSc(Hons), MSc, PhD
M. A. J. WILLIAMS, BA(Hons), MA, PhD, ScD

Printed by Graphic Print Group, 10-14 Kingston Avenue, Richmond, S.A. 5033